Radiative forcing of climate: the historical evolution of the radiative forcing concept, the forcing agents and their quantification, and applications

Article

Accepted Version

It is advisable to refer to the publisher's version if you intend to cite from the work. See Guidance on citing.

www.reading.ac.uk/centaur

CentAUR

Central Archive at the University of Reading

Reading's research outputs online

Radiative Forcing of Climate: The Historical Evolution of the Radiative Forcing Concept, the Forcing Agents and their Quantification, and Applications

V. Ramaswamy[1,c], W. Collins[2], J. Haywood[3], J. Lean[4],

N. Mahowald[5], G. Myhre[6], V. Naik[1], K.P. Shine[7], B. Soden[8],

G. Stenchikov[9], and T. Storelvmo[10]

32

1.   NOAA/ Geophysical Fluid Dynamics Laboratory, Princeton University, Princeton, NJ 08540.

2.   Lawrence Berkeley National Laboratory and University of California, Berkeley, CA 94720.

3.   University of Exeter, and United Kingdom Met Office, Exeter, EX4 4QF, UK.

4.   U. S. Naval Research Laboratory, Washington, DC 20375 (Retired).

5.   Department of Earth and Atmospheric Sciences, Cornell University, Ithaca, NY 14853.

6.   CICERO, Pb. 1129 Blindern, 0318, Oslo, Norway.

7.   Department of Meteorology, University of Reading, Reading RG6 6BB, UK.

8.   Rosentiel School of Marine and Atmospheric Science, University of Miami, Miami, FL 33124.

9.   King Abdulla University of Science and Technology, Thuwal, Jeddah 23955-6900, Saudi Arabia.

10.   University of Oslo, Postboks 1022, Blindern 0315, Norway.

c – Corresponding Author

1

Abstract

We describe the historical evolution of the conceptualization, formulation, quantification, application and utilization of "radiative forcing (RF, see e.g., IPCC, 1990)" of Earth's climate.

Basic theories of shortwave and long wave radiation were developed through the 19th and 20th centuries, and established the analytical framework for defining and quantifying the perturbations to the Earth's radiative energy balance by natural and anthropogenic influences. The insight that the Earth's climate could be radiatively forced by changes in carbon dioxide, first introduced in the 19th century, gained empirical support with sustained observations of the atmospheric concentrations of the gas beginning in 1957. Advances in laboratory and field measurements, theory, instrumentation, computational technology, data and analysis of well-mixed greenhouse gases and the global climate system through the 20th Century enabled the development and formalism of RF; this allowed RF to be related to changes in global-mean surface temperature with the aid of increasingly sophisticated models. This in turn led to RF becoming firmly established as a principal concept in climate science by 1990.

The linkage with surface temperature has proven to be the most important application of the RF concept, enabling a simple metric to evaluate the relative climate impacts of different agents. The late 1970s and 1980s saw accelerated developments in quantification including the first assessment of the effect of the forcing due to doubling of carbon dioxide on climate (the "Charney" report, National Research Council, 1979). The concept was subsequently extended to a wide variety of agents beyond well-mixed greenhouse gases (WMGHGs: carbon dioxide,

2

86   methane, nitrous oxide, and halocarbons) to short-lived species such as ozone. The WMO

87   (1986) and IPCC (1990) international assessments began the important sequence of periodic

88   evaluations and quantifications of the forcings by natural (solar irradiance changes and

89   stratospheric aerosols resulting from volcanic eruptions) and a growing set of anthropogenic

90   agents (WMGHGs, ozone, aerosols, land surface changes, contrails). From 1990s to the

91   present, knowledge and scientific confidence in the radiative agents acting on the climate

92   system has proliferated. The conceptual basis of RF has also evolved as both our understanding

93   of the way radiative forcing drives climate change, and the diversity of the forcing

94   mechanisms, have grown. This has led to the current situation where "Effective Radiative

95   Forcing (ERF, e.g., IPCC, 2013)" is regarded as the preferred practical definition of radiative

96   forcing in order to better capture the link between forcing and global-mean surface temperature

97   change. The use of ERF, however, comes with its own attendant issues, including challenges in

98   its diagnosis from climate models, its applications to small forcings, and blurring of the

99   distinction between rapid climate adjustments (fast responses) and climate feedbacks; this will

100   necessitate further elaboration of its utility in the future. Global climate model simulations of

101   radiative perturbations by various agents have established how the forcings affect other climate

102   variables besides temperature e.g., precipitation. The forcing-response linkage as simulated by

103   models, including the diversity in the spatial distribution of forcings by the different agents, has

104   provided a practical demonstration of the effectiveness of agents in perturbing the radiative

105   energy balance and causing climate changes.

106
107   The significant advances over the past half-century have established, with very high

108   confidence, that the global-mean ERF due to human activity since preindustrial times is

109   positive (the 2013 IPCC assessment gives a best estimate of 2.3 W m^{-2}, with a range from 1.1

110   to 3.3 W m^{-2}; 90% confidence interval). Further, except in the immediate aftermath of

111   climatically-significant volcanic eruptions, the net anthropogenic forcing dominates over

112   natural radiative forcing mechanisms. Nevertheless, the substantial remaining uncertainty in

113   the net anthropogenic ERF leads to large uncertainties in estimates of climate sensitivity from

114   observations and in predicting future climate impacts. The uncertainty in the ERF arises

115   principally from the incorporation of the rapid climate adjustments in the formulation, the well-

116   recognized difficulties in characterizing the preindustrial state of the atmosphere, and the

117   incomplete knowledge of the interactions of aerosols with clouds. This uncertainty impairs the

118   quantitative evaluation of climate adaptation and mitigation pathways in the future. A grand

119   challenge in Earth System science lies in continuing to sustain the relatively simple essence of

120   the radiative forcing concept in a form similar to that originally devised, and at the same time

121   improving the quantification of the forcing. This, in turn, demands an accurate, yet increasingly

122   complex and comprehensive, accounting of the relevant processes in the climate system.

123
124
125

Radiative influences driving climate change since preindustrial times: Segue to the RF

Concept

1. Introduction

Interactions of the incoming solar radiation and outgoing longwave radiation with the Earth's

surface and atmosphere affect the planetary heat balance and therefore impact the climate

system. The growth in fundamental knowledge of physics and chemistry via observational and

theoretical developments through the 18th, 19th and 20th centuries became the platform for

describing the agents driving Earth's climate change since preindustrial times (1750) and the

formulation of the "Radiative Forcing (RF)" (see Section 2) of climate change. The central

purpose of this paper is to trace the progression in the RF concept leading to our current

knowledge and estimates of the major agents known to perturb climate. Below, we give a

perspective into the key milestones marking advances in the knowledge of RF. Subsequent

sections of the paper focus on the evolution of: the concept including its formulation; the known

major forcing agents; and various applications of the concept. We attempt to capture the

historical evolution of the above foci through approximately the mid-2010. Of necessity, given

the nature of the paper for the American Meteorological Society Centennial monograph volume

and the vast domain of the topic, the principal aim of this manuscript is to describe the evolution

as evidenced through the literature, particularly the major international assessment reports. We

refer the reader to the richness of the references cited for the in-depth scientific details marking

the steps over the past three centuries to the present state-of-the-art.

Section 1.1 Growth of atmospheric radiation transfer (pre-20th C to mid-20th C)

The basic concepts of planetary energy budget and the greenhouse effect were put forward in the early nineteenth century by Fourier (1824), although the term "greenhouse" was not mentioned. Fourier recognized that the atmosphere is opaque to "dark heat" (infrared radiation), but could not identify the factors. Laboratory experiments related to transmission of light by atmospheric gases at different wavelengths were the subject of atmospheric radiation inquiries as far back as the early 19th century. One of the very first laboratory measurements of infrared absorption was reported by Tyndall (1861). Based on a series of carefully designed laboratory experiments, Tyndall discovered that infrared absorption in the atmosphere is largely due to carbon dioxide and water vapour. Tyndall thought that variations in the atmospheric concentrations of CO_2 and water vapour account for "all the mutations of climate which the researches of geologists reveal" (see Anderson et al., 2016). Very soon after that came spectral measurements, prompted by both scientific curiosity and a quest to explain the then known variations in earth's climate.

Arrhenius (1896) made the quantitative connection to estimate the surface temperature increase due to increases in CO_2. He relied on surface radiometric observations (Langley, 1884), used or inferred a number of fundamental principles in shortwave and longwave radiation, pointed out the greenhouse effect of water vapor and CO_2, and made simple assumptions concerning exchange of heat between surface and atmosphere to deduce the temperature change (see Ramanathan and Vogelmann, 1997). In the same study, Arrhenius also discussed the solar absorption in the atmosphere. Arrhenius' systematic investigation and inferences have proven to be pivotal in shaping the modern-day thinking, and computational modeling of the climate effects due to CO_2 radiative forcing.

6

180

181   Advances in theoretical developments in classical and, later on, in quantum physics, through the

182   19th and early 20th centuries laid the groundwork concerning light (photon) absorption/emission

183   processes and their linkage to the laws of thermodynamics. This led to the enunciation of basic

184   concepts in the 19th century e.g., Kirchhoff's deductions concerning blackbody radiation, and

185   the associated laws byPlanck, Wien, Rayleigh-Jeans, Stefan-Boltzmann. These laws, and the

186   physics of thermal absorption and emission by gases and molecules, were applied to the context

187   of the atmosphere, leading to the formalism of atmospheric longwave radiative transfer (see

188   Chapter 2 in Goody and Yung, 1989).

189
190   Discovery and understanding of observed phenomena played a role throughout in the

191   development of methodologies that were to become building blocks for the quantification of

192   perturbations to the shortwave and longwave radiative fluxes. A combination of fundamental

193   theoretical developments, observations, simple calculations, and arguments sowed the advances,

194   for example, Lord Rayleigh's (Hon. J. W. Strutt) treatise on skylight and color (1871) and the

195   electromagnetic scattering of light (1881). Another example isMie's theory of electromagnetic

196   extinction (1908) which unified the laws of light reflection, refraction, and diffraction following

197   Huygens, Fresnel, Snell, (see van de Hulst, 1957), and inferred the disposition of light at any

198   wavelength when it interacts with homogeneous spherical particles. Advances in the knowledge

199   of gaseous absorption and emission processes through laboratory-based quantification of

200   absorption lines and band absorption by the important greenhouse gases marked the further

201   growth of atmospheric longwave radiative transfer from the late 19th century into the mid-and-

202   late 20th century (see Chapter 3 in Goody and Yung, 1989). Experimental developments, along

203   with advances in conceptual thinking on the heat balance of the planet, began to provide the

7

204   platform for quantifying the radiation budget e.g., solar irradiance determination by Abbott and

205   Fowle (1908), and an early estimate of the Earth's global-average energy budget by Dines

206   (1917). Dines' effort was a remarkable intellectual attempt given there was very little then by

207   way of observations of the individual components. Figure 1.1 provides a comparison of the

208   values estimated by Dines (1917) compared to one modern analysis (L'Ecuyer et al. 2015). What

209   we term as radiative forcing (RF) of climate change today can be regarded as a result of this early

210   thinking about the surface-atmosphere heat balance.

211
212   Callendar's work in the 1930s-1950s built upon the earlier explorations of Arrhenius and Ekholm

213   (1901) to relate global temperature to rising CO_2 concentrations. Callendar (1938) compiled

214   measurements of temperatures from the 19th century onwards and correlated these with

215   measurements of atmospheric CO_2 concentrations. He concluded that the global land

216   temperatures had increased and proposed that this increase could be an effect of the increase in

217   CO_2 (Fleming, 1998). Callendar's assessment of the climate sensitivity (defined as surface

218   temperature change for a doubling of CO_2) was around 2 °C (Archer and Rahmstorf, 2010)

219   which is nowadays regarded as being at the lower end of the modern-day computed values (e.g.,

220   IPCC, 2013). His papers in the 1940s and 1950s influenced the study of CO_2-atmosphere-surface

221   interactions vigorously, both on the computational side which introduced simplified radiation

222   expressions (e.g., Plass, 1956; Yamamoto and Sasamori, 1958) and in initiating the organization

223   of research programs to measure CO_2 concentrations in the atmosphere. Plass recognized the

224   importance of CO_2 as a greenhouse gas in 1953 and published a series of papers (e.g., Plass,

225   1956). He calculated that the 15-micron CO_2 absorption causes the temperature to increase by 3.6

226   C if the atmospheric CO_2 concentration is doubled and decreases by 3.8 C when it is halved.

227   These early calculations helped guide future works. Modern monitoring of CO_2 concentrations

8

228   began with Keeling's pioneering measurements of atmospheric CO_2 concentrations, begun in

229   connection with the International Geophysical Year in 1957 (e.g., Keeling, 1960). This soon

230   spurred the modern computations of the effects due to human-influenced CO_2 increases, and

231   initiated investigations into anthropogenic global warming. The historical developments above,

232   plus many others, beginning principally as scientific curiosity questions concerning the Earth's

233   climate, have formed the foundational basis for the contemporary concept of RF and the

234   estimation of the anthropogenic effects on climate.

235
236   A major part of the work related to radiative drivers of climate change came initially on the

237   longwave side, and more particularly with interest growing in the infrared absorption by CO_2 and

238   H_2O. This came about through the works of many scientists (see references in Chapters 3 and 4,

239   Goody and Yung, 1989). Research expansion comprising theoretical and laboratory

240   measurements continued into the late 20th Century (see references in Chapter 5, Goody and

241   Yung, 1989). Importantly, from the 1960s, existing knowledge of spectral properties of gaseous

242   absorbers began to be catalogued on regularly updated databases, notably HITRAN (see

243   references in Chapter 5, Goody and Yung, 1989).

244
245   On the shortwave measurements side, the Astrophysical Observatory of the Smithsonian

246   Institution (APO) made measurements of the solar constant (now more correctly referred to as

247   the "total solar irradiance" as it is established that this is not a constant) at many locations on the

248   Earth's surface from 1902 to 1962 (Hoyt, 1979). While there were interpretations from these

249   observations about change and variations in the Sun's brightness, the broad conclusion was that

250   the data reflected a strong dependency on atmospheric parameters such as stratospheric aerosols

251   from volcanic eruptions, as well as dust and water vapor. Research into shortwave and longwave

252   radiation transfer yielded increasingly accurate treatments of the interactions with atmospheric

253   constituents (Chapters 4-8 in Goody and Yung, 1989; and Chapters 1-4 in Liou, 2002).

254

255

256

1.2 Advent of the RF concept and its evolution (since the 1950s)

Advances in computational sciences and technology played a major role alongside the growth in

basic knowledge. The increases in computational power from 1950s onwards, with facilitation

of scalar and later vector calculations, enhanced the framework of "reference" computations

(e.g., Fels et al., 1991; Clough et al., 1992). This enabled setting benchmarks for quantifying the

radiative forcing by agents. With developments in community-wide radiative model

intercomparisons (e.g., Ellingson et al., 1991; Fouquart et al., 1991; Collins et al., 2006), the

comparisons against benchmarks established a definitive means to evaluate radiative biases in

global weather and climate models, one of the best examples of a "benchmark" and its

application in the atmospheric sciences. The advance in high-performance computing since

2000 has endowed the benchmark radiative computations with the ability to capture the details

of molecular absorption and particulate extinction at unprecedented spectral resolutions in both

the solar and longwave spectrum.

Relative to the previous decades, the 1950s also witnessed the beginning of increasingly

sophisticated and practical numerical models of the atmosphere and surface that included

radiative and then radiative-convective equilibrium solutions. Hergesell's (1919) work had

superseded earlier calculations in describing the radiative equilibrium solutions using a grey-

atmosphere approach. Subsequent studies further advanced the field by recognizing the

existence of a thermal structure, making more realistic calculations based on newer

spectroscopic measurements and observations (e.g., Murgatroyd, 1960; Mastenbrook, 1963;

Telegadas and London, 1954), developing simplified equations (parameterizations) for use in

11

281   weather and climate models, and exploring how the radiation balance could be perturbed

282   through changes in the important atmospheric constituents e.g., water vapor and carbon dioxide

283   (Kaplan, 1960; Kondratyev and Niilisk, 1960; Manabe and Moller, 1961; Houghton, 1963;

284   Moller, 1963; Manabe and Strickler, 1964). Manabe and Strickler (1964) and Manabe and

285   Wetherald (1967) set up the basis for the more modern-day calculations in the context of one-

286   dimensional models, invoking radiative-convective equilibrium, where the essential heat

287   balance in the atmosphere-surface system involved solar and longwave radiative, and

288   parameterized convective (latent+sensible heat) processes. In this sense, the 1960s efforts went

289   significantly ahead of Arrhenius' pioneering study and other earlier insightful investigations to

290   recognize and calculate the effects of carbon dioxide in maintaining the present-day climate.

291
292   The foundational model calculations of radiative perturbations of the climate system arose from

293   publications beginning in the 1960s. Manabe and Wetherald (1967) demonstrated how changes

294   in radiative constituents (CO_2, H_2O, O_3) as well as other influences (solar changes, surface

295   albedo changes) could affect atmospheric and surface temperatures. The field of modeling grew

296   rapidly over the 1960s to 1980s period and three-dimensional models of the global climate

297   system came into existence, enabling an understanding of the complete latitude-longitude-

298   altitude effects of increasing CO_2. The acceleration of modeling studies resulted in an ever-

299   increasing appreciation of CO_2 as a major perturbing agent of the global climate [Manabe and

300   Bryan, 1969; Manabe and Wetherald, 1975; Ramanathan et al., 1979; Manabe and Stouffer,

301   1980; Hansen et al., 1981; Bryan et al., 1988; Washington and Meehl, 1989; Stouffer et al.,

302   1989; Mitchell et al., 1990]. The growth in the number of studies also galvanized CO_2-climate

303   assessments using the numerical model simulations (e.g., NRC, 1979, now famously referred to

304   as the "Charney" report,). The Charney study was the first institutionally sponsored scientific

12

305   assessment based on then available studies. The report concluded a RF due to CO_2 doubling of

306   about 4 W m-2 and estimated the most probable global warming to be near 3°C with a probable

307   error of ± 1 .5°C. This was a landmark report, has influenced the community immensely, and

308   became a trendsetter for climate science assessments. A second assessment followed (NRC,

309   1982, referred to as the "Smagorinsky" report) which essentially reiterated the conclusions of

310   the Charney report.

311

312   The above studies and assessments established a useful basis for a formalized perspective into

313   mathematical linkages between global-mean RF by greenhouse gases and surface temperature

314   changes, with the applicability extending to global climate impacts. The modern definition and

315   equations for RF took root during this period. The conceptual development that has lent

316   powerful significance to characterizing radiative perturbations via "RF" came through in the

317   1970s with the first formal phrasing (Ramanthan, 1975), and got solidified as a concept in the

318   late 1970s and 1980s (e.g., Ramanathan et al., 1979; Dickinson and Cicerone, 1982) especially

319   through the major international assessment reports e.g., WMO (1986, volume III). Eventually,

320   the IPCC scientific assessments, beginning with IPCC (1990), made this a robust terminology.

321
322   This continues through today even though there have been substantial refinements in the past

323   decade (see Section 2). As the RF concept settled into more rigorous formulations in the 1970s

324   and 1980s, a spate of research extended this exercise to other well-mixed greenhouse gas

325   changes such as methane, nitrous oxide and chlorofluorocarbons (Ramanathan, 1975; Wang et

326   al., 1976; Donner and Ramanathan, 1980; Hansen et al., 1981). This became possible as

327   spectroscopic data and knowledge of their atmospheric concentration changes grew. In later

328   years and decades, the list of well-mixed greenhouse gases grew to include a plethora of

329   halocarbons, sulfur hexafluoride etc. (e.g., Fisher et al., 1990; Pinnock et al., 1995).

330

331   Although the RF concept was developed to quantify the changes in radiation balance due to

332   well-mixed greenhouse gases and solar irradiance changes, this was extended to short-lived

333   gases, such as ozone, which exhibit strong spatial and temporal variability (Ramanathan et al. in

334   WMO, 1986; Shine et al., 1990; Isaksen et al., 1992). The concept was also applied to an entire

335   category of effects referred to as "indirect" which accounted for changes in atmospheric

336   concentrations of a radiative constituent affected by non-radiative effects such as chemical or

337   microphysical interactions (see Sections 4 and 5). These were first derived for the case of

338   tropospheric and stratospheric ozone changes occurring through chemical reactions in the

339   atmosphere involving anthropogenic precursor species. Indirect effects also were uncovered for

340   aerosol-related radiative effects obtained through their interactions with water and ice clouds

341   (Charlson et al., 1992, Penner et al., 1992; Schimel et al., 1996).

342
343   The impact of emissions of anthropogenic aerosols, or their precursors, on climate had been

344   recognized as early as the 1970s while recognition of their effects on air pollution goes back

345   more than a century (Brimblecombe and Bowler, 1990). The first quantification, however, in

346   the context of preindustrial to present-day emissions came through Charlson et al. (1991). The

347   forcing connected with the anthropogenic aerosol emissions has acquired a more diverse picture

348   now with the complexity associated with the various species (e.g., different types of

349   carbonaceous aerosols), existence of a variety of mixed states (i.e. aerosols consisting of more

350   than one component), and the influence of each species on the formation of water drops and ice

351   crystals ("indirect" forcing referred to above). Additional complexities with aerosols as

14

352   compared to the well-mixed greenhouse gases arise because of their inhomogeneous space and

353   time distribution. Estimating preindustrial concentrations of important short-lived gases and

354   aerosols and their precursors is difficult, and is a major contributor to uncertainty in their RF

355   (e.g., Tarasick et al. 2019; Carslaw et al. 2017).

356
357   Besides atmospheric constituents, other radiative influences also began to be quantified under

358   the broad concept of "radiative forcing". These included land-use and land-cover changes due to

359   vegetation changes, primarily in the Northern Hemisphere. The initial considerations were for

360   the changes induced in the albedo of the surfaces due to human activity (Sagan et al., 1979).

361   Later, other physical factors in the context of forced changes such as surface roughness, trace

362   gas and aerosol emissions, water and water-related changes as a consequence of land surface

363   changes were also considered as it was realized that these too affected the planetary heat

364   balance (e.g., IPCC, 2013).

365
366   A relatively recent entry under the anthropogenic RF label includes the attempts to quantify the

367   forcing due to aviation-induced aerosols and contrails, reported as early as beginning of 1970s,

368   and quantitatively assessed beginning with IPCC (1999) (e.g., Fahey et al., 1999). Emissions

369   from various industrial sectors including transportation (aircraft, shipping, road transport) have

370   been comparatively evaluated and assessed (see Unger et al., 2010). While anthropogenic

371   forcings became increasingly better quantified in the 20th Century, so too were the natural

372   agents, such as solar irradiance changes (see Hoyt and Schatten, 1997) and aerosols formed in

373   the stratosphere in the aftermath of explosive or climatically-significant volcanic eruptions

374   (Franklin, 1784, Robock, 2000). The qualitative recognition of the potential climatic effects due

375   to powerful volcanic eruptions (e.g., Toba, Tambora, Krakatoa eruptions), and solar changes,

15

376   possibly goes more than two centuries back. As an example, solar irradiance changes and the

377   resultant ransmission of sunlight through the atmosphere began to be pursued as both questions

378   of scientific curiosity and for potential impacts on surface climate.

379
380
381

1.3 Scope of the paper

In this paper we trace the evolution of the knowledge base that began with recognizing the

importance of changes in atmospheric composition, how they alter the radiative balance of the

planet, and the resulting growth in understanding that has enabled quantification of the radiative
effects.

Notably, this began with considerations of the roles of water vapor and carbon dioxide in the

longwave spectrum, and the naturally arising solar irradiance changes and particulates from

volcanic eruptions in the shortwave spectrum. The early discoveries and theories on the role of

radiation in the planet's heat equilibrium state paved the way for defining the

forcing of the Earth's climate system, with gradually increasing attention to the range of

anthropogenic influences. The forcing used in this context was meant to characterize the agents

driving climate change and nominally on a global-average basis, rather than regional or local

scales. In describing the evolution of the RF concept and its applications, we follow a strategy of

describing the principal advancements over time, with references to a few of the seminal

investigations. Included in these are the well-known chapters on radiative forcing appearing in

various assessments and reports e.g., IPCC (e.g., 1990, 1996, 2001, 2007, 2013), WMO (e.g.,

1986), NRC (e.g., 1979). Our aim is not to summarize from the assessments but instead to

document the key elements happening over time that pushed the frontiers to the state-of-the-art

in its successive evolutionary stages through to today. We hew fairly strictly to RF only. We do

not discuss "climate feedbacks" *per se* which are an integral part of climate response, but that

discussion is outside the scope of this paper.

Figure 1.2 illustrates the radiative forcing quantification in each of the 5 major IPCC WGI

17

414
415 Assessments to date (1990, 1996, 2001, 2007, and 2013). All the forcings on the illustration
416 represent a measure of the radiative perturbation at the tropopause brought about by the change
417 in that agent relative to its value/state in 1750. As the knowledge has advanced, there
418
419 has been a growth in the number of forcing agents and an evolution in the estimates of the
420
421 magnitudes of the agents. The increased attention to scientific uncertainties also becomes
422
423 evident, representing an advance in the measure of the scientific understanding of.

424 Quantification of the anthropogenic WMGHG and the secular solar forcing began from the 1st

425 IPCC assessment (IPCC, 1990, or "FAR"). While aerosol radiative effects were recognized in

426 FAR, the tropospheric aerosol quantification was reported in an interim IPCC Special Report

427 (IPCC, 1995) which was reaffirmed in the Second Assessment Report (IPCC, 1996 or SAR).

428 RF from ozone changes was recognized in FAR but quantified later. The RF from stratospheric ozone

429 losses due to the halocarbon-catalyzed chemical reactions, and that due to tropospheric ozone increases from

430 anthropogenic precursor emission increases and related chemistry-climate interactions was first quantified in a

431 special IPCC (1992) report followed by IPCC (1995). A special report on aviation-related impacts appeared as

432 IPCC (1999).

433 The Third Assessment Report (IPCC, 2001, or TAR) added a few more agents that were able to

434 be quantified besides updating the estimates of the greenhouse gas and aerosol agents. This

435 occurred in part due to accounting for the increased knowledge about changes in the species

436 concentrations, and to a lesser extent, due to improvements in the treatment of the processes.

437

438

439 The Fourth Assessment Report (IPCC, 2007, or AR4) introduced new methodologies to

440 estimate short-lived gas RF, and

441

18

442 to express the uncertainty due to tropospheric aerosols which continue to be the principal reason

443

444 for the large uncertainty in the anthropogenic forcing (Section 10). AR5, the Fifth Assessment

445

446 Report (IPCC, 2013) introduced a major change in the manner of expressing the radiative

447 forcing by making the transition from radiative forcing (RF) to the effective radiative forcing

448 (ERF). Further details on the progress through the IPCC assessments appear in Section 2. The

449 change in radiative forcing due to CO_2 is due to increase in the concentration between the IPCC

450 assessments, except between SAR and TAR where there was an update in the expression for

451 calculating the radiative forcing. On the other hand, the changes in the short-lived compounds

452 such as ozone and aerosols from one assessment to the other are mainly results of improvements

453 based on observations and modeling representing the knowledge prevailing at the time of the

454 IPCC assessments.

455
456
457 The presentation in this paper aims to capture the principal developments of each forcing and

458
459 their chief characteristics as they developed over time, and thus does not insist on discussions of

460
461 all forcing agents to hew to the same format in the discussions. The sections below discuss the

462
463 major facets of the radiative forcing concept, beginning with its formulation in Section 2.

464
465 Sections 3, 4, 5, 6, 7 address the development of the quantified knowledge, including

466

467 uncertainties, of the anthropogenic forcing agents, in tandem with the

468 developments in the IPCC assessments beginning with the first assessment report in 1990.

469 Sections 8 and 9 discuss the natural drivers of climate change.

470 The totality of the forcing of the climate system i.e., a synthesis by accounting for all the agents

471 in a scientifically justified manner is examined in Section 10. The role of

19

472   RF in enabling the development of metrics to allow emissions of different gases to be placed on

473   an equivalent scale is discussed in Section 11 while the connection of response to the forcing

474   culled from observations and climate model simulations follows in Section 12. Section 13 traces

475   the development of the newest ideas in the application of forcing concept viz.,

476   management of solar and terrestrial radiation in the planet's heat budget based on the RF

477   discussed in the previous Sections regarding well-mixed greenhouse gases and aerosols. The

478   concluding section summarizes the major points of the paper's presentation of the development

479   and utilization and application of radiative forcing, lists the strengths and limitations of the

480   simple concept, and portrays the unresolved issues and grand challenge related to the viability of

481   this concept, and the quantification for climate change determination in the future.
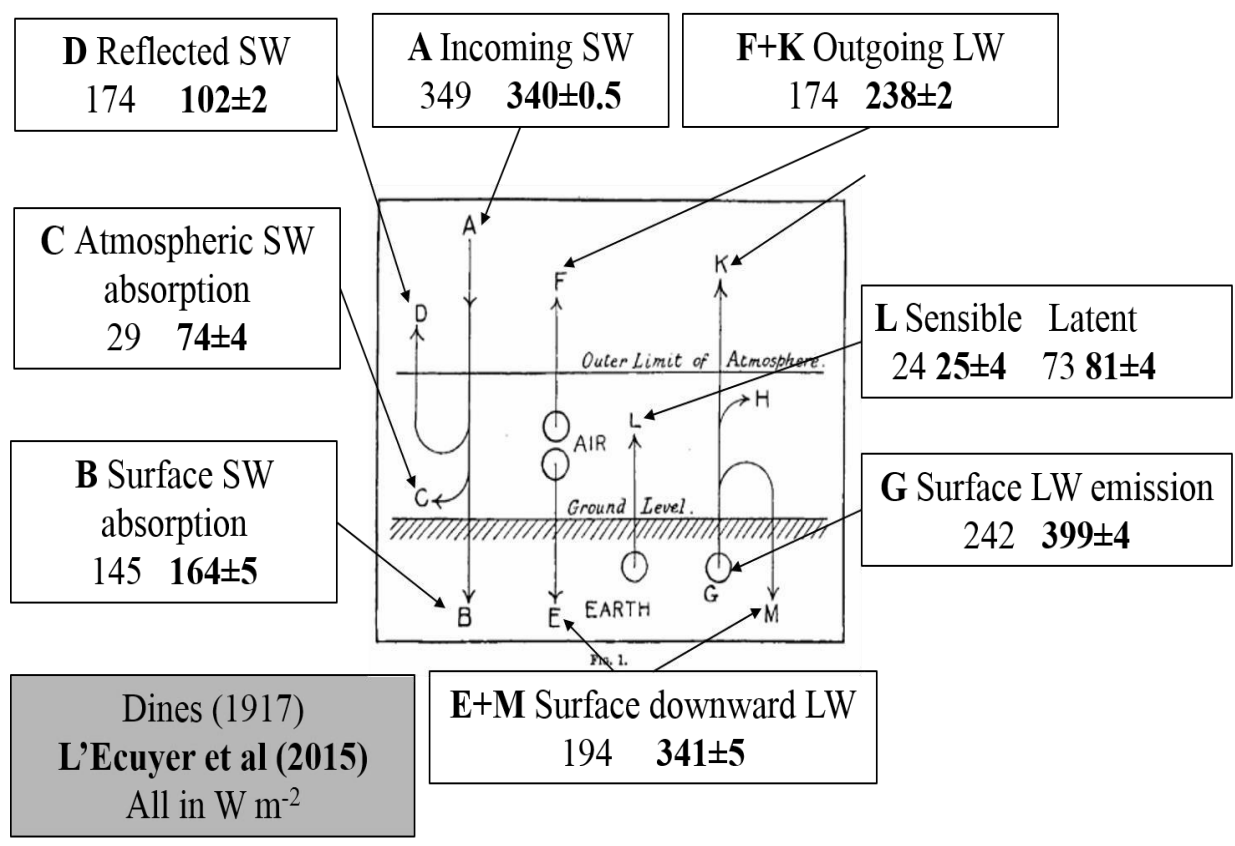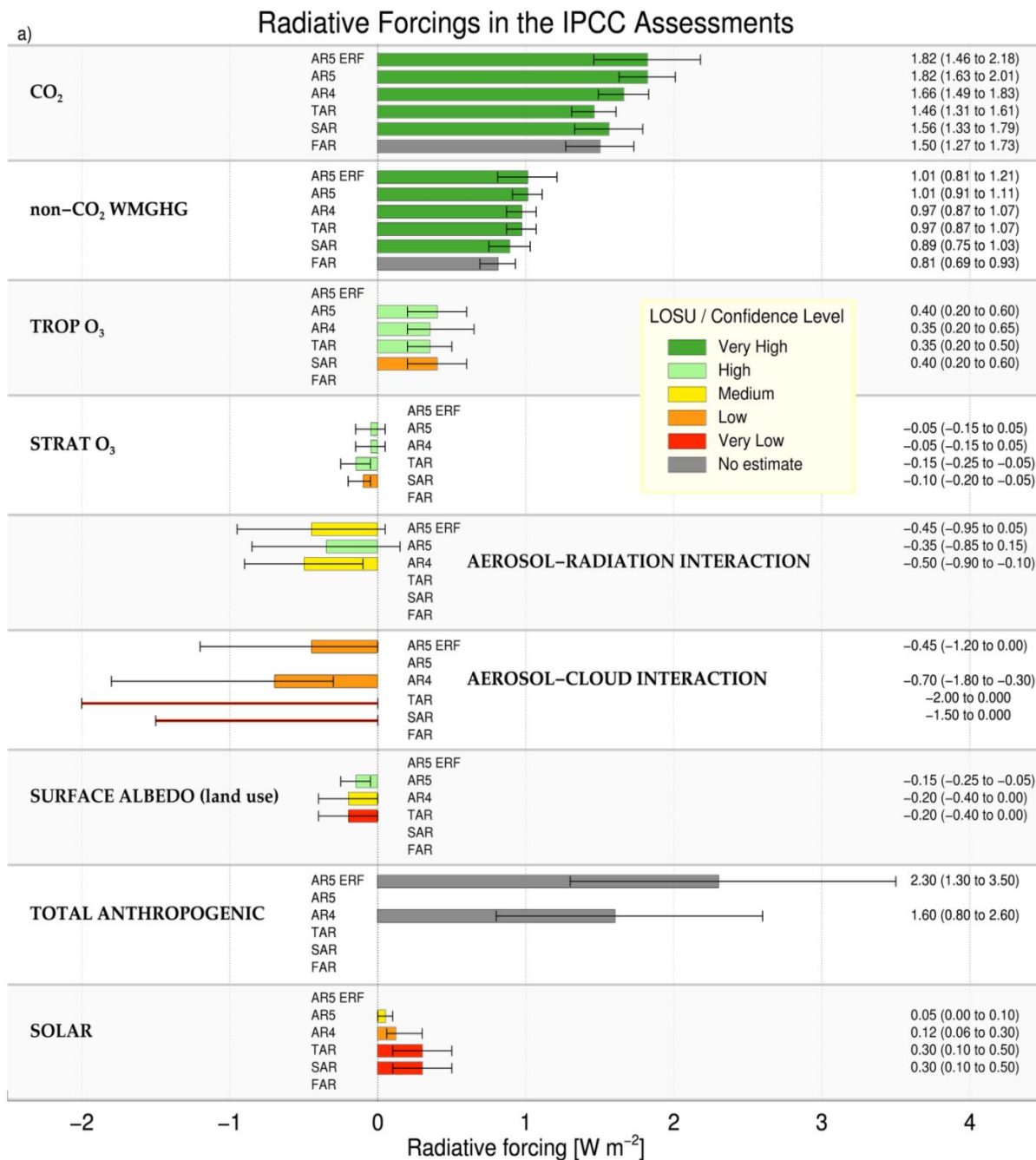
482

483
484

485

486   Figure 1.1: Comparison of one early estimate of the Earth's global-average energy budget (Dines

487   1917) with the contemporary estimates of L'Ecuyer et al. (2015) by annotating the original

488   figure from Dines (1917). All values are given in W m^{-2}, with Dines' values in plain font, and

489   L'Ecuyer et al. in bold font. Dines' value for the surface LW emission is low probably because

490   he adopted a value for Stefan's Constant which was "decidedly lower than that usually given"

491   although the assumed surface temperature is not stated either. For some components, Dines also

492   gave an estimate the uncertainty. The L'Ecuyer et al. (2015) values are from their Figure 4 which

493   applies energy and water balance constraints.

494

495
496

Radiative Forcings in the IPCC Assessments

b) Radiative Forcing of aerosol–radiation interactions in the IPCC Assessments

SULFATE	AR5		−0.40 (−0.60 to −0.20)
	AR4		−0.40 (−0.60 to −0.20)
	TAR		−0.40 (−0.80 to −0.20)
	SAR		−0.40 (−0.80 to −0.20)
BLACK CARBON	AR5		0.40 (0.05 to 0.80)
	AR4		0.20 (0.05 to 0.35)
	TAR		0.20 (0.10 to 0.40)
	SAR		0.10 (0.03 to 0.30)
BIOMASS BURNING	AR5		0.03 (−0.2 to 0.20)
	AR4		0.03 (−0.0 to 0.09)
	TAR		−0.20 (−0.60 to −0.07)
	SAR		−0.20 (−0.60 to −0.07)
ORGANIC AEROSOLS	AR5	AR5 / SOA, AR5 / POA	−0.03 (−0.27 to 0.20) & −0.09 (−0.16 to −0.03)
	AR4		−0.05 (−0.10 to 0.00)
	TAR		−0.10 (−0.30 to −0.03)
	SAR		
DUST	AR5		−0.10 (−0.30 to 0.10)
	AR4		−0.10 (−0.30 to 0.10)
	TAR		−0.60 to 0.40
	SAR		
NITRATE	AR5		−0.11 (−0.30 to −0.03)
	AR4		−0.10 (−0.20 to 0.00)
	TAR		
	SAR		
TOTAL	AR5		−0.35 (−0.85 to 0.15)
	AR4		−0.50 (−0.90 to −0.10)
	TAR		
	SAR		

Radiative forcing [W m^{-2}]

501
502
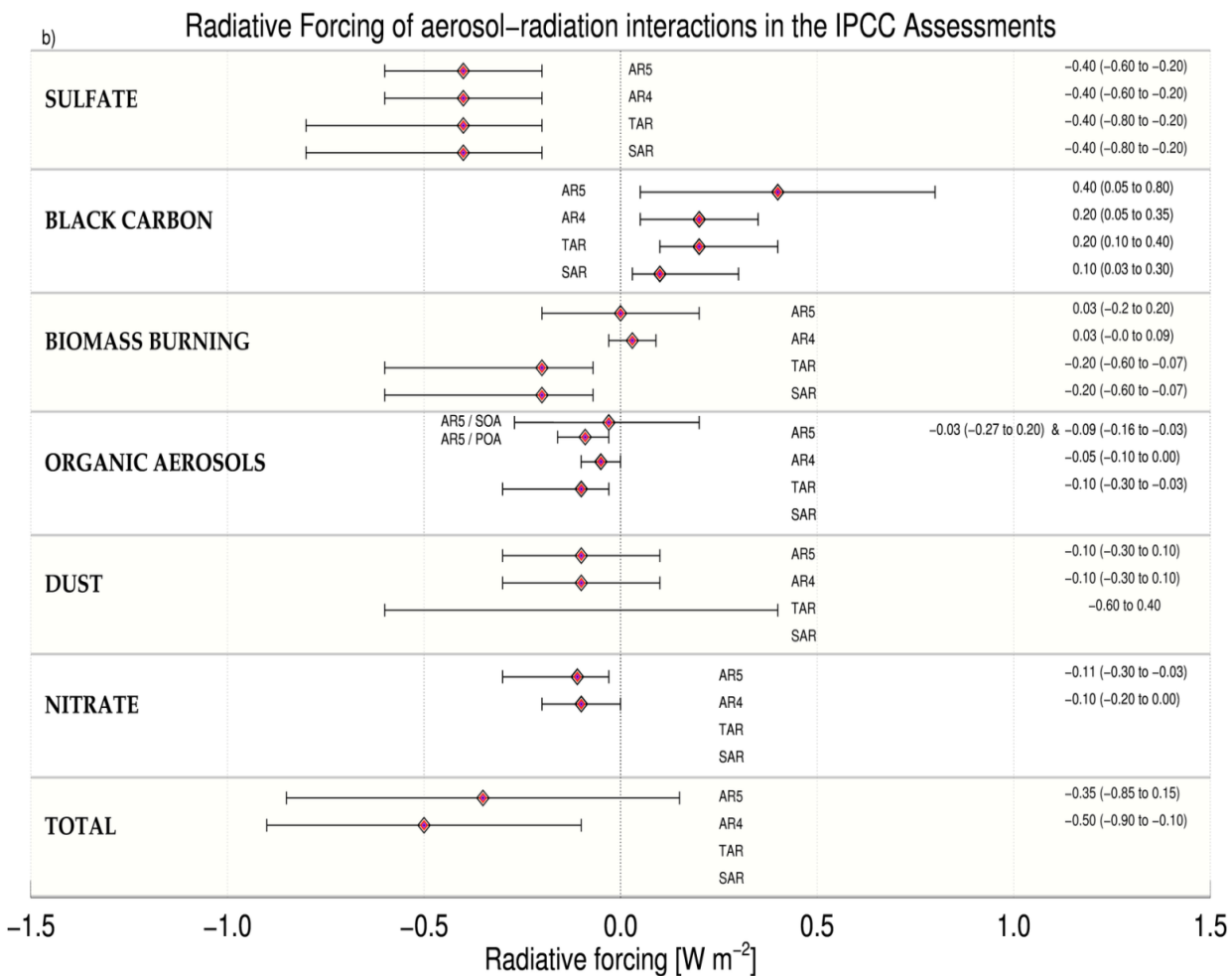503
504
505
506

23

507   Figure 1.2: Summary of the evolution of the global-mean radiative forcings from IPCC reports,

508   where available, from FAR (1765-1990), SAR (1750-1992), TAR (1750-1998), AR4 (1750-

509   2005) and AR5 (1750-2011). The RF and/or the ERF presented in AR5 are included.

510   Uncertainty bars show the 5-95% confidence ranges.

511

512   (a) From top to bottom, the forcings are due to changes in CO_2, non-CO_2 well-mixed

513   greenhouse gases (WMGHGs), tropospheric ozone, stratospheric ozone, aerosol-radiation

514   interaction, aerosol-cloud interaction, surface albedo, total anthropogenic RF, and solar

515   irradiance. The forcings are color coded to indicated the "confidence level" (or "level of

516   scientific understanding (LOSU)", as was presented in and before AR4, which used

517   "consensus" rather than "agreement" to assess confidence level). Dark green is "High

518   agreement and Robust evidence"; light green is either "High agreement and Medium evidence"

519   or "Medium agreement and Robust evidence"; yellow is either "High agreement and limited

520   evidence" or "Medium agreement and Medium evidence" or "Low agreement and Robust

521   evidence"; orange is either "Medium agreement and Limited evidence" or "Low agreement and

522   Medium evidence"; red is "Low agreement and Limited evidence". Several minor forcings

523   (such as due to contrails, and stratospheric water vapor due to methane changes) are not

524   included. The information used here, and information on excluded components, can be mostly

525   found in Myhre et al. (2013) Tables 8.5 and 8.6 and Figure 8.14 and Shine et al. (1990) Table

526   2.6. The decrease in CO_2 RF between SAR and TAR was due to a change in the simplified

527   expressions used to compute its RF; the CO_2 concentration has increased monotonically

528   between each successive IPCC report. No central estimate was provided for aerosol-cloud

529   interaction in SAR and TAR, and a total aerosol-radiation interaction (see panel (b)) and a total

530   anthropogenic RF was not presented in assessments prior to AR4. Stratospheric aerosol RF

531   resulting from volcanic aerosols is not included due to their episodic nature; estimates can be

532   seen in Figure 10.3.

533

534   (b) Individual components of RF due to changes in aerosol-radiation interaction. From top to

535   bottom these are sulfate, black carbon from fossil fuel or biofuel burning, biomass

536   burning, -organic aerosols, dust, nitrate, and total (also shown on panel (a)). In AR5, the

537   organic aerosol RF was separated into primary organic aerosol (POA) from fossil fuel and

538   biofuel, and secondary organic aerosol (SOA), due to changes in source strength, partitioning

539   and oxidation rates. Separate confidence levels were not presented for individual components

540   of the aerosol-radiation interaction in AR4 and AR5, and hence none are shown-. The

541   information used here is mostly drawn from Myhre et al. (2013) Tables 8.4.

542

543
544

545

2. Radiative Forcing – its origin, evolution and formulation

547
548

2.1 The utility of the forcing-feedback-response framework

550
551

552   Radiative forcing provides a metric for quantifying how anthropogenic activities and natural

553   factors perturb the flow of energy into and out of the climate system. This perturbation initiates

554   all other changes of the climate due to an external forcing. The climate system responds to

555   restore radiative equilibrium through a change in temperature, known as the Planck response or

556   Planck feedback. A positive forcing (i.e., a net radiative gain) warms the climate and increases

557   the thermal emission to space until a balance is restored. Similarly, a negative forcing (i.e., a net

558   radiative loss) cools the climate, decreasing the thermal emission until equilibrium is restored.

559
560   The change in temperature required to restore equilibrium can induce other surface and

561   atmosphere changes that impact the net flow of energy into the climate system, and thus

562   modulate the efficiency at which the climate restores equilibrium. Borrowing terminology from

563   linear control theory, these secondary changes can be thought of as feedbacks that serve to

564   further amplify or dampen the initial radiative perturbation. The use of radiative forcings and

565   radiative feedbacks to quantify and understand the response of climate to external drivers has a

566   long and rich history (Schneider and Dickinson 1976; Hansen et al. 1984; Cess, 1976; Cess et

567   al., 1990, NRC 2005; Stephens 2005; Sherwood et al 2015).

568

569   Consider a perturbation in the global-mean net downward irradiance at the top-of-atmosphere,

570     $d\bar{F}$ (which we call the radiative forcing or RF) that requires a change in global-mean surface

571   temperature, $d\bar{T}$ to restore radiative equilibrium (overbars indicate a global-average quantity). If

572   the changes are small and higher order terms can be neglected, and $d\bar{F}$ is time independent, the

573   change in upward radiative energy, $d\bar{R}$ induced by the change in surface temperature, $d\bar{T}$, can

574   be decomposed into linear contributions from changes in temperature and other radiative

575   feedbacks X_i

576
577
578                 $$d\bar{R} = \left[\frac{\partial \bar{R}}{\partial \bar{T}} + \sum_i \frac{\partial \bar{R}}{\partial X_i} \frac{\partial X_i}{\partial \bar{T}}\right] d\bar{T} \qquad (2.1)$$

579

580

581   Equilibrium is restored when $d\bar{R} = d\bar{F}$. The ratio, $\alpha = d\bar{R}/d\bar{T}$, called the "climate feedback

582   parameter", quantifies the efficiency at which the climate restores radiative equilibrium

583   following a perturbation. In the absence of feedbacks, the Planck response is $\alpha_i \approx 3.3$ W m^{-2} K^{-1}

584   (e.g. Cess 1976). In current climate models, radiative feedbacks from water vapor, clouds, and

585   snow/sea ice cover act to reduce α to a range $\approx$1-2 W m^{-2} K^{-1}; this amplifies the change in

586   temperature in response to a given radiative forcing. Most of the intermodel spread in α is due

587   to differences in predicting the response of clouds to an external forcing (Cess et al. 1990).

588   Feedbacks from water vapor, clouds, snow and sea ice cover, have been well documented in

589   both models (Bony et al. 2006) and, to a lesser extent, in observations (Forster 2016). Less well

590   studied are feedbacks from the carbon cycle, ice sheets and the deep ocean that occur on much

591   longer time scales (e.g., Gregory et al. 2009; Forster 2016).

592   While attempting to characterize global climate changes using a single scalar quantity may seem

593   overly simplistic, many aspects of climate do respond in proportion to $d\bar{T}$, regardless of the

594   spatial and temporal scales being considered and are of much greater societal relevance than

595   global mean temperature (e.g., the magnitude of regional rainfall change). To the extent that

596    $d\bar{F}$ can be used to estimate $d\bar{T}$, radiative forcing then provides a simple but crude metric for

597   assessing the climate impacts of different forcing agents across a range of emission scenarios.

598   Here we write the relationship between $d\bar{T}$ and $d\bar{F}$ as

599
600    $$d\,\bar{T} \approx \lambda\,d\bar{F} \qquad (2.2)$$
601
602
603   where λ is usually referred to as the "climate sensitivity parameter", the inverse of α. It

604   is worth noting that equilibrium climate sensitivity is often written in terms of the

605   equilibrium surface temperature response, in K, to a doubling of CO_2 (about 3.7 W m^{-2}).

606

607
608   An important driver in the early development of RF as a metric was the chronic uncertainty

609   in the value of λ, which persists to this day; this meant that quantifying the drivers of

610   climate change, and intercomparing different studies, was easier using $d\bar{F}$ rather than $d\bar{T}$.

611   However, such a comparison of different climate change mechanisms relies on the extent to

612   which λ is invariant (in any given model) to the mechanism causing the forcing; early

613   studies demonstrated similarity between the climate sensitivity parameter for CO_2 and solar

614   forcing (e.g. Manabe and Wetherald 1975) but subsequent work (see Section 2.3.4) has

615   indicated limitations to this assumption. The conceptual development in the subject, which

616   will be discussed in the following sections, has adopted progressively more advanced

617   definitions of RF with the aim of improving the level of approximation in Expression (2.2).

618
619

620
621

622

2.2 Origin of the radiative forcing concept (1970s-1980s)

623

624

625

626 Ramanathan (1975) presents the first explicit usage of the RF concept, as currently recognised

627 (although the term "radiative forcing" was not used), in an important paper quantifying, for the

628 first time, the potential climate impact of chlorofluorocarbons (CFCs). Ramanathan computed

629 the change in the top-of-atmosphere (TOA) irradiance due to increased CFC concentrations and

630 directly related this to the surface temperature change, via an empirical estimate of the

631 dependence of the irradiance on surface temperature; this is the climate feedback parameter

632 discussed in Section 2.1. Ramanathan noted that the surface temperature calculations using this

633 "simpler procedure" were identical to those derived using a "detailed" radiative-convective

634 model. Ramanathan and Dickinson (1979) extended the Ramanathan (1975) framework in

635 important ways, in a study of the climate impact of stratospheric ozone changes. First, there was

636 an explicit recognition that changes in stratospheric temperature (in this case driven by

637 stratospheric ozone change) would influence the tropospheric energy balance. Second, these

638 calculations were latitudinally-resolved. While the global-average stratosphere is in radiative

639 equilibrium (and hence temperature changes can be estimated via radiative calculations alone),

640 locally dynamical heat fluxes can be important. Ramanathan and Dickinson considered two

641 "extreme" scenarios to compute this temperature change without invoking a dynamical model.

642 One assumed that dynamical feedbacks were so efficient that they maintained observed

643 latitudinal temperature gradients; given subsequent developments, this is of less interest here.

644 The other scenario assumed that, following a perturbation, dynamical fluxes remain constant, and

645 temperatures adjust so that the perturbed radiative heating rates equal unperturbed heating rates

646 (and thus balance the unperturbed dynamical heat fluxes). This second method was originally

29

647   referred to as the "no feedback case" (the "feedback" referring to the response of stratospheric

648   dynamics to a forcing); it has since become more widely known as "Fixed Dynamical Heating"

649   (FDH) (Fels et al. 1980; WMO 1982) or more generally "stratospheric (temperature)

650   adjustment". FDH has also been used for stratospheric temperature trend calculations, and shown

651   to yield reasonable estimates of temperature changes derived from a general circulation model

652   (GCM) (e.g. Fels et al. 1980; Kiehl and Boville 1988; Chanin et al., 1998; Maycock et al 2013;

653   ).

654

655

656   Ramanathan et al. (1979) applied the same methodology to CO_2 forcing. Their estimate of RF

657   for a doubling of CO_2 of about 4 W m^{-2} was adopted in the influential Charney et al (1979)

658   report and has been an important yardstick since then. Although not explicitly stated until

659   subsequent papers in the 1980s (see later), one key reason for including stratospheric

660   temperature adjustment as part of RF, rather than as a climate feedback process, was that the

661   adjustment timescale is of order months; this is much faster than the decadal or longer timescale

662   for the surface temperature to respond to radiative perturbation, which is mostly driven by the

663   thermal inertia of the ocean mixed layer. A second, related, key reason is that the tight coupling

664   of the surface and troposphere, via convective heat fluxes, (and, conversely, the limited

665   coupling between the surface and the stratosphere) means that ΔT at surface is largely driven by

666   the RF at the tropopause. A consequence of applying stratospheric temperature adjustment

667   (which returns the stratosphere to global radiative equilibrium) is that tropopause and top-of-

668   atmosphere forcings are identical. This removes an important ambiguity in the definition of RF,

669   although the definition of the tropopause still has to be considered (see Section 2.3.5).

670

671

672   These timescales were made explicit by Hansen et al. (1981) who demonstrated the evolution of

673   the irradiance changes in their radiative-convective model, following a doubling of CO_2 (see Fig.

674   2.1). This tracked the changes from: (i) the immediate response (nowadays called the

675   instantaneous RF (IRF)); (ii) the response after a few months (which is close to the RF

676   incorporating stratospheric temperature adjustment); in the case of a CO_2 increase, the increased

677   emittance of the stratosphere leads to a cooling which increases the magnitude of the

678   perturbation of the top-of-atmosphere irradiance from -2.4 to -3.8 W m^{-2}; and (iii) "Many years

679   later" when the surface temperature has equilibrated (following Expression (2.2)) and the

680   resulting irradiance change at the top of the atmosphere has cancelled out the forcing. Hansen et

681   al. (1981) seem to be the first to use the terminology "radiative forcing", although they used it in

682   a general rather than a quantitative sense.

683

684   Several contributions to the edited volume by Clark (1982) also used the RF concept, at least in

685   an illustrative way, although using a variety of names. For example, Chamberlain et al. (1982)

686   compared different climate change mechanisms using what would now be called as surface

687   radiative forcing; their use of this (rather than tropopause or top-of-atmosphere RF) as a

688   predictor of surface temperature change was strongly disputed in the same volume by

689   Ramanathan (1982) (and earlier in Ramanathan et al., 1981), Hansen et al. (1982) and Luther

690   (1982). Hansen et al. (1982) briefly presented values of top-of-atmosphere radiative flux changes

691   for idealised changes in concentrations of 5 gases, and refer to these as "radiative forcings" in

692   their text. At around the same time, WMO (1982), in a brief report on a meeting on the potential

693   climate effects of ozone and other minor trace gases, refer explicitly to "the net outgoing

31

694 longwave flux at the tropopause" as determining "the radiative forcing of the surface-troposphere

695 system", and present values for idealised perturbations of 6 greenhouse gases.

696

697 Ramanathan et al (1985) also used the term "radiative forcing" in the context of Expression

698 (2.2) and Dickinson and Cicerone (1986) appear to be the first to use the concept to quantify the

699 climate impact of changes in concentrations of several greenhouse gases relative to pre-

700 industrial times in W m^{-2} (using the term "trapping" rather than RF).

701

702 "Radiative forcing" became firmly established as accepted terminology in Chapter 15 of the

703 1985 WMO Ozone Assessment (WMO 1985) (which was largely reproduced in Ramanathan et

704 al. (1987)) and the term was widely used in their discussion; however, much of their overall

705 comparison of the impacts of climate forcing agents was still posed in terms of surface

706 temperature change.

707

708

709
710

711   **2.3 The evolution of the radiative forcing concept during the IPCC era**

712

713   Assessment of RF has been firmly embedded in IPCC assessments from it's First Assessment

714   Report (FAR) onwards. FAR (Shine et al. 1990) took as its starting point the fact that the

715   climate impact of a range of different climate forcing agents could be compared using RF, in W

716   m^{-2}, even though this was only starting to be done routinely in the wider literature at the time. A

717   significant motivator for the use of RF in all IPCC reports was as input to climate emissions

718   metrics (such as the Global Warming Potential, see Section 11). This section focuses mostly on

719   developments in understanding of anthropogenic forcings – more detailed discussions of the

720   evolution of the understanding of solar and volcanic aerosol forcings is given in Sections 8 and

721   9 respectively.

722

723
724

725

2.3.1 The IPCC First Assessment Report 1990 (FAR)

727

728

729 FAR discussed the concept of RF, stressing the utility of including stratospheric

730 temperature adjustment. Building on earlier work (e.g. Ramanathan et al. 1987) it also

731 emphasized the importance of indirect forcings, such as the impact of changes in methane

732 concentrations on ozone and stratospheric water vapor. The main focus was on greenhouse

733 gases, including extended tabulations of forcing due to CFCs and their potential replacements.

734 FAR also popularized the use of simplified expressions for calculating RF, which were

735 empirical fits to more complex model calculations. The expressions used in FAR were based on

736 two studies available at the time (Wigley et al. 1987; Hansen et al. 1988). Updated versions of

737 the simplified expressions are still widely used in simple climate models and for assessing

738 potential future scenarios of trace gas concentrations.

739

740 FAR also included, together in a single section, the roles of solar variability, direct aerosol

741 effects, indirect aerosol effects and changes in surface characteristics. The literature on these

742 was sparse. The section on direct aerosol forcing focused mostly on volcanic aerosol; it did not

743 attempt to quantify the impact of human activity because of "uncertainties in the sign, the

744 affected area and the temporal trend". Perhaps surprisingly more attention was given to the

745 indirect aerosol effects (now more generally known as "aerosol cloud interactions"); although

746 FAR stated that "a confident assessment cannot be made", due to important gaps in

747 understanding, a 1900-1985 estimate of -0.25 to -1.25 W m^{-2} (based on Wigley 1989) was

34

748   provided. FAR did not include estimates for pre-industrial to present-day RF across all forcing

749   agent, but restricted itself to two then-future periods (1990-2000 and 2000-2050).

750

751   Soon after FAR, an IPCC Supplementary Report provided an update (Isaksen et al. IPCC,

752   1992). Significant developments since FAR included more advanced RF estimates due to ozone

753   change (Lacis et al. 1990), and the first calculation of the forcing due to latitudinally-resolved

754   observed stratospheric ozone depletion (Ramaswamy et al., 1992). The indirect forcing due to

755   methane's impact on tropospheric ozone and stratospheric water vapour were quantified. The

756   first geographically-resolved estimates of sulphate aerosol direct forcing (now referred to as

757   aerosol-radiation interaction) (Charlson et al. 1991) had become available, indicating a

758   significant offset (in the global-mean sense) of greenhouse gas RF.

759

760

761

762

2.3.2 IPCC Special Report on Radiative Forcing and the IPCC Second Assessment Report (SAR)

765

The SAR discussion on RF was partly based on the analysis of Shine et al. (1995) in an IPCC

Special Report. Since FAR there had been several important developments. The 1992 Pinatubo

volcanic eruption had allowed unprecedented global-scale observations of the impact of such a

large eruption on the radiation budget (Minnis et al. 1993) and the subsequent climate response

was well predicted (Hansen et al. 1993 updated in Shine et al. 1995); because of the transient

nature of the forcing, this still arguably constitutes the most direct evidence of the linkage

between transient forcing and transient response to date. Understanding of ozone RF continued

to develop as a result of ongoing analyses of observational data and the advent of (then 2-D,

latitude-height) chemistry models allowing improved estimates of the longer-term increases in

tropospheric ozone (e.g. Wang et al., 1993; Hauglustaine et al. (1994)). More sophisticated RF

calculations due to sulphate aerosol-radiation interaction were becoming available (e.g. Kiehl

and Briegleb, 1993; Hansen et al. 1993; Taylor and Penner 1994), as were the first climate

model simulations of aerosol cloud-interaction (Jones et al. 1994). Early attempts to estimate the

direct RF from biomass burning (Penner et al. 1992; Hansen et al. 1993) were presented. Shine

et al. (1994) produced the first of IPCC's many figures of the pre-industrial to present-day

global-mean forcing incorporating both an estimate of the uncertainty range and a subjective

confidence level. Shine et al. (1994) also extended the discussion of the utility of the radiative

forcing concept; the chapter included clear demonstrations of the need to include stratospheric

temperature adjustment to compute ozone forcings, as IRF and RF could differ in sign.

785

786 Climate models were beginning to be used to test the forcing-response relationships for a wide

787 variety of forcings, including the impact of the spatial distribution of forcing; an unpublished

788 study by Hansen et al. (1993b) (a precursor to Hansen et al. (1997)) reported experiments with

789 an idealised GCM that indicated that extratropical forcings had almost double the impact on

790 global mean surface temperature change as the same (in the global-mean sense) tropical forcing;

791 ongoing work (e.g. Taylor and Penner 1994) also clearly demonstrated that while forcing in one

792 hemisphere was felt mostly in that hemisphere, there was still a large non-local response. By the

793 time of the SAR update (Schimel et al. 1996), attention had begun to focus on the (positive)

794 direct forcing due to soot (or black carbon) (Chylek and Wong 1995; Haywood and Shine 1995)

795 (see Section 5 for details), which highlighted the dependence of the computed forcing on

796 whether the aerosol population was internally or externally mixed. More studies of aerosol

797 indirect forcing were emerging (e.g. Boucher and Lohmann, 1995; Chuang et al, 1994) which

798 continued to indicate a significant negative forcing, as well as discussing indirect effects beyond

799 the impact on cloud effective radius. SAR updated the earlier RF figure most notably by

800 splitting the direct effect into its sulphate, biomass burning and soot components, but refrained

801 from giving a central estimate for the aerosol indirect forcing, "because quantitative

802 understanding of this process is so limited".

803

804

37

805

806 **2.3.3 IPCC Third Assessment Report (TAR)**

807

808

809 After four IPCC reports with a focus on RF in the space of just 6 years, TAR's analysis

810 (Ramaswamy et al. 2001) was able to assimilate developments over a much longer period, using

811 a much larger body of literature. This was particularly so for tropospheric ozone and aerosol

812 forcing, as a result of many more chemistry-transport and GCM studies. These included early

813 studies investigating mineral dust and nitrate aerosols. The sophistication and range of studies

814 on aerosol indirect forcing had increased, with much more effort to separate out first (droplet

815 radii) and second indirect (liquid water path) effects. The associated uncertainty in the first

816 indirect effect could not be reduced beyond that given in SAR; no estimate was given for the

817 second indirect effect because it was "difficult to define and quantify" but it was noted that it

818 "could be of similar magnitude compared to the first (indirect) effect". Ramaswamy et al. (2001)

819 also reassessed the simple formulae used by IPCC to compute greenhouse gas RF, which led to

820 a 15% reduction in CO_2 forcing relative to the FAR formula; this and subsequent reports mostly

821 adopted the expressions presented by Myhre et al. (1998).

822
823
824 TAR also included in its RF summary figure, for the first time, the effect of contrails and

825 contrail-induced cirrus, partly based on work presented in the IPCC Special Report on Aviation

826 and the Global Atmosphere (Prather et al. 1999) and the effect of land-use change on surface

827 albedo.

828
829 TAR continued the important discussion on the utility of the RF concept. A larger number of

830 GCM studies, with a more diverse set of forcing mechanisms, were available, leading to the

831 important conclusion that "radiative forcing continues to be a good estimator of global-mean

38

832   surface temperature response, but not to a quantitatively rigorous extent as in the case of …

833   radiative convective models". Most notably, Hansen et al. (1997) had presented a wide-ranging

834   study with a simplified configuration of their climate model which examined the response to

835   both latitudinally and vertically constrained forcings. They showed that forcings confined to

836   specific altitudes could lead to specific cloud or lapse rate responses, and these resulted in

837   marked variations in climate sensitivity for a given forcing. This weakened the perception that

838   the global-mean climate sensitivity for spatially inhomogeneous forcings could be used to

839   determine quantitative aspects of the spatial responses. This important work also presaged later

840   developments in the definition of RF, and appears to be the first explicit usage of the concept of

841   "efficacy" (although it was not given that name) that is discussed in the next subsection.

842

843

844
845 **2.3.4 IPCC Fourth Assessment Report (AR4)**
846
847
848 AR4's assessment of RF (Forster et al. 2007) brought together many important advances in both

849 its concept and utility of and the quantification of a number of new RF mechanisms. Notably, it

850 was the first report to formally combine all anthropogenic forcings via a Monte Carlo

851 simulation; it concluded that the net anthropogenic forcing since 1750 was "extremely likely" to

852 be positive (central estimate of 1.6 W m^{-2}) and that in the period since 1950, the impact of

853 natural forcings was considered "exceptionally unlikely" to have been comparable to the

854 anthropogenic forcings. A central estimate of the first indirect aerosol forcing (which was

855 labelled the "cloud albedo effect") was presented (-0.7 W m^{-2} with "low level of

856 understanding").

857

858 RF from changes in surface albedo due to black carbon on snow and stratospheric water vapor

859 from CH_4 oxidation were now included on the summary figure; it was noted that the total

860 stratospheric water vapor forcing, based on available observations, could be higher than the

861 methane-only component. In addition to the now-standard IPCC forcing diagram based on

862 changes in concentrations (see summary in Fig. 1.2), an emissions-based version (Fig 2.2) was

863 presented – this particularly served to highlight the fact that methane emissions (combining the

864 effect of methane change and the indirect forcings from changes in tropospheric ozone,

865 stratospheric water vapor and CO_2) led to a forcing equivalent to about half that of CO_2. The

866 combined impact of NOx emissions on tropospheric ozone, methane and nitrate aerosols, was

867 found to be negative.

868

40

869   Forster et al. (2007) detailed significant advances in the understanding of the utility of RF. In

870   particular, a number of GCM studies (e.g. Hansen et al. 2005; Shine et al. 2003; Gregory et al.

871   2004) had explored RF definitions which went beyond the then- standard RF with stratospheric

872   temperature adjustment; this framework allowed for rapid tropospheric adjustments (i.e. those

873   that occur independent of surface temperature change, and on timescales of up to a few months)

874   due to changes in clouds, water vapor and lapse rate, to be incorporated in the definition of

875   forcing. These were shown to have greater utility, in that the climate sensitivity showed less

876   dependence on the forcing mechanism. This framework would then lead to the AR5 definition of

877   effective radiative forcing (Section 2.3.5).

878
879   Forster et al. (2007) instead adopted the framework of efficacy, that had been developed in

880   earlier work discussed above, whereby Equation 2.1 is modified to

881

882 $$d\bar{T} \approx E_i \lambda_{CO_2} \, d\bar{F} \qquad\qquad (2.3)$$

883
884
885   where $d\bar{F}$ still represents the (stratospheric-temperature-adjusted) radiative forcing, E_i

886   represents the efficacy of a given climate change mechanism, which is given by the ratio of the

887   climate sensitivity for that mechanism to that for CO_2; formally, since the CO_2 forcing varies

888   slightly with the magnitude of the CO_2 change (e.g. Hansen et al. 2005), a more robust

889   definition should be specific to the size of the CO_2 perturbation.

890

891   The product $E_i d\bar{F}$ was then labelled "effective radiative forcing", a definition that would be

892   elaborated on in AR5 (Section 2.3.5). A significant number of climate modelling papers had, by

893   then, computed efficacies, with varying levels of agreement; this allowed Forster et al. (2007) to

41

894   draw tentative conclusions; for example, the combined efficacy for long-lived greenhouse gas

895   forcing was unity, to within 10%; solar forcing, tropospheric ozone and scattering aerosol

896   forcings had efficacies of 0.7 to 1.0, 0.6 to 1.1, and 0.7 to 1.1 respectively (all with "medium

897   confidence"). There was no consensus on an efficacy for black carbon.

898
899
900
901

902 **2.3.5 IPCC Fifth Assessment Report (AR5)**
903
904
905 In AR5 the effective radiative forcing (ERF) concept was introduced to allow rapid adjustment

906 processes in the troposphere but avoiding changes that are associated with climate feedbacks

907 (and in the conventional framework, mediated by surface temperature change – see Section

908 2.1) (Boucher et al., 2013; Myhre et al., 2013). ERF is defined in Myhre et al. (2013) as

909 "Change in the net top of atmosphere (TOA) downward radiative flux after allowing for

910 atmospheric temperatures, water vapour and clouds to adjust, but with surface temperature or a

911 portion of surface conditions unchanged". Figure 2.3, from AR5, summarizes the progression

912 from instantaneous radiative forcing, through RF and ERF, to climate response. AR5 also

913 retained discussion of RF.

914

915 No new forcing mechanisms were included in AR5, but the confidence level was raised,

916 relative to earlier IPCC assessments for stratospheric water vapor, aerosol-radiation

917 interactions, surface albedo due to land use, contrails, contrail-induced cirrus, solar irradiance

918 changes and volcanic aerosols. The only 'very low' confidence level was given to rapid

919 adjustment of aerosol-cloud interactions (earlier denoted as aerosol indirect effects). See the

920 summary in Fig. 1.2.

921

922 The motivation for introducing the ERF concept was that efficacies (see expression 2.2) for

923 many climate drivers were different to unity when applying RF. This was particularly so for

924 black carbon (Ban-Weiss et al., 2011; Hansen et al., 2005; Ming et al., 2010) and for aerosol-

925 cloud interactions beyond the cloud albedo effect (Twomey effect) (e.g. Lohmann et al., 2010).

926 There was also a growing understanding that rapid adjustments were important for CO_2

43

927   (Andrews and Forster, 2008; Andrews et al., 2012; Doutriaux-Boucher et al., 2009).

928   Furthermore, a clearer distinction between the fast changes (including instantaneous radiative

929   perturbations and the rapid adjustments) and the slow climate feedback processes in terms of

930   their importance for the climate response was elaborated (Andrews et al., 2010; Bala et al.,

931   2010). Importantly, in single model studies, ERF was shown to provide an efficacy much

932   closer to unity than the traditional RF concept (Hansen et al., 2005; Shine et al., 2003). The

933   stratospheric temperature adjustment, which is included in the definition of RF, is also included

934   in ERF. An additional advantage of ERF compared to RF is that a tropopause definition is

935   avoided in the quantification of the forcing (e.g. Shine et al., 2003).

936

937   Two methods have been widely adopted to calculate the ERF. One method (Gregory et al.,

938   2004) regresses TOA net radiative imbalance against surface temperature change in coupled

939   climate model simulations. The extrapolation of that regression line to zero surface temperature

940   change then yields the ERF. The second method computes the TOA net radiative fluxes in

941   fixed sea surface temperature (SST) climate model simulations (Hansen et al., 2005); while it is

942   arguably more consistent to fix both land and surface temperatures (Shine et al. 2003), this is

943   difficult to implement in advanced climate models. Instead Hansen et al. (2005) suggested

944   adjusting the derived ERF to account for the impact of the land-surface temperature change on

945   TOA radiative fluxes.

946

947   The primary advantage of adopting ERF is that it reduces the level of approximation inherent

948   in Expression 2.2 across a wide range of climate forcing mechanisms. Nevertheless, there are

949   several limitations associated with its adoption. To some extent these are reflected in AR5

44

950   where the uncertainties in RF of WMGHGs were quantified as 10%, in agreement with earlier

951   IPCC assessments, whereas AR5 assessed WMGHG ERF to have uncertainties of 20%.

952

953   The necessity of climate model simulations to calculate tropospheric adjustments makes ERF

954   distinct from either IRF (see Section 2.2) or RF in several ways. IRF and RF can be quantified

955   using more sophisticated radiative transfer schemes than are typically available in climate

956   models, and, for example, can be more easily applied to a wider range of greenhouse gases. In

957   addition, the ERF technique is limited to forcing mechanisms that are of a sufficient size for

958   the impact on TOA fluxes to emerge from the noise of the climate model's own internal

959   variability (see Section 2.3.6).

960

961   Since rapid tropospheric adjustment processes are likely to be climate-model dependent this

962   introduces further uncertainties beyond those involved in more traditional forcing definitions.

963   For example, IRF are pure radiative transfer calculations that can be constrained reasonably

964   well with detailed models and a high degree of physical understanding. The stratospheric

965   temperature adjustment that is incorporated in the RF has a well-understood theoretical basis

966   (resulting from the balance between changes in absorption by and emission from the

967   stratosphere). By contrast, tropospheric adjustments are much more complicated. There is less

968   theoretical underpinning with which to constrain these adjustments; this is particularly so for

969   cloud adjustments which result from the complex interplay between different processes that

970   may or may not be well-represented in individual climate models. This complicates the

971   distinction between adjustments and feedbacks that are mediated by surface temperature

972   change and there is no obvious way to quantify the adjustments with observations.

45

973
974
975   One consequence of these shortcomings is a blurring of the lines between forcings and

976   feedbacks. While the tropospheric adjustments are defined to have a shorter time scale than

977   feedbacks, they also generally involve some coupling to the surface; e.g., land warming (in

978   the fixed-SST approach to ERF calculation) or pattern of SST change (in the regression

979   approach). Hence there is a need to further develop techniques that enable a robust

980   separation of adjustment and feedback processes.

981

982   A specific difficulty is that it is increasingly hard to compare different types of forcing.

983   IRF, which involves purely radiative transfer calculations, has generally not been computed

984   in climate model simulations (see section 2.3.6 for future efforts) due to computational

985   considerations; instead, ERF has become the preferred approach to quantifying RF.

986   Attempts to isolate IRF from ERF using radiative kernels have noted that most of the

987   intermodel spread in ERF from CO_2 forcing does not arise from differences in tropospheric

988   adjustments, but rather from differences in IRF (Chung and Soden 2015). Indeed,

989   intermodel differences in the calculation of IRF have been a persistent problem in GCMs

990   (Cess et al. 1993; Soden et al 2018) despite the presence of accurate and observationally

991   verified line-by-line calculations to constrain their counterparts in climate models (Collins

992   et al. 2006).

993

994

2.3.6 Developments since AR5

Marvel et al. (2015) and Shindell (2014) indicate that even for the ERF concept, efficacies (see

Expression 2.3) may be different for short-lived and regionally heterogeneous compounds like

aerosols, ozone, and land use compared to greenhouse gases using various CMIP5 simulations.

This would have implications for estimates of climate sensitivity using temperature changes

over historical period. However, the cause of the findings on the efficacies in CMIP5 is under

debate   (Richardson et al., 2019). The ERF has been further described (Sherwood et al., 2015)

and methods to calculate ERF have been better compared (Forster et al., 2016). Forster et al.

(2016) find that uncertainties in ERF from fixed SST simulations are much lower than using the

regression technique. ERF from the fixed SST simulations can be quantified to an accuracy of

0.1 W m^{-2} at the 5-95% confidence interval in 30-year simulations. This implies that ERF from

very small forcings (<0.1 W m^{-2}) would require many ensembles or very long simulations.

The ERF framework has allowed a clearer understanding of the forcing and climate response of

a climate driver; it is now constructive to distinguish into "instantaneous", "rapid adjustment",

and "equilibrium". Figure 2.4 shows how radiative fluxes and surface sensible and latent heat

fluxes change for a doubling of CO_2 in multi-model simulations and is a modern version of

Figure 2.1, explicitly using the ERF concept. The instantaneous radiative forcing due to CO_2 is

well known to be primarily due to the longwave (LW), with a weak solar (shortwave (SW))

effect (Fig 2.4 left) shown as the positive values at TOA. Positive values at the surface in Fig

2.4 indicate that the surface gains energy. If the difference between the flux changes at TOA

and surface is positive, it means the atmosphere gains energy. The SW absorption by CO_2

47

1019   reduces the solar absorption at the surface and causes a weak change at the TOA where it is

1020   very small compared to LW TOA.

1021

1022   By contrast, the SW contribution to atmospheric absorption is 35-40% of the LW trapping of

1023   energy in the atmosphere. The instantaneous part involves only the initial radiative perturbation.

1024   The rapid adjustments (Figure 2.4 middle) are processes that occur to equilibrate the atmosphere

1025   with no SST changes. A doubling of CO_2 gives an initial heating of the troposphere and a

1026   cooling of the stratosphere. The cooling of the stratosphere is well known (see Section 2.2) and

1027   the consequent adjustment in the radiative fluxes was included in the early applications of the

1028   RF concept. The initial radiative perturbation in the troposphere increases temperature and

1029   water vapor, and changes clouds. The increase in tropospheric temperature reduces the net

1030   atmospheric absorption (giving a radiative cooling) but the reduction in stratospheric

1031   temperature has a larger impact on the net atmospheric absorption. The overall rapid

1032   adjustments of temperature, water vapor and clouds lead to an enhanced atmospheric absorption

1033   of similar size to the initial heating (Myhre et al., 2018). The atmospheric equilibrium is

1034   achieved by reduction in the surface latent and sensible heat fluxes, thereby making a clear link

1035   between the atmospheric absorption and precipitation changes, at the global-mean level (e.g.

1036   Andrews et al., 2010). The fast response of global-mean precipitation can be estimated, to

1037   reasonable accuracy, from the atmospheric component of the ERF (e.g. Samset et al. 2016).

1038

1039   In the full climate response to doubling of CO_2 (Fig 2.4 right), the surface temperature changes

1040   to bring TOA and the atmosphere net fluxes into equilibrium (see section 2.1). Note that the

1041   initial atmospheric radiative heating (which leads to a precipitation decrease) when ERF is

48

1042   diagnosed, turns into a radiative cooling, when the full surface temperature response is allowed.

1043   Since AR5 there has been an improved quantification of the rapid adjustment processes and

1044   their inter-model diversity. Double radiation calls (Ghan, 2013) and radiative kernels (Soden et

1045   al., 2008) allow a differentiation of the instantaneous radiative perturbation and the rapid

1046   adjustment and individual rapid adjustment terms, respectively.

1047

1048   Smith et al. (2018) quantify the rapid adjustment contributions to ERF based on radiative

1049   kernels in multi-model simulations for various climate drivers. Figure 2.5 shows the rapid

1050   adjustment terms for two scenarios: a doubling of CO2, and a tenfold increase in the black

1051   carbon (BC) abundance. In fact, the IRF at TOA for a doubling of CO2 and tenfold increase in

1052   BC is very similar (Smith et al., 2018), but their total rapid adjustment (the bars on the yellow

1053   background in Fig 2.5) is strong and of opposite signs. Temperature increases enhance the

1054   outgoing longwave radiation and are thus a negative rapid adjustment, which can be seen both

1055   for land surface and tropospheric temperature for increase in CO2 and BC.

1056

1057   The stratospheric cooling due to the CO_2 increase, on the other hand, gives a positive rapid

1058   adjustment. Increases in the tropospheric temperature increase water vapor, thus a positive rapid

1059   adjustment by increasing the greenhouse effect. For a doubling in CO_2, the high cloud cover

1060   increases with a reduction in the lower clouds, but these features are opposite for BC explaining

1061   the different sign of rapid adjustment of clouds for these two climate drivers. For CO_2 the rapid

1062   adjustments other than the stratospheric temperature adjustment happen to cancel each other

1063   out, making ERF and RF quite similar in that case. Based on available estimates for doubling of

1064 CO_2 this was already noted in AR5.

49

1065

1066   The total rapid adjustment for BC is strongly negative; nevertheless, individual rapid

1067   adjustments vary in sign, so that the net effect is a residual of these competing effects. Soden et

1068   al. (2018) indicate that the large diversity in ERF due to change in CO_2 among GCMs arise from

1069   differences in the instantaneous forcing. Results from Smith et al. (2018) support this by having

1070   a range of less than 10% (5-95% confidence interval) of the non-stratospheric temperature rapid

1071   adjustments. Combining the uncertainty in the tropospheric rapid adjustment with 10%

1072   uncertainty in RF derived from detailed off-line radiation schemes as given in AR5 provides an

1073   uncertainty in ERF of 14%. Section 10 describes the implication of a reduced uncertainty range

1074   of WMGHG forcing compared to that given in IPCC AR5 (20%) for the uncertainty in the total

1075   anthropogenic ERF.

1076

1077
1078

2.4 Summary and challenges

A future challenge with respect to the forcing concept is to quantify whether the efficacy is

unity when adopting the current definition of ERF for all drivers of climate change and various

models, and thus to understand the diversity among some previous results (Shine et al., 2003;

Hansen et al., 2005; Shindell 2014; Marvel et al., 2015; Richardson et al., 2019).

Further there is a need to better understand the rapid adjustment processes in climate models,

both the degree of influence of diversity in IRF as indicated in Smith et al. (2018), but also

dedicated process studies comparing GCMs with high resolution models with weaker degrees of

parametrization, such as convection permitting models. There is a high potential for progress to

be made using results from the ongoing CMIP6 model intercomparison project, which is

supporting IPCC AR6 (Eyring et al., 2016); efforts have been made to ensure that more

diagnostics are available to enable the drivers of ERF to be better quantified and hence for inter-

model diversity to be better characterized. Such studies will aid the understanding of whether

uncertainties in ERF of CO_2 and other greenhouse gases are substantially larger than using RF,

as was indicated in Myhre et al. (2013).

Lastly, there is a need to develop methodologies to compare weak radiative perturbations,

which will continue to need to be quantified using RF, with the major climate drivers which are

increasingly being quantified from various model simulations using the ERF concept. It is

possible that once the generic understanding of the rapid adjustments has improved, it can be

applied to the weak forcings and enable ERF to be estimated from their RFs.

1104
1105
1106
1107
1108
1109
1110
1111
1112
1113
1114
1115
1116
1117
1118
1119
1120
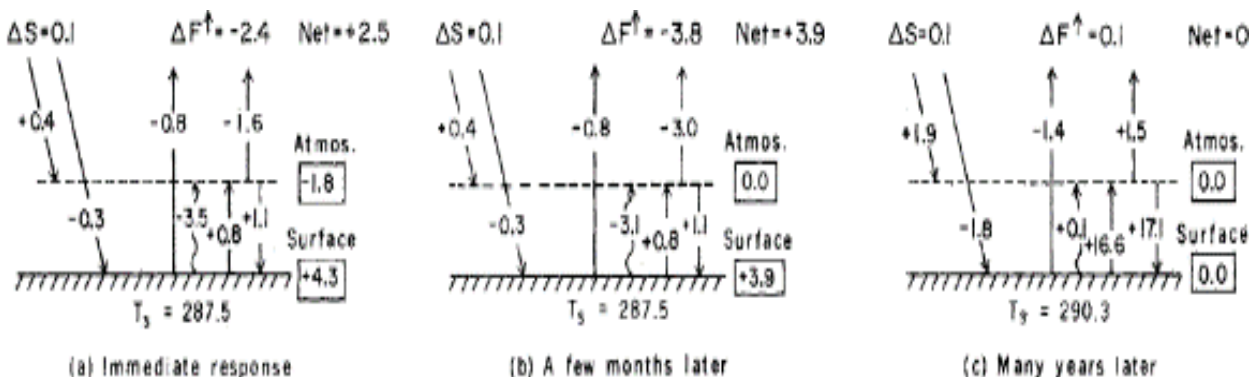
Fig. 4. Change of fluxes (watts per square meter) in the 1-D RC model when atmospheric CO_2 is doubled (from 300 to 600 ppm). Symbols: ΔS, change in solar radiation absorbed by the atmosphere and surface; $\Delta F\uparrow$, change in outward thermal radiation at top of the atmosphere. The wavy line represents convective flux; other fluxes are radiative.

1121

1122 **Figure 2.1**: Changes in top-of-atmosphere shortwave (ΔS) and longwave ($\Delta F^{\uparrow}$) irradiances

1123 following a doubling of CO_2 from 300 ppm, in a one-dimensional radiative-convective model.

1124 Wavy lines represent changes in convective fluxes, with all other lines radiative. The values in

1125 boxes show the net flux changes at the surface and for the atmosphere. (a) the instantaneous

1126 flux change, (b) the change after a few months and includes the effect of stratospheric

1127 temperature adjustment and other rapid adjustments represented in the model and (c) the flux

1128 changes when the system has come to equilibrium following a change in surface temperature

1129 (T_S). Figure taken from Hansen et al. (1981).
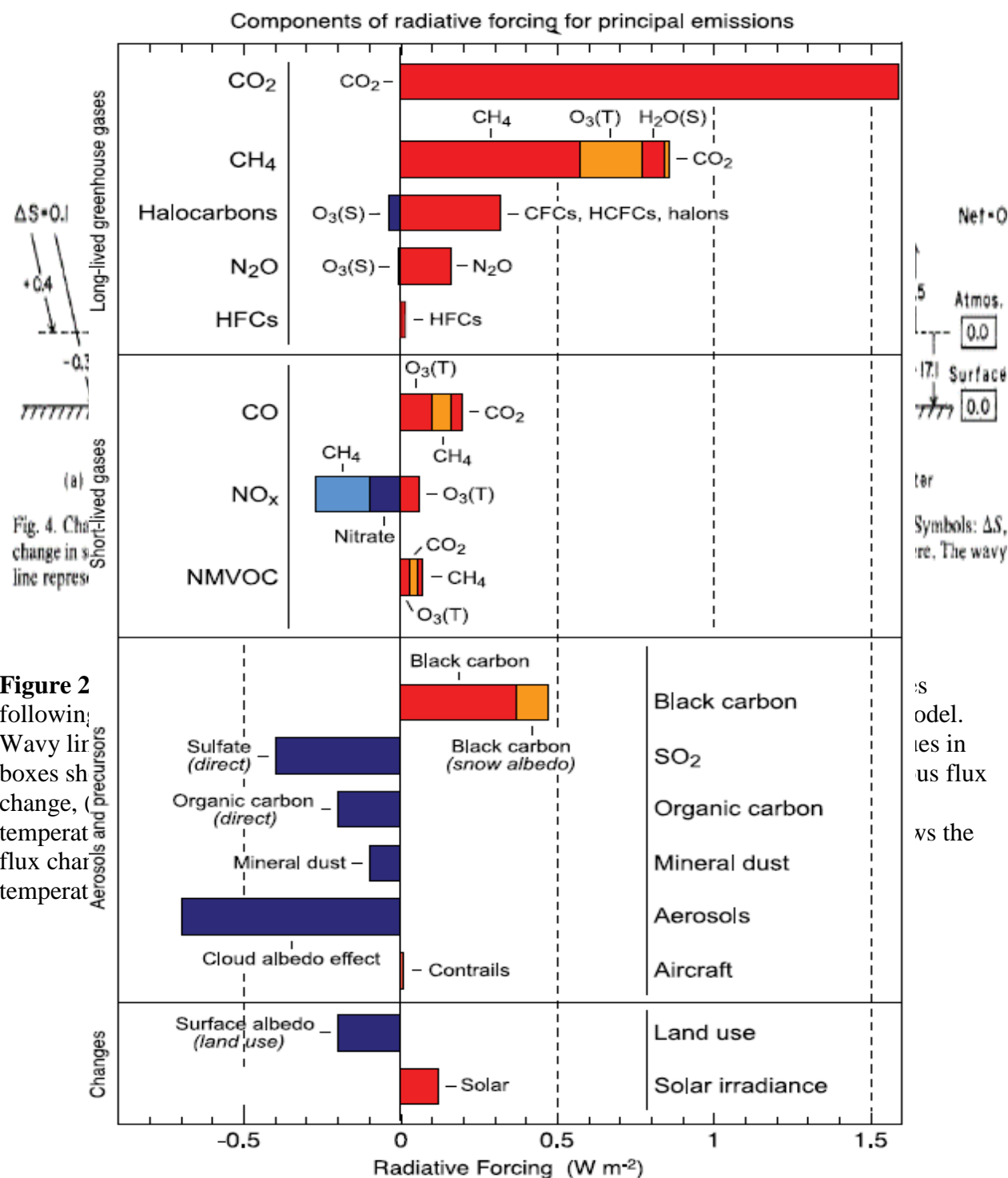
1130

1131

1132

Components of radiative forcing for principal emissions

Figure 2.21. Components of RF for emissions of principal gases, aerosols and aerosol precursors and other changes. Values represent RF in 2005 due to emissions and changes since 1750. (S) and (T) next to gas species represent stratospheric and tropospheric changes, respectively. The uncertainties are given in the footnotes to Table 2.13. Quantitative values are displayed in Table 2.13.

53

1160   **Figure 2.2**

1161

1162

1163   Components of RF by emissions of gases, aerosols, or their precursors for the period 1750-

1164   2005. $O_3(T)$ and $O_3(S)$ indicate tropospheric and stratospheric ozone respectively. Figure from
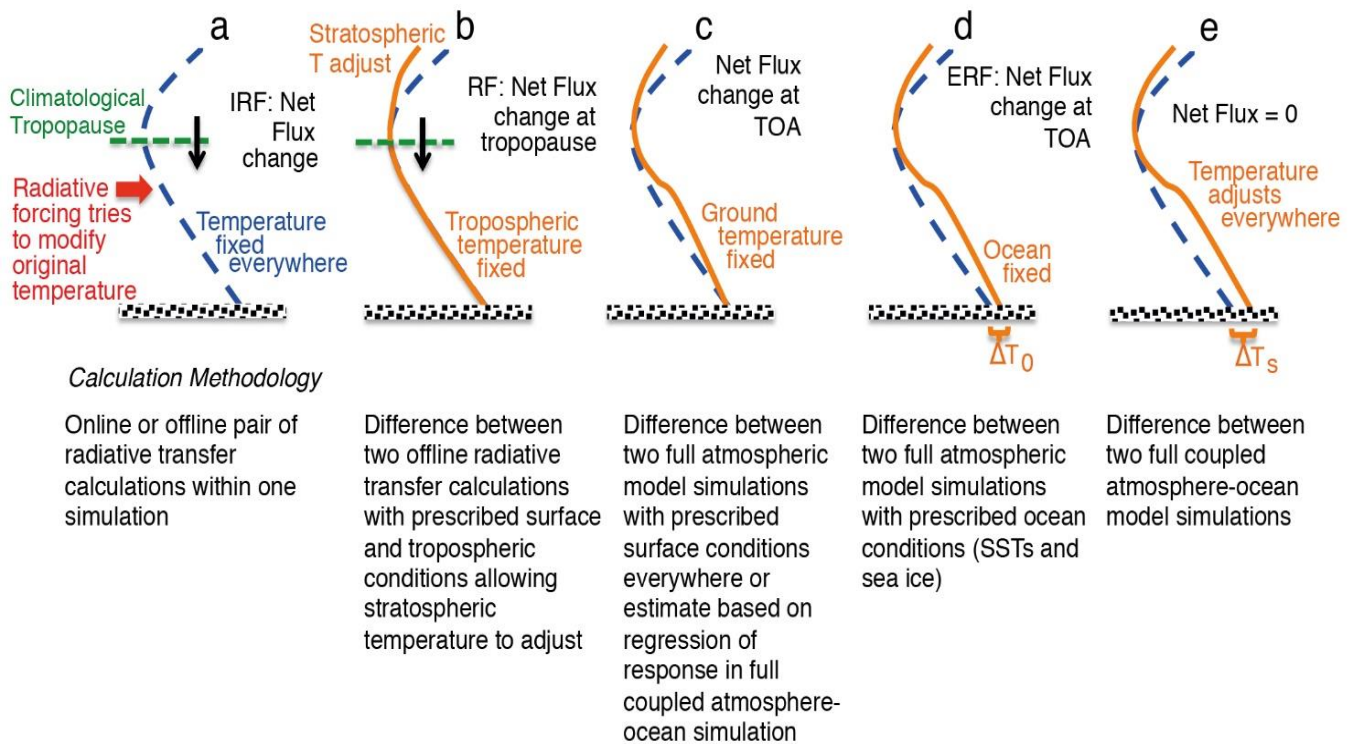
1165   Forster et al. (2007).

1166

1167   [Jpeg can be obtained from

1168   https://archive.ipcc.ch/report/graphics/images/Assessment%20Reports/AR4%20-%2

1169   WG1/Chapter%2002/fig-2-21.jpg].

1170
1171
1172
1173

Figure 2.3 Schematic comparing (a) instantaneous RF, (b) RF, which allows stratospheric temperature to adjust, (c) flux change when the surface temperature is fixed over the whole Earth (a method of calculating ERF), (d) the ERF calculated allowing atmospheric and land temperature to adjust while ocean conditions are fixed and (e) equilibrium response. (Figure taken from Myhre et al. 2013).

1174
1175

1176
1177 JPEG can be obtained from:

1178 https://archive.ipcc.ch/report/graphics/images/Assessment%20Reports/AR5%20-

1179 %20WG1/Chapter%2008/Fig8-01.jpg

1180
1181 **Figure 2.3** Schematic comparing (a) instantaneous RF, (b) RF, which allows stratospheric

1182 temperature to adjust, (c) flux change when the surface temperature is fixed over the whole

1183 Earth (a method of calculating ERF), (d) the ERF calculated allowing atmospheric and land

1184 temperature to adjust while ocean conditions are fixed and (e) equilibrium response. (Figure

1185 taken from Myhre et al. 2013).

1186
1187
1188

1189

1190
1191
1192
1193
1194 **Figure 2.4:** Illustration of the change in the global energy balance (top of the

1195 atmosphere -TOA, atmosphere - Atmos., and surface) from a doubling of the CO_2

1196 concentration for an instantaneous perturbation, instantaneous and rapid adjustment,

1197 and the climate system in new equilibrium. Changes in the energy fluxes of solar

1198 radiation (SW) is given in yellow bars, longwave (LW) in red bars, latent heat (LH) in

1199 blue bars and sensible heat (SH) in green bars. The net flux changes at TOA, Atmos.,

1200 and surface are given in numerical values in boxes. This figure can be considered as a

1201 modern day-version of Figure 2.1.

1202

1203

Figure 2.5: Instantaneous radiative forcing (IRF), individual and total rapid adjustments, and
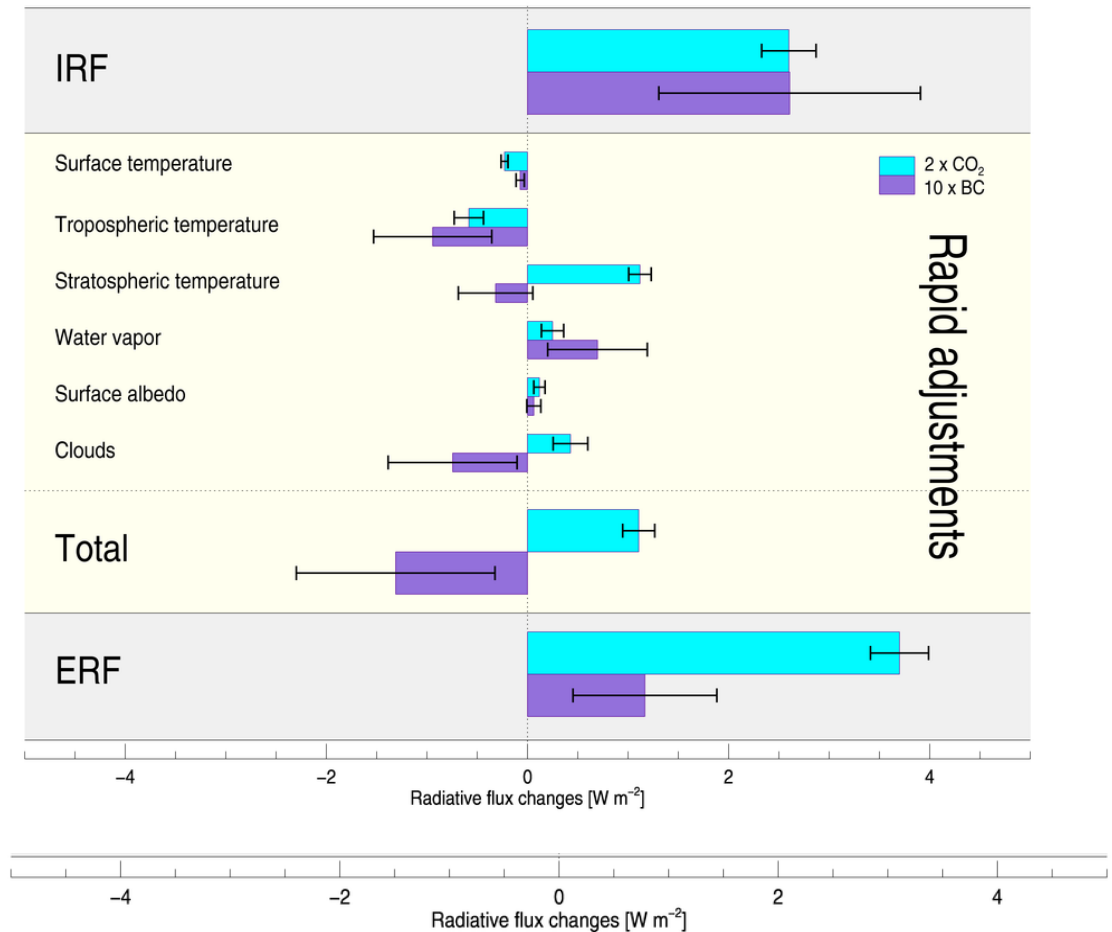
1206   effective radiative forcing (ERF) at the top of the atmosphere for a doubling of CO_2 and a

1207   tenfold increase in the BC concentration. The total rapid adjustment is the sum of the individual

1208   terms of surface temperature change (only land), tropospheric temperature, stratospheric

1209   temperature, water vapor, surface albedo change, and clouds. The uncertainties are one standard

1210   deviation among the PDRMIP models. It is a coincidence that the IRF for CO_2 and BC is almost

1211   identical. The figure is modified from Smith et al. (2018).

1212

57

Section 3: CO$_2$ and other well-mixed greenhouse gases

Accurate computation of the radiative forcing by CO$_2$ and other gaseous constituents of the

Earth's atmosphere only became possible with the advent of accurate spectroscopic

measurements in the laboratory. While these measurements still serve as the primary

foundation for calculations of the greenhouse effect, for some simple molecules the

combination of quantum and statistical mechanics provides a complementary framework for

interpreting the observations and extending them to conditions that have not been directly

observed. The inputs to this framework are the energies, numbers (degeneracies), and

occupation numbers of excited states of each constituent, the transitions among these

excited states, and the interactions of these transitions with light and heat following

Einstein's quantum theory of radiation. One of the first attempts to compute the effects of

doubling CO$_2$ in an atmosphere in radiative-convective equilibrium produced a remarkably

good estimate of 4 K (Hulburt, 1931). However, this finding and other supporting evidence

was largely unappreciated due to prevailing assumptions prevalent that the strong broadband

absorption of water vapor would dominate the regions of the spectrum where CO$_2$ is

radiatively active and that the logarithmic curve of growth of CO$_2$ radiative effects in these

regions would further constrain the impact of rising CO$_2$ on the climate system.

Parameterizations of the rudimentary laboratory measurements of CO$_2$ with ambient and

prescribed amounts of water vapor accumulated by the mid-20$^{\text{th}}$ century contradicted the

assumption that water vapor would saturate the primary CO$_2$ bands (Callendar, 1941), but

did little to change the balance of opinions held by the scientific community. Further, more

58

1238   detailed information on the bands of CO_2 based on its structure and more accurate

1239   spectrometers revealed the potential for additional absorption of terrestrial radiation at the

1240   edges of these bands and in the upper atmosphere, where the overlap among neighboring

1241   absorption lines is greatly reduced (Martin & Barker, 1932).

1242
1243
1244   Further progress had to await the need for operational weather forecasting and active and

1245   passive remote sensing during and after the Second World War together with the subsequent

1246   military investments in computing infrastructure, spectroscopic characterization of the

1247   Earth's atmosphere, and the theory of radiative transfer (see historical description by Weart,

1248   1997). One of the first applications of the new digital computers to atmospheric science

1249   revealed that the absorption by CO_2 of upwelling terrestrial radiation in the stratosphere had

1250   been systematically underestimated in prior studies based on manual calculations (Kaplan,

1251   1952). Subsequent computational solutions to the infrared radiative transfer for the whole

1252   atmosphere (Plass, 1956, 1956bb) revealed that the forcing by doubling CO_2 is sufficient to

1253   change the mean surface temperature of the Earth by about 3.6 K (Plass, 1956, 1956aa).

1254
1255
1256   In the 1960s, general circulation models of the atmosphere were developed that included

1257   reasonably complete parameterizations of solar and infrared radiative transfer together with

1258   detailed treatments of the radiative properties of the Earth's atmosphere and surface.

1259   Pioneering calculations with one-dimensional (Manabe & Wetherald, 1967) and three-

1260   dimensional (Manabe & Wetherald, 1975) models demonstrated the effects of CO_2 on the full

1261   climate system and suggested that the surface temperature would increase by approximately

1262   2.5 to 3 K for a doubling of carbon dioxide concentrations (Fig. 3.1). These models and other,

59

1263   simper energy balance models (Ramanathan et al., 1979) formed the basis for one of the first

1264   comprehensive reviews of the state of climate change science for policy makers, the pivotal

1265   Charney Report (National Research Council, 1979).

1266

1267   Due to rapid increases in computing power, much more exact treatments of radiative transfer

1268   known as line-by-line (LBL) codes were developed starting in the 1970s. Early examples

1269   include the Fast Atmospheric Signature Code (Smith et al., 1978), a rapid method for

1270   computing the Voigt line shape profile that includes line broadening and Doppler shifting

1271   (Drayson, 1976) , and the Automated Atmospheric Absorption Atlas (Scott and Chedin 1981).

1272   These codes are based upon comprehensive tabulations of all known absorption lines for over

1273   fifty radiatively active gaseous species in the Earth's atmosphere. An early example that has

1274   grown significantly and is in widespread usage is the high-resolution transmission molecular

1275   absorption (HITRAN) database, which was first developed by the Air Force Cambridge

1276   Research Laboratories (McClatchey et al., 1973) and subsequently maintained and updated by

1277   the Harvard Smithsonian Center for Astrophysics; the most recent version is HITRAN2016

1278   (Gordon et al. 2017). A parallel European-led line database called GEISA (Gestion et Etude des

1279   Informations Spectroscopiques Atmosphériques) was launched in 1974 at the Laboratoire de

1280   Météorologie Dynamique (LMD) in France (Chédin et al, 1982; Husson et al, 1992) has been

1281   updated most recently in 2015 (Jacquinet-Husson et al, 2016). These LBL codes now serve as

1282   the reference radiative transfer codes for calculation of CO_2 forcing and its representation in

1283   Earth System Models (e.g., Collins et al., 2006).

1284

1285

1286

1287   While most climate models compute radiative transfer using full codes, in many applications

1288   simple formula, based on more detailed calculations, are useful for computing the global

1289   annual- mean greenhouse gas radiative forcing from changes in their concentration; such

1290   formulae appear in the First Assessment Report of the Intergovernmental Panel on Climate

1291   Change (IPCC; Shine, Derwent, Wuebbles, & J-J. Morcrette, 1990) and have been utilized and

1292   updated in subsequent IPCC Assessment Reports. For CO_2, to leading order, the forcing in the

1293   infrared is proportional to the logarithm of the concentration (Goody & Yung, 1989;

1294   Pierrehumbert, 2011), and in the Third Assessment Report (Ramaswamy et al. 2001) the IPCC

1295   formula was augmented to include absorption of solar radiation by CO_2 (Myhre et al., 1998).

1296

1297   One of the lingering uncertainties in the radiative forcing by CO_2 is due to remaining

1298   uncertainties in its spectroscopic characterization. If we assume that the energies associated

1299   with the most important excited states of the CO_2 molecule are known precisely, then three

1300   principal spectroscopic properties of CO_2 involved in computing its radiative forcing are its

1301   line strengths, line half widths, and line shapes, in addition to line overlaps with other

1302   absorbers. Systematic propagation of these uncertainties through to the radiative forcing

1303   from doubling CO_2 concentrations suggeststhat the combined effects of residual errors in

1304   these properties are less than approximately 0.7%; this suggests that current LBL models are

1305   more than sufficient for accurately computing the climate forcing from this WMGHG

1306   (Mlynczak et al., 2016).

1307

3.1 CH₄, N₂O, CFCs and halogenated compounds:

Since the atmospheric concentrations of CH4 are two orders of magnitude lower than those

of CO2, it was historically difficult to detect through chemical sampling. Methane was first

detected under ambient conditions in the 1940s using purely spectroscopic techniques

(Migeotte, 1948). In turn, the atmospheric concentrations of N2O, the third most important

anthropogenic greenhouse gas, are three orders of magnitude lower than those for CO2. The

common assumption was that these trace species were present at insufficient levels to have

an appreciable impact on the climate system.

As a result, the importance of the radiative forcings by long-lived greenhouse gases other

than CO2 went largely unappreciated. Wang et al. (1976) and Donner and Ramanathan

(1980) were amongst the first to compute the impact of increasing concentrations of methane

and nitrous oxide and show that the effect could be substantial. Wang et al (1976) computed

the effects of doubling the concentrations of CH4, N2O (as well a NH3 and HNO3) as a

simple proof-of-principle test of anthropogenic perturbations to the concentrations of these

compounds.

They found that the combined effects of doubling concentrations of CH4 and N2O also

approached 1K once the climate system had re-equilibrated to the elevated concentrations

and forcing. To advance beyond these simpler tests required modeling the joint interactions

between the physical climate system and the radiatively active species together with the

associated networks of chemical sources and sinks for these species More advanced models

that include these interactions can treat the nonlinear effects of spectral overlap among the

1333   well-mixed greenhouse gases, ozone, and water vapor. Ramanathan (1980) constructed a

1334   prototype of this class of coupled chemistry-climate model and showed that the non-CO2

1335   WMGHGs could contribute nearly half the warming projected for 2025 assuming persistence

1336   of extant emissions trends. This conclusion was buttressed in subsequent studies starting with

1337   Ramanathan et al (1985) who concluded that the minor well-mixed greenhouse gases could

1338   contribute as much warming as projected increases in CO2 concentrations. Indirect effects of

1339   CH4 and N2O were also uncovered in this time frame and are discussed in greater detail in

1340   Section 4.1.

1341

1342   Because chlorofluorocarbons (CFCs) have strong bands in the mid-infrared window, a region

1343   of the spectrum otherwise largely transparent to terrestrial infrared radiation, increasing

1344   concentrations of these gases leads to rapid increases in the Earth's greenhouse effect (Fig.

1345   3.2). Lovelock et al. (1973), after discovering the ubiquity of CFCs in the Earth's

1346   atmosphere, suggested that it might serve as a greenhouse gas. The implications of

1347   unchecked historical emissions of these gases (prior to the imposition of the Montreal

1348   Protocols in 1987) and the consequent increase in the total greenhouse effect for the mean

1349   surface temperature were first calculated by Ramanathan (1975). He found that continuing

1350   emissions unabated until the year 2000 would ultimately lead to increases in surface

1351   temperature approaching 1 K. Unlike CO2, the major absorption bands of the CFCs are far

1352   from saturated, and therefore the forcing increases linearly and rapidly with increasing

1353   concentration.

1354

1355 Ramanathan et al (1985 investigated a larger set of compounds, including several CFCs, one

1356 HCFC and some fully fluorinated compounds (Fig 3.3). Fisher et al. (1990) expanded the

1357 number of halocarbons having a greenhouse effect by providing radiative forcing for a large

1358 group of CFC replacements including HCFCs and HFCs. Some of the halocarbons have

1359 major absorption bands outside the The mid-infrared window and thus have strong overlap

1360 with water vapor and even some with CH4 and N2O (Ramanathan et al., 1985). Pinnock et

1361 al. (1995) illustrated how the radiative forcing varies over the infrared spectral region for an

1362 increase in 1 ppb of an idealized halocarbon absorbing equally at all wavelengths (Fig. 3.4).

1363 The figure shows that halocarbons absorbing particularly in the region 800-1000 cm^{-1} are

1364 very efficient compared to e.g. compounds like CF4 with strong absorption band located

1365 closer to 1300 cm^{-1}.

1366

1367 Due to the weak absorption by the halocarbons and weak overlap by other gases in the mid-

1368 infrared window region Dickinson et al. (1978) showed that these compounds warm the

1369 lower stratosphere. This is unlike CO2 and most halocarbons therefore have a positive

1370 contribution to radiative forcing from the stratospheric adjustment rather than the negative

1371 contribution from CO2 (see section 2). The state of knowledge of radiative forcing per unit

1372 concentration change for halocarbons is discussed in section 11.3 on Radiative Efficiency.

1373 While much of the work to date had stressed the climatic effects of the infrared bands of

1374 these minor well-mixed gases, the fact that the shortwave bands also contribute non-

1375 negligible forcing was first highlighted by Collins et al. (2006).

1376

1377   Their study showed that all of the atmosphere-ocean global climate models participating in

1378   the Fourth Assessment Report of the IPCC omitted the shortwave effects of CH4 and N2O.

1379   This omission was starting to be corrected by the time of the Fifth Assessment, and these

1380   effects have now been incorporated into the simple bulk formulas for forcing by these

1381   greenhouse gases (Collins et al.,, 2018; Etminan et al., 2016). The simple formula in Etminan

1382   et al. (2016) includes in addition to direct shortwave effect the shortwave contribution due to

1383   stratospheric temperature adjustment and updated water vapor overlap with methane,

1384   resulting in a 25% enhancement in the radiative forcing of methane

1385

1386

1387
1388

3.2 Summary and Challenges

1389
1390
1391

1392 While current LBL models are more than sufficient for accurately computing the climate

1393 forcing from WMGHG (Mlynczak et al., 2016), unfortunately this accuracy has not been

1394 propagated to the radiation codes used in the ensemble of climate models used for climate

1395 projections. The first systematic quantifications of the spread in CO_2 radiative forcing were

1396 conducted using the generation of models used in the first IPCC assessment (Cess et al., 1993;

1397 Ellingson & Fouquart, 1991; Fels et al. 1991), followed by evaluations of modeled forcings

1398 used in the fourth (W. D. Collins et al., 2006) and fifth (Soden, Collins, & Feldman, 2018)

1399 IPCC assessments.

1400
1401
1402 The 1-sigma relative range in the TOA forcings for the latter two studies is 20%, approximately

1403 1.5 decades larger than the LBL uncertainty (Fig. 3.5). This has significant implications for the

1404 interpretation of historical climate change simulations. Reduction and ideally elimination of this

1405 large range in CO_2 radiative forcing remains an ongoing challenge for the climate modeling

1406 community, with efforts continuing under the WCRP/CMIP6 Radiative Forcing Model

1407 Intercomparison Project (RFMIP) (Pincus et al., 2016). Better agreement of ESM radiative

1408 parameterizations with LBL models is both feasible and highly desirable. It would help ensure

1409 more accurate interpretations of the historical climate record and more actionable projections of

1410 future climate and climate-change mitigation scenarios.

1411

1412

1413

Figure 3.1: Vertical distributions of temperature in radiativeconvective equilibrium for various values of CO2 content. (Manabe and Wetherald, 1967).
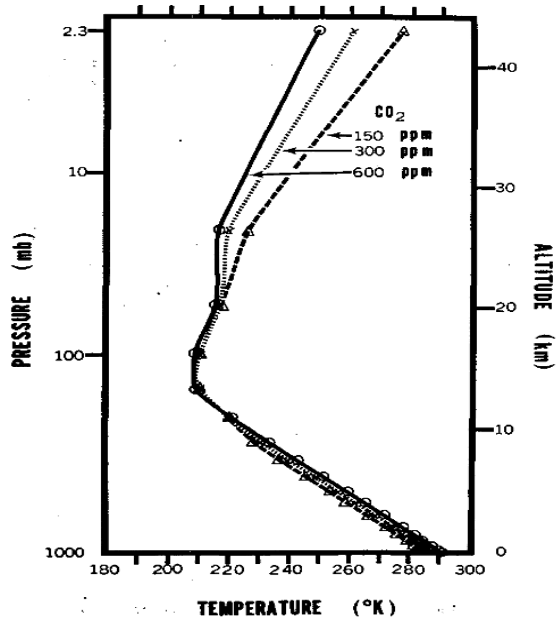
FIG. 16. Vertical distributions of temperature in radiative convective equilibrium for various values of CO_2 content.

1418
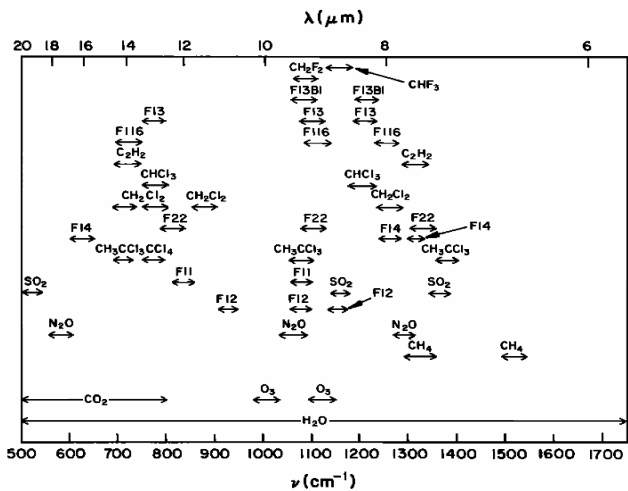
Fig. 3. Spectral locations of the absorption features of various trace gases. The spectral region between 7 and 13 μm is referred to as the atmospheric "window." The anthropogenic trace gases have the potentials for making it into a "dirty window." This figure was provided by J. T. Kiehl (private communication, 1986).

1419

67

Figure 3.2: Spectral locations of the absorption features of various trace gases. The spectral region between 7 and 13 *μm* is referred to as the atmospheric "window" because of its relative transparency compared to neighbouring spectral regions. The anthropogenic trace gases have the potentials for making it into a "dirtier window." (Ramanathan et al, 1987).

1420
1421
1422
1423
1424
1425
1426
1427
1428
1429
1430
1431
1432
1433
1434
1435
1436
1437
1438
1439
1440
1441
1442
1443
1444
1445
1446
1447

RAMANATHAN ET AL.: TRACE GAS CLIMATE EFFECTS

SENSITIVITY TO UNIFORM INCREASE IN MIXING RATIO
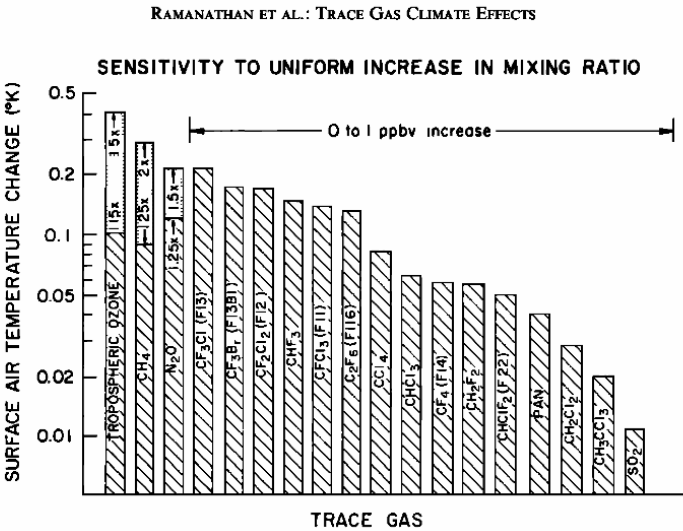
Fig. 1. Surface temperature increase due to a 0–1 ppbv increase in trace gas concentration. Tropospheric O_3, CH_4, and N_2O increases are also shown for comparison.

1448   **Figure 3.3**: Surface temperature increase due to a 0-1 ppbv increase in

1449   trace gas concentration. Tropospheric O3, CH4, and N2O increases are also

1450   shown for comparison (Ramanathan et al, 1985).

1451
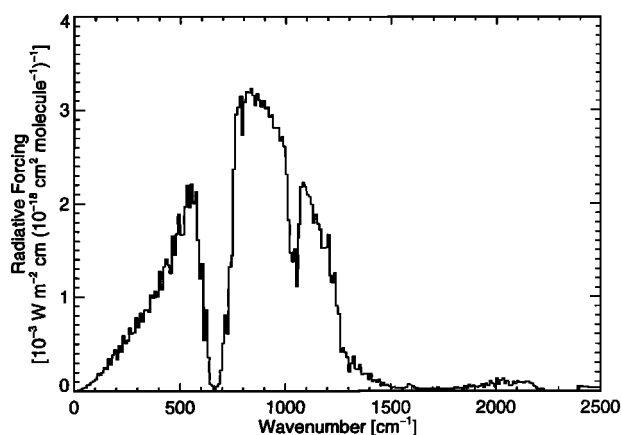
Figure 3. Radiative forcing per unit cross section for the GAM atmosphere including clouds, for a 0–1 ppbv increase in mixing ratio. This graph is repeated in tabular form in the Table 8.

1452

1453   **Figure 3.4**: Radiative forcing per unit cross section for a 0-1 pp by increase

1454   in mixing ratio of a gray-body absorber (Pinnock et al, 1995).

1455
1456

69

Reducing the uncertainty
Radiative forcing uncertainty in GCMs has remained high over the past 25 years. LBL calculations show that this uncertainty can be substantially reduced.

Legend:
- 200 mbar (~12 km above ground level)
- TOA (top of the atmosphere)
- GCM results
- LBL results

y-axis: $2 \times CO_2$ radiative forcing (W/m²)

x-axis: Cess *et al.* (2) 1993 | Collins *et al.* (3) 2006 | Chung & Soden (6) 2015
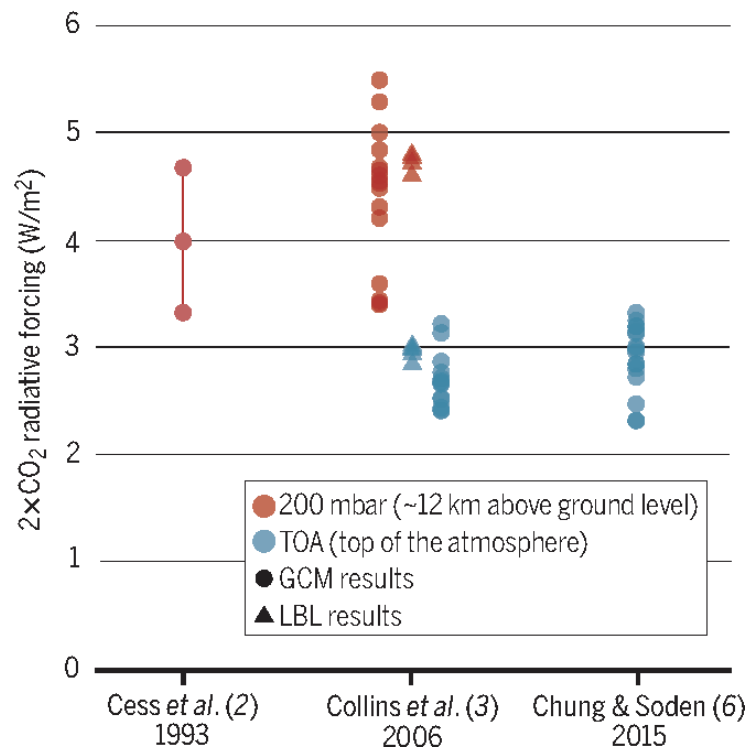
Figure 3.5: Estimates of radiative forcing from doubling CO_2 from three multi-model intercomparisons spanning 1993 to 2015, at the top of the atmosphere and a pseudo-tropopause at 200 mb (Soden et al., 2018).

70

1465
1466

1467 **Section 4: Short-lived trace gases and chemistry-climate interactions**
1468

1469

1470 The importance of atmospheric chemistry for climate began to be recognized after a

1471 multitude of advances in the early 1970s revealed a chemically active atmosphere that

1472 could be perturbed both by natural and anthropogenic activities (National Research

1473 Council, 1984). The foundation for these advances was laid over the preceding four to five

1474 decades. This included the knowledge of stratospheric ozone photochemistry (Chapman

1475 1930; Hampson 1965; Bates and Nicolet 1950), urban photochemical air pollution

1476 (Haagen-Smit 1952; Altshuller and Bufalini 1965) and tropospheric composition and

1477 photochemistry (Cadle and Allen 1970; Bates and Witherspoon (1952). Developments

1478 were also dependent on quantitative but (initially) highly uncertain estimates of

1479 atmospheric amounts of several trace gases including ozone (in the stratosphere only),

1480 nitrogen, oxygen, noble gases, CO_2, H_2O, CH_4 and N_2O (below the tropopause) (see

1481 section 1 for more details). We review below developments in atmospheric chemistry that

1482 set the stage for the recognition of chemistry as an integral part of the climate system and

1483 process- level advances made thereafter that have shaped our knowledge of radiative

1484 forcing from short- lived trace gases and chemistry-climate interactions.

1485
1486
1487
1488

Section 4.1 Atmospheric Chemistry and Climate Connections in 1970s-1980s

The importance of chemistry for the radiative forcing of climate change was recognized by studies in the early 1960s that highlighted the important role of ozone in maintaining stratospheric temperature and the tropopause (Manabe and Möller 1961; Manabe and Strickler 1964). The seminal work of Manabe and Wetherald (1967) demonstrated that stratospheric ozone is not only important for maintaining stratospheric temperature but also influences tropospheric and surface temperature though the effect is small compared to that of CO_2.

A series of new developments in atmospheric chemistry through the 1970s and 1980s established the close links between stratospheric and tropospheric composition and chemistry and how human activities can perturb these linkages with consequences for climate change. The first of these developments was the discovery of human influence on stratospheric ozone through catalytic ozone destruction via nitrogen oxide (NO_x) (Crutzen 1970). Studies showed that increases in NO_x due to human activities leading to enhanced fossil fuel combustion (such as from a planned fleet of high-altitude supersonic transport planes) (Johnston 1971; Crutzen 1972a; McElroy et al. 1974) or changes in its primary source gas, N_2O (McElroy et al. 1977; Wang and Sze 1980) could cause significant stratospheric ozone loss in the future with consequences for climate (Ramanathan et al. 1976).

1511   Around the same time, Molina and Rowland (1974) identified the role of

1512   chlorofluorocarbons (CFCs) as a major source of chlorine responsible for catalytic ozone

1513   destruction. Further developments in the understanding of the evolution of stratospheric

1514   ozone depletion during this time period are reviewed elsewhere (Wallington et al. 2018;

1515   Solomon 1999; Crutzen and Lelieveld 2001).

1516

1517   The next key development in atmospheric chemistry was the identification of the

1518   hydroxyl (OH) radical as the primary driver of tropospheric chemistry by Levy (1971).

1519   Observational evidence of large concentrations of tropospheric OH (Wang and Davis

1520   1974; Wang et al. 1975; Perner et al. 1976) combined with theoretical and modeling

1521   work established that OH plays an extremely important role in controlling the

1522   abundance and lifetime of several trace gases emitted at the Earth's surface were either

1523   directly radiatively active (e.g., methane, halogenated hydrocarbons) or affected the

1524   abundance of other radiatively active gases by influencing OH concentrations (e.g.,

1525   CO, NMHCs (McConnell et al. 1971; Wofsy et al. 1972; Singh 1977; Chameides and

1526   Cicerone 1978; Logan et al. 1981). Thus, OH came to be recognized as the chemical

1527   filter or cleansing agent in the troposphere with important consequences for

1528   calculations of radiative forcing.

1529

1530   Finally, a major development that solidified the focus on chemistry-climate

1531   interactions was the recognition of the essential role of tropospheric ozone in

1532   determining the chemical composition and the radiation budget of the Earth's

1533   atmosphere. Till the work of Levy (1971), ozone was assumed to be, except over

73

1534   polluted regions, injected into the troposphere from the stratosphere due to mixing

1535   processes, chemically inert, and destroyed at the Earth's surface (Regener 1938; Junge

1536   1962; Fabian and Pruchniewicz 1977). The understanding evolved as both theoretical

1537   and observational analysis showed that the photochemical source of tropospheric

1538   ozone from OH-initiated oxidation of CO, methane, and other hydrocarbons in the

1539   presence of NO_x dominates over that provided via transport from the stratosphere

1540   (Crutzen 1972b, 1973; Chameides and Walker 1973; Fishman et al. 1979b; Fishman

1541   and Crutzen 1978). Subsequently, Fishman (1979a) quantified the climate influence of

1542   tropospheric ozone using its observed distribution.

1543

1544   Advances in understanding of atmospheric chemistry in both the troposphere and

1545   stratosphere, therefore, led to better understanding of its interactions with climate.

1546   Before elaborating on the calculation of ozone radiative forcing, we summarize below

1547   the key chemical interactions leading to indirect radiative forcing of climate change

1548   that were recognized by the end of 1980s based on modeling studies with simplistic

1549   representation of physical, chemical, and dynamical processes (see Wang et al. 1986;

1550   Ramanathan et al. 1987; Wuebbles et al. 1989 for more details). Tropospheric

1551   hydroxyl radical, as the primary sink for many trace gases, was at the center of these

1552   chemistry-climate interactions as illustrated in Figure 4.1.

1553   •   Since reaction with OH is the primary removal mechanism for methane, CO, non-

1554   methane hydrocarbons, many halogenated hydrocarbons, DMS, and SO2 any

1555   changes in the abundance of these gases would alter OH with subsequent

74

1556   feedbacks on the lifetime and abundance, and therefore climate effects of methane

1557   and halogenated hydrocarbons.

1558

1559   • Changes in the emissions of NO_x, methane, CO and non-methane hydrocarbons

1560   would affect tropospheric ozone with subsequent climate effects via tropospheric

1561   ozone changes or OH induced changes in the abundances as mentioned above.

1562

1563   • Changes in stratospheric ozone would impact tropospheric OH concentrations by

1564   influencing the rate of photolysis of tropospheric ozone resulting in the formation

1565   of O1(D) – the primary source of tropospheric OH.

1566

1567   • Increased water vapor in a warmer climate would enhance OH with impacts on

1568   abundances of tropospheric ozone (depending on the levels of tropospheric NO_x)

1569   and methane.

1570

1571   • Oxidation of methane is a major source of stratospheric water vapor. Hence, any

1572   changes in methane would also influence stratospheric water vapor with

1573   subsequent climate implications due to water vapor radiative effects.

1574

1575   By mid-1980s, the scientific community recognized that a full understanding of the

1576   possible changes in ozone distribution and its subsequent effects on climate and

1577   biologically important UV radiation would require not only consideration of

1578   stratospheric processes but also knowledge of often coupled and non-linear, physical,

75

1579   chemical and biological processes controlling the chemical composition of the

1580   troposphere. This was reflected in the first international scientific assessment of ozone

1581   sponsored by the World Meteorological Organization (WMO 1985).

1582

1583   The inhomogeneous distribution of ozone coupled with the different interactions of

1584   stratospheric and tropospheric ozone with solar and longwave radiation necessitated

1585   calculations of radiative forcing due to changes in stratospheric and tropospheric ozone

1586   separately. The net effect of a reduction in stratospheric ozone on surface temperature

1587   depends upon the balance between warming due to enhanced solar radiation reaching

1588   the surface-troposphere system and cooling due to reduced longwave radiation emitted

1589   by the stratosphere both because of the reduction in stratospheric ozone and the

1590   consequent cooling (the "stratospheric temperature adjustment" process described in

1591   section 2). Studies relying on model predictions of ozone distribution showed that the

1592   sign of surface temperature change depends on the vertical distribution of the

1593   stratospheric ozone change (Ramanathan and Dickinson 1979; Wang et al. 1980;

1594   Ramanathan et al. 1985). Further progress on the sensitivity of surface temperature to

1595   observed changes in the vertical distribution of ozone came in 1990 with the iconic

1596   work of

1597   Lacis et al (1990) who showed that ozone changes in the upper troposphere and lower

1598   stratosphere are most effective in forcing climate change. Surface temperature is much

1599   more sensitive to tropospheric ozone perturbations relative to stratospheric ozone

1600   changes because the longwave opacity of tropospheric ozone is nearly the same as that

1601   of stratospheric ozone, and the solar and longwave effects of tropospheric ozone change

1602 affect surface temperature in the same direction (Ramanathan et al. 1985). Studies

1603 estimated the net radiative effect of ozone changes from preindustrial up to 1980s to

1604 cause warming despite a net reduction in ozone column (driven by CFC induced

1605 stratospheric ozone depletion) because of the greater radiative efficiency of

1606 tropospheric ozone (Owens et al. 1985;Lacis 1985; Ramanathan and Dickinson 1979).

1607

1608

Section 4.2. Radiative Forcing due to Short-lived Trace Gases: 1990 to 2000

By the early 1990s, a better understanding of the effect of ozone on radiative forcing and its
strong dependence on the vertical profile of ozone change throughout the troposphere and
stratosphere as well as on its total amount had emerged (Schwarzkopf and Ramaswamy 1993
Lacis et al. 1990; Ramaswamy et al. 1991; Shine et al. 1990). Unlike sparse observational
constraints on tropospheric ozone trends, better constraints on stratospheric ozone trends (e.g.
Stolarski et al. 1991) facilitated quantitative assessment of its radiative forcing indicating that
ozone reductions between 1979 to 1990 caused a negative radiative forcing (Ramaswamy et al.
1991).

Estimates of radiative forcing due to ozone continued to be refined through the mid-1990s
(IPCC 1994, 1995) though the level of confidence was low around this time (Figure 1.2 in
section 1). Low confidence in stratospheric ozone forcing was largely driven by more than a
factor of two spread in model computed values of stratospheric ozone forcing (Shine et al.
1995a,c,b; Schimel et al. 1996). Similarly, for tropospheric ozone, studies based on modeled or
limited observations of ozone trends agreed that increases in tropospheric ozone since
preindustrial times have resulted in a positive forcing (e.g., Hauglustaine et al. 1994; Marenco et
al. 1994; Mohnen et al. 1993) but there was large uncertainty as summarized in the IPCC 1994
special report and SAR (Shine et al. 1995b; Schimel et al. 1996). The major difficulty in
accurately estimating global ozone forcing was limitations in the knowledge of changes in
vertical, horizontal and temporal distributions of ozone (Prather et al. 1995; Stordal et al. 1995;
Ko et al. 1995). This was particularly true for tropospheric ozone whose distribution was

1632   difficult to capture in the two-dimensional models used widely until the mid 1990s (Prather et

1633   al. 1994; see Peters et al. 1995 for a review of tropospheric chemistry models until 1995).

1634   Furthermore, it was difficult to demonstrate confidence in model-derived trends because of the

1635   lack of strong observational constraints. Chemistry-climate interactions were recognized to have

1636   a significant effect on the total radiative forcing of climate and were deemed important to be

1637   accounted for in the assessment of potential future climate change as highlighted in Chapter 2 of

1638   the FAR (Shine et al. 1990) (Figure 4.1).

1639

1640

1641

1642   The first quantitative estimate of the indirect radiative effects, in terms of Global Warming

1643   Potentials (GWPs; see section 11.2 for definition), from increases in emissions of methane, CO

1644   and NO_X was based on results from a two-dimensional model representing the fundamentals of

1645   atmospheric chemistry known at the time (Hough and Derwent 1990). Although there was a fair

1646   degree of confidence in the sign of the indirect effects (Isaksen et al. 1991), these early

1647   estimates were found to be too uncertain and likely overestimated (Johnson et al. 1992; Isaksen

1648   et al. 1992; Lelieveld and Crutzen 1992; Isaksen et al. 1991). Two-dimensional tropospheric

1649   chemistry models that had been primarily used until the mid-1990s were of limited scope in

1650   adequately characterizing the complex chemical and physical processes and the nonlinear

1651   interactions between them (Prather et al. 1995; Olson et al. 1997; Stordal et al. 1995) hampering

1652   the accurate quantification of indirect radiative forcing (Shine et al. 1995b,c; Schimel et al.

1653   1996). Limited atmospheric measurements on global scale for many species, including ozone,

1654   CO, NOx, and NMHCs, needed to characterize historical trends and provide constraints on

1655   models, further restricted the ability to robustly quantify indirect radiative forcing..

1656

1657

1658   Progress was however made in better definition and quantification of indirect forcing

1659   from methane increases driven by theoretical (Prather 1994) and multi-model analysis (Prather et

1660   al. 1995; Stordal et al. 1995). Forcing due to the chemical feedback of methane increases on its

1661   own lifetime via reduced tropospheric OH (OH changes discussed in section 4.3) was no longer

1662   considered an indirect effect as this effect would be implicitly included in the estimates for the

1663   forcing due to historical methane changes (Schimel et al. 1996). The influence of methane

1664   increases on tropospheric ozone and stratospheric water vapor was estimated to add about 25%

1665   to the direct methane forcing (Schimel et al. 1996; Prather et al. 1995).

1666

1667   From the late 1990s onwards, the development and application of sophisticated global climate

1668   models with some representation of atmospheric chemistry (see Zhang 2008; Young et al. 2018

1669   for a historical overview of atmospheric chemistry in global models) combined with

1670   improvements in the knowledge of chemical and physical processes affecting the distributions

1671   of short-lived gases, and better atmospheric observations led to significant improvements in

1672   forcing estimates as assessed in the TAR (Ramaswamy et al. 2001). Results from several studies

1673   applying various approaches and observational evidence of ozone loss for a longer period (e.g.,

1674   MacKay et al. 1997; Forster 1999; F. Forster and Shine 1997; Hansen et al. 1997; Granier et al.

1675   1999) enhanced the level of scientific understanding of stratospheric ozone forcing of -0.15±0.1

1676   Wm^{-2} for the period 1979 to 1997 (Ramaswamy et al. 2001). Approximate consistency between

80

1677   observed lower stratospheric temperature trends since the late 1970s and that simulated by global

1678   climate models forced with observed ozone losses confirmed that forcing from the decline in

1679   ozone is indeed negative (Hansen et al. 1997a). However, a clear attribution was complicated by

1680   the possible role of cooling from increasing stratospheric water vapor (Forster and Shine 1999),

1681   observations of which were limited.

1682

1683   Results based on global three-dimensional model studies of preindustrial to present-day

1684   tropospheric ozone changes driven by precursor emissions (e.g., Roelofs et al. 1997;

1685   Haywood et al. 1998; Dorland et al. 1997; Berntsen et al. 1997; Mickley et al. 1999;

1686   Brasseur et al. 1998; Stevenson et al. 1998) along with those based on satellite-inferred

1687   ozone column changes (Portmann et al. 1997; Kiehl et al. 1999) alleviated uncertainties

1688   in the tropospheric ozone forcing estimates (Granier et al. 1999; Ramaswamy et al.

1689   2001). Process studies provided better understanding of the sensitivity of surface

1690   temperature to the vertical distribution of ozone and clouds, and the spatial distribution

1691   of ozone forcing (e.g., Forster and Shine 1997; Hansen et al. 1997b; Hauglustaine and

1692   Brasseur 2001).

1693

1694   Although the level of confidence in tropospheric ozone forcing had increased,

1695   uncertainties remained because of the large model diversity in predicted historical ozone

1696   changes and limited observational constraints on ozone trends (Prather et al. 2001 and

1697   references therein). Limitations in our understanding of not only the complex non-linear

1698   chemical interactions between ozone precursors but also the historical evolution of the

1699   emissions of specific precursors impeded the quantitative attribution of ozone forcing up

1700   until this time (Prather et al. 2001 and references therein).

1701

1702   Studies also highlighted the importance of including feedbacks between climate and

1703   chemistry on the assessment of the climate impact of short-lived species (Prather et al.

1704   2001). Here, we do not cover the details of this feedback but refer to past IPCC reports

1705   and several review papers on this topic (Prather et al. 2001; Jacob and Winner 2009;

1706   Fiore et al. 2012, 2015; Isaksen et al. 2009; Denman et al. 2007; Von Schneidemesser et

1707   al. 2015; Brasseur 2009; Kirtman et al. 2013; Monks et al. 2015).

1708

1709   Much progress was made in the quantitative estimates of forcings from chemistry-

1710   climate interactions in the latter half of the 1990s as assessed in the TAR. The indirect

1711   forcing from methane changes continued to be the best studied, with explicit

1712   quantification of the individual effects on its own lifetime, tropospheric ozone,

1713   stratospheric water vapor, and CO2 (e.g., Hauglustaine et al. 1995; Lelieveld et al. 1998;

1714   Fuglestvedt et al. 1996). Modeling studies also quantified indirect forcing from changes

1715   in CO and a suite of NMHCs through their influence on methane lifetime, tropospheric

1716   ozone and CO_2 (Daniel and Solomon 1998; Johnson and Derwent 1996).

1717

1718   Accurate calculation of the indirect forcing of NO_x remained challenging because of

1719   counteracting effects– increased NO_x emissions increase tropospheric ozone producing

1720   a short- lived regional positive forcing, but increase OH concentration lowering methane

1721   abundance (with a consequent decrease in ozone) that produces a longer-lived global

82

1722   negative forcing partially offsetting the short-lived positive ozone forcing (Ramaswamy

1723   et al. 2001 and references therein). Studies showed that the ozone and OH perturbations

1724   strongly depended on the location of NO_x emission perturbations because of the non-

1725   linear ozone chemistry and differences in mixing regimes (e.g., Fuglestvedt et al. 1999).

1726

1727   Diversity in results of model studies that resolved the complex and non-linear effects of

1728   emission changes on ozone and OH radical and limitations in observational constraints

1729   to build confidence in them remained a significant source of uncertainty in these

1730   estimates of indirect forcings (Ramaswamy et al. 2001).

1731

1732
1733
1734

Section 4.3. Emission-based radiative forcing for Short-lived Climate Forcers (SLCFs):

2000-present

Over the past two decades, the development of increasingly sophisticated comprehensive

global chemistry models in terms of their design (e.g., models with coupled

stratospheric-tropospheric chemistry, global climate model with online chemistry) and

the representation of complex physical and chemical processes (e.g., trace gas-aerosol

interactions, interactive natural emissions), combined with better estimates of trace gas

emissions and the availability of longer observational records has facilitated advances in

the attribution of the changes in short-lived trace gases and their forcings (Forster et al.

2007; Myhre et al. 2013).

Consideration of coupled stratospheric and tropospheric chemistry in global models has

facilitated greater understanding of the influence of changes in stratospheric ozone and

ozone depleting substance (ODSs) on tropospheric ozone and the effect of tropospheric

ozone precursors on stratospheric ozone (e.g., Shindell et al. 2006; Hegglin and Shepherd

2009; Eyring et al. 2013; Young et al. 2013), which has led to better accounting of these

impacts on the radiative forcing due to ozone (Gauss et al. 2006; Stevenson et al. 2013;

Myhre et al. 2013; Forster et al. 2007; Shindell et al. 2013; Banerjee et al. 2016).

Coupled chemistry-climate models have enabled assessment of the changes in ozone

induced by climate change (i.e., chemistry-climate feedbacks; see Isaksen et al. 2009;

more refs), and the resulting radiative forcing (e.g., Gauss et al. 2006; Stevenson et al.

1757   2013; Forster et al. 2007) and feedbacks on climate (e.g., Nowack et al. 2015; Chiodo et

1758   al. 2018; Marsh et al. 2016).

1759

1760   A major development in the quantification of forcing due to tropospheric ozone and

1761   chemistry-climate interactions over this period has been the adoption of an emissions-

1762   based approach (Shindell et al. 2009, 2005) to estimate the contribution of anthropogenic

1763   emissions of individual ozone (or aerosol) precursors to the preindustrial to present- day

1764   radiative forcing either via direct influences (e.g., ozone, methane, or aerosols) or

1765   indirect effects (Myhre et al. 2013; Forster et al. 2007). With this approach, model

1766   representation of couplings between gas-phase and aerosol chemistry in the troposphere

1767   has helped elucidate indirect effects of trace gases on aerosols via influences on ozone

1768   and OH and the resulting forcing (Shindell et al. 2009; Von Schneidemesser et al. 2015).

1769   Additionally, indirect forcing through detrimental ozone effects on vegetation (see

1770   section 6 for discussions on forcing from land and biogeochemical interactions) have

1771   also been explored (Sitch et al. 2007; Collins et al. 2010; Kvalevag and Myhre 2013).

1772   These emissions-based radiative forcing estimates (Figure 4.2) give a significantly

1773   different relative importance to various emissions (Forster et al. 2007; Myhre et al. 2013)

1774   than that suggested by abundance-based assessments in the past. Radiatively active short-

1775   lived trace gases (and aerosols; see section 5) and their precursors are now collectively

1776   termed as Short-lived Climate Forcers (SLCFs) as their climate impact is mainly felt

1777   within the first one to three decades (near term) of their emissions (Myhre et al., 2013;

1778   Fiore et al., 2015) in contrast to long-lived greenhouse gases. Furthermore, the short

1779   lifetimes of SLCFs result in spatially inhomogeneous abundances and associated forcings

1780   highly sensitive to the location of emissions. Consequently, climate influence from

1781   SLCFs is more important on a regional scale (e.g., Fry et al. 2012; Collins et al. 2013;

1782   Aamas et al. 2017) contrary to the relatively homogeneous spatial influence from well-

1783   mixed greenhouse gases.

1784

1785   The question of how global mean hydroxyl radical has evolved in the past and will

1786   change in the future in response to anthropogenic emission and climate change remains

1787   highly relevant to the estimates of SLCF radiative forcing given the dependence of SLCF

1788   atmospheric lifetimes on OH (section 4.1). Significant progress has been made in the

1789   understanding of fundamental atmospheric chemistry of OH with advances in both

1790   observations and modeling (e.g., Stone et al, 2012; Rohrer et al., 2014), however the

1791   answer to this question remains at an impasse. The atmospheric chemistry community

1792   has mostly relied on global chemistry models to derive past changes and predict future

1793   evolution of OH over long time scales, and on proxies, such as methyl chloroform, to

1794   derive OH variability over the past ~35 years during which we have observations (e.g.,

1795   Prinn et al., 2001; Bousquet et al., 2005; Montzka et al., 2011; Rigby et al., 2017; Turner

1796   et al., 2017). There is no consensus in the global model estimates of changes in

1797   tropospheric mean OH abundance from preindustrial to present-day based on studies

1798   over the past ~40 years as displayed in Table 4.1. The simulated change in present day

1799   OH relative to preindustrial ranges from a decline to no change to an increase due to

1800   varying levels of offsetting effects from increases in OH sinks (methane, CO, NMHCs)

1801   and increases in factors that increase OH (water vapor, tropospheric ozone, NOx, and

1802   UV radiation) (e.g., Naik et al., 2013). This is in contrast to the 30% decline in present-

1803   day OH relative to preindustrial inferred from ice core measurements, although with

1804   large uncertainties (Alexander and Mickley 2016). There are also large discrepancies in

1805   the projections of global OH levels with implications for estimates of future SLCF

1806   forcing (e.g., Voulgarakis et al. 2013). Changes in OH over the past ~35 years and their

1807   role in the renewed growth in atmospheric methane since 2007 are intensely debated in

1808   the literature with no consensus view (Turner et al., 2019).

1809

1810   Global chemistry-climate models have remained the tools of choice to quantify the

1811   contribution of SLCF emissions to radiative forcing of climate change as observational

1812   constraints are sparse (e.g., for tropospheric ozone Bowman et al., 2013). Multi-model

1813   intercomparison projects (MIPs) involving coordinated experiments with chemistry

1814   models provide a means of exploring structural uncertainty related to model

1815   representation of various physical and chemical processes determining the distribution

1816   and budgets of SLCFs and have informed IPCC as well as other international

1817   assessments (see Young et al. 2018 for a brief history of MIPs for chemistry).

1818

1819   Similar to climate model intercomparisons (e.g., Meehl et al., 2007), analysis is focused

1820   on multi-model means because the ensemble average across structurally different models

1821   shows better agreement with available observations with individual model biases

1822   canceling out, while the spread across models is considered a measure of uncertainty

1823   (e.g., Young et al. 2013). However, because these ensembles represent "ensembles of

1824   opportunity", the spread across models does not necessarily span the full range of

1825   structural as well as process uncertainty (Tebaldi and Knutti 2007).

87

1826

1827 For chemistry models, early MIPs focused on exploring the uncertainty in model

1828 representation of specific processes affecting the distribution and budget of tropospheric

1829 ozone and related trace gases (e.g., PhotoComp in Olson et al., 1997 and OxComp in

1830 Prather et al., 2001). Computation of ozone radiative forcing within MIPs came about

1831 later in the 2000s beginning with the framework of Atmospheric Chemistry Composition

1832 Change: an European Network (ACCENT; Gauss et al. 2006) that informed the AR4

1833 report (Forster et al. 2007). The specifications of the simulations for MIPs improved with

1834 the development of a consistent set of gridded anthropogenic precursor emissions

1835 describing their preindustrial to present day evolution (Lamarque et al. 2010). This

1836 common dataset employed by the more recent ACCMIP (Atmospheric Chemistry and

1837 Climate Model Intercomparison Project) (Lamarque et al. 2013) allowed for increased

1838 comparability of model simulations of tropospheric ozone (and aerosols) abundances and

1839 resulting radiative forcings as assessed in AR5 (Myhre et al. 2013). Uncertainties in

1840 emission estimates (e.g., Granier et al., 2011; Bond et al., 2013) have consequences for

1841 SLCF radiative forcing. New and revised estimates of the historical evolution of SLCF

1842 and their precursor emissions (Hoesly et al, 2018; van Marle et al. 2017) provide a means

1843 of exploring the contribution of emission uncertainty to SLCF forcing uncertainty. The

1844 Aerosol Chemistry Model Intercomparison Project (AerChemMIP) in support of the

1845 forthcoming IPCC assessment (AR6) is designed to quantify and explore uncertainties in

1846 the forcing due to anthropogenic emissions of SLCFs thereby providing better constraints

1847 on the role of SLCFs in climate forcing (Collins et al. 2017).

1848

1849

Section 4.4. Summary and Challenges

1851

1852 In this section, we have reviewed the evolution of our knowledge of radiative forcing from

1853 short-lived trace gases and chemistry-climate interactions over the past approximately four

1854 decades.

1855

1856 Significant progress has been made beginning with the recognition of the role of

1857 stratospheric ozone on climate change to the scientific understanding and quantitative

1858 estimate of the contribution of emissions of a suite of SLCFs to Earth's radiative forcing.

1859 The use of comprehensive global chemistry-climate models combined with observational

1860 constraints where available have enhanced our ability to capture complex chemical

1861 interactions in the computation of SLCF radiative forcing. However, challenges remain in

1862 quantifying the forcing due to anthropogenic emissions of SLCFs as outlined below:

1863

1864 ● A persistent uncertainty in constraining the radiative forcing from SLCFs is

1865 the limited or no knowledge of preindustrial precursor emissions and atmospheric burdens

1866 (e.g., for tropospheric ozone as highlighted by Stevenson et al., 2013).

1867

1868 ● The spatial distribution of ozone precursor emissions has undergone a

1869 dramatic change over the last couple of decades with emissions declining in the developed

1870 mid-latitude and rising in the developing tropical regions (e.g., Zhang et al., 2016). The

1871 consequences of such emission distribution for chemistry-climate interactions and

1872 consequent SLCF forcing is not clear.

1873

1874   ●   The debate over how global mean OH is changing in response to changing

1875   anthropogenic emissions and climate change, and the implications of this change for the

1876   abundance and lifetime of SLCFs is yet to be resolved. It has been a challenge to narrow

1877   down the reasons for differences in global model simulations of the evolution of

1878   atmospheric OH (e.g., Naik et al., 2013; Voulgarakis et al., 2013). Recent efforts

1879   combining observations and model results in novel ways show promise in understanding

1880   the causes of model disagreement (e.g., Nicely et al., 2017; Prather et al., 2018).

1881

1882

Tables:

Table 4.1. Percent change in present day OH relative to preindustrial compiled from

literature (based on Murray et al. 2014). The definition of present day varies depending

on the year of publication of the study.

Reference	% Change in OH since preindustrial	Method
McElroy (1989)	+60%	1-D model
Hough and Derwent (1990)	-19%	2-D model
Valentin (1990)	-9%	2-D model
Law and Pyle (1991)	-13%	2-D model
Pinto and Khalil (1991), Lu and Khalil (1991)	-4%	1-D model, multi 1-D model
Staffelbach et al. (1991)	-30%	ice core measurements of formaldehyde
Crutzen and Zimmerman (1991)	-10% to -20%	3-D model
Thompson et al. (1993)	-20%	Multi 1-D model
Martinerie et al. (1995)	+6%	2-D model
Berntsen et al. (1997)	+6.8%	3-D model
Roelofs et al. (1997)	-22%	3-D model
Brasseur et al. (1998)	-17%	3-D model
Wang and Jacob (1998)	-9%	3-D model
Mickley et al. (1999)	-16%	3-D model
Grenfell et al. (2001)	-3.9%	3-D model, NMHCs
Hauglustaine and Brasseur (2001)	-33%	3-D model
Shindell et al. (2001)	-5.9%	3-D model
Lelieveld et al. (2002)	-5%	3-D model

Lamarque et al. (2005)	-8%	3-D model
Shindell et al. (2006)	-16%	3-D model

1888

1889

Sofen et al. (2011)	-10%	3-D model
John et al. (2012)	-6%	3-D model
Naik et al. (2013)	-0.6±8.8%	Multi 3-D model
Murray et al. (2014)	+7.7±4.3%	Multi 3-D model
Achakulwisut et al. (2015)	-8 to +17%	Multi 3-D Model

1890

1891

1892

1893

1894

1895

1896

1897

1898

1899

1900

1901

1902

1903

1904

92

1905
1906 **Figure 4.1** Historical evolution of the consideration of chemistry-climate interactions

1907 in international assessments. The figure displays in clockwise order beginning from the

1908 top left, the interactions of short-lived gases considered in WMO (1985), IPCC AR1

1909 (1990), IPCC AR4 (2007), and IPCC AR5 (2013).
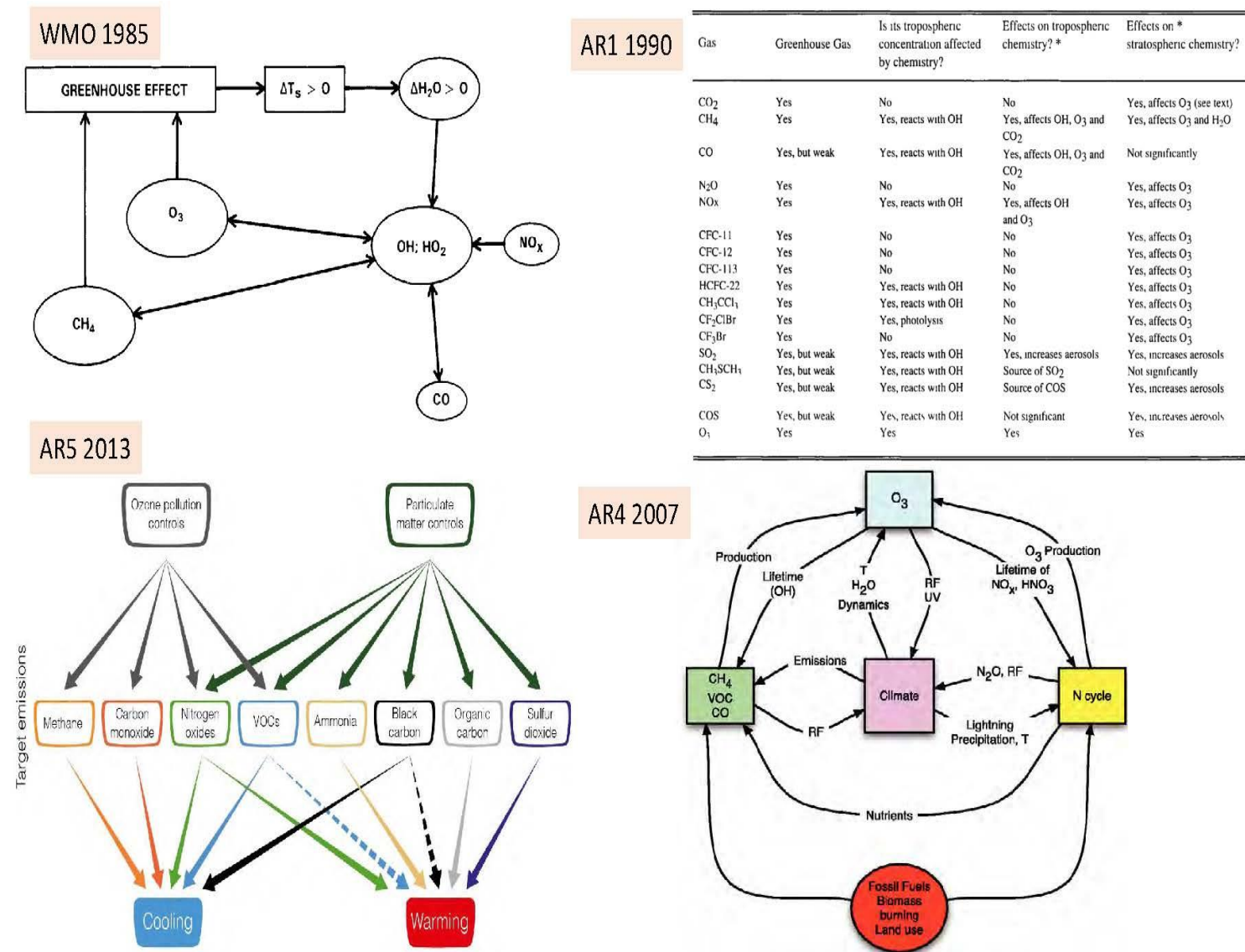
1910

1911

1912
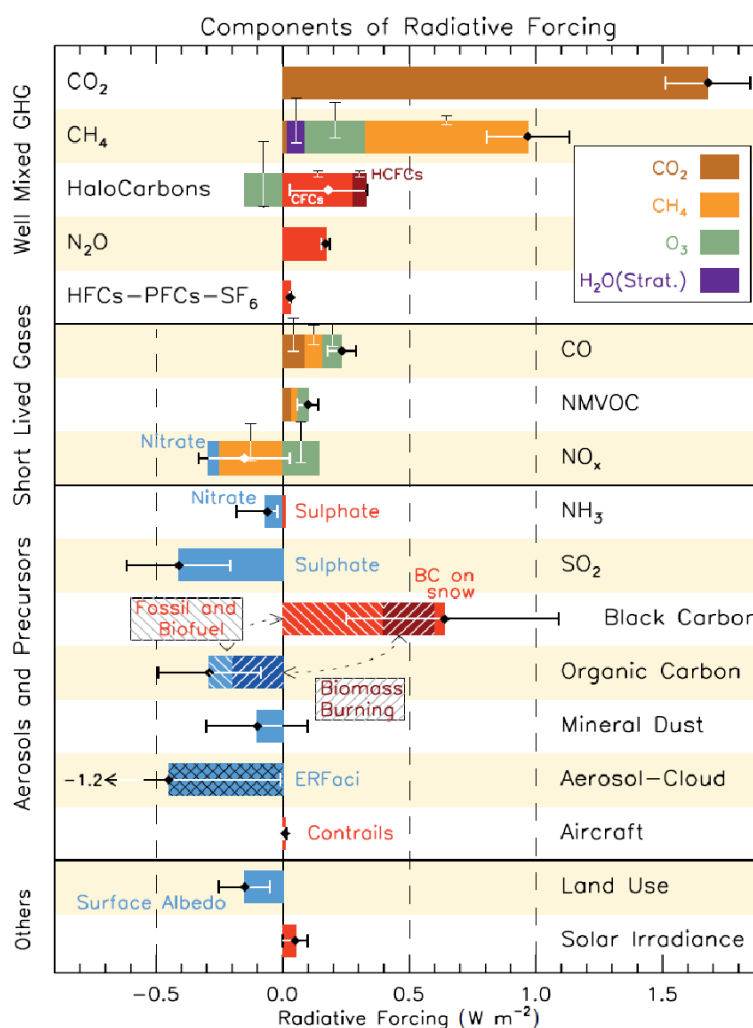
Figure 4.2. Best estimate of global average radiative forcing for the period 1750 to 2011 for emitted chemical species (well-mixed and short-lived gases, aerosols and their precursors) or other factors (from Myhre et al. (2013)). As shown in the inset in the top portion of the figure, many colors are used to represent RF from emitted species affecting several chemicals while red (positive forcing) and blue (negative forcing) are used for emitted components that affect fewer forcing agents. The vertical bars represent the relative uncertainty of the RF induced by each component. See Myhre et al. (2013) for more details.

Section 5. Tropospheric aerosols

Aerosols scatter and absorb radiation (the direct effect), and also act as cloud condensation

nuclei whereby they modify the microphysical and macrophysical properties of clouds (the

indirect effect). Increased concentrations of aerosols from anthropogenic activity therefore exert

a radiative forcing of climate. The importance of atmospheric aerosols had been long

established in the areas of atmospheric visibility (Koschmeider, 1924) and human health (e.g.

Lippmann and Albert, 1969), but aerosols were originally considered to be of only minor

consequence in terms of their impact on climate via direct and indirect effects (Twomey, 1959;

McCormick and Ludwig, 1967; Bolin and Charlson, 1976). Simple models of the impact of

aerosols on planetary albedo in terms of their absorptance and the reflectance of the underlying

surface had been developed (e.g. Ensor et al., 1971; Reck, 1974, Chylek and Coakley, 1974),

but the radiative forcing was not quantified owing to the lack of knowledge of the

anthropogenic aerosol perturbation.

Observational evidence of aerosol-cloud interactions was hypothesized from observations of

ship-tracks after satellite sensors were launched (Conover, 1966) but quantifying their radiative

effect was only possible once detailed spectral information from satellites became available

(Coakley et al., 1987). Observations of surface solar insolation suggested a widespread

reduction in irradiance at the surface (Stanhill and Moreshet, 1992) although the causes were

difficult to attribute. Thus, until the late 1980s, aerosols were considered insignificant in terms

of radiative forcing when compared to that from changes in atmospheric concentrations of

greenhouse gases. This view changed in the early 1990s. Global chemical transport models

(CTMs) that were able to model the aerosol lifecycle of emission, chemical transformation,

1970   transportation and deposition and hence model the anthropogenic perturbation to aerosol

1971   concentrations were combined with relatively simple radiative transfer models.

1972

1973

1974

1975

5.1.   Simple models of aerosol-climate interactions: the early 1990s

1976

1977

1978

1979   Sulfate aerosol was the first aerosol species to be comprehensively investigated owing to the

1980   anthropogenic emissions of the SO_2 gaseous precursor being ~100 Tgyr^{-1}, i.e. exceeding natural

1981   emissions by around a factor of five (Langner and Rodhe, 1991). These early global CTMs

1982   typically had a spatial resolution of 10°x10° latitude/longitude with ~10 coarsely-spaced

1983   atmospheric levels in the troposphere (Zimmermann et al., 1989). The impact of anthropogenic

1984   emissions of sulfur dioxide and the resulting sulfate aerosols on the radiative forcing of the

1985   Earth's climate was initially quantified by Charlson et al., (1991, 1992) who used a multiple

1986   scattering approximation to derive an equation for the change in the planetary albedo owing to a

1987   purely scattering aerosol and focused on the change in cloud free regions.

1988

1989   This related the direct radiative forcing of sulfate aerosol, F_{direct}, to the total solar irradiance , S_o,

1990   the atmospheric transmission, T_{at}, the cloud fraction, A_c, the surface reflectance, R_s, the aerosol

1991   single scattering albedo, ω_o, the fraction of light backscattered to space, β_{aer}, and the

1992   perturbation to the aerosol optical depth since pre-industrial times, $d\tau_{aer}$:

$$F_{direct} = -\frac{1}{2}S_o T_{at}^2 (1 - A_c)(1 - R_s)^2 \beta_{aer} d\tau_{aer}$$

1993

1999

1994   Charlson et al (1992) also derived an expression for the Twomey effect, which is the aerosol

1995   impact on the cloud droplet effective radius under the assumption of constant cloud liquid water

1996   (Twomey et al., 1977). Charlson et al (1992) used global mean estimates of the various

1997   parameters coupled to newly available estimates of the perturbation to the total aerosol

1998   concentrations caused by anthropogenic emissions (Langner and Rodhe, 1991) and concluded

97

2000   that the resulting global-mean radiative forcing for aerosols (pre-industrial to circa 1980s) was

2001 F_{direct}= -1.3 W m^{-2} and F_{Twomey}= -1 W m^{-2} with significant uncertainty owing to the neglect of

2002   subsequent impacts on cloud liquid water (i.e. the Albrecht effect, Albrecht, 1989), the

2003   simplicity of the models used and the lack of account of spatial correlation between the various

2004   parameters. Penner et al (1992) used a similar method to derive an initial estimate of the

2005   radiative forcing due to biomass burning aerosols from combined direct and indirect effects as

2006   strong as -2 W m^{-2}.

2007

2008   Simple representations of the direct radiative forcing of sulfate aerosol were straightforward to

2009   implement in fully coupled ocean-atmosphere models (Mitchell et al., 1995) because, for cloud-

2010   free regions, the local surface reflectance could simply be increased in proportion to $d\tau_{aer}$:-

2011

2012
2013
2014
2015

$$dR_s = (1-R_S)^2 \beta_{aer} \frac{d\tau_{aer}}{\mu_0} \qquad \underline{\hspace{3cm}}$$

2016
2017   Implementing this parameterization in the UK Met Office climate model showed a reduced rate

2018   of warming particularly in the northern hemisphere in their climate model simulations, bringing

2019   the simulated surface temperature change into better agreement with observations.

2020   Because the radiative forcing due to aerosols could conceivably outweigh that of increased

2021   concentrations of well-mixed greenhouse gases there were significant efforts to better quantify

2022   aerosol radiative forcing.

2023

2024
2025

5.2.Refinement of aerosol direct and indirect effect modelling studies: the mid-1990s

Simple models continued to play a significant role. Early simple theoretical models of radiative

impacts of partially absorbing aerosols (e.g. Ensor et al., 1971; Reck, 1974; Chylek and Coakley,

1974) were now extended (Haywood and Shine, 1995; Chylek and Wong,1995) by accounting

for aerosol absorption via the aerosol single scattering albedo, ω_o, day-length fraction, D, and

spatially resolved parameter values rather than global mean values:

$$F_{direct} = -DT_{at}^2(1 - A_c)[\omega_0\beta_{aer}(1 - R_s)^2 - 2(1 - \omega_0)R_s]d\tau_{aer}$$

Assuming a mass fraction between absorbing black carbon (BC) and scattering sulfate based on

in-situ measurements weakened the sulfate F_{direct} from -0.34 W m-2 (already much weaker than

that diagnosed by Charlson et al., 1991, 1992) to between -0.10 to -0.30 W m-2 depending on

the assumed sulphate climatology and mixing state and that there was no direct radiative forcing

in cloudy areas. This study established the importance of aerosol absorption, particularly when

it was recognized that the positive radiative forcing impact would be amplified if absorbing

aerosols resided above underlying cloud (e.g. Haywood and Shine, 1997). Regionally, dF_{direct}

can be either positive (for low ω_o and high Rs or above reflective cloud) or negative (for high ω_o

and low Rs) as demonstrated by the 'real color' image (Fig 5.1).A more comprehensive estimate

of Fdirect for sulfate aerosol was performed by Kiehl and Briegleb (1993) who imposed

monthly mean climatologies of sulfate mass burden (Langner and Rodhe,1991), an aerosol size

distribution and suitable refractive indices to derive aerosol optical properties. These optical

properties were then included in off-line radiative transfer calculations using meteorological

fields from observations. The F_{direct} of sulfate was evaluated as being a modest -0.3 W m-2 (this
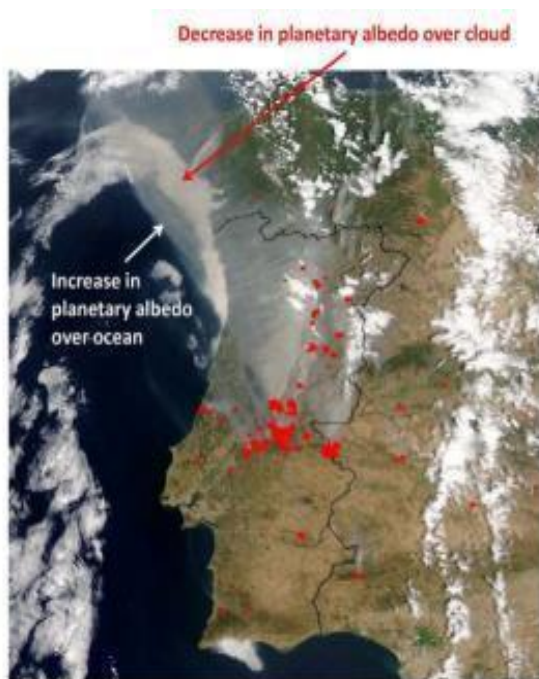
Fig 5.1. A real-colour MODIS satellite image showing the impact of smoke from biomass burning fires off the coast of Portugal on 3 August 2003. Fires are shown by the red spots and the smoke plume is shown in grey (from Haywood, 2016).

2053 affirmed the simple model of
2054 Haywood and Shine (1995)).
2055 Similarly, previous results for
2056 biomass burning aerosol were
2057 regarded as too strongly negative
2058 owing to lack of account of aerosol
2059 absorption, pre-industrial biomass
2060 burning and the lack of a
2061 discernible cooling trend in the
2062 climatic record. GCM
2063 investigations of the aerosol
2064 indirect effect were also performed
2065 (Jones et al., 1994; Boucher and
2066 Lohmann, 1995) using the model-
2067 simulated clouds.
2068 Climatological sulfate

2069 concentrations (Langner and Rodhe, 1991) were utilized together with parameterisations based

2070 on airborne observations that related the cloud droplet effective radius to the aerosol number

2071 concentration in marine and continental environments (Martin et al., 1994). These

2072 simulations indicated a F_{Twomey} of -1.3 W m^{-2} (Jones et al.,1994) and -0.5 to -1.5 W m^{-2}

2073 (Boucher and Lohmann, 1995), but the uncertainty remained significant. Boucher (1995)

2074 made a first estimate using satellite observations of the difference between inter- hemispheric

2075 cloud effective radius (northern hemisphere 11.0μm, southern hemisphere 11.7μm; Han et al.,

100

2076   1994) but acknowledged that the contribution of aerosols from natural land surfaces made the

2077   results difficult to interpret in the context of anthropogenic radiative forcing. Recognizing the

2078   fidelity of the refinements, IPCC (Schimel et al., 1996) suggested a best estimate for F_{direct} of -

2079   0.5W m^{-2} (range -0.25 to -1.0 W m^{-2}) which was derived from a combination of the radiative

2080   forcing of sulfate (-0.4W m^{-2}), biomass burning (-0.2W m^{-2}) and fossil-fuel black carbon

2081   (FFBC; +0.10W m^{-2}). IPCC (Schimel et al., 1996) recognized that a best estimate of F_{Twomey}

2082   was impossible to establish without further model simulations and observational constraints

2083   and suggested a range of 0 to -1.5W m^{-2}

2084

2085

2086

2087 **5.3. The proliferation of GCM-based estimates and the requirement for validation data:**

2088 **late 1990s to early 2000s**

2089

2090 The development of global model-based estimates of aerosol species other than sulfate

2091 continued apace. Tegen and Fung (1995) developed a global model of mineral dust and

2092 highlighted that, in addition to impacts in the solar region of the electromagnetic spectrum,

2093 coarse mode aerosols can have a significant impact by absorbing and re-emitting terrestrial

2094 radiation. Any anthropogenic fraction of mineral dust was recognized as being very uncertain.

2095 A first black carbon climatology was also produced (Cooke and Wilson, 1996) reiterating that

2096 global black carbon emissions ($\sim$14 Tg yr^{-1} cf SO$_2$ at $\sim$100 Tg yr^{-1}) would lead to anthropogenic

2097 aerosol that was partially absorbing i.e. grey rather than white (Figure 5.1). The first estimates of

2098 nitrate aerosol direct radiative forcing were also produced (Van Dorland et al., 1997) but were

2099 highly uncertain owing to differences in the partitioning between the accumulation and coarse

2100 modes (Adams et al., 2001; Jacobson, 2001). The recognition that the different aerosol types

2101 needed to be represented for accurate determination of total aerosol radiative forcing led to a

2102 rapid expansion of GCM estimates based on aerosol climatologies derived from global CTMs.

2103

2104 Aerosol optical properties are determined by the (wavelength-dependent) refractive index of the

2105 particles and the particle size distribution. Recognizing that aerosol direct effects were be

2106 represented using more flexible radiative transfer codes that allowed integration over the full

2107 solar spectrum and range of solar zenith angles led to a comprehensive multi-model radiative

2108 transfer inter-comparison for sulfate aerosol (Boucher et al., 1998).

2109   This study showed a relatively modest variation in radiative effect between the radiative transfer

2110   models, indicating that the radiative transfer codes of reduced complexity in GCMs, but more

2111   refined than those used in the earlier simplified model calculations, could adequately describe

2112   aerosol direct radiative effects.

2113

2114   It was recognized that GCMs were a suitable tool for allowing representation of the variability

2115   in humidity, surface reflectance, aerosol and cloud but computational expense meant that CTMs

2116   were used for computing e.g. monthly mean distributions of sulfate aerosol and these monthly

2117   mean fields were then input to the GCMs, which computed the direct and indirect effects using

2118   their internal radiative transfer models (e.g. Kiehl and Briebleb, 1993; Boucher and Anderson,

2119   1995; Boucher and Lohmann, 1995; Kiehl and Rodhe, 1995; Haywood et al., 1997; Haywood

2120   and Ramaswamy, 1997; Hansen et al., 1998). However, CTMs and GCMs were increasingly

2121   combined so that the sulfur chemistry, transport, deposition and direct and indirect radiative

2122   forcing could be explicitly calculated. This method had the benefit that aerosol concentrations

2123   could be precisely correlated with fields determining aerosol production and removal i.e. clouds

2124   and precipitation (e.g. Graf et al., 1997; Feichter et al, 1997; Myhre et al., 1998; Iversen et al,

2125   2000; Ghan et al., 2001; Jacobson, 2001; Jones et al., 2001). Nevertheless, the limitations of

2126   model resolution were recognized; GCMs with their coarse resolution of ~100s of km were

2127   unable to represent the sub- gridscale details such as relative humidity and detailed distributions

2128   of gas phase and aqueous phase production of sulfate aerosol (Ghan et al., 2001).

2129
2130   Direct radiative forcing calculations were made for fossil-fuel BC (Haywood and Ramaswamy,

2131   1998; Penner et al., 1998; Cooke et al., 1999), fossil-fuel organic carbon (Penner et al., 1998;

2132   Cooke et al., 1999), biomass burning aerosol (Penner et al., 1998; Iacobellis et al., 1999), total

2133 BC (Hansen et al., 1998; Haywood and Ramaswamy, 1998; Jacobson, 2001) and fossil-and

2134 biomass- burning organic carbon (Hansen et al., 1998; Jacobson, 2001). These models treated

2135 each of the aerosol types separately (i.e. an external mixture) although some of these models

2136 began to represent multi-component aerosols as internal mixtures which can have particular

2137 relevance for inclusion of absorbing BC cores within scattering shells (e.g. Jacobson, 2001)

2138 producing a 'lensing' effect that enhances the absorption (e.g. Lesins et al., 2002).

2139

2140 GCM studies of indirect effects tended to rely on empirical relationships between aerosol

2141 number (e.g. Jones et al., 1994) or mass (Boucher and Lohmann, 1995) and cloud droplet

2142 number concentrations (CDNC), but prognostic mechanistic parametrizations that attempted to

2143 explicitly account for aerosol activation and cloud nucleation began to appear (e.g. Lohmann et

2144 al. (2000), Ghan et al. (2001)). By contrasting polluted and unpolluted clouds, comprehensive

2145 aircraft-based observational measurement campaigns (e.g. ACE-2, Brenguier et al., 2000) were

2146 able to show clear evidence of aerosol Twomey effects, but definitive evidence of Albrecht

2147 effects remained elusive.

2148

2149 Until this point, there was little/no information available from observational sources with a

2150 global reach (i.e. satellites or global surface networks) with which the global models could be

2151 challenged. The first satellite retrievals of τ_{aer} (at midvisible wavelength) appeared, based on

2152 the reflectance from a single visible spectral channel from the AVHRR satellite sensor (Husar et

2153 al., 1997; Fig 5.2).

2154
2155 These retrievals were restricted to cloud-free regions over ocean owing to difficulties in

2156 accurately characterizing surface reflectance properties over land and cloudy regions, but for the

2157 first time these retrievals were able to detect the geographic distribution of aerosols, and how

2158 these distributions shifted according to the season. These observations emphasized that, to

2159 compare model results against those from observations, both natural and anthropogenic aerosols

2160 need to be modelled, particularly those of mineral dust (e.g. Woodward, 2001) and sea-salt

2161 aerosol (Fig 5.2).

2162

2163

2164

2165

2166 **Fig 5.2**. The equivalent aerosol optical thickness EAOT) derived from a single channel

2167 (algorithm of the AVHRR satellite sensor (reproduced from Husar et al., 1997).

2168

2169

2170

2171
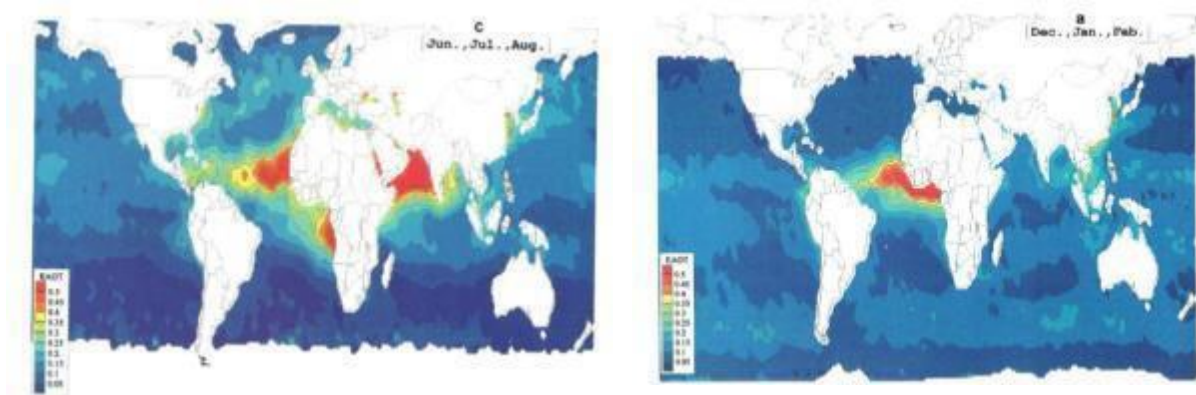
2178 Improved detection algorithms soon followed using 2-channels (AVHRR; Mishchenko et al.,

2179 1999) or polarization (POLDER; Deuzé et al., 1999). The use of 2-channel retrievals and

2180   polarization allowed, for the first time, separation between coarse and fine mode aerosol

2181   particles based on the measured Angstrom exponent (i.e. the wavelength dependence of τaer)

2182   and depolarization respectively. Initial estimates of the direct radiative effect were also made

2183   over the cloud-free oceans (e.g. Haywood et al., 1999; Boucher and Tanré, 2000), but the

2184   problem of deriving a radiative forcing (i.e. the change in the radiative effect since pre-

2185   industrial times) remained. Concurrently with satellite observations, significant investment was

2186   made in the global network of aerosol sun-photometers (Holben et al., 1998) that were able to

2187   measure τ_{aer} from direct sun measurements. The first sun photometer was deployed in 1993, but

2188   this network was to blossom over the next two decades with the number of sites operational in

2189   June 1998/2008/2018 increasing from 33/>200/>400 globally. AERONET has become a

2190   mainstay for checking both the calibration of satellite τ_{aer} retrievals and modelled τ_{aer}.

2191

2192   Given the rapid growth in model estimates of direct and indirect effects, IPCC (2001)

2193   commissioned an Intercomparison workshop (Penner et al., 2001) to provide global model

2194   estimates of various aerosol parameters such as speciated natural and anthropogenic burdens,

2195   direct and indirect radiative forcings; in many ways this may be considered the forerunner of the

2196   Aerosol Comparisons between Observations and Models project (AeroCom; Kinne et al., 2006).

2197   Because of the rapid expansion of estimates of both direct and indirect effects, IPCC

2198   (Ramaswamy et al., 2001) expanded the number of aerosol species assigned a direct radiative

2199   forcing; sulfate (- 0.40W m-2, x2 uncertainty), biomass burning aerosols (-0.20W m-2, x3

2200   uncertainty), BC from fossil fuel use (FFBC) (+0.2W m-2, x2 uncertainty), organic carbon from

2201   fossil-fuel use (FFOC; -0.10W m-2, x3 uncertainty), mineral dust (range -0.6 to +0.40W m-2)

2202   and estimated the total combined Fdirect to be -0.6W m-2 (range -0.1 to 1 W m-2). While

2203   diagnosing aerosol direct radiative effects within GCMs was straightforward, diagnosing aerosol

2204   indirect forcing beyond the Twomey effect became problematic because the strict definition of

2205   radiative forcing required "surface and tropospheric temperatures and state held fixed at the

2206   unperturbed values" (Ramaswamy et al., 2001). This definition precluded allowing changes in

2207   cloud macrophysical properties such as cloud liquid water path (Albrecht, 1989) and subsequent

2208   impacts on cloud fraction, cloud height etc. Thus, in a strict radiative forcing sense, only

2209   FTwomey could be calculated within GCMs, although some studies simply used the difference

2210   between two simulations with pre-industrial and present-day aerosols with fixed sea-surface

2211   temperatures to attempt to diagnose aerosol-cloud impacts beyond Twomey effects

2212   (Rotstayn,1999; Jones et al, 2001). These studies can be thought of as forerunners of the

2213   "Effective RadiativeForcing (ERF) concept" (section 2). The fidelity and utility of ERF was far

2214   from proven however,so IPCC (2001) assigned only the Twomey effect with a radiative forcing,

2215   with an increased uncertainty range of 0 to -2 W m^{-2}. A comprehensive discussion of the basis

2216   and quantitative estimates of the direct and indirect radiative forcing is provided by Haywood

2217   and Boucher (2000).

2218

2219

2220

5.4.Explicit treatment of aerosols within GCMs and improved observational capability:

2000s.

2224

As computing power increased and advances were made through observations and fundamental

developments in the physics of aerosols, GCMs increasingly incorporated detailed aerosol

chemistry, transport and microphysics schemes, frequently on a species-by-species basis under

the assumption of external mixing. Models began to incorporate enough of the natural and

anthropogenic species prevalent in the atmosphere to make meaningful inter-comparisons

against observations from e.g. surface-based AERONET sun photometer sites and satellite

retrievals. However, determining differences in performance between the models was

complicated by the impacts of differing emissions, differing time-periods of analysis, and

different analyses of observational constraints (Textor et al., 2007). Hence, many modelling

centres joined the AeroCom initiative (Kinne et al., 2006, Schulz et al., 2006) which provided

a platform for consistent model-model and model-observation intercomparisons. AeroCom

initially focused on inter-comparison of aerosol optical properties (Kinne at al., 2006) and

aerosol direct radiative forcing (Schulz et al., 2006). AeroCom's remit rapidly expanded

considerably to include a wide range of intercomparisons such as aerosol indirect effects

(Penner et al., 2006; Quaas et al., 2009) along with more specific objectives such as

comparisons of model derived vertical profiles against satellite-borne lidars (Koffi et al., 2011)

and in-situ black-carbon profiles (Schwarz et al., 2010), enabling refinements of model

performance.

2243

2244   The majority of aerosol schemes at this time treated aerosols in 'bulk' form i.e. aerosol mass

2245   was transported, but the detailed description of aerosol microphysics was not included. Aerosol

2246   size distributions and hygroscopic growth factors were assumed based on in-situ measurements

2247   of aerosol properties from surface sites, in-situ aircraft-based measurements, or validated

2248   AERONET sky-radiance-based retrievals (Dubovik and King, 2000, Haywood et al., 2003). At

2249   the time, the impacts of relative humidity on the radiative forcing of aerosols via their influence

2250   on optical properties and in particular the specific extinction coefficient were frequently

2251   accounted for via measurements of the hygroscopic growth using e.g. airborne humidified

2252   nephelometer systems. For example, Kotchenruther and Hobbs (1998) and Kotchenruther et al.

2253   (1999) provided hygroscopic growth parameterisations for biomass burning aerosols in Brazil

2254   and industrial pollution off the east coast of the USA, respectively.

2255

2256   In addition to aerosol direct effects and aerosol indirect effects, the aerosol semi-direct effect

2257   started to receive some considerable attention. The semi-direct effect is the mechanism

2258   whereby aerosol absorption leads to heating of the atmospheric column, increasing atmospheric

2259   stability and decreasing the relative humidity. These impacts were postulated to inhibit cloud

2260   formation in the layer of absorbing aerosols, but also alter cloud cover in other parts of the

2261   troposphere (e.g. Ackerman et al., 2000; Johnson et al., 2004; Hansen et al., 1997). Diagnosing

2262   the semi-direct effect of aerosols using the strict definition of radiative forcing (holding all

2263   other atmospheric variables fixed) was not possible; as for aerosol indirect effects beyond the

2264   Twomey effect this posed a significant problem in quantification of radiative forcing.

2265

2266   MODIS TERRA started producing τ_{aer} data in 2002, with MODIS AQUA following in 2002

2267   (Remer et al., 2002); they are still providing essential data for validation and data assimilation

2268   to this day. Other satellite sensors provided considerable additional information (e.g. MISR,

2269   Kahn et al., 2002; AATSR/AATSR-2, Table 2.2 of Forster et al., 2007). However, the

2270   combination of the near-global daily coverage, developments of retrievals over land surfaces

2271   (Hsu et al., 2006), cross calibration with the highly accurate AERONET network, ease of data

2272   access and the longevity of this data-set has resulted in MODIS becoming the mainstay for

2273   model validation for both τ_{aer} and for examining aerosol indirect effects via relationships

2274   between aerosol and clouds (Quaas et al.,2009). Development of near-global coverage of τ_{aer}

2275   from satellites and accumulation mode fraction from the MODIS instrument augmented by in-

2276   situ aircraft-based measurements allowed the first mainly observational estimate of aerosol

2277   direct effects (Bellouin et al., 2005) compared to the earlier efforts using model-observation

2278   analysis. The anthropogenic fraction was recognized as being almost entirely in the

2279   accumulation mode, while natural aerosols in the form of sea-salt and mineral dust are typically

2280   in the coarse mode allowing a first observational estimate of the perturbation of τ_{aer} by

2281   anthropogenic emissions and an associated F_{direct} of -0.8W m^{-2}. Similar methods followed

2282   (Chung et al., 2005, -0.35W m^{-2}; Yu et al., 2006, -0.5W m^{-2}); these estimates were generally

2283   rather stronger than those from models, potentially due to the fact that absorbing aerosols (e.g.

2284   anthropogenic biomass burning aerosols above clouds) were neglected which can frequently

2285   produce positive radiative forcings (e.g. Keil and Haywood, 2003)

2286
2287   More sophisticated estimates of the direct radiative effect of aerosol in cloud-free skies over

2288   oceans were also developed by correlating the cloud-free TOA upward solar irradiance

2289   (frequently derived from CERES) against the aerosol optical depth derived from other

2290 instruments such as VIRS or MODIS (Loeb and Kato, 2002; Zhang et al., 2005, Loeb and

2291 Manalo-Smith, 2005). These estimates provide additional validation data for testing

2292 relationships in GCMs, but cannot be used to infer the radiative forcing by themselves owing to

2293 lack of knowledge of pre-industrial conditions.

2294

2295 Aerosol indirect forcing based on satellite retrievals were also developed. Typically these

2296 studies developed relationships between CDNC and fine mode aerosol concentrations or optical

2297 depth (Quaas, 2005; Quaas and Boucher, 2005). For example, Quaas and Boucher (2005)

2298 developed relationships between observed cloud properties from MODIS and observed aerosol

2299 properties from POLDER for stratiform marine clouds and for convective clouds over land and

2300 utilized these relationships within GCMs. Various methods for partitioning the observed

2301 relationships as a function of meteorology, above cloud moisture, and SSTs were to be

2302 developed to account for the impacts of meteorology that can confound derived relationships in

2303 observational studies. However, a persistent problem with these correlative studies is the mutual

2304 exclusivity of aerosol and cloud satellite retrievals and the lack of account of the relative

2305 vertical profile of aerosol and cloud.

2306

2307 IPCC (2007) and Forster et al (2007) recognized that the growing number of different aerosol

2308 species that were being considered in climate models was becoming unwieldy; while aerosol

2309 components were still assigned individual radiative forcing values, only the total aerosol direct

2310 effect and cloud albedo effect were included on the bar chart. Direct radiative forcing estimates

2311 were predominately model-based relying on a combination of AeroCom/non-AeroCom

2312 estimates and revealed F_{direct}=-0.5±0.4W m^{-2} (5% to 95% confidence), while the Twomey effect

2313   was estimated to be -0.7W m^{-2} (best estimate) with a 5% to 95% range of -0.3 to -1.8W m^{-2}

2314   (Forster et al., 2007). For the first time, Forster et al (2007) presented the spread in the long-

2315   lived GHG, aerosol and total radiative forcing using a Monte-Carlo simulation of the

2316   uncertainties associated with each of the forcing mechanisms (Boucher and Haywood, 2001) to

2317   demonstrate that the uncertainty in the total radiative forcing was dominated by that of aerosols,

2318   particularly owing to uncertainties in the aerosol indirect effects, and that the total radiative

2319   forcing was positive, consistent with the observed warming of climate. Forster et al (2007)

2320   recognized that interactions of aerosols with mixed-phase and ice-clouds continued to be

2321   impossible to quantify on a global mean basis owing to the even greater complexity of these

2322   clouds when compared to warm liquid- phase clouds.

2323

2324

2325
2326

112

2327

2328   **5.5.Increases in aerosol model complexity – 2nd generation models: 2010s**

2329

2330   As aerosol modelling matured, further refinements of aerosol direct and indirect effects were

2331   included in GCMs. Further components of aerosol were included; Bellouin et al (2011) included

2332   nitrate aerosol and pointed out that as sulphur dioxide emissions decrease in the future owing to

2333   emission control, the radiative forcing of nitrate will likely increase owing to the availability of

2334   excess ammonia in the atmosphere. However, nitrate continues to remain a difficult aerosol to

2335   model owing to the dissociation to nitric acid and ammonia under ambient temperature and

2336   humidities.

2337

2338   The development of aerosol mass spectrometers and their location at surface sites and airborne

2339   platforms enabled, for the first time, a full appreciation of the complexity of optically active sub-

2340   micron aerosol composition as a function of location and altitude to be deduced (Jimenez et al.,

2341   2011) with sulphate, organic and nitrate highlighted as the dominant sub-micron components. The

2342   problems of the mutual exclusivity of satellite-retrievals of aerosol and cloud can be avoided using

2343   active satellite sensors such as CALIPSO lidar aerosol data collocated with MODIS cloud data

2344   (e.g. Costantino and Bréon, 2013). However,in-situ airborne platforms with dedicated

2345   instrumentation such as nephelometers, and aerosol optical particle counters continued to provide

2346   vital information on the aerosol vertical profiles at a level of detail and vertical resolution

2347   impossible to achieve with satellite mounted lidars.

2348

113

2349

2350

2351   In modelling, dual-moment schemes became more common, treating both aerosol number and

2352   aerosol mass prognostically (Stier et al., 2005) and both internal and external mixtures. This has

2353   particular relevance to estimates of aerosol-cloud-interactions because, for single-moment

2354   schemes with prognostic mass only, any increase in the aerosol mass (e.g. via condensation or

2355   coagulation), must artificially increase the aerosol number and hence CCN which then produces

2356   stronger aerosol indirect effects. The use of dual-moment state-of-the-art aerosol schemes in

2357   GCMs is now common-place.

2358

2359   Lohmann et al. (2010) examined the differences between i) the radiative flux perturbation (RFP;

2360   Haywood et al., 2009) which is calculated as the difference in the top-of-the-atmosphere

2361   radiation budget between a present-day simulation and a preindustrial simulation, both using the

2362   same sea surface temperatures and ii) the radiative forcing computed from two–calls to the

2363   radiative transfer code in GCMs holding the atmospheric state fixed. The RFP calculation allows

2364   for rapid responses (e.g. in clouds), that occur on a faster time-scale than the large-scale shifts in

2365   climate response thaare induced through SST responses. RFP has become more commonly

2366   known as the effective radiative forcing (ERF – see Section 2.3.6). Allowing rapid adjustment to

2367   occur in diagnosing the ERF allowed isolation of both the Twomey (1977) and the Albrecht

2368   (1989) aerosol indirect effects and also aerosol semi-direct effects.

2369

2370

2371

2372   Myhre (2009) suggested that the discrepancy between observational (stronger) and modelled

2373   (weaker) estimates of aerosol direct forcing highlighted in IPCC (2007) was due to the lack of

2374   account of aerosol absorption above clouds and (ii) relatively larger fractional increase in BC

2375   containing absorbing than scattering aerosols since pre-industrial times. Analysis of models

2376   reported an aerosol direct radiative forcing of -0.3W m^{-2} which was found to be consistent with

2377   observational estimates. Aerosol absorption was again highlighted as a major uncertainty in

2378   accurate determination of aerosol direct radiative forcing (Bond et al., 2013) owing to aspects such

2379   as the morphology of the black carbon as a function of age and the impact of coatings of organic

2380   and inorganic components, the heating in the atmospheric column and subsequent rapid

2381   adjustment. Again this suggested that diagnosing the radiative forcing in a strict sense could not

2382   capture the rapid adjustment associated with atmospheric processes.

2383

2384   Boucher et al. (2013), Myhre et al (2013) and IPCC (2013) recognized that retaining the strict

2385   definition of radiative forcing as in previous IPCC reports was becoming untenable because it

2386   did not reflect the growing consensus that rapid responses can and should be isolated in any

2387   metric ofclimate change, but also because of the ease of application to GCM simulations. Hence

2388   the growth of ERF as the preferred metric for assessing potential climate impacts. Indeed, IPCC

2389   also chose the term aerosol-radiation-interactions over the aerosol direct forcing and aerosol-

2390   cloud interactions over aerosol indirect with rapid adjustment of aerosol-radiation interaction as a

2391   term for the semi-direct effect (Boucher et al., 2013). By this time there were many mature

2392   estimates of the impact of aerosol-radiation-interactions and aerosol-cloud-interactions from

2393   sophisticated GCMs and satellite-based estimates (e.g. Fig 5.3; see also Table 7.4 and 7.5 of

2394   Boucher et al. , 2013) allowing Myhre et al (2013) to estimate the magnitude of pre-industrial to

2395   present-day aerosol-radiation-interactions (-0.45W m^{-2} with a 95% uncertainty range of -0.9 to

2396   +0.05W m^{-2})and aerosol-cloud-interactions (-0.45W m^{-2} with a 95% uncertainty range of -1.2

2397   to 0 W m^{-2}).

2398

2399
2400

2401
2402
2403
2404   **5.6. Current promising lines of research**
2405

2406   We have seen that the radiative forcing (or effective radiative forcing, ERF) has changed

2407   significantly from best estimates of stronger than -2 W m-2 (Charlson et al., 1991; 1992)

2408   to weaker than -1 W m-2. Much of this reduction in magnitude of the radiative forcing via the

2409   direct effect (aerosol-radiation-interactions) was captured by the late 1990s owing to the use of

2410   GCMs (e.g. Kiehl and Briegleb, 1993) and by accounting for the effects of aerosol absorption by

2411   black carbon (Haywood and Shine, 1995). However, uncertainties in both the aerosol-radiation

2412   and aerosol-cloud interactions have remained stubbornly difficult to reduce owing to structural

2413   and parametric uncertainties. Here we ask what progress has been made in the 5-years since

2414   IPCC (2013) in terms of promising avenues of research.

2415

2416   The direct radiative effect/forcing of aerosols above clouds has remained a contentious issue

2417   with some very strong instantaneous positive radiative effects (greater than +130 to +150 W m-2)

2418   being diagnosed from various satellite instruments (e.g. de Graaf et al., 2012; Meyer et al., 2015;

2419   Peers et al., 2016) over the S.E. Atlantic; values that are stronger than those from climate models

2420   (de Graaf et al., 2014). Zuidema et al (2016) highlights that global models diverge when

2421   determining the direct radiative effect in the region. This is because the direct radiative forcing of

2422   a partially absorbing aerosol such as biomass burning aerosol depends not just on determination of

2423   the aerosol optical depth and aerosol absorption properties, but on the cloud amount, cloud reflectance

2424   and the relative vertical profile of cloud relative to the aerosols (see Fig 5.4). The ORACLES, LASIC,

117

2425   CLARIFY and AeroClo-SA in-situ aircraft-based measurement campaigns have targeted deriving

2426   better estimates of the direct effect

2427

2428
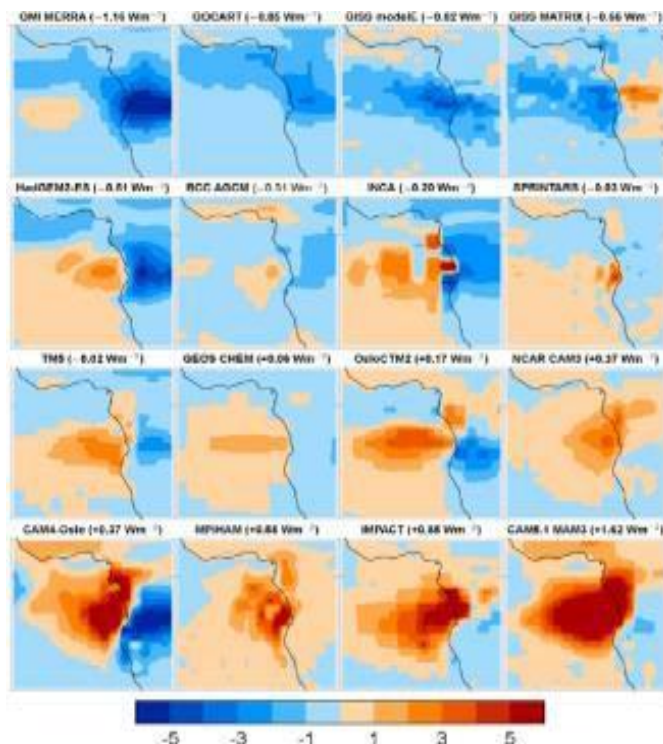
Figure 5.3. Showing the direct radiative effect of partially absorbing biomass burning aerosols diagnosed from 16 different climate models. The model with the strongest negative direct radiative effect is shown on the top left, while that with the strongest positive forcing is on the bottom right.

2429   of absorbing aerosols over clouds as one of their primary objectives (Zuidema et al., 2016).

2430   These measurement campaigns will undoubtedly give a better understanding of direct radiative

2431   effects of partially absorbing aerosols above clouds in the key-region of the SE Atlantic, but the

2432   change inconcentration from pre-industrial times may well preclude accurate determination of

2433   the radiative forcing.

2434

2435

2436

2437

2438   Accurate representation of pre-industrial aerosol concentrations is also highlighted as a key

2439   uncertainty by Carslaw et al. (2013), who used a statistical emulator approach to examine the

2440   sensitivity of the aerosol forcing to a wide range of parameters including uncertainties in

2441   anthropogenic and natural emissions. The variance caused by uncertainties in natural aerosol

2442   concentrations accounted for around 45% of the variance, while uncertainty in anthropogenic

2443   emissions accounted for around 35% of the variance due to the impact that natural

2444   backgroundaerosols have on the susceptibility of clouds to anthropogenic perturbations. Based

2445   on the limited paleodata, desert dust may have increased by almost 40% over the twentieth

2446   century due to a combination of climate change and land use (Mahowald et al., 2010; Ginoux et

2447   al., 2012). An important and likely source of higher preindustrial aerosols, which is currently

2448   poorly constrained, are wildfires. Recent studies have suggested that due to uncertainties in

2449   preindustrial wildfire emissions alone, the range of anthropogenic indirect effects could be

2450   between -0.1 W/m2 to -1.1 W/m2 (Hamilton et al., 2018). If these estimates are supported by

2451   more studies, we would have to rethink how we constrain estimates of both aerosol indirect

2452   effects from anthropogenic aerosols and climate sensitivity (see Section 6.0 for more discussion).

2453

2454   Progress been made in understanding the impact of anthropogenic emissions on mixed-phase

2455   cloud by contrasting observations of their behavior against liquid-phase clouds. Christensen et

2456   al., (2014) examined ship-track data in mixed-cloud environments and found a more muted

2457   indirect radiative forcing impact owing to enhanced glaciation induced precipitation that limited

2458   the total water path of the clouds. Christensen et al. (2016) extended these observations by using

2459   multiple sensors over millions of atmospheric profiles and concluded that liquid clouds

120

2460   dominate any negative radiative forcing for the aerosol indirect effects owing to the muted

2461   impacts of mixed-phase clouds and a counterbalancing positive radiative forcing from

2462   convective clouds. These observations call into question whether net aerosol indirect effects

2463   have been overestimated.

2464

2465   Ghan et al. (2016) performed an intercomparison to isolate the strength of the Twomey and

2466   Albrecht aerosol-cloud-interaction effects in GCMs, and showed that while all models exhibited

2467   a reasonably consistent Twomey effect, the strength of the Albrecht effect essentially fell into

2468   two clusters. The cluster were i) an almost negligible impact, ii) a strong positive forcing that

2469   acted to reinforce the radiative forcing from the Twomey effect, but observational evidence

2470   remained lacking as to which one of these responses was correct. However, one interesting line

2471   of evidenceto elucidate the strength of the Albrecht effect was the use of large-scale SO_2-

2472   degassing volcanic eruptions in relatively pristine environments to examine the impact on

2473   satellite-derived cloud properties. This technique was first used by Gasso (2008), on relatively

2474   modest degassing events and has been the subject of further research (Toll et al., 2017). These

2475   smaller scale degassing eruptions can be used to examine relationships between cloud and

2476   aerosol in a similar way to ship- tracks (Christensen et al., 2014; Chen et al., 2015), but are

2477   frequently on too small a scale for the impacts to be directly compared against GCMs capable of

2478   diagnosing a radiative forcing. This situation changed in 2014 with the fissure eruption at

2479   Holuhraun, Iceland which emitted a huge plume of SO_2 across the entire north Atlantic

2480   (Gettelman et al., 2015) causing a clear, statistically significant reduction in the cloud effective

2481   radius in the MODIS satellite record (McCoy and Hartmann, 2015, Malavelle et al., 2017), but

2482   no discernible impact of the cloud liquid water path. Malavelle et al. (2017) were able to show

2483   that only models with a modest Albrecht effect were consistent with observations for a host of

2484   liquid-water cloud conditions. In a similar vein, Chen et al (2014) showed that variations in

2485   cloud liquid water paths are dominated by other meteorological factors such as the state of

2486   precipitation, humidity and atmospheric stability rather than aerosol microphysical processes

2487   making definitive detection and attribution difficult.

2488

2489   These advances provide an opportunity to better constrain aerosol indirect effects in the future;

2490   without pursuing these opportunities to confront model performance, an accurate

2491   characterization of aerosol radiative forcing is likely to prove elusive. There is however, a

2492   growing consensus that, in the future, the importance of the radiative forcing of aerosols will

2493   begin to be a less important uncertainty as the radiative forcing from greenhouse gases continues

2494   to increase. Global emissions of sulphur dioxide have plateaued at around 1990, and have begun

2495   to fall on a global mean basis owing to effective clean-air policies targeted at reducing

2496   particulate pollution. Areas such as the US and Europe have already seen reductions in sulphur

2497   dioxide emissions of around a factor of 5 since their peak. This reduction in emissions, coupled

2498   with the ever increasing radiative forcing from greenhouse gases may result in significant rates of

2499   global warming over the next few decades (e.g. Andreae et al., 2005).

2500

2501   Where aerosols may start to play an increasing role is in the, currently theoretical, field of

2502   geoengineering i.e. the deliberate injection of aerosols or their precursors into the stratosphere to

2503   mimic the cooling impacts of explosive volcanic eruptions such as Pinatubo or the deliberate

2504   injection of aerosols into stratocumulus clouds to mimic the impacts of natural degassing

2505   volcanoes. The use of such techniques would have many, many consequences (e.g. Robock et al.,

122

2506   2008), not least that, if proven effective, it could reduce the drive for reduced use of fossil-fuels

2507   (see Section 13 for a comprehensive discussion).

2508
2509

2510   1990   2000   2010   2020+

2511
2512
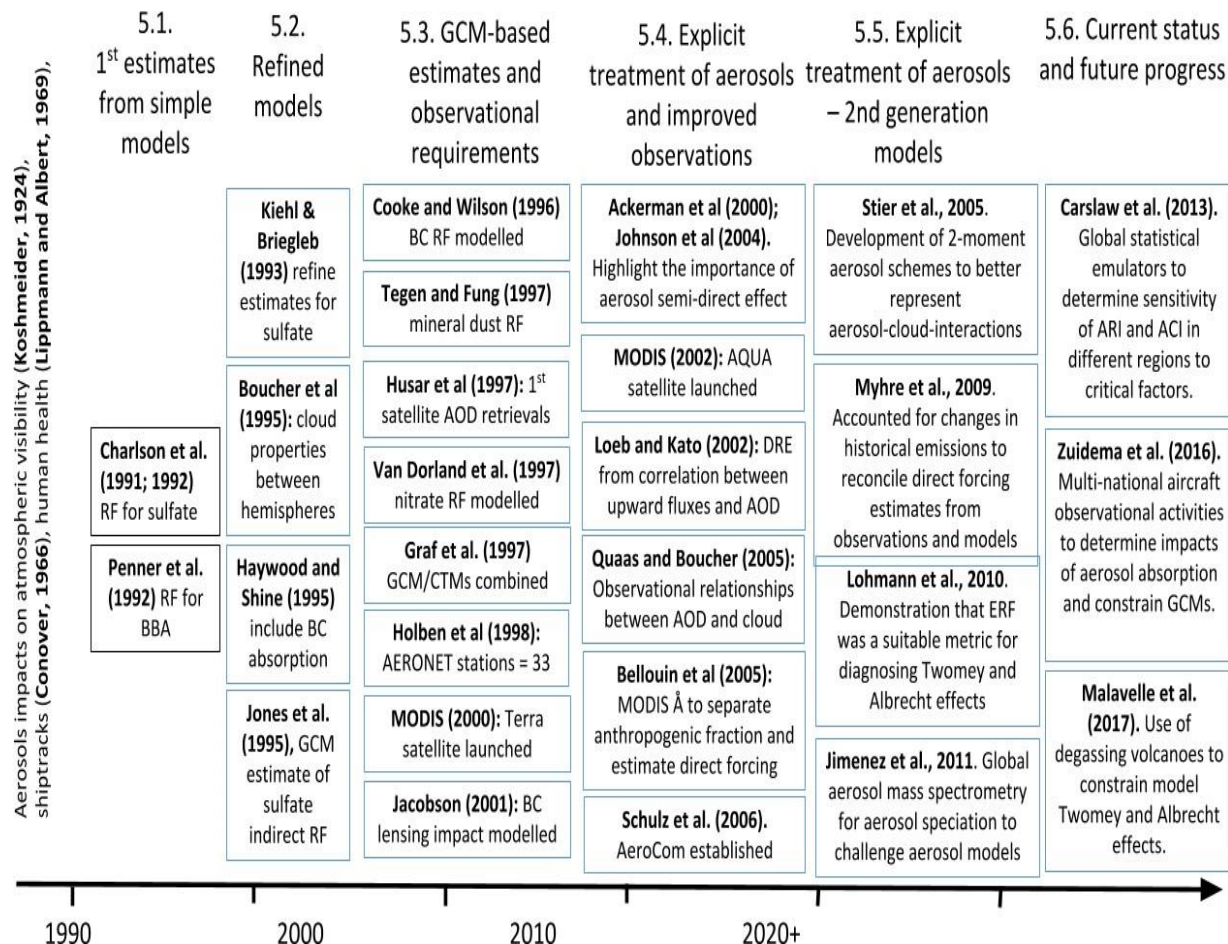
2513   **Figure 5.4.** Illustrating the time evolution of some of the most significant findings that

2514   are discussed in the text. Keil, A., and Haywood, J.M., Solar radiative forcing by

2515   biomass aerosol particles over marine clouds during SAFARI-2000. J. Geophys. Res.,

2516   8467, 108(D13), doi:10.1029/2002JD002315, 2003.

2517
2518
2519

123

6. Land and biogeochemistry interactions

Human activities do not only directly emit gases and aerosols which impact climate, as

described above, they also modify the land surface, which can directly change the surface

properties, and both directly and indirectly change the emissions of different gases and aerosols

(Feddema et al., 2005; Heald and Spracken, 2015; Myhre et al., 2013; Pielke, 2005; Ward et al.,

2014). Land conversion of forests, for example to croplands, emits carbon dioxide immediately,

and the land cover change and the land management has many implications for albedo changes,

and emissions Feddema et al., 2005; Heald and Spracken, 2015; Myhre et al., 2013; Pielke,

2005; Ward et al., 2014). Changes in land surface, such as urbanization or deforestation, can

also change the local experience of climate in substantial ways, but these are not contributing to

changes in the top of atmosphere radiative forcing directly, and thus are not discussed here

(Field et al., 2014; Hartmann et al., 2013; Lejeune et al., 2018). We also do not consider longer

term feedbacks, such as the fertilization of land or ocean ecosystems by anthropogenic aerosols,

which could be as large as the direct radiative effects of anthropogenic aerosols (Mahowald,

2011). Generally speaking, understanding and quantifying how changes to the land surface are

impacting the climate are more difficult than some of the direct emissions from human activities

described previously (Boucher et al., 2013; Myhre et al., 2013).

The most important impact of human land use and land cover change (LULCC), in terms of

radiative forcing of climate, and one of the first processes included in the IPCC assessment

reports are the direct emissions of CO2 from deforestation, and the indirect emissions of CO2

from forest degradation and land management (IPCC, 1990). Other processes, such as the

albedo changes, interactions with wildfires and other processes, were mentioned in the first

2544   report, but not quantified (IPCC, 1990). In subsequent AR, these processes were expanded upon

2545   and quantified, as described below.

2546
2547   For long-lived gases, which can be assumed to be relatively well-mixed across the troposphere,

2548   such as carbon dioxide, methane or nitrous oxides, estimates of changes in the atmospheric

2549   composition rely on ice core and other observational records, as discussed previously (Forster et

2550   al., 2007; Myhre et al., 2013). But for short-lived gases and aerosols, an important difficulty in

2551   understanding how human activities have changed past atmospheric conditions, especially for

2552   example, in understanding base line preindustrial chemistry or aerosol conditions, is that there

2553   are no direct observations of preindustrial conditions for short lived gases or aerosols, since the

2554   ice core records from just a few sites cannot characterize the global average for short-lived

2555   constituents (Myhre et al., 2013). For short-lived gases and aerosols, their emissions are

2556   estimated based on simple assumptions or modeling studies (Boucher et al., 2013; Collins et al.,

2557   2017; Lamarque et al., 2010; Van Marle et al., 2017; Myhre et al., 2013; Shindell et al., 2013).

2558   Recent studies have highlighted the importance of potential changes in emissions from 'natural'

2559   sources due to human activities, especially on the land surface (Carslaw et al., 2010, 2013;

2560   Hamilton et al., 2018; Mahowald et al., 2011, 2010; Myhre et al., 2013; Ward et al., 2014), so

2561   here we review the state of knowledge on how humans can perturb natural sources. We will also

2562   review evolution of the representation of human land use forcings of climate in the IPCC

2563   reports, as an indication of how the understanding of how human activities on the land surface

2564   impacting natural sources of different important radiative constituents has evolved.

2565

2566
2567

6.1 Land use and land cover change climate forcers

The interactions of land use and land cover change are shown in Figure 1 and described in more detail in each section below.

6.1.1 Albedo impacts from land use and land cover change

The direct modification of the surface from land use, land management or land cover change can be through albedo changes or through changes in the energy fluxes locally (Andrews et al., 2017; Bonan, 2008; Feddema et al., 2005; Myhre et al., 2013; Pielke, 2005). The surface albedo (ratio of the reflected and incoming solar radiation) varies between dark forests, lighter grasslands or crops, and often even lighter barren deserts or snow covered surfaces. Consequently, deforestation tends to increase the Earth's albedo, and cause more light to be reflected, cooling the Earth. The largest impacts of land use and deforestation will occur at higher latitudes because snow covered forests retain a low albedo, while snow covered crop-lands will have a high albedo (IPCC, 2001). Recently satellite measurement have been used to estimate the impact of land use on radiative forcing (Myhre et al., 2013; Zhao and Jackson, 2014). Estimates of the changes since preindustrial require the use of models, and the biophysical impacts of LULCC are sensitive to the model's used; a Land Use Model Inter-comparison project (LUMIP) is underway to better constrain the impacts on radiative forcing (Lawrence et al., 2016). Changes in the land surface, such as changes in vegetation, and their impact on the surface albedo have been included in the assessments since the first report (IPCC, 1990), but not quantified until the third report, to be -0.2 +/- 0.2 W/m2 (IPCC, 2001). The

126

2593   estimates and uncertainty stayed the same in the AR4, but became slightly smaller, with smaller

2594   uncertainties in the AR5 (-0.15 +/- 010 W/m2) (Myhre et al., 2013).

2595

2596

6.1.2. Carbon dioxide emissions

The gross carbon dioxides emissions or uptake from natural ecosystems, both land and ocean, are much larger than the fluxes from anthropogenic emissions but the net emissions are close to zero (Ciais et al., 2013; Le Quere et al., 2013; Le Quéré et al., 2016; Sitch et al., 2015). Deforestation and conversion of natural lands for human management tend to directly release carbon dioxide into the atmosphere, while reforestation, afforestation, or carbon dioxide fertilization will increase the uptake of carbon dioxide into the terrestrial system, including soils (Ciais et al., 2013; Friedlingstein et al., 2006; Houghton, 2018; Le Quere et al., 2013). In addition, the change in land cover and land management changes the longer term uptake of carbon dioxide (Ciais et al., 2013; Friedlingstein et al., 2006; Houghton, 2018; Le Quere et al., 2013). Over all of the IPCC assessment reports, ice core data is used for carbon dioxide changes, which does not require the attribution of the change in carbon dioxide from land surface changes versus direct emission (Ciais et al., 2013; Denman et al., 2007; IPCC, 1996, 2001; Stocker et al., 2013). However, starting already in the FAR, there was an important division between land use emissions and other emissions identified in the reports (IPCC, 1990). The 2000 Special report on land use, land use change and forestry was written in support of the Kyoto Protocol and provided

6.1.3 Wildfires and biomass burning

Natural ecosystems can emit short-lived gases and aerosols through a variety of processes, and these processes can be modified by human activities (Carslaw et al., 2010, 2013; Hamilton et al., 2018; Mahowald et al., 2011, 2010; Myhre et al., 2013; Ward et al., 2014) (Figure 6.1). Of the most important is likely to be changes in wildfire regimes (Arneth et al., 2010; Carslaw et

128

2622   al., 2010; Ward et al., 2014). Intermittent wildfires release substantial amounts of carbon

2623   dioxide, carbon monoxide, sulfur dioxide, methane and other organic gases, and carbonaceous

2624   aerosols (Andreae and Merlet, 2001). Wildfire sources of methane were identified already in the

2625   FAR. Biomass burning aerosols were one of the first three aerosols considered in the TAR

2626   (along with industrial sources of sulfate and black carbon). For AR4 and AR5, studies suggested

2627   that preindustrial wildfires were much less than in current climate, as they attributed wildfires to

2628   deforestation fires (Boucher et al., 2013; Forster et al., 2007; Lamarque et al., 2010). Recent

2629   evidence suggests strong changes in wildfire over the last 250 years, with a large increase in

2630   fires about 200 years ago, and then a decrease (Kloster et al., 2010; Marlon et al., 2008, 2012;

2631   Pechony and Shindell, 2010; Zennaro et al., 2014). Recently, evidence from satellites has

2632   suggested a 25% decrease in fires over the last 18 years, likely to due to the expansion of

2633   agriculture (Andela et al., 2017). While increases in biomass burning due to deforestation and

2634   climate change are assumed to have occurred since preindustrial times in the standard estimates

2635   used for CMIP6 (Van Marle et al., 2017), some estimates suggest a decline instead, due largely

2636   to a change in human fire and land management (Hamilton et al., 2018; Marlon et al., 2008;

2637   Zennaro et al., 2014). These large decreases in wildfire emissions, over the Anthropocene are

2638   large enough to have an impact on indirect and direct aerosol radiative forcing so that they

2639   offset those from direct anthropogenic emissions (Hamilton et al., 2018). For example, that

2640   study suggested that new wildfire emission estimates increase estimated anthropogenic aerosol

2641   indirect forcing from -1.1 W/m2 using the CMIP6 emission datasets to 0.1 W/m2 using LMfire

2642   estimates of wildfire (Figure 6.1; using global averages from Hamilton et al., 2018). In other

2643   words, because the preindustrial wildfire emissions are poorly constrained,

2644   current day anthropogenic aerosol radiative forcing could be -1.1 W/m2 or 0.1 W/m2 using the

129

2645 same model but different emission estimates. This has profound implications for our

2646 understanding, not only of anthropogenic aerosol radiative forcing, but also climate sensitivity,

2647 which is very sensitive to assumptions about the size of the anthropogenic aerosol radiative

2648 forcing (Knutti et al., 2002; Myhre et al., 2013).

2649
2650
2651 **6.1.4. Agricultural activity and soils**
2652
2653 Soils naturally release nitrogen oxides, nitrous oxide and ammonia: changes in nitrogen inputs

2654   or temperature can radically modify the amount of nitrogen oxides or ammonia released (Ciais

2655   et al., 2013; Fowler et al., 2013). Since agriculture, and especially the green revolution, there

2656   has been a substantial modification of the nitrogen budgets of regions with land use, modifying

2657 substantially the nitrogen inputs (Ciais et al., 2013; Fowler et al., 2013). In terms of direct

2658 radiative forcing of nitrogen-based species, nitrous oxide is the most important and is a long-

2659 lived greenhouse gas, with a lifetime on the order of 100 years (Ciais et al., 2013). Already in

2660 the FAR, the agricultural sources of nitrous oxide were identified, if not quantified (IPCC,

2661 1990), while in the SAR and later reports, estimates for the agricultural sources of nitrous

2662 oxides were quantified (Ciais et al., 2013; Denman et al., 2007; Forster et al., 2007; IPCC, 1996,

2663 2001; Myhre et al., 2013). The ice core changes over the last hundred years in nitrous oxide

2664 have been attributed to changes in land management (Ciais et al., 2013; Ward et al., 2014).

2665 Nitrogen oxide and ammonia emissions from soils are thought to be enhanced by agricultural

2666 activities, especially nitrogen fertilizers (Fowler et al., 2013; Myhre et al., 2013), and the role of

2667 human land use in modifying these emissions from soils is first mentioned in the TAR (IPCC,

2668 2001). Nitrogen oxide emissions are important climatically for their impact on tropospheric

130

2669   ozone and methane lifetime (section 4), but the anthropogenic part is dominated by combustion

2670   sources (Myhre et al., 2013; Shindell et al., 2017). On the other hand, ammonia emissions are

2671   predominantly from nitrogen fertilization as part of agriculture or pasture usage, which

2672   contribute to a change in ammonium aerosols (Myhre et al., 2013; Riddick et al., 2016; Shindell

2673   et al., 2017; Sutton et al., 2013).

2674
2675
2676
2677

6.1.5. Methane

2678

2679

2680 In inundated regions, methanogens thrive, producing methane from organic material in the soil

2681 (Mathews and Fung, 1987). Changes in the area of inundated areas (for example, due to

2682 expansion of rice paddies or filling of wetlands), productivity of these regions, temperatures and

2683 carbon dioxide itself have impacted the methane emissions from these regions (Kirschke et al.,

2684 2013; Myhre et al., 2013; Paudel et al., 2016; Zhang et al., 2017). In addition to changes in

2685 natural wetland area, rice paddy expansion and ruminant animal husbandry has increased land

2686 use methane production (Kirschke et al., 2013; Myhre et al., 2013). Emissions of methane from

2687 land use change were already considered early in the IPCC process (IPCC, 1990, 2000).

2688

2689

6.1.6. Mineral aerosols (Dust)

2690

2691

2692 Dry, unvegetated land subject to strong winds allow the entrainment of soils into the

2693 atmosphere, causing the largest source of aerosols by mass into the atmosphere (Mahowald et

2694 al., 2011).Desert dust is one of the few aerosols for which we have paleo-records, since it can be

2695 retrievedfrom ice, marine, terrestrial and land records (Albani et al., 2018; Kohfeld and

2696 Harrison, 2001;Mahowald et al., 2010). AR4 assumed that <10% of mineral aerosols were from

2697 anthropogenic sources (Forster et al., 2007). A reconstruction based on paleo-data suggests that

2698 dust may have increased by a factor of almost two across the 20th century (Mahowald et al.,

2699 2010), due to either aridification from climate change (Mahowald, 2007) or land use (Ginoux et

2700 al., 2012). However, between the AR4 and AR5, estimates of the radiative forcing from mineral

2701 aerosols became closer to zero because of a shift in dust properties (Albani et al., 2014;

2702 Mahowald et al., 2010; Perlwitz et al., 2001; Sinyuk et al., 2003), suggesting small

2703 contributions from anthropogenic desert dust to radiative forcing. Mineral aerosols absorb and

132

2704   scatter in both the short wave and long wave, making them complicated in their impacts

2705   (Sokolik and Toon, 1996). The shift to a smaller magnitude radiative forcing for mineral

2706   aerosols is due to both an improved estimate that mineral aerosols are likely more absorbing in

2707   the short wave than previously thought from remote sensing data (Sinyuk et al., 2003), as well

2708   as a consensus that mineral aerosols tends to be larger than previously thought (Kok et al., 2017;

2709   Mahowald et al., 2014). Future projections vary depending on whether they include climate

2710   change impacts (Evan et al., 2016), land use impacts or both (Ward et al., 2014). While the SAR

2711   included the possibility of anthropogenic land use sources of desert dust, (IPCC, 2001; Tegen et

2712   al., 1996) the radiative forcing of this constituent was not included in the report until the TAR

2713   (Forster et al., 2007).

2714
2715
2716   **6.1.7 Organic compounds**

2717
2718   Some plants emit volatile organic compounds (Guenther et al., 2006), which can interact with

2719   nitrogen oxides to change the cycling of tropospheric ozone (Collins et al., 2017; Myhre et al.,

2720   2013), as well as produce secondary organic aerosols (Arneth et al., 2010; Carslaw et al., 2010;

2721   Mahowald et al., 2011; Myhre et al., 2013). Natural ecosystems also emit primary biogenic

2722   aerosols, from fungi, pollen or plant or insect pieces (Despres et al., 2012; Graham et al., 2003;

2723   Mahowald et al., 2011).   Deforestation, climate change or changes in fire frequency can

2724   modify the amount of forests, thereby modifying the emissions from natural forests of these

2725   important constituents (Arneth et al., 2010; Mahowald et al., 2011; Unger, 2014; Ward et al.,

2726   2014). The importance of biogenic derived organics for modifying both ozone and secondary

2727   organic aerosol formation was established by the TAR, although no explicit calculation of the

2728   impact of human land use or fires onto the radiative forcing was performed until after the last

133

2729   assessment (Forster et al., 2007; IPCC, 2001; Myhre et al., 2013), and is thought to be a small,

2730   but important feedback (Unger, 2014; Ward et al., 2014)

2731
2732
2733
2734
2735
2736

2737 **6.2 Snow albedo changes**
2738

2739

2740 Anthropogenic aerosol deposition of black carbon onto snow can change the albedo of the

2741 snow, darkening the snow and warming the globe (Hansen and Nazarenko, 2004) as well as

2742 modifying the melting of the snow and glaciers (Painter et al., 2013). This effect was first

2743 included in the AR4 as a slight warming: +0.1 [0.0 to 0.2] W/m2 (Forster et al., 2007). The

2744 AR5 estimate is slightly smaller at +0.04 (0.02 to 0.09) W/m2.

2745
2746
2747

2748

2749 **6.3. Estimates of the net effect of land use land cover change (LULCC) on radiative**
2750 **forcing.**
2751
2752
2753
2754   In order to better understand the relative role of LULCC compared to other sources of radiative

2755   forcing, one set of studies split the emissions into those from LULCC from non-LULCC based

2756   on standard CMIP5 and IPCC AR5 input datasets and approaches, including using the ERF

2757   concept (Mahowald et al., 2017; Ward et al., 2014; Ward and Mahowald, 2015). Similar to most

2758   climate models, the model used in this set of studies overpredicted aerosol direct and indirect

2759   effects compared to IPCC AR5 assessed RF, and thus the aerosol radiative forcings from

2760   LULCC results were tuned to the AR5 estimates (Mahowald et al., 2017; Ward et al., 2014;

2761   Ward and Mahowald, 2015). Radiative forcing from LULCC sector represents 40% of the

2762   current anthropogenic forcing (Figure 6.3a). This is due to the carbon dioxide emissions from

2763   conversion of natural lands to managed lands, in addition to substantial radiative forcing from

2764   methane and nitrous oxide emitted from agriculture and changes in land (Mahowald et al., 2017;

2765   Ward et al., 2014; Ward and Mahowald, 2015). Anthropogenic aerosol changes from land use

2766   are thought to be large individually, due to changes in desert dust, agricultural aerosols, forest

2767   biogenic aerosol emissions and wildfires, but have a net zero impact on radiative forcing in this

2768   set of studies (Ward et al., 2014), so that most of anthropogenic aerosol radiative forcing is due

2769   to non-LULCC (Figure 6.3a), which is a net negative radiative forcing. The fraction of the

2770   Total radiative forcing from LULCC (40%) is larger than the fraction of the CO2 radiative

2771   forcing attributable to LULCC (20%). Over time, the LULCC radiative forcing has grown

2772   gradually over the 20th century, while non-LULCC radiative forcing was close to zero until

2773   1970s, and now is growing very quickly to positive values as CO2 is accumulating the

2774   atmosphere (Figure 6.3b).

2775
2776
2777
2778
2779
2780
2781

6.4. Future projections

LULCC RF for future are even more difficult to estimate than that for past, and are highly dependent on driving assumptions, especially how much land use conversion will occur (Ward etal.,2014). Integrated assessment models which were used to create the forcing scenarios for the earth system models (Gidden et al., 2018; Hurtt et al., 2011; Moss et al., 2010), tended to underestimate current deforestation rates in the AR5, especially in the tropics, and tended to have very similar deforestation rates, compared with possible futures (Ciais et al., 2013; Ward et al., 2014). This suggests that future estimates from IAMs or IAMs coupled to earth system models may underestimate the impact of LULCC (Mahowald et al., 2017). The land use model intercomparison (LUMIP) has the goal to explore more fully the possible LULCC pathways as well as the radiative forcing resulting from the land biophysics component (Lawrence et al., 2016).

The emission datasets used in the CMIP5 and CMIP6 include some of processes which might impact radiative forcing from LULCC: generally only direct emissions from agriculture are included in emission changes, including some estimates of changes in wildfires in the past and future but with no changes in desert dust (Collins et al., 2017; Gidden et al., 2018; Lamarque et al., 2010, 2011). However the CMIP6 studies, currently underway, will include idealized sensitivity studies for the different natural aerosols to understand their impact on current radiative forcing, providing some bounding on their current and future role (Collins et al., 2017).
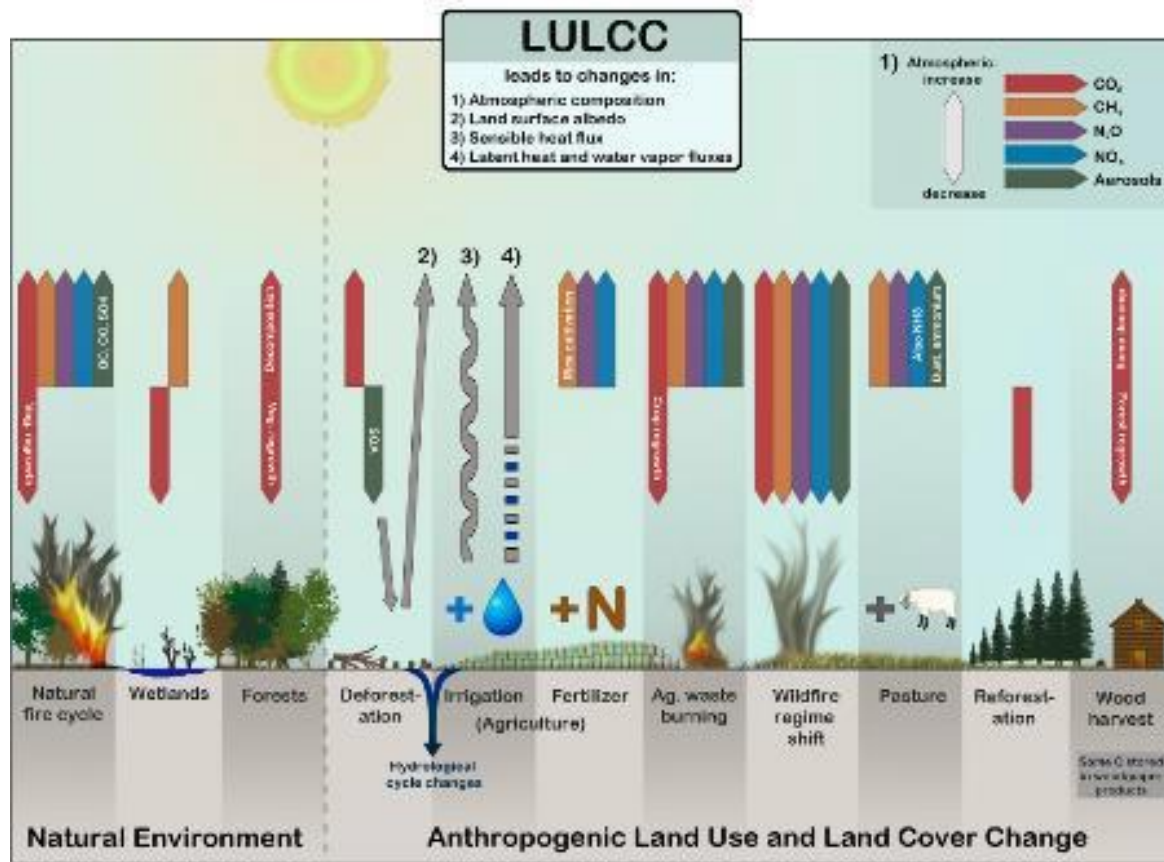
2807
2808
2809
2810
2811 **Figure 6.1:** A schematic illustration of the climate impacts of land use and land cover change

2812 from Ward et al., 2014.

2813

2814

2815

139
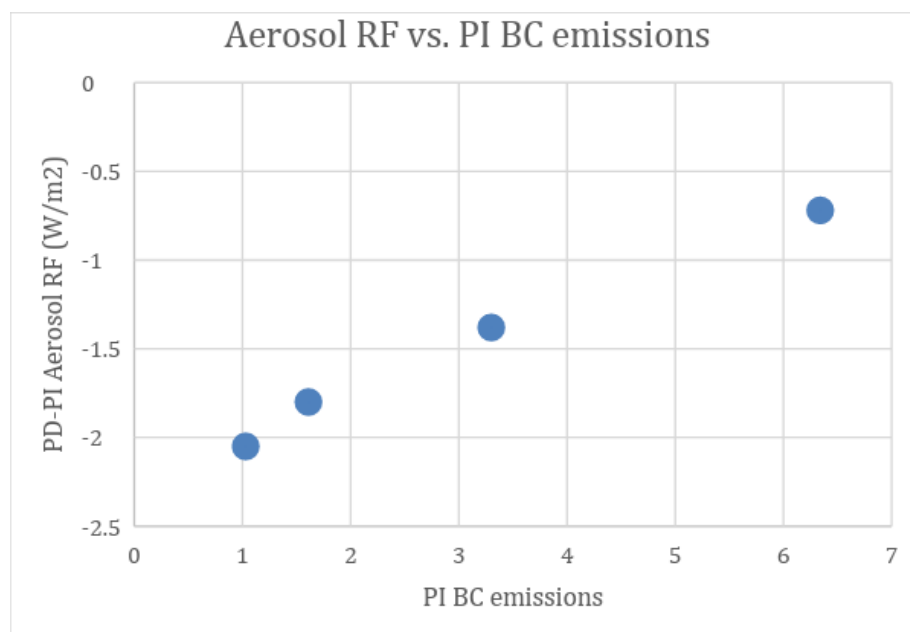
Figure 6.2: Graph showing the relationship between estimated preindustrial black

carbon missions (PI BC) from different fire models and the total indirect

anthropogenic radiative forcing based on Hamilton et al., 2018 numbers. Notice

that estimates of current anthropogenic indirect radiative forcing are linearly

dependent on estimates for preindustrial emissions of

2844
2845
2846
2847
2848
2849
2850
2851
2852
2853
2854
2855
2856
2857
2858
2859
2860
2861
2862
2863
2864
2865
2866
2867
2868
2869
2870
2871
2872
2873
2874

2875
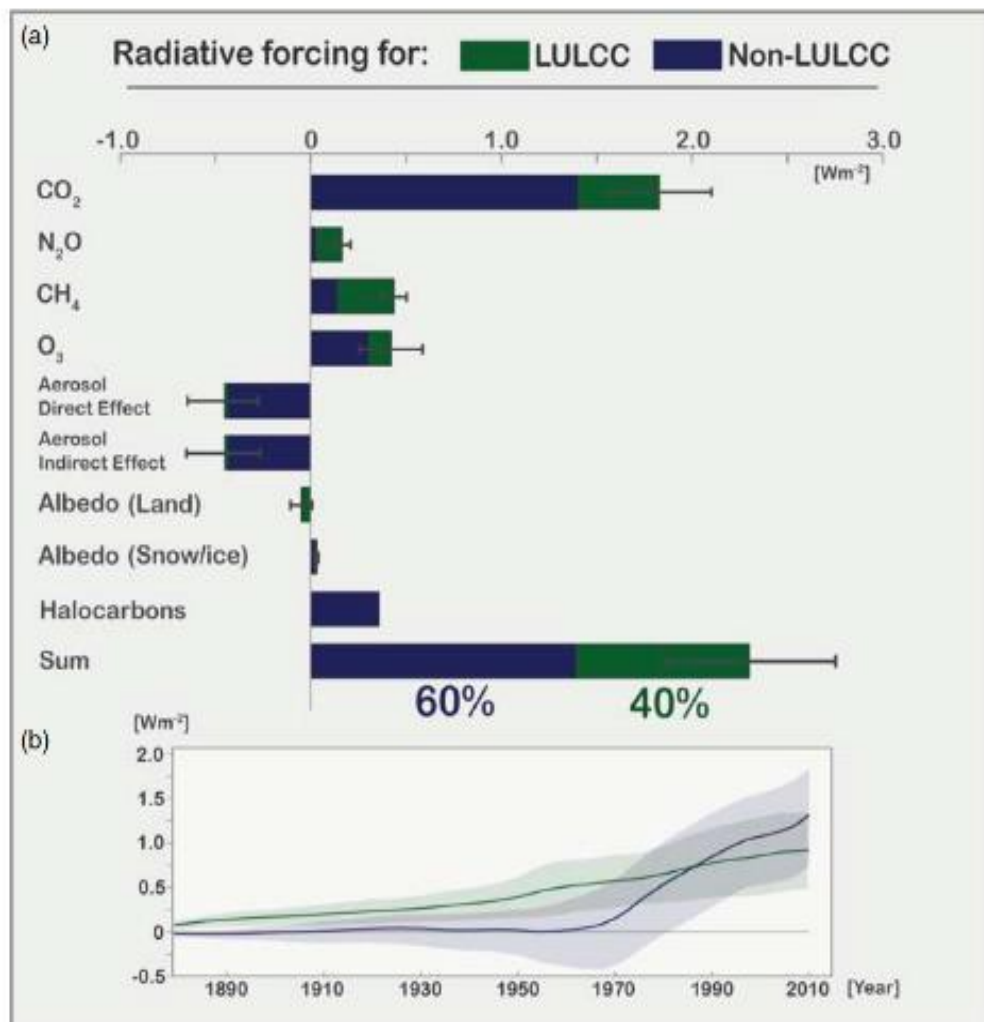
Figure 6.3: a) Anthropogenic radiative forcing (W/m2) for the year 2010 relative to 1850

partitioned into LULCC and non-LULCC sources for different forcing agents, with uncertainty

in the portion of total radiative forcing due to LULCC given by the error bars (adapted from

Ward et al., 2014). b) time series of anthropogenic radiative forcing (W/m2) for LULCC and

non-LULCC sources with uncertainty represented by the shading. (from Mahowald et al.,

2017).

141

Section 7. Contrails and contrail-induced cloudiness

One important component to the RF from subsonic and supersonic aircraft operations (in

addition to its direct emissions of CO_2 and the indirect effects of NO_x emissions) arises from

the ejection of hot moist air (and aerosols and their precursors) from jet engines into air which

is supersaturated (with respect to ice) in the upper troposphere and lower stratosphere (e.g.

Heymsfield et al. 2010; Kärcher 2018). This leads to the formation of persistent linear

condensation trails (contrails) that can evolve into persistent cirrus (e.g. Minnis et al.,1998;

Boucher, 1999; Fahey et al., 1999), comprised mostly of ice condensates. Contrail

characteristics are influenced by humidity and temperature along aircraft flight tracks. In

addition, aerosols from aviation can alter the properties of existing clouds or influence their

subsequent formation. The potential impact of aviation contrails on climate was recognized in

the early 1970s. Machta and Carpenter (1971) presented evidence of changes in high cloud

cover over Denver and Salt Lake City, USA, which they tentatively attributed to aviation; in

the same volume Matthew et al. (1971) noted that while this would increase the albedo, a

compensating change in longwave emissivity could reverse the sign of the climate effect.

Assessments of contrail RF have mostly concluded that, when diurnally averaged, the net

effect of contrails is a positive, due to the dominance of the longwave component. An early

quantification of persistent linear contrails consisted of using meteorological and air traffic

data scaled to regional observations of contrail cover (Minnis et al., 1999; Fahey et al., 1999).

These studies yielded an estimate of 0.02 W m^{-2}.

(with Fahey et al. (1999) estimating a range: 0.005 to 0.06 W m^{-2}) (IPCC, 1999, 2001). The

uncertainty factors included contrail cover, optical depth and cloud microphysical properties

2909   which runs true even today. Sausen et al. (2005) updated the IPCC estimate, giving a year 2000

2910   forcing of 0.01 W m^{-2} for persistent linear contrails and a total (including the impact on cirrus)

2911   of 0.05 W m^{-2}. Soot emissions from aircraft can also affect the cirrus cloud processes

2912   especially the nucleation of ice crystals, but the effects are deemed highly uncertain.

2913   Sedimentation of ice crystals from contrails may remove water vapor from the upper

2914   troposphere with resultant impacts on vertical profiles of cloud condensates and humidity.

2915

2916

2917

2918   Boucher et al. (2013) used more advanced model results to support the view that the longwave

2919   forcing dominates over the shortwave(e.g. Stuber and Forster, 2007); however, models

2920   disagree on the relative importance of the two effects. Contrails have been observed to spread

2921   into cirrus sheets which can persist for several hours, and observations confirm their overall

2922   positive RF (Haywood et al., 2009). Boucher et al. (2013) gave a global-mean RF estimate of

2923   0.01 (0.005 to 0.03) W m^{-2} for persistent linear contrails. Based on Schumann and Graf (2013)

2924   and Burkhardt and Kärcher (2011), the combined linear contrails and contrail-induced cirrus

2925   ERF for the year 2011 was assessed to be 0.05 (0.02 to 0.15) W m^{-2}, with the principal

2926   uncertainties still occurring due to gaps in the knowledge of the spreading rate, physical

2927   properties including optical depth and shape, radiative transfer, as well as the lack of

2928   knowledge of actual aircraft trajectories. This emphasizes the importance of ongoing

2929   measurement campaigns that target contrail properties (e.g. Voigt et al. 2017) as well as the

2930   systematic collation of existing knowledge emerging from such campaigns (Schumann et al.

2931   2017). Analysis of satellite data, especially in the context of detecting line-shaped contrails,

2932   remains important in the assessment of contrail RF. The recent estimate of Duda et al. (2019),

2933   using MODIS data for the period 2006-2012, yielded global-mean RF of 0.008 – 0.009 W m^{-2},

2934   supporting the values assessed earlier in Boucher et al. (2013).

2935

2936   Bock and Burkhardt (2016) have produced a more-refined model estimate of contrail-induced

2937   cirrus (including line-shaped contrails) forcing of 0.056 W m^{-2} for a 2006 aviation inventory.

2938   Although this seemed in good agreement with the earlier Burkhardt and Kärcher (2011) results,

2939   it arose from a different balance between the longwave and shortwave RF components.

2940
2941   Both Chen and Gettelman (2016) and Bock and Burkhardt (2019) have performed detailed

2942   modelling studies of the possible contrail RF in 2050. There are formidable challenges in

2943   making such estimates, in addition to those that are relevant to estimating present-day forcing.

2944   These include assumptions on the growth in air traffic, and the regional distribution of that

2945   growth, changes in engine technology and fuel type, and how changes in climate may impact

2946   the occurrence of ice supersaturated regions in which contrails form. Chen and Gettelman

2947   (2016) predict a seven-fold increase in contrail forcing from 2006 to 2050, which is

2948   substantially more than the four-fold increase in global-flight distance - they attribute this to

2949   stronger growth in flight distances in low latitudes. Bock and Burkhardt (2019) obtain a more-

2950   modest factor of 3 increase in global-mean forcing and find that growth in air traffic is the

2951   predominant cause, with other effects only impacting the regional distribution. The absolute

2952   2050 forcing differs significantly between these studies, with Chen and Gettelman (2016)

2953   obtaining a value of 87 mW m^{-2} while Bock and Burkhardt (2019) obtain 160 to 180 mW m^{-}

2954 ^{2}. Bock and Burkhardt (2019) attribute the differences to different assumptions of ice crystal

2955   size in newly-formed contrails; additional effects include differences in the simulation of

2956   changes in the distribution of ice supersaturated regions in a future climate in the two models.

2957

2958   A significant issue in understanding the importance of contrail RF arises from uncertainty in

2959   the efficacy of that forcing (see Section 2.3.4). There is a sparse literature on the topic. In GCM

2960   studies, Ponater et al. (2006) found an efficacy of 0.6, while Rap et al. (2010) obtained a value

2961   of 0.3. Both studies pre-date the uptake of ERF as a concept and the reason/

2962   s for these low values remains unclear; however, if confirmed by later work, it would imply a

2963   significantly lower impact of contrails on surface temperature than implied by the radiative

2964   forcing. Schumann and Mayer (2017), using results from a simple global-mean model,

2965   speculate that the climate sensitivity to the (negative) shortwave contrail forcing may exceed

2966   that due to the (positive) longwave forcing, because of differences in the partitioning of the

2967   surface and top-of-atmosphere forcings in the two cases. As they note, there is a need to test

2968   this hypothesis in a comprehensive global model.

2969
2970

2971
2972

Section 8. Solar Radiative Forcing

Three primary foci compose contemporary solar radiative forcing research; 1) space-based

measurements of solar irradiance, which explicitly define the forcing over the past 40 years, 2)

modelling observed irradiance variability in terms of proxies that expand understanding across

wavelengths and to multi-centennial time scales, and 3) detection and understanding of

terrestrial responses to solar irradiance variability for indirect assessment of the forcing.

Following an historical overview, this section addresses the development and current status of

these three primary topics, concluding with a summary of successes, uncertainties and

challenges.

8.1 Historical Overview

Solar photons at all wavelengths of the electromagnetic spectrum interact with the terrestrial

system over a range of altitudes, via multiple processes that depend on the composition of

Earth's land, atmosphere, ice and ocean. The processes couple radiatively, chemically and

dynamically to distribute incoming solar energy from low to high latitudes and among different

altitude regimes. Solar radiation is Earth's primary energy source, and pursuit of possible

terrestrial influences of its variability has a long history. The discovery in 1843 of an 11-year

cycle in the occurrence of dark sunspots on the Sun's surface initiated efforts to detect,

understand and specify variability in solar radiative output and Earth's response that continue

today (see e.g., reviews by Hoyt & Schatten, 1997; Gray et al., 2010; Lean 2017).

From the mid 19th century until the late 20th century, correlations between solar indices such as

sunspots and climate indices such as temperature afforded the primary evidence in support of a

solar influence on climate. However, the phase and magnitude of correlations from individual

sites sometimes differed from each other and during different epochs, making their significance

difficult to establish. Moreover, the Sun's total irradiance was assumed to

be invariant; solar-related changes at the level of 0.1% detected in a few decades of ground-

based observations made in the early-to-mid 20th Century were attributed to changes in

atmospheric transmission and speculated to be due to changes in ozone concentrations in

response to the Sun's more variable ultraviolet radiation (Foukal, Mack & Vernazza, 1977).

Sporadic balloon and rocket-borne measurements did detect variations in solar ultraviolet

irradiance but with large uncertainties. Exploratory studies of the terrestrial impacts of solar

147

3021   variability using physical models of climate and, independently, of ozone suggested that an

3022   increase in total solar irradiance of 2% was equivalent to doubling CO_2 concentrations

3023   (Wetherald& Manabe, 1975) and that a 30% increase in solar UV irradiance would increase

3024   total ozone by 5% (Penner & Chang, 1978).

3025

3026   Space-based observations of the Sun transformed knowledge of solar radiative forcing. They

3027   quantify unequivocal changes in the Sun's total irradiance over the past forty years (Fröhlich &

3028   Lean, 2004; Dudok de Wit et al., 2017) and characterize concurrent spectral irradiance changes

3029   at all wavelengths (Haberreiter et al., 2017). Models successfully simulate the observed

3030   irradiance changes in terms of the occurrence of dark sunspots and bright faculae on the solar

3031   disc (Fröhlich & Lean, 2004, Lean et al., 2005) and estimate solar radiative forcing during past

3032   millennia using solar activity proxies (Jungclaus et al., 2017; Matthes et al., 2017; Lean, 2018a).

3033   In 2015 NOAA implemented a Solar Irradiance Climate Data Record (CDR, Coddington et al.,

3034   2016) in support of multiple solar-terrestrial endeavors.

3035

3036   Space-based and expanded ground-based observations of Earth's surface and atmosphere

3037   provide compelling terrestrial evidence for solar radiative forcing (Gray et al., 2010; Lilensten

3038   et al., 2015; Lean, 2017). Solar signals are affirmed in surface and atmospheric temperature and

3039   ozone concentrations over multiple recent decades, providing a new framework for verification

3040   and interpretation of site-specific sun-climate paleo connections evident in multiple

3041   paleoclimate records, especially of hydrological variables (e.g., Haug et al., 2003; Antico &

3042   Torres, 2015). State-of-the-art physical general circulation climate models, such as those used in

3043   recent IPCC assessments, couple surface, atmosphere and ocean processes, include interactive

3044   ozone, and input spectral – not just total – irradiance. They indicate detectable responses to

3045   solar radiative forcing throughout the ocean, surface and atmosphere (Mitchell et al., 2015;

3046   Misios et al., 2015; Hood et al., 2015), as do statistical models of the direct observations (Lean

3047   & Rind, 2008; Lean 2017; Foster & Rahmstorf, 2011).

3048
3049
3050

8.2 Space-Based Observations of Solar Irradiance Variability

The launch into space of electrical substitution "active" cavity radiometers enabled the

detection of real changes in total solar irradiance, beginning with the Hickey-Friedan

radiometer on the Nimbus 7 satellite in November 1978 (Hickey et al., 1980). The radiometers

compare solar radiant heating of a black cavity of known aperture area with equivalent

electrical power. The Active Cavity Radiometer Irradiance Monitor (ACRIM) on the Solar

Maximum Mission (SMM, 1980-1989), Upper Atmosphere Research Satellite (UARS, 1992-

2005) and ACRIMSAT (1999-2013) comprised multiple cavities each with different solar

exposure (Willson, 1979, 2014), thereby isolating real solar irradiance changes during the 11-

year solar cycle from changes in radiometer sensitivity. Radiometers with different

configurations of cavity geometry, surface coating, baffles and aperture placement continue to

measure total solar irradiance on the Solar and Heliospheric Observatory (SOHO) since 1996

(Fröhlich et al., 1995; Fröhlich, 2013), the Solar Radiation and Climate Experiment (SORCE)

since 2003 (Kopp & Lawrence, 2005; Kopp & Lean, 2011) and on the International Space

Station since 2018 (ISS, Richard et al., 2011). By virtue of advanced radiometric design and

signal detection, etched cavity surface, extensive characterization and ground-based absolute

calibration, the Total and Spectral Solar Irradiance Sensor (TSIS) on the International Space

Station (ISS) is expected to measure total solar irradiance with <100 ppm uncertainty and 10

ppm per year repeatability (Richard et al., 2011; Pilewskie et al., 2018).

Space-based observations show unequivocal total solar irradiance variability on time scales

from days to decades as the sun rotates on its axis (every 27-days) and in concert with the 11-

year activity cycle. Initial ACRIM observations readily detected the day-to-day variations

3076   (Willson et al., 1981; Hudson et al., 1982), with solar cycle changes subsequently established

3077   in the longer ACRIM dataset (Foukal & Lean, 1988). Total solar irradiance can decrease by a

3078   few tenths percent over a few days but the Sun is brighter overall when solar activity is higher,

3079   as indicated by higher sunspot numbers.

3080

3081   Figure 8.1 shows monthly mean values of sunspot numbers and total solar irradiance since

3082   1978 according to five different composite records constructed by cross-calibrating and

3083   combining multiple observations. The absolute value of total solar irradiance during the 2008

3084   solar minimum period is 1360.8 ± 0.5 W m^{-2} (Kopp & Lean, 2011) and the change in total

3085   solar irradiance, ΔTSI, of 1.3 W m^{-2} (0.1%) in solar cycles 22 (1986-1996) and cycle 23

3086   (1996-2008) produced decadal solar radiative forcing $\Delta F_S = 0.7\Delta TSI/4 = 0.23$ W m^{-2} (Hansen

3087   & Lacis, 1990). For comparison, radiative forcing by greenhouse gases over the five-year

3088   period of solar irradiance's increase from solar minimum to maximum is less than 0.25 W m^{-2}.

3089   Such forcing estimates assume full adjustment of terrestrial climate processes to a new

3090   "equilibrium" state.

3091

3092   Absolute solar spectral irradiance is less well specified observationally, especially at infrared

3093   wavelengths (Meftah et al., 2018), than is its integral, the total solar irradiance and spectral

3094   irradiance variability, which also depends (differently) on wavelength, is similarly less well

3095   specified observationally than is total solar irradiance variability. This is especially true over the

3096   solar cycle because drifts in spectral radiometer sensitivity during space operation can produce

3097

3098   measurement uncertainties that are larger than the magnitude of the solar cycle changes (Lean

3099   & DeLand, 2012; Mauceri et al., 2018). Conclusive detection of real spectral irradiance

3100   changes was achieved initially at ultraviolet wavelengths, where the relative changes are about

3101   an order of magnitude larger than at visible wavelengths. Spectroradiometers onboard the Solar

3102   Mesosphere Explorer (SME, 1980-1989), UARS (1992-2005) (Lean et al., 1997; Rottman,

3103   2006) and SORCE (2003-), as well as Solar Backscatter Ultraviolet (SBUV) instruments on

3104   multiple NASA and NOAA spacecraft (DeLand & Cebula, 1998) all record spectral irradiance

3105   variability at wavelengths less than 400 nm. The launch of SORCE in 2003 successfully

3106   extended the detection of solar spectral irradiance variability to visible and near infrared

3107   wavelengths (Rottman et al., 2005; Mauceri et al., 2018).

3108

3109   Figure 8.1 shows monthly mean variations in solar spectral irradiance in four broad wavelengths

3110   bands measured by SORCE since 2003 (green lines); 11-year cycle variability is in the range

3111   0.7% to 1.4% in the wavelength band 200-300 nm, 0.1% to 0.2% in the band 300-600 nm,

3112   0.06% to 0.1% in the band 600-900 nm and <0.05% in the band 900-1200 nm. Composite

3113   records of solar UV irradiance have been constructed by combining observations over multiple

3114   solar cycles (DeLand and Cebula, 2008; Haberreiter et al., 2017) but their repeatability is

3115   generally insufficient to reliably specify the magnitude of solar cycle variability because of

3116   instrument sensitivity drifts and the lack of overlap needed to cross calibrate spectroradiometers

3117   with different absolute scales. The exception is the H I Lyman α emission line whose variability

3118   has been constructed since 1947 (Woods et al., 2000); solar Lyman α irradiance (at 121.5+0.5

3119   nm) increased 3.5 mW m^{-2} (60%) in solar cycle 22 and 2.5 mW m^{-2} W m^{-2} (40%) in cycle 24

3120   (Snow et al., 2018).

8.3 Modelling Solar Irradiance Variability

Climatological time scales, on which radiative forcing is typically defined, are considerably longer than the four-decades of space-based solar irradiance observations. Models that relate the observed irradiance variations to historical indices of solar activity are therefore necessary to reconstruct solar radiative forcing prior to 1978. The primary causes of solar irradiance variability are dark sunspots and bight faculae which respectively reduce and enhance the Sun's local radiative output (Foukal, 1981), by different amounts at different wavelengths (Unruh et al., 2000; Lean et al., 2005). Solar rotation imposes a 27-day cycle on solar irradiance by altering the heliographic locations of dark sunspots and bright faculae on the disk, and the growth, transport and decay of sunspots and faculae in response to a sub-surface solar dynamo generates 11-year irradiance cycles. Models that utilize indices of sunspot darkening and facular brightening reproduce the observed variations in total solar irradiance with high fidelity, including decreases up to a few tenths percent during solar rotation and cycle increases of 0.1% (Foukal & Lean, 1988, 1990; Fröhlich & Lean, 2004, Lean, 2017).

Examples of solar irradiance variability models are those of the Naval Research Laboratory (NRLTSI2, NRLSSI2, Lean et al, 2005), which the NOAA CDR utilizes to estimate present and historical irradiance variations (Coddington et al., 2016), and the Spectral and Total Irradiance Reconstructions (SATIRE, Krivova & Solanki, 2008; Krivova et al., 2010). The NRL models input a sunspot darkening function calculated from direct observations of sunspot areas and locations on the Sun's surface and the Mg irradiance index facular proxy; multiple regression

153

3146   against observations determines the relative contributions of the two influences bolometrically

3147   and at individual wavelengths. The SATIRE model derives its two sunspot (dark sunspot umbra

3148   and penumbra) and two facular (bright faculae and network) inputs from solar magneto grams; a

3149   theoretical stellar atmosphere model specifies their wavelength-dependent contrasts relative to

3150   the background "quiet" Sun (Unruh et al., 2000).

3151

3152   To assess the fidelity of such models by comparisons with extant, albeit imperfect,

3153   observations, Figure 8.1 also shows monthly values of total solar irradiance and spectral

3154   irradiance in four broad wavelength bands according to the NRLSSI2 and SATIRE models.

3155   Figure 8.2 compares their total solar irradiance reconstructions over multiple solar cycles and

3156   corresponding spectral irradiance changes in selected epochs. Compared with the SATIRE

3157   model the NRL model has a negligible downward trend during recent cycle minima (e.g., from

3158   1986 to 2008 in Figure 8.1), somewhat smaller solar cycle increases at near ultraviolet

3159   wavelengths and larger increases at longer wavelengths. In solar cycle 23, for example (Figure

3160   8.2), irradiance from 300 to 400 nm increases 0.4 W m^{-2} in the NRLSSI2 model and 0.59 W

3161   m^{-2} in the SATIRE model while visible irradiance from 500 to 750 nm increases 0.42 W m^{-2}

3162   in the NRLSSI2 model and 0.35 W m^{-2} in the SATIRE model.

3163

3164   Reliable historical reconstructions of solar irradiance depend on the availability of suitable

3165   sunspot and facular indices and on understanding plausible irradiance variability mechanisms.

3166   The lack of sunspots on the Sun's disk for several years during the Maunder Minimum (1645-

3167   1715) indicates anomalously low solar activity relative to the contemporary epoch (Eddy,

3168   1976). The possibility that solar irradiance was reduced during such periods relative to

3169   contemporary minima derives from the overall higher levels of ^{14}C in tree-rings and ^{10}Be in

3170   ice-cores (respectively) during the Spörer, Maunder and Dalton Minima. Cosmogenic isotope

3171   levels increase when solar activity decreases because the reduced solar magnetic flux in the

3172   heliosphere facilitates a great flux of galactic cosmic rays at Earth (McCracken et al., 2013).

3173   That cycles near 80, 210 and 2400 years manifest in cosmogenic isotope records of solar

3174   activity suggests the likelihood of similar periodicities in irradiance (e.g., Damon & Jirikowic,

3175   1992).

3176

3177   Initial estimates of the reduction in solar irradiance during the Maunder Minimum below

3178   contemporary solar minima considered two different scenarios (Lean et al., 1992; White et al.,

3179   1992). In one scenario total irradiance decreased 1.5 Wm^{-2} (about 0.1%) due to the

3180   disappearance of faculae; a second scenario estimated a larger decrease of 2.6 Wm^{-2} (about

3181   0.2%) because of an additional reduction in the background "quiet" Sun, inferred from the

3182   reduced emission in non-cycling Sun-like stars (assumed to be in states of suppressed activity

3183   similar to the Maunder Minimum) relative to overall higher emission in cycling stars. Questions

3184   about the applicability of Sun-like stars for solar variability made these initial estimates

3185   speculative (Foukal et al., 2004). Current estimates of the solar irradiance increase from the

3186   Maunder Minimum to the present derive from a model of the transport of magnetic flux on the

3187   Sun's surface. The simulations suggest an increase of 0.5 Wm^{-2} (about 0.04%) in total solar

3188   irradiance at cycle minima over the past ~300 years, from the accumulation of magnetic flux

3189   during successive 11-year cycles of increasing strength (Wang et al., 2005). This estimate of

3190   long-term solar irradiance variability is a factor of five smaller than inferred from Sun-like stars

3191   (Lean et al., 2005, Table IV summarizes estimates of total solar irradiance reduction in the

3192   Maunder Minimum). Figure 8.2 shows reconstructions of total solar irradiance from 850 to

3193   2300 using the ^{14}C cosmogenic isotope record of Roth & Joos (2013), assuming a reduction in

3194   the Maunder Minimum of 0.5 Wm^{-2}. Figure 8.2 also shows spectral irradiance changes in the

3195   NRLSSI2 and SATIRE models from the Maunder Minimum to the present and to the Medieval

3196   Maximum.

3197

3198   Both the magnitude and temporal structure of longer-term irradiance changes remain uncertain.

3199   The only direct index of solar activity prior to 1882 is the sunspot number, which is undergoing

3200   renewed scrutiny and debate (Clette & Lefèvre, 2016; Kopp et al., 2016). The two historical

3201   irradiance reconstructions in Figure 8.2 differ notably prior to 1882 because of their different

3202   parameterizations of irradiance in terms of sunspot numbers and cosmogenic isotopes (Lean,

3203   2018a). The relationship between solar irradiance and cosmogenic isotopes is complex and

3204   poorly known, in part because the magnetic fields that produce sunspots and faculae at the

3205   Sun's surface are not the same as those that modulate galactic cosmic rays in the heliosphere

3206   (Lean et al., 2002). As well, distinctly different terrestrial processes produce cosmogenic

3207   archives in tree- rings and ice-cores (Delaygue & Bard, 2011; Steinhilber, et al., 2012; Roth &

3208   Joos, 2013).

3209
3210
3211

8.4 Climate Response to Solar Radiative Forcing

Just as the detection of terrestrial responses to solar activity initially signified the relevance of solar radiative forcing for understanding climate change, in lieu of direct observations of the forcing itself, so too does ongoing analyses of ever-lengthening terrestrial observations and newly extracted, high fidelity paleoclimate records continue to strengthen and expand the evidence. Using indicators such as sunspots and cosmogenic isotopes to identify times of high and low solar activity during the 11-, 80- and 210-year cycles, solar-related changes are identified in diverse climate parameters that range from low latitude drought and rainfall (e.g., Verschuren et al., 2000; Neff et al., 2001; Haug et al., 2003; Antico & Torres, 2015), associated with Intertropical Convergence Zone displacement (Novello et al., 2016) and a La-Nina type response in the tropical Pacific (Mann et al., 2005), to mid-and high latitude 'centers of action' (Christoforou & Hameed, 1997), storm tracks and winter intensity (e.g., Barriopedro et a., 2008; Mann et al., 2009; Lockwood et al., 2010), associated with the North Atlantic Oscillation and the circumpolar vortex.

On global scales, climate signals related to the 11-year solar cycle were detected first in basin-wide ocean temperatures (White et al., 1997) then in global lower tropospheric temperature (Michaels & Knappenberger, 2000). Observational temperature and ozone databases are now sufficiently long that statistical analyses readily isolate in them solar responses, both globally and regionally, from other concurrent influences (Douglass & Clader, 2002; Lean and Rind, 2008; Foster & Rahmstorf, 2011). Figure 8.3 shows the solar cycle component, thus extracted, of <0.1°C in global surface temperature and <3 DU (1%) in total ozone compared with natural

157

Accepted for publication in *Meteorological Monographs*. DOI 10.1175/AMSMONOGRAPHS-D-19-0001.1.

3237   (volcanic, ENSO, QBO) and anthropogenic (greenhouse gases and ozone depleting substances)

3238   components and Figure 8.4 shows the corresponding geographical response patterns. These

3239   estimates of climate's response to solar forcing are attained by linearly regressing indices of the

3240   simultaneous natural and anthropogenic influences against (de-seasonalized) monthly mean surface

3241   temperature (Figure 8.3a) and total ozone (Figure 8.3b) observations from 1979 to 2017 (Lean,

3242   2017, 2018b).

3243

3244   Time dependent simulations of climate's response to solar radiative forcing on climatological

3245   time scales became possible with the reconstruction of historical solar irradiance. Simulations

3246   using energy balance models initially suggested that the global surface temperature response to

3247   reconstructed solar irradiance cycles since 1874 (Foukal & Lean, 1990) was likely undetectable,

3248   the transient response of 0.03°C being notably smaller than the equilibrium response because of

3249   attenuation (~80%) by the thermal inertia of the ocean (Wigley & Raper, 1990). But subsequent

3250   analysis of historical surface temperature observations did detect a solar cycle response of

3251   0.06°C by statistically extracting the modelled spatial pattern of the response to the forcing

3252   (Stevens & North, 1996).

3253

3254   The first general circulation model simulations of climate's response to time-dependent solar

3255   radiative forcing found a global surface temperature increase of ~0.5°C since the Maunder

3256   Minimum (Cubacsh et al., 1997; Rind et al., 1999). Decreased solar irradiance during the

3257   Spörer, Maunder and Dalton solar activity minima (Eddy, 1976) and enhanced volcanic activity

3258   are posited causes of anomalously cold surface temperatures from ~1300 to 1850, during the

3259   Little Ice Age (e.g., Mann et al., 2005, 2009). Even though the simulations input a factor of five

3260   – or more - larger increase in total solar irradiance (Lean et al., 1995) than current estimates

3261   (Wang et al., 2005), they nevertheless identified that water vapor feedbacks, cloud cover

3262   changes and land-sea contrasts contribute to the surface response to solar radiative forcing, with

3263   enhanced warming in sub-tropical regions similar to that forced by increasing greenhouse gas

3264   concentrations. The simulations further established that variations in solar irradiance were

3265   unlikely to be the primary cause of global warming in the postindustrial period, as some

3266   statistical correlations between solar cycle length and northern hemisphere temperature had

3267   suggested (Friis-Christensen & Lassen, 1991).

3268

3269   State-of-the-art general circulation models now include couplings between the land, ocean and

3270   atmosphere, functional middle atmospheres with ozone chemistry, and the ability to input

3271   realistic solar spectral irradiance changes. Analyses of ensembles of simulations made with

3272   various such models, designed to isolate responses of different terrestrial regimes to solar

3273   radiative forcing, demonstrate both a direct response of the land and ocean, dependent in part on

3274   the regional distribution of clouds, and an indirect response facilitated by stratospheric ozone

3275   and temperature changes (Rind et al., 2008; Meehl et al., 2009). Convective and dynamical

3276   processes disperse the forcing geographically and altitudinally, altering extant dynamical

3277   patterns such as the Hadley and Walker circulations and impacting, in particular, the

3278   hydrological cycle. IPCC's AR5 climate assessment included simulations made with 13 models

3279   that resolve the stratosphere (Mitchell et al., 2015), 6 of which include interactive ozone

3280   chemistry (Hood et al., 2015). Modeled responses to solar cycle irradiance changes are evident

3281   at the surface, in the ocean (Misios et al., 2015) and in the troposphere, stratosphere and ozone

3282   layer (Hood et al., 2015). While the simulated responses are generally of smaller magnitude

3283   than in observations (e.g., global mean surface warming of 0.07oC), the processes and patterns

3284   are qualitatively similar, including changes in precipitation and water vapor leading to weaker

3285   Walker circulation (Misios et al., 2015) and a stratosphere-related North Atlantic surface

3286   response (Mitchell et al., 2015).

3287

3288   Figure 8.4 compares statistically-extracted geographical patterns of the terrestrial response to

3289   solar radiative forcing with estimates made by a physical climate model (Rind et al., 2008).

3290   Differences between the physical and statistical model patterns suggest that deficiencies remain

3291   in one or both. Uncertainties in the hundreds of parameterizations that seek to account for the

3292   multiple integrated processes that heat the land and ocean, and redistribute this heat regionally

3293   and vertically, compromise physical model simulations. Statistical models suffer from

3294   uncertainties in the predictors and covariance among them (such as between solar and

3295   anthropogenic indices), including distinguishing whether covariance is physically based or

3296   random. The limited duration of the most reliable observations and indices exacerbate such

3297   uncertainties. Articulating and reconciling differences between the statistical and physical

3298   models is expected to improve understanding of process that facilitate terrestrial responses to

3299   solar radiative forcing, and may help improve physical model parameterizations of these

3300   processes. It is increasingly apparent that solar radiative forcing initiates a continuous spectrum

3301   of coupled interactions throughout Earth's land, ocean and atmosphere on multiple time scales

3302   with different and interrelated regional dependencies. Differential heating of the land and

3303   oceans, equator and poles, and surface and atmosphere drive these responses; the processes

3304   involved are those by which climate responds to other radiative forcings, including by

3305   increasing greenhouse gas concentrations, albeit with different, magnitude, timing and regional

3306   detail.

3307

8.5 Summary: Successes, Uncertainties, Challenges

3309

3310   *Successes*

3311

3312   Both measurements and models have now established that solar irradiance varies at all

3313   wavelengths, with different magnitudes at different wavelengths. Total (spectrally integrated)

3314   solar irradiance increased 1.3+0.2 Wm-2 (0.1%) in solar cycle 23 (1996-2008) producing radiative

3315   forcing of 0.22 Wm-2. Spectrally, the energy change maximizes at 300-400 nm, which increased 0.4 W

3316   m-2 in solar cycle 23.

3317

3318   Solar irradiance variability is a result of the Sun's magnetic activity, which alters radiative

3319   output locally in dark sunspots and bright faculae. Models of the net, global influence of

3320   sunspots and facular reproduce observed total solar irradiance variability with high fidelity on

3321   time scales of the Sun's 27-day rotation.

3322

3323   Observations and models of Earth's surface and atmospheric temperature and ozone amount

3324   indicate that terrestrial responses to solar radiative forcing have detectable magnitudes during

3325   the 11-year solar cycle. Global responses are ~0.1°C in surface temperature, ~0.3°C in lower

3326   stratospheric temperature and ~3 DU (1%) in total ozone; the response patterns are regionally

3327   inhomogeneous and differ from that of the incident solar radiative forcing. There is abundant

3328   terrestrial evidence in paleoclimate records and solar activity proxies for solar radiative forcing

3329   with cycles near 80 and 210 years, in addition to the 11-year cycle.

3330

3331   *Uncertainties*

3332

161

3333   Not yet known with the needed certainty is the magnitude of spectral irradiance changes in the

3334   solar cycle. This is because observations lack the long-term stability to establish this

3335   unequivocally and models disagree about the apportioning of the changes to near-UV versus

3336   visible-near IR wavelengths. Less certain still are the magnitudes of multi-decadal irradiance

3337   variations and their possible mechanisms. Yet to be proven is the assumption in historical

3338   reconstructions that solar irradiance varies on time scales longer than the 11-year activity

3339   cycle, and whether observations of Sun-like stars can provide useful estimates of the

3340   magnitude of this variability.

3341

3342   Physical processes that connect variations in solar irradiance and cosmogenic isotopes,

3343   including modulation by solar magnetic flux, the flow of galactic cosmic rays through the

3344   heliosphere and production of isotopes in terrestrial archives are conceptually established but

3345   not yet quantified with the needed certainty. Similarly, the terrestrial processes and model

3346   parameterizations thereof that facilitate the multiple pathways that transform solar radiative

3347   forcing to climate variability are generally recognized but their specifications require validation

3348   and improvement. This includes the deposition of incident solar in c) for total ozone and in d)

3349   for surface temperature spectral energy, direct chemical and dynamical responses to this

3350   forcing, and the modulation of extant circulation patterns throughout the integrated system.

3351

3352   *Challenges*

3353

3354

3355   The highest priority going forward is the continuous monitoring of solar irradiance with the

3356   highest possible accuracy and repeatability to extend the extant record of solar radiative

3357   forcing, exemplified by the launch in 2018 of the Total and Spectral Solar Irradiance Sensor

3358   (TSIS) on the International Space Station.

3359

3360   Differences among observed and modelled absolute irradiance and irradiance variations,

3361   require resolution, including the magnitude of inter-minima changes in the space era and the

3362   spectral dependence of the variability.

3363

3364   Physical climate models of the future are challenged to fully capture and parameterize the

3365   multiple pathways by which solar radiation enters and alters the integrated terrestrial

3366   environment, including under different conditions of other natural and anthropogenic forcings.

3367   The reconciliation of the magnitude, pattern and time lags of terrestrial responses to solar

3368   radiative forcing extracted statistically from observations with those calculated by physical

3369   models may aid the pursuit of this challenge.

3370
3371

Figure captions

3373

3374

3375

3376   **8.1.** Shown are monthly means in the space era of a) sunspot numbers, b) total solar irradiance,

3377   TSI, and solar spectral irradiance in broad bands from c) 100-300 nm, d) 300-600 nm, e) 600-

3378   900 nm and f) 900-1200 nm. The five green lines in b) are composite records of TSI constructed

3379   from different combinations of observations. Also shown are estimates of the irradiance

3380   variations by two models, the NRLTSI2 and NRLSSI2 models (black lines) and the SATIRE

3381   model (orange lines).

3382

3383   **8.2.** Reconstructed historical and projected future variations in total solar irradiance are shown

3384   in a) from 850 to 2300 according to two different models, the NRLTSI2 model (black lines)

3385   and the SATIRE model (orange lines, recommended for use in PMIP4). Shown in b), c) and d)

3386   are the spectral irradiance changes for three selected periods, specifically solar cycle 23 (1996

3387   to 2009), the Maunder Minimum (1645–1715) to Modern Maximum (1950-2009) and the

3388   Maunder Minimum to the Medieval Maximum (1100-1250).

3389

3390

3391   **8.3**. Shown as the black lines are observed changes from 1979 to 2017 in a) monthly-averaged

3392   global surface temperature and b) monthly-averaged global total ozone. Also shown by the

3393   blue lines in a) and b) are the changes in the respective observations according to statistical

3394   models. The statistical models are constructed by using linear least squares regression of the

3395   observations against indices of the known sources of their variability. The relative

3396   contributions of the individual components to the observed changes are identified in the lower

3397 two panels; these include the El Niño southern oscillation (ENSO), quasi biennial oscillations

3398 (QBO), volcanic aerosols, the solar irradiance cycle, changes in the concentrations of

3399 anthropogenic greenhouse gases (GHG) and the effective equivalent stratospheric chlorine

3400 (EESC) of ozone-depleting substances (adapted from Lean, 2017, 2018b).

3401

3402 **8.4**. Shown in the top image is the annually averaged relative distribution of received solar

3403 radiation at Earth. The regional patterns of terrestrial responses to changes in solar radiation

3404 during the 11-year cycle, statistically extracted from observations (Lean, 2017, 2018b), are

3405 shown in a) for total ozone and in b) for surface temperature. For comparison, the terrestrial

3406 responses to the solar cycle simulated by a general circulation model (GISS Model 3; Rind et

3407 al., 2008) are shown.

3408

3409

3410

3411

3412   **Figure 8.1**

3413

a) Sunspot Number

b) Total Solar Irradiance

Observational Composites (5)
NRLTSI2
SATIRE

c) Solar Spectral Irradiance 100−300 nm

SORCE×1.0160
NRLSSI2
SATIRE×1.1860

d) Solar Spectral Irradiance 300−600 nm

SORCE×0.9941
NRLSSI2
SATIRE×1.0108

e) Solar Spectral Irradiance 600−900 nm

SORCE×1.1138
NRLSSI2
SATIRE×1.0977

f) Solar Spectral Irradiance 900−1200 nm

SORCE×0.9901
NRLSSI2
SATIRE×0.9319

3414

3415

3417   **Figure 8.2**

a) Total solar irradiance

b) Spectral irradiance change

167

3422   **Figure 8.3**

3423

a) Global Surface Temperature
— observations, average
— model, r=0.91

b) Total Ozone
— observations, MOD V8.6
— model, r=0.89

ENSO
Volcanic Aerosols

QBO
ENSO
Volcanic Aerosols

Solar Cycle
Anthropogenic Effect

Solar Cycle
EESC
GHG

3424

3425

3426

3427

3428

3429
3430   **Figure 8.4**

Annually Averaged Distributon of Received Solar Radiation

Terrestrial Responses to Solar Irradiance Cycle

3431
3432
3433
3434
3435

169

9. Stratospheric Aerosols

9.1 Introduction

An important discovery of the 20th century is that some amount of submicron sulfate

particles are permanently present in the stratosphere perturbing the Earth's radiative balance,

climate, and weather (Junge et al., 1961; Turco et al., 1982; Pueschel, 1996; Hamill et al.,

1997). The abundance of stratospheric aerosols greatly increases after explosive volcanic

eruptions that inject materials directly in the stratosphere. The tremendous success in

observations and theoretical understanding of stratospheric aerosols achieved during recent

decades is briefly reviewed in this Section.

Volcanic hazards have been documented since antiquity. Pompeii in the ancient Roman

Empire was destroyed by the eruption of Vesuvius in 79 AD (Zeilinga de Boer and Sanders,

2002). Plutarch mentioned that the Etna eruption in 44 B.C. dimmed the Sun and killed the

crops causing famine in Rome and Egypt (Forsyth, 1988). The systematic compilation of

active volcanoes and past volcanic eruptions started in the mid-nineteenth century (Scope,

1862). Coming to the present times, there is now available a comprehensive database of

active volcanoes (Simkin et al, 1981; Simkin, 1993).

It was long suspected that explosive volcanic eruptions affect the weather, climate, and

human health through the injection into the atmosphere of large amounts of solid particles

(i.e., volcanic ash) and gases (Coakley, 1981; Robock, 2000; Timmreck, 2012; Stenchikov,

2016). Benjamin Franklin, then a US ambassador to the court of Louis XVI, related the 1783

170

3462   Laki eruption in Iceland with the dry fog and anomalously cold weather in Europe (Franklin,

3463   1784). Grattan et al. (1998) found an increase in mortality caused by the Laki's plume. Sereno

3464   Bishop was the first who described the diffuse halo that forms around the sun due to the

3465   optical effect of volcanic aerosols (now called Bishop's ring) after the eruption of Krakatau

3466   in Indonesia in 1883. Much later Humphreys (1913, 1940) correctly pointed out the radiative

3467   effect of volcanic aerosols as a physical cause of volcanically-induced cold weather.

3468
3469
3470

3471

9.2 Origin of Stratospheric Aerosols

3472

3473

3474

3475 During the sufficiently prolonged volcanically quiescent periods, stratospheric aerosols do

3476 not disappear but reduce to background levels. Gruner and Kleiner (1927) first suggested the

3477 existence of a persistent non-volcanic aerosol layer in the stratosphere. It was instrumentally

3478 confirmed in1961 (Junge et al., 1961; Junge and Manson, 1961) 59 years after the

3479 stratosphere itself was documented by a pioneering balloonist Leon Tisserenc de Bort in 1902

3480 (Greene, 2000). Currently, the stratospheric aerosol layer is often referred to as Junge layer

3481 both for volcanically quiescent and active periods, although the aerosol abundance, vertical

3482 extent, and horizontal spread drastically change after an explosive volcanic eruption.

3483

3484 In the volcanically quiescent periods, the background Junge layer height varies around 20 km

3485 and is modulated by the quasi-biennial oscillation (QBO). The aerosol abundance is

3486 maintained by the mostly tropical cross-tropopause transport (Fueglistaler et al., 2009) of

3487 sulfur-containing gases, carbonyl sulphide (OCS) (Crutzen, 1976) and SO_2 (Bruhl et al.,

3488 2012; Sheng et al., 2015), as well as aerosols of natural and anthropogenic origin (Brock et

3489 al., 1995). Deep convective cells could also overshoot tropospheric materials into the

3490 stratosphere (Stenchikov et al., 1996). The much-debated contribution of anthropogenic sulfur

3491 from highly polluted East Asia is found to be of minorimportance (Deshler et al., 2006;

3492 Vernier et al., 2011; Thompson and Peter, 2006). This is consistent with the observation

3493 that despite the increase in anthropogenic emissions there is no measurable long-term trend

3494 in background aerosols (Deshler et al., 2006; Vernier et al., 2011; Thomson and Peter, 2006)

3495 during 1970-2005. The estimated total net flux of sulfur into the stratosphere is about 180

3496 GgS/year but this figure has an uncertainty of at least 50% (Thompson and Peter, 2006;

3497 Kremser et al., 2016). The input of other aerosols, meteoric from the middle atmosphere,

3498 organic from troposphere, and mixed from air traffic and rocket exhaust, is little by mass but

3499 may affect aerosol microphysics (Turco et al., 1982; Bardeen et al., 2008; Kremser et al.,2016;

3500 Gomez Martin et al., 2017).

3501

3502 The diameters of background aerosol particles range from 10 to 100 nm and their total

3503 optical depth is of the order of 0.001 in visible (Vernier et al., 2011) resulting in radiative

3504 forcing (compared to zero concentrations) of about -0.01 to -0.05 W/m2. So, although

3505 background stratospheric aerosols are important indicators of the stratosphere-troposphere

3506 chemical exchange and chemical processes in the stratosphere itself, their radiative effect is

3507 relatively small, but not completely negligible. Note that radiative forcing in the present

3508 paper is with reference to preindustrial times when there was likely a small but non-zero

3509 background concentration.

3510 However, the pure background Junge layer is rarely observed as it is frequently perturbed by

3511 explosive volcanic eruptions that directly inject into the lower stratosphere volcanic ash,

3512 sulfur-containing gases, mostly SO_2 and H_2S, water vapor, CO_2, halogens, nitrogen (N_2),

3513 and other species. After such emissions the thermal and chemical relaxation of the

3514 stratosphere to background level takes 7-8 years (Brasseur and Granier, 1992; Thomason and

3515 Peter, 2006). So during the observation period that started in the 1970s there are only a few

3516 time-windows when the background Junge layer could be sampled.

3517

3518

3519

3520   Volcanic ash particles, mainly re-condensed silicates, usually exceed 2 μm in diameter.

3521   Although ash immediately after eruption develops a measurable radiative forcing, it does not

3522   produce a long- term climate effect as it gravitationally deposits in an about a week or two.

3523   The finest ash particles might be present in the stratosphere for a few months but their

3524   radiative effect is negligible (Niemeier et al., 2009; Guo et al., 2004a, 2004b).

3525

3526

3527   The model studies suggest that the aerosol plume from a strong equatorial volcanic eruption

3528   could heat the tropical tropopause layer (TTL) facilitating the tropospheric water vapor

3529   penetration into the stratosphere (Joshi and Shine, 2003; Robock et al., 2009; Löffler et al.,

3530   2016). The heating of the TTL after volcanic eruptions appears challenging to detect in

3531   observations even for the most recent strong eruption of Mt. Pinatubo (Fueglistaler et al.,

3532   2013; Randel et al., 2004; Chiou et al., 2006). This is because the TTL temperature and

3533   water vapor flux into the stratosphere are also affected by QBO, El Nino Southern

3534   Oscillation (ENSO), and the strength of the Brewer-Dobson Circulation. Dessler et al.

3535   (2014) used multiple regression analysis to account for all those factors and have shown the

3536   increase of the water vapor mixing ratio in the air entering the tropical stratosphere both for

3537   El Chichon and Pinatubo eruptions.

3538

3539

3540

3541   Volcanic SO_2 and H_2S are oxidized in the stratosphere by a photochemically produced

3542   hydroxyl radical to form sulfate aerosols with a characteristic conversion time of about one

3543   month (Bluth et al., 1992, 1993; Read et al., 1993), although, this rate could vary at different

3544   stages of the process (LeGrande et al., 2016). Initially, aerosol particles are formed due to

3545   binary nucleation of sulfuric acid and water vapor and are subject to coagulation and

3546   diffusional growth as well as gravitational settling (Turco et al., 1982; Pueschel, 1996;

3547   Hamill et al., 1997). They exert substantial perturbation of the radiative energy budget of the

3548   planet (Lambert et al., 1993; Baran and Foot, 1994; Minnis et al., 1993; Barns and Hoffman,

3549   1997; Lacis et al., 1992; Stenchikov et al., 1998).

3550

3551   Volcanic aerosols are dispersed in the stratosphere by wave-driven Brewer-Dobson

3552   circulation (Holton et al., 1995) modulated by the QBO phase (Trepte and Hitchman, 1992)

3553   to be deposited at high latitudes. The stratospheric e-folding residence time of equatorial

3554   injections with respect to Brewer-Dobson transport is about two years (Hamill et al., 1997).

3555   The lifetime of high-latitude volcanic injections is somewhat shorter than the low-latitude

3556   ones because of proximity to a pole and absence of the slowly emptying aerosol equatorial

3557   reservoir blocked by the subtropical barrier (Oman et al., 2006b). For large eruptions,

3558   gravitational settling of quickly growing sulfate particles intensifies aerosol removal

3559   restricting the magnitude of the climate impact of super-eruptions (Pinto et al., 1989;

3560   Timmreck et al., 2010). Volcanic aerosols deposited to Antarctica and/or Greenland snow

3561   affect the chemical composition of ice, thus recording the history of the Earth's volcanism

3562   for thousands of years (Zielinski, 2000; Cole-Dai, 2010).

3563
3564

3565

9.3 Observations Of Stratospheric Aerosols

3566

3567
3568

3569

3570   The first generation of aerosol viewing instruments provided invaluable empirical

3571   knowledge about stratospheric loadings and optical properties, however, with some

3572   significant gaps in spaceand time (Deshler, 2008; Deshler et al., 2003; Hofmann et al., 1975;

3573   Baumgardner et al., 1992; Borrmann et al., 2000; Fiocco and Grams, 1964; Stothers, 1996;

3574   1997; 2001a, 2001b; Krueger et al., 2000; Carn et al., 2003; McCormick et al., 1987;

3575   Antuña et al., 2003; Thomason and Taha, 2003; Randall et al., 2000; 2001). Thomson and

3576   Peter (2006) and Kremser et al. (2016) overview extensively the available observations.

3577

3578   The recognized deficiency of existing observations is that aerosol size distribution, which

3579   affects both aerosol optical characteristics and sedimentation velocities, suffers from

3580   significant retrieval uncertainties (Kremser et al., 2016; Bingen et al., 2004a, 2004b;

3581   Bourassa et al., 2008; Malinina et al., 2018). During the recent decade, a new generation of

3582   instruments for monitoring aerosols and precursor gases has emerged. Among them are the

3583   Michelson Interferometer for Passive Atmospheric Sounding (MIPAS), Ozone Mapping

3584   Profiler Suite (OMPS), Ozone Monitoring Instrument (OMI), InfraRed Atmospheric

3585   Sounding Interferometer (IASI), Cloud-Aerosol Lidar and Infrared Pathfinder Satellite

3586   Observations (CALIPSO), Cloud-Aerosol Transport System (CATS), Optical Spectrograph

3587   and InfraRed Imager System (OSIRIS), SCanning Imaging Absorption SpectroMeter for

3588   Atmospheric CHartographY (SCIAMACHY). OMI and OMPS continue the Total Ozone

176

3589   mapping Spectrometer (TOMS) measurement record providing SO2 loadings used to

3590   document the global volcanic degassing (Carn et al., 2016). MIPAS sees the

3591

3592   vertically resolved SO2 and aerosol volume (Hopfner et al., 2013; 2015). The vertically

3593   resolved aerosol extinctions are detected by the limb profiling SCHIAMACHY (Burrows et

3594   al., 1995; Bovensmann et al., 1999; von Savigny et al., 2015), OSIRIS (Bourassa et al.,

3595   2007), and Lidar instruments, CATS (Yorks et al., 2015) and CALIOP (Vernier et al.,

3596   2009). The new limb-scattering instruments observe aerosol plume more frequently than

3597   those based on the solar occultation technique and allow reliably retrieve more parameters

3598   of aerosol Particle Size Distribution (PSD) then were possible in the past (Malinina et al.,

3599   2018). For the forcing calculations, it is important to smoothly merge the past and current

3600   aerosol observations to produce seamless datasets of stratospheric aerosol parameters for an

3601   extended period of time (Thomason et al., 2018).

3602
3603
3604

9.4 Radiative Forcing Of Stratospheric Aerosols

Stratospheric aerosols, both volcanic and background, scatter the incoming shortwave radiation depleting the direct and enhancing the diffuse downward solar fluxes; they also absorb shortwave near infrared, and absorb and emit outgoing terrestrial radiation. The cumulative radiative effect of stratospheric aerosols is to cool the Earth's surface and heat the aerosol layer in the lower stratosphere.

Volcanic eruptions that have historically exerted the strongest radiative forcing, have i) significant SO2/H2S injected into the stratosphere (although there is growing evidence of non-linearity of injections strength and radiative forcing (e.g. Niemeier and Tilmes, 2017) , ii) tend to occur in tropical regions where both hemispheres of the globe are impacted by the subsequent perturbation to the aerosol optical depth and iii) inject SO2 to sufficiently high altitudes within the stratosphere (e.g. Jones et al., 2017).

The large perturbations of the Earth's radiative balance caused by explosive volcanic eruptions e.g., Pinatubo, are discernible in observations; however, this does not lend itself readily to quantifying their actual radiative forcing (Dutton and Christy, 1992; Minnis et al., 1993; Russell et al., 1993). The theoretical calculations of the radiative forcing of stratospheric aerosols were first attempted using conceptual models (Lacis et al., 1992; Harshvardhan, 1979; Toon and Pollack, 1976). Because aerosol microphysical and optical

178

3629   characteristics, which have to be compiled from observations or calculated within the

3630   model, are the major input into the radiative forcing calculations, we discuss both these

3631   aspects together here.

3632

3633   The first generation of the atmospheric general circulation models simulated the impact of

3634   volcanic aerosols using simplified approaches, i.e., assuming a reduction of the solar

3635   constant, increase of planetary albedo, or representing stratospheric aerosols by a single

3636   reflecting layer (e.g., Broccoli et al., 2003; Soden et al., 2002).

3637

3638   The existing aerosol observations were used to build the global aerosol datasets with pre-

3639   calculated aerosol optical/microphysical characteristics that could be implemented in

3640   climate models (Stenchikov et al., 1998; Stenchikov, 2016; Ramachandran et al., 2000; Sato

3641   et al., 1993; Hansen et al., 2002; Schmidt et al., 2011; Tett et al., 2002; Ammann et al.,

3642   2003). One approach is to use the observed/reconstructed aerosol optical depth (usually in

3643   visible) and assume aerosol composition and size distribution to calculate aerosol extinction,

3644   single scattering albedo, and asymmetry parameter required for radiative transfer models as

3645   input (Stenchikov et al., 1998; Sato et al., 1993). Another approach uses the empirical

3646   estimates of SO2 emissions and a simplified model to distribute them globally and to obtain

3647   the aerosol optical parameters (Ammann et al., 2003; Gao et al., 2008). Ammann et al.

3648   (2003) and Sato et al. (1993) datasets have essentially provided the bases for

3649

3650   implementing volcanic aerosols in virtually all of the climate models that have performed the

3651   20th-century climate integrations within IPCC AR4 (Stenchikov et al., 2006; Forster et al.,

3652   2007).

3653

3654   For the IPCC AR5 and CMIP6, the improved "gap-filled" SAGE II Version 6 aerosol

3655   product from (Thomason and Peter, 2006) was employed (Arfeuille et al., 2013; Zanchettin

3656   et al., 2016). All three stratospheric optical depths (SATO, AMMAN, and CMIP6) in Figure

3657   9.1 vary by about 30%, with Amman's optical depth being the largest and CMIP6 being the

3658   smallest.

3659

3660   Figure 9.2 and 9.3 compare the all-sky shortwave (SW), longwave (LW), and SW+LW

3661   instantaneous radiative forcing at the top of the atmosphere and perturbations of heating rates

3662   calculated using SATO and CMIP6 inputs within the GFDL CM2.1 (Delworth et al., 2006)

3663   employing a double radiation call. To calculate optical characteristics of stratospheric

3664   aerosols for the SATO case, it was assumed that the aerosol has lognormal distribution with

3665   the time-and-latitude-varying effective radii and a fixed geometric width of 1.8 μm

3666   (SATO1.8) or 2.0 μm (SATO2). Despite the differences in the input information and

3667   assumptions, the changes in total radiative balance for the three datasets appear to be quite

3668   close. Both SATO's datasets slightly overestimate the SW radiative forcing in comparison

3669   with (Minnis et al. 1993). The CMIP6 heating rates appear to be higher than expected

3670   (Stenchikov et al., 1998) and shifted toward theSW heating. Typical stratospheric sulfate

3671   particles absorb SW radiation only in near-IR starting

180

3672

3673   from 2.5 µm where solar flux is weak. This is why LW heating is expected to prevail

3674   contributing about 70% of the effect (Stenchikov et al., 1998). The stratospheric heating is

3675   important, as it controls stratospheric dynamic responses (Ramaswamy et al., 2006).

3676

3677   The complexity of radiative, microphysical, and transport processes forced by volcanic

3678   aerosols suggests that it is important to calculate aerosol radiative effects interactively with

3679   the aerosol plume development rather than use a pre-calculated set of aerosol optical

3680   parameters. To accomplish this, it is necessary to know the SO2 volcanic emissions (Krueger

3681   et al., 2000; Hopfner et al., 2013; 2015) and be able to calculate development, transport, and

3682   decay of a volcanic aerosol layer.

3683

3684   The "bulk" aerosol models calculate SO2 to H2SO4 conversion and transport their bulk

3685   concentrations. Sulfate aerosols are assumed to form instantaneously with the prescribed size

3686   distribution (Timmreck et al., 1999; Oman et al., 2006a; and Aquila et al., 2012) that defines

3687   aerosol optical properties and deposition rates.   Modal aerosol models keep track of

3688   aerosol number-density approximating the aerosol size distribution by a few log-normal

3689   modes with the prescribed width and varying modal radii, accounting for coagulation,

3690   condensation growth, and size-dependent gravitational settling (Niemeier et al., 2009; Bruhl

3691   et al., 2015; Dhomze et al., 2014; LeGrande et al., 2016; Sekiya et al., 2016). The aerosol

3692   sectional microphysical models are the most accurate but computationally more demanding

3693   (English et al., 2013; Mills et al., 2016).

181

3694

3695

3696   There are still significant discrepancies between models, and between the models and

3697   observations. This remains a challenging issue. The 1991 Pinatubo case-study is an important

3698   testbed where different approaches have been compared and could be further investigated.

3699   For example, in (Bruhl et al., 2015) the aerosol optical depth relaxes too fast, but in (Mills et

3700   al., 2016) the stratospheric aerosol plume decays too slowly and the initial SO2 loading has

3701   to be decreased by almost a factor of two to make the results consistent with observations.

3702

9.5 Small Volcanoes, Climate Hiatus, and Geoengineering Analogs

The slowing of global warming, or climate hiatus, in 2000-2013, despite continued emission of greenhouse gases, attracted widespread attention (Meehl et al., 2011; Myhre et al., 2013). Many mechanisms were suggested as causal factors. These included natural variability associated with increased ocean heat uptake (Balmaseda et al., 2013) and cooling forced by small volcanic eruptions (Fyfe et al., 2013; Haywood et al., 2014; Santer et al., 2014; Solomon et al., 2011). The latter refers to eruptions of Kasatochi in August of 2008, Sarychev in June 2009, and Nabro in June 2011. They were the most significant recent events, however, 15-20 times weaker in terms of SO_2 injection than for the Pinatubo eruption. The estimated global mean surface temperature perturbations that they could cause range from 0.02 K to 0.07 K (Haywood et al., 2014; Santer et al., 2014). However, Andersson et al. (2014) reported that about 30% of aerosols from these small volcanoes were retained in the lowermost stratosphere and their total optical depth was underestimated in observations.

The deliberate injection of aerosols and aerosol precursors in the lower stratosphere suggested to reduce greenhouse warming (Crutzen, 2006; Wigley, 2006; Govindasamy and Caldeira, 2000; Robock et al., 2010; Heckendorn et al., 2009) is discussed in detail in Section 17. The associated processes have much in common with the effects of volcanic aerosols. Therefore the understanding of all aspects of stratospheric aerosols and climate links, which we gain from investigating the climate consequences of volcanic eruptions, is important for a feasibility assessment of solar management schemes (Pitari et al., 2014; Tilmes et al., 2009; Aquila

183

3726   et al., 2014; Haywood et al, 2013; Aquila et al., 2012; Kravitz et al., 2013; Tilmes et al.,

3727   2013).

3728

9.6 Dynamic and Thermal Responses To Volcanic Eruptions

3729
3730

3731 Improvements in our understanding of volcanic forcing help to better understand past climate

3732 and make a better climate prediction. It also enables the radiative forcing and accompanying

3733 transient response due to volcanic aerosols to be placed in perspective, relative to the forcing

3734 and responses due to the increases in the anthropogenic well-mixed greenhouse gas emissions.

3735 Since 1850 volcanic forcing has offset the ocean heat content increase due to the global-mean

3736 warming by about 30% (Delworth et al. 2005). Comparison of simulated and observed climate

3737 responses to the major volcanic eruptions helps to evaluate volcanic forcing itself. The

3738 relatively large transient forcing by volcanic aerosols offers a platform to test climate model

3739 simulations of stratospheric and surface temperature perturbations against observations.

3740 The net radiative effects of volcanic aerosols on the thermal and hydrologic balance (e.g.,

3741 surface temperature and moisture) have been highlighted in (Kirchner et al., 1999; Free and

3742 Angell, 2002; Jones et al., 2004; Trenberth and Dai, 2007). Atmospheric temperature after

3743 volcanic eruptions relaxes for 7-10 years, while the deep ocean retains a thermal perturbation

3744 for about a century (Stenchikov et al., 2009; Delworth et al., 2005). Gregory et al. (2013)

3745 indicated the importance of the pre-industrial volcanic forcing to predict future climate

3746 correctly. The prolonged volcanic activity could be a reason for a long-term climate cooling as

3747 it had arguably happened during the medieval Little Ice Age in 1300-1850 (Free and Robock,

3748 1999) when in the middle of this period the cooling was enhanced by the Maunder Minimum

3749 in Solar Irradiance (Eddy, 1976).

3750

3751   In addition, the differential heating/cooling due to volcanic aerosols affect atmospheric

3752   circulation. It is believed these circulation responses could cause a positive phase of the

3753   Arctic oscillation and winter warming in high northern latitudes (Ramaswamy et al., 2006;

3754   Shindell et al., 2003, 2004; Stenchikov et al., 2002, 2004, 2006; Perlwitz and Graf, 2001;

3755   Toohey et al., 2014;), prolong or even initiate El Nino (Adams et al., 2003; Pausata et al.,

3756   2015; Predybaylo et al., 2017; McGregor et al., 2011; Ohba et al., 2013), or damp monsoon

3757   circulations (Trenberth and Dai, 2007; Anchukaitis et al., 2010; Iles et al., 2013; Schneider et

3758   al., 2009). There are still large discrepancies between the models on the magnitude and the

3759   leading mechanism that forces those dynamic responses, and observations are not long

3760   enough to provide empirical proof of a concept. E.g., (Polvani et al., 2019) argued that the

3761   positive phase of Arctic Oscillation in winter of 1991/1992 was not casually forced by the

3762   1991 Pinatubo eruption, as it was not associated with the strong northern polar vortex.

3763   However, one has to take precaution making a far-reaching conclusion from their analysis as

3764   the authors only considered one volcanic winter that does not exhibit a statistically

3765   significant climate signal.

3766

3767   One robust finding in terms of dynamical response to high latitude eruptions that

3768   preferentially load one hemisphere relative to the other, is that tropical precipitation

3769   associated with the Inter-Tropical Convergence Zone is shifted towards the unperturbed

3770   hemisphere in both observations and global climate models (Oman et al., 2006 Haywood et al.,

3771   2013). Thus, significant high latitude ruptions in the northern hemisphere (e.g., Katmai which

3772   erupted in 1913) can lead to drought in sub-Saharan Africa and cause the North Atlantic

3773   hurricane frequency to dramatically reduce in years subsequent to the eruptions (Evan, 2012;

186

3774 Jones et al., 2017). These impacts are relatively well understood from theoretical constraints

3775 on cross equatorial energy and moisture transport (e.g. Bischoff and Schneider, 2014; 2016).

3776 Equatorial eruptions also can affect the position of African rain-belt by the combined effect

3777 of the preferential hemispheric summer cooling and damping of Indian Monsoon (Dogar et

3778 al., 2017).

3779

3780 **9.7 Summary**
3781
3782

3783 Stratospheric aerosols exert a substantial, albeit transient, impact on climate after the Junge

3784 layer is replenished by strong volcanic injections. For the equatorial eruptions, the radiative

3785 forcing peaks in about a half a year after a volcanic explosion and relaxes with the e-folding

3786 time of one-two years. For the high-latitude eruptions, the e-folding time is shorter than for

3787 tropical ones. Despite the transient nature of the volcanic forcing, the global ocean integrates

3788 the cooling from multiple eruptions extending the climate response to decades and even

3789 centuries (Delworth et al., 2005; Stenchikov et al., 2009).

3790

3791 Our understanding of the effect of stratospheric aerosols has grown substantially over the last

3792 century, from descriptive and intuitive knowledge base to the full-scale first-principle

3793 modeling supported by ground-based and satellite observations. Despite this progress, the

3794 error bars in volcanic radiative forcing probably remain larger than 20-30%. Because we

3795 have a limited ability to reconstruct volcanic forcing in the past, it is extremely important to

3796 further develop models that could interactively simulate volcanic plume development and its

3797 radiative effect. The best models so far demonstrate a sizable discrepancy with available

3798   observations that also may bear a significant uncertainty. One important bottle-neck is

3799   aerosol particle size distribution that is controlled by fine-scale microphysical processes.

3800   Particle sizes are important as they define both radiative effects of aerosols and their

3801   lifetime with respect to gravitational settling. The accumulation of the effect of small

3802   volcanic eruptions has to be better understood as it contradicts the expectation of a smaller

3803   lifetime of above-tropopause emissions. The pre-calculated, based on observations, aerosol

3804   datasets have their value in helping to better calibrate simulated climate

3805   responses to volcanic forcing.

3806

3807   It is important to consider radiative forcing and climate responses in combination, as this

3808   gives important feedback on how well a model reproduces the observed climate variations.

3809   The climate models are capable of calculating the thermodynamic responses to the volcanic

3810   aerosols forcing, but fail to consistently reproduce the circulation anomalies forced by

3811   volcanic eruptions. Further development of model capabilities and stratospheric aerosol

3812   monitoring are necessary to reduce uncertainties in past and future climate simulations

3813

3814

3815

Figure captions

Figure 9.1

Global mean optical depth of stratospheric sulfate aerosols for 0.55 um calculated using

CMIP6, Sato et al. (1993) with (Schmidt et al., 2011) corrections, and Amman et al.

(2003) data sets

Figure 9.2.

Global mean radiative forcing (clear-sky and all-sky) at top of the atmosphere after the

1991 Pinatubo eruption as a function of time calculated using different volcanic aerosol

datasets

Figure 9.3.

Zonal mean SW (top row) and LW (bottom row) Heating Rates after the 1991 Pinatubo

eruption calculated using CMIP6 (left column), Sato1.8 (middle column), and Sato2

(right column) datasets averaged over the equatorial belt of 5S-5N as a function of time

and pressure.
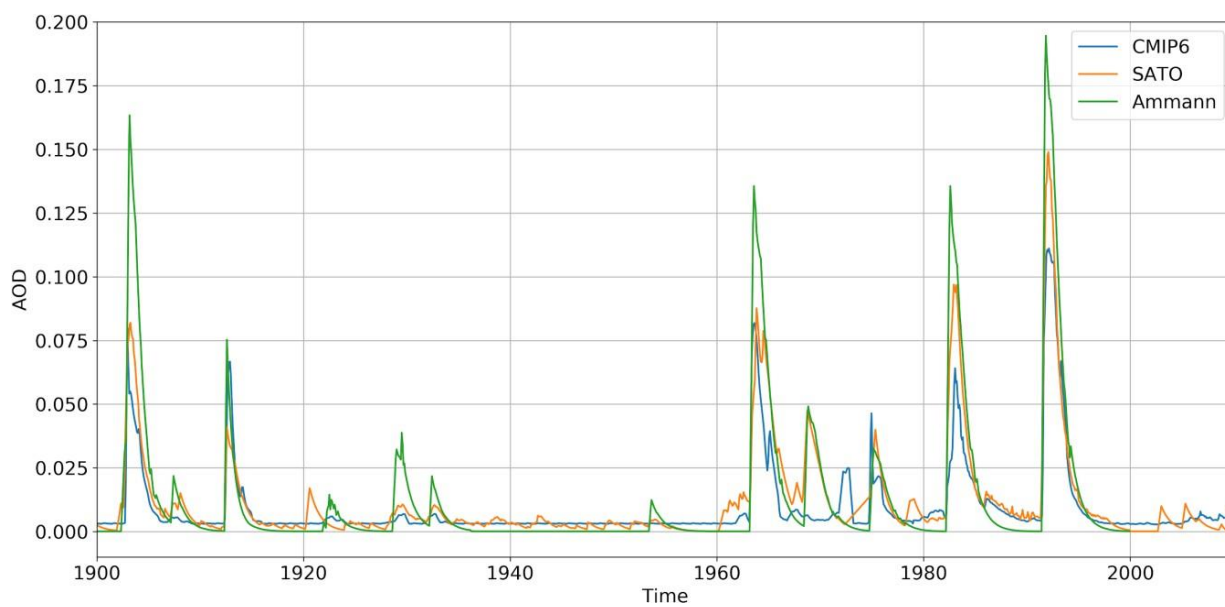
3836

3837

3838

3839

3840

3841

3842

3843

3844

3845

3846

3847

3848

3849

3850

3851

3852
3853 **Figure 9.1**

3854

3855
3856

Shortwave (down - up) flux at TOA — Outgoing longwave flux at TOA — Total (SW + LW) flux at TOA

3857
3858 **Figure 9.2.**

3859   .

3860
3861
3862 **Figure 9.3**.

3863
3864
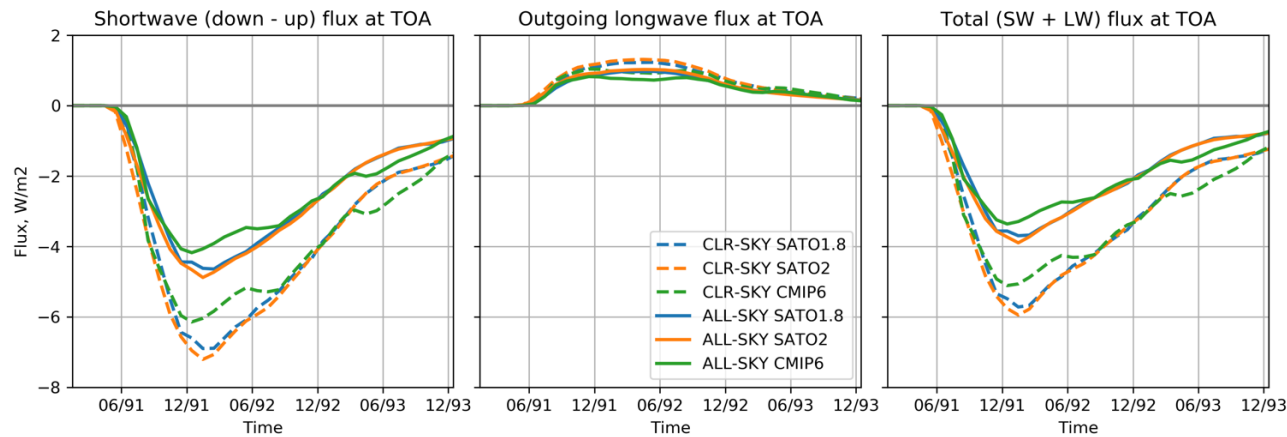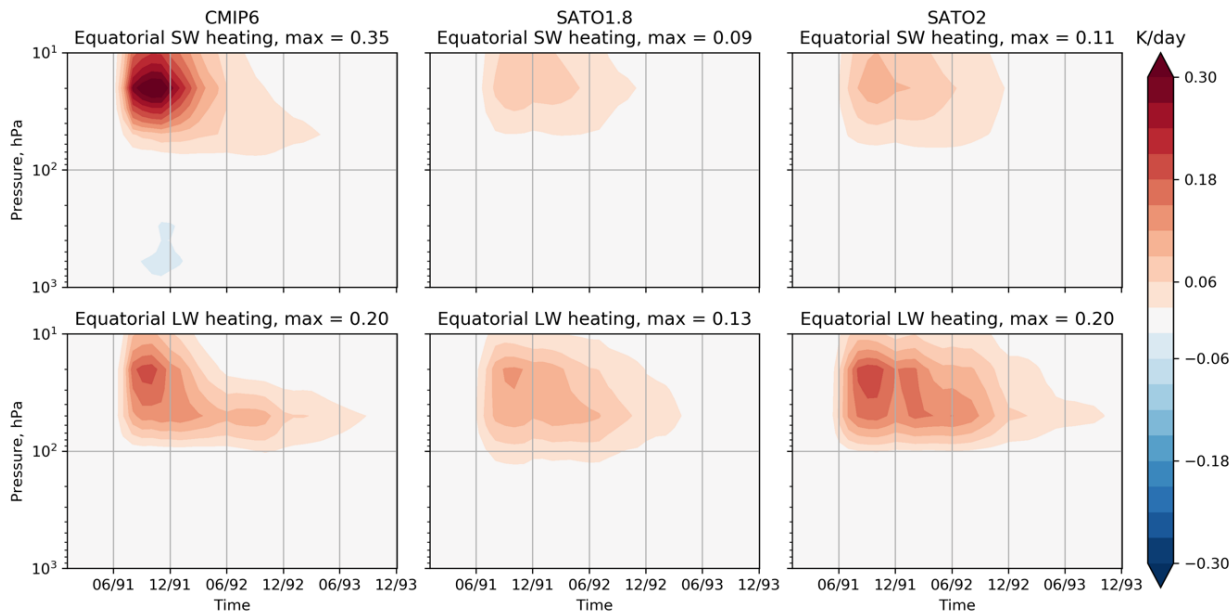
3865

3866   **10. Total natural and anthropogenic radiative forcing**

3867

3868   This section describes developments in the comparison of different forcing agents which then

3869   naturally leads to estimates of the total forcing and its time evolution, and thus acts as a

3870   synthesis of the material in the previous Sections. The nature of the forcing agents is

3871   very different in terms of magnitude, uncertainty, spatial distribution and time evolution

3872   (see sections 2-9).

3873

3874

3875

3876

3877

10.1 Complexity in comparing forcing agents

Kiehl and Briegleb (1993) were the first to provide model estimates of the geographical

distribution of the net forcing of WMGHGs and the direct sulfate aerosol effect. The results

showed that the WMGHG forcing in northern industrialized regions at mid-latitudes was

strongly offset by the direct aerosol effect, but the offset was much weaker in the tropics where

WMGHG forcing is at maximum. A distinct spatial distribution was also found in modelling

studies for tropospheric ozone and biomass burning by Penner et al. (1992) with a maximum

near the emission regions located over the continents, and for stratospheric ozone forcing by

Ramaswamy et al. (1992) with a negative forcing in the middle to high latitudes but near-zero

or small negative in the low latitudes.

Geographical distributions of various climate drivers, and further estimates of RF and their

uncertainties, were given in Shine and Forster (1999), Hansen et al. (2000), and assessed in

TAR. All these estimates showed a large difference in the uncertainty of WMGHG forcing and

other climate drivers, in particular, aerosol effects. The much larger uncertainties are due to

known factors such as the aerosol distribution and optical properties, as well as uncertainties in

the physical process of aerosol-cloud interactions. Compared to relatively low uncertainties for

WMGHGs, this made it difficult to provide a net RF. In addition to providing uncertainty

ranges for the climate drivers, TAR presented the "Level of Scientific Understanding" which

showed large difference among the climate drivers. This illustrated the difficulty at that time of

providing a net forcing for both global and annual means and geographical distributions.

Ramanathan et al. (2001) and Kaufman et al. (2002) on regional scale and AR4 globally pointed

out the distinct differences in the net anthropogenic forcings at TOA and surface, which

193

3903   demonstrates the sharp differences between the relatively homogeneous WMGHG forcings and

3904   the much more spatially inhomogeneous aerosol forcing.

3905

10.2 Applications of probability distribution functions to derive total anthropogenic forcing

Boucher and Haywood (2001) provided a method to estimate a net global-mean RF from components with different uncertainties, a method which has since been used in IPCC assessments beginning with AR4. The method used probability distribution functions (PDFs) for the individual climate drivers and a Monte-Carlo approach to estimate the net RF. In Boucher and Haywood (2001) various assumptions on the shape of the PDFs such as normal and log-normal distributions were investigated. They found a higher sensitivity to how uncertainty ranges should be interpreted than to the shape of the PDFs. This has led to an improved quantification of uncertainty range and confidence levels in later research and whether RF numbers are given as e.g. one standard deviation or 5-95% confidence intervals. The method of Boucher and Haywood (2001) allows the calculation of a mean net RF (with an uncertainty range) and the quantification of the probability of the RF falling outside a certain range, e.g. the probability for a negative RF given the time period for the selection of climate drivers.

Fig 10.1 shows PDFs for global-mean forcing, relative to 1750, due to total aerosols, total WMGHGs, and the net of all climate drivers for IPCC AR4 and AR5 as well as two scenarios for 2030 (RCP2.6 and RCP8.5). RFs are presented for AR4 PDFs. All the other results use ERF, but the AR5 WMGHG RF is also shown to illustrate the larger uncertainty in ERF (20%) relative to RF (10%). The mean estimates of ERF and RF for WMGHGs in AR5 are the same, but the much wider PDF for ERF relative to RF is evident.

195

3929

3930   The change in net forcing between AR4 (1750-2005) and AR5 (1750-2011) results partly from

3931   the introduction of ERF, partly from the increase in the WMGHG forcing of 8% due to changes

3932   in concentrations between 2005 and 2011, and partly from a wide range of other updates based

3933   on a better understanding of processes important for forcing

3934

3935   The change in the forcing for the two RCPs compared to AR5 (1750-2011) is solely due to the

3936   trends in atmospheric composition. The main change in the scenarios are due to aerosols and

3937   WMGHGs; the changes to other climate drivers are small (less than 0.1 W m^{-2}) (Myhre et al.,

3938   2015). The weaker aerosol forcing and increased WMGHG forcing enhance the net forcing quite

3939   substantially in 2030 (for both RCPs) relative to AR5 (1750-2011) forcing. Furthermore, the

3940   weaker contribution from aerosols (with its high uncertainty) and a stronger dominance of

3941   WMGHGs (with its relatively low uncertainty) contributes to a smaller uncertainty in the future

3942   forcing in both absolute and relative terms. The increase in CO_2 in the two scenarios is

3943   responsible for between 80 and 100% of the increase in WMGHG forcing, and is a strong

3944   contributor to the lower uncertainty in the net forcing. The reduction in the magnitude of the

3945   aerosol forcing is consistent with recent developments in trends of aerosol abundance (e.g.

3946   Paulot et al., 2018).

3947

3948   Since AR5, the WMGHG concentration has increased and there have been updates to RF and

3949   the quantification of rapid adjustments (see sections 2 and 3). The upper bar in Figure 10.2

3950   shows the net anthropogenic ERF from AR5 (which was for the period 1750-2011) with an

3951   absolute (5-95%) uncertainty range of 2.2 W m^{-2} (1.1 to 3.3 W m^{-2}). Keeping everything the

3952   same as in the upper bar, except updating WMGHG concentrations (to 2018) using the growth

3953   rates from NOAA (https://www.esrl.noaa.gov/gmd/aggi/aggi.html) and the methane forcing

3954   expression (to include the solar absorption component from Etminan et al. 2016) gives the

3955   middle bar of Figure 10.2. The best estimate increases from 2.3 W m^{-2} in AR5 to 2.7 W m^{-2}.

3956   With a better quantification of rapid adjustments (see Smith et al., 2018 and section 2) the

3957   uncertainties in tropospheric rapid adjustment to ERF of CO_2 is about 10% leading to a total

3958   ERF uncertainty of 14% compared to the 20% uncertainty assumed in AR5. A large part of the

3959   diversity in the ERF of CO_2 is likely to be from the instantaneous RF (Soden et al., 2018). The

3960   lower bar in Figure 10.2 combines the contribution of uncertainties in detailed off-line

3961   calculations (10%) with the 10% uncertainty from climate model simulated rapid adjustment.

3962

3963

3964   **10.3 Time evolution of forcing**

3965
3966   The natural climate drivers from volcanic eruptions and solar irradiance changes have large

3967   interannual variations (Section 8 and 9) and because of that, it is difficult to include these in the

3968   PDF of climate drivers for a time period. The time evolution of the natural climate drivers

3969   represents their relation to anthropogenic drivers much better than providing forcing over a

3970   fixed time period. Hansen et al. (1993) provided, for the first time, the evolution of various

3971   forcing agents and the net RF (Figure 10.3). Figure 10.3 shows that there is a remarkable

3972   similarity between the evolution of net forcing until 2000 between Hansen et al. (1993) and the

3973   estimate in IPCC AR5, given all the new insights since early 1990s. A strengthening in the

3974   aerosol forcing especially in the period 1950 to 1980 is further illustrated in Figure 10.3 as is the

3975   strengthening of WMGHG forcing since 1960.

3976
3977
3978
3979
3980

10.4 Summary and challenges

The AR5 result shown in Figure 10.1 led Myhre et al. (2013) to conclude that "it is certain that the total anthropogenic forcing is positive" strengthening the "extremely likely" wording used in AR4 (Forster et al. 2007). Nevertheless, despite this strengthened language, the AR5 1750-2011 net anthropogenic forcing (2.3 (1.1 to 3.3) W m^{-2}) indicates that uncertainties remain very large compared to the best-estimate net forcing; this significantly hinders efforts to derive, for example, climate sensitivity given observed temperature changes, and inhibits understanding of the effectiveness of proposed mitigation pathways, with consequent impacts on the confidence in the advice given to policymakers.

Challenges to decreasing the spread in the estimated net forcing include (i) ensuring adequate monitoring of changes in concentrations of drivers of forcing, and improved understanding of the pre-industrial background values, especially for aerosols and ozone and (ii) improving methods of calculating the forcing, given these constituent changes. It is particularly notable that the introduction of ERF in AR5 led to an increase in the uncertainty of the WMGHG forcing. While the relative uncertainty in WMGHG is lower than other components, Myhre et al. (2013) give the absolute 5-95% % uncertainty for the 1750-2011 ERF as 1.14 W m-2; this is only slightly less than the corresponding values for the aerosol-cloud interaction (1.2 W m-2). Recent results indicate progress in understanding rapid adjustment. Given the expected increasing dominance of WMGHG forcing in coming decades (Figure 10.1) this indicates the importance of improved estimates of the rapid adjustments in order to reduce the WMGHG ERF uncertainty, as well as efforts to better characterize the other remaining uncertainties in WMGHG forcing. It is also clear that, to date, most efforts on estimating the net forcing have

199

focused on the global-mean; further attempts to provide geographical distributions of the net

forcing, and the associated confidence levels, would allow additional insights into the drivers of

climate change.
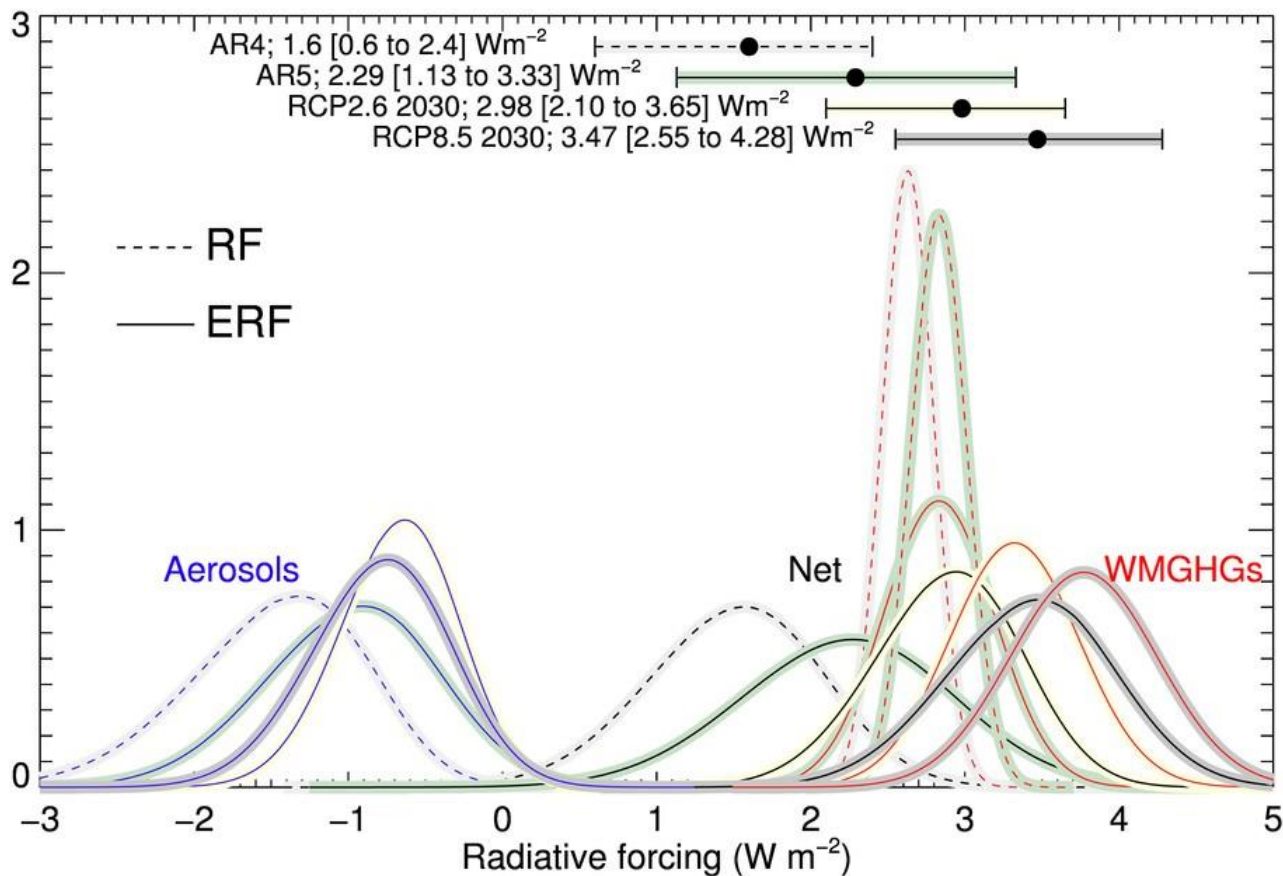
Figure 10.1: Probability distribution functions of forcing from IPCC AR4 (1750-2005) (Forster et al., 2007), IPCC AR5 (1750-2011) (Myhre et al., 2013) and two scenarios for year 2030 relative to 1750 (RCP2.6 and RCP8.5) (Prather et al., 2013). Black lines show net forcing, blue lines show total aerosol forcing, and red lines show WMGHG forcing. The colors around the lines provide information on AR4, AR5 and RCPs. Unlike AR5, the red line includes solely the WMGHGs and does not include ozone and stratospheric water vapor.
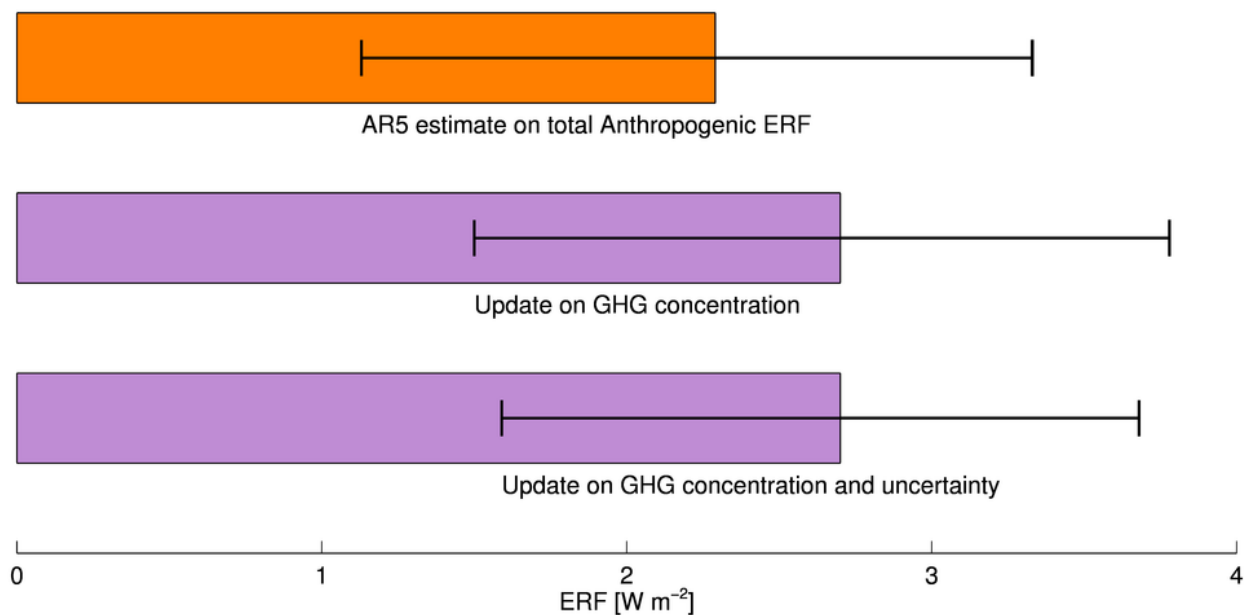
Figure 10.2: Estimates of the net anthropogenic ERF from AR5 (1750-2011) (upper bar),   the effect of updates to WMGHG concentrations (1750-2018) and to the methane RF expression (middle bar), and updates to the uncertainty range due to improved understanding of rapid adjustments (lower bar).
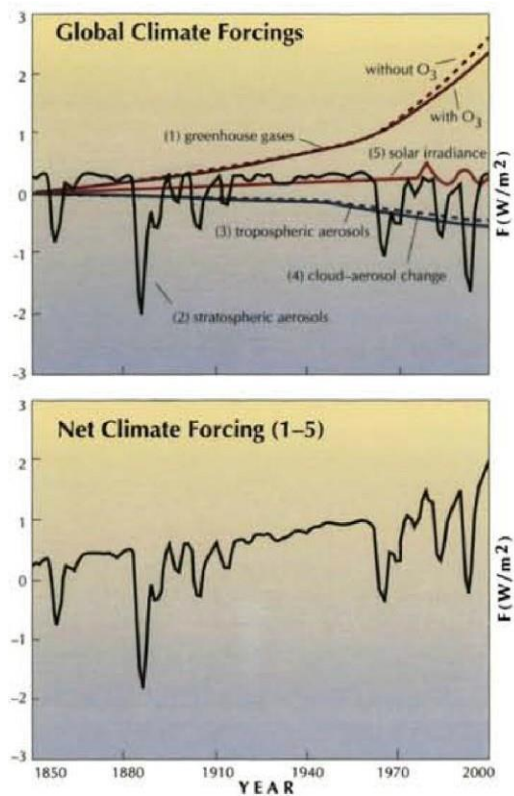
4031
4032
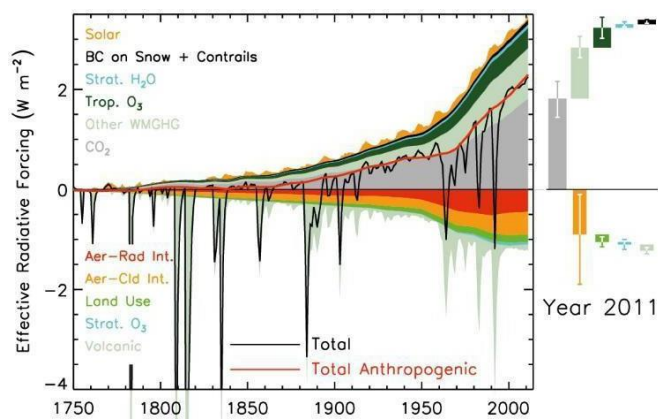
4033

4034   **Figure 10.3**: Time evolution of radiative forcing for individual and net forcings 1850-

4035   2000 (Hansen et al., 1993) (left) and IPCC AR5 estimates of individual and net forcings

4036   1750-2011 (right).

4037
4038

11. Emission metrics and radiative efficiencies

As described in previous sections, RF has great utility in quantifying the radiative impact of changes in concentrations of different atmospheric constituents, and in assessing their relative importance. RF has also found an important usage in serving climate policy, by enabling methodologies, which are simple to apply in a policy context, to compare the climate impact of *emissions* of different species; this role is discussed in this section.

11.1 Background

RF at a given time (e.g. present day), relative to some past time (e.g. pre-industrial), is an

important indicator of the absolute and relative importance of different drivers of climate

change. That forcing depends on the past history of emissions. In the case of CO_2, because of

the long persistence times of atmospheric perturbations, emissions over a century ago are still

impacting present-day RF; at the other extreme, the present-day RF due (directly) to aviation

contrails is mostly the result of contrails formed in the preceding few hours. The influence of

the lifetime of perturbations is implicit in, for example, the standard IPCC forcing bars (Fig

1.2), but this provides little guide to future influence of present-day forcing agents. Fig 11.1

(from Fuglestvedt et al. 2010) illustrates this point for an extreme scenario when a selection of

emissions from the transport sector are instantaneously reduced to zero. The forcing due to CO_2

emissions persists for centuries, while most of the forcing due to short-lived species reduces to

zero within a few weeks.

From a policy perspective, the explicit consideration of these timescales is important, for

example in assessing the future impact of present-day emissions. In addition, in the context of

climate agreements which cover emissions of a range of different gases (sometimes called multi-

gas agreements), it is necessary to place the climate impact of different emissions on a common

scale. Via the application of a climate emission metric (henceforth "metric"), it is (at least in

principle) possible to aggregate all emissions into a single "CO_2-Equivalent" value.

There are many aspects and choices, some contentious, to consider in the design and application

of such metrics and there is no agreed metric which is suitable for all purposes. The issues have

4077   been extensively discussed in various reviews and assessments and

4078

4079   has continued through all IPCC ARs (e.g. Fuglestvedt et al. 2010, Myhre et al. 2013). Some

4080

4081   of the issues extend beyond physical science, and reflect policy choices on, for example the

4082

4083   appropriate timescales and the extent to which the chosen metric serves the aims of a particular

4084

4085   policy. Here the focus will be on the role of RF in computing these metrics.

4086

4087
4088
4089

11.2 The Global Warming Potential

By way of illustration, one metric, the Global Warming Potential (GWP), is considered briefly

here; it is the most widely used metric in international policymaking

. The GWP was presented in FAR, based on rather

few precursor studies (Derwent, 1990; Fisher et al., 1990; Lashof and Ahuja 1990; Rodhe 1990)

and has been assessed in all IPCC assessments since then. The GWP is, for example, used by

parties to the 1997 Kyoto Protocol to the United Nations Framework Convention on Climate

Change (UNFCCC) to place emissions of more than 20 gases on a common CO_2-equivalent

scale, and in the UNFCCC's 2015 Paris Agreement. It is also used within the 2016 Kigali

Amendment to the UN's Montreal Protocol on Substances that Deplete the Ozone Layer, to

place targets on emissions of many hydrofluorocarbons.

The GWP measures the time-integrated RF of a pulse emission of a unit mass of a

climate forcing agent (or its precursor) relative to the time-integrated RF of a pulse

emission of a unit mass of CO_2. For each agent, it is necessary to know the radiative efficiency

(i.e. the RF per molecule or per kilogram) and its lifetime, which determines the

decay of the pulse after emission. In addition, indirect forcings resulting from that emission

should be incorporated; one example is the impact of methane emissions on ozone, stratospheric

water vapour and CO_2. In almost all policy applications of the GWP, the integration is

performed over 100 years (the "time horizon"), and denoted GWP(100). However, there is no

compelling scientific reason for that choice, and the perceived importance of emissions of a gas

(i.e. their contribution to CO_2-equivalent emissions) can depend markedly on that choice,

4128   especially for short-lived species. For example, for methane, AR5 (Myhre et al. 2013) reports
4129
4130   values of GWP(20) and GWP(100) of 84 and 28 respectively.
4131
4132
4133
4134   All IPCC assessments have presented values of GWPs for a range of gases (more than 200 are

4135   included in Myhre et al. (2013)) and have discussed scientific issues in determining the input

4136   parameters. The reported values of GWP(100) for some species have varied quite strongly over

4137   time. For example, the GWP(100) for methane has increased from 21 to 28 between FAR (Shine

4138   et al., 1990) to AR5 (Myhre et al. 2013) as a result of changes in the recommended values of

4139   methane's radiative efficiency, lifetime and indirect effects, as well as changes in the radiative

4140   efficiency and lifetime of CO_2. Advances in understanding since AR5 (for example, the effect of

4141   methane's near-infrared

4142   absorption bands (Section 3)), and the incorporation of the influence of carbon-climate feedbacks

4143   (e.g. Gasser et al. 2016, Sterner and Johansson 2017), could see the recommended

4144   GWP(100) value for methane change significantly in future.

4145

4146

4147
4148
4149

11.3 Radiative efficiency

Radiative efficiency (RE) is a key input to all the main emission metrics that have been

proposed to support multi-gas agreements. By convention, IPCC assessments have computed

the RE for a small perturbation to present-day concentrations for the more major greenhouse

gases (CO_2, CH_4, N_2O), for which forcing does not increase linearly with

concentration; for more minor species, present in sub-ppbv concentrations, the forcing

is assumed to be linear in concentration. RE calculations need to be

representative of global-average conditions including the effects of clouds (e.g. Myhre and

Stordal 1997). Irrespective of its use in metrics, the RE gives insights into the role of different

gases. For CO_2., Myhre et al. (2013) report a value of 1.37×10^{-5} W m^{-2} ppb^{-1}. The RE of methane

is 26 times higher and nitrous oxide's is 220 times higher. Halocarbons are often greater than

10,000 times more effective, per molecule. There are multiple reasons for these differences in

RE (e.g. Shine 1991). These include the fundamental spectroscopic intensity of each molecule,

which is determined by the probabilities of vibration-rotation transitions, the wavelengths of

absorption features relative to the Planck function at typical atmospheric temperatures, the pre-

existing atmospheric concentrations of the molecule (as RE decreases with concentration), and

overlap with absorption features of other atmospheric gases (notably water vapor and CO_2).

Hodnebrog et al. (2013) attempted to characterize the sources of uncertainty in calculating REs,

focusing particularly on the halocarbons. The overall conclusion was that REs were accurate to

within 15% for longer-lived gases and to within about 25% for the

shorter-lived gases.

209

4174

4175

4176   Compilations of halocarbon REs and the associated emission metrics in many earlier

4177   IPCC assessments drew values from different sources which used various techniques to

4178   compute the forcing. This inhibited a reliable comparison of the RE of different gases. AR5

4179   (Myhre et al. (2013)), using the Hodnebrog et al. (2013) calculations, tried to enhance the

4180   consistency between   gases, by adopting a single method for calculating the RE.

4181

4182   To date REs have mostly been computed using RF (i.e. accounting for stratospheric temperature

4183   adjustment in some way), rather than using ERFs for several reasons. First, computing ERFs for

4184   such large numbers of gases using GCMs would be a formidable task; in future, a simpler

4185   generic framework for estimating rapid adjustments could be developed if it was shown to be

4186   applicable to a wide range of gases. Second, , GCM radiation codes do not have the spectral

4187   resolution that is necessary for reliable RE calculations for gases with generally quite narrow

4188   spectral features. Finally, because of the noise inherent in GCM calculations of ERF, estimation

4189   of REs for sub-ppbv concentrations (and hence radative forcings below about 0.2 W m^{-2}

4190   (Forster et al. 2016) would be difficult; while artificially high perturbations could be imposed in

4191   GCMs, this would raise questions about the applicability of the results to more realistic

4192   concentrations found, or likely to be found, in the atmosphere.

4193

Molecule	Radiative Efficiency (W m^{-2} ppb^{-1})	Radiative Efficiency relative to CO_2
CO_2	1.37×10^{-5}	1
CH_4	3.63×10^{-4}	26
N_2O	3.00×10^{-3}	219
CFC-12	0.32	23,360

| HFC134a | 0.16 | 11,680 |
| SF_6 | 0.57 | 41,600 |

4194

4195   Table 11.1 Radiative efficiencies (in W m^{-2} ppb^{-1}, and relative to CO_2) for a selection

4196   of gases (values from Myhre et al. 2013).

4197

4198

4199

4200
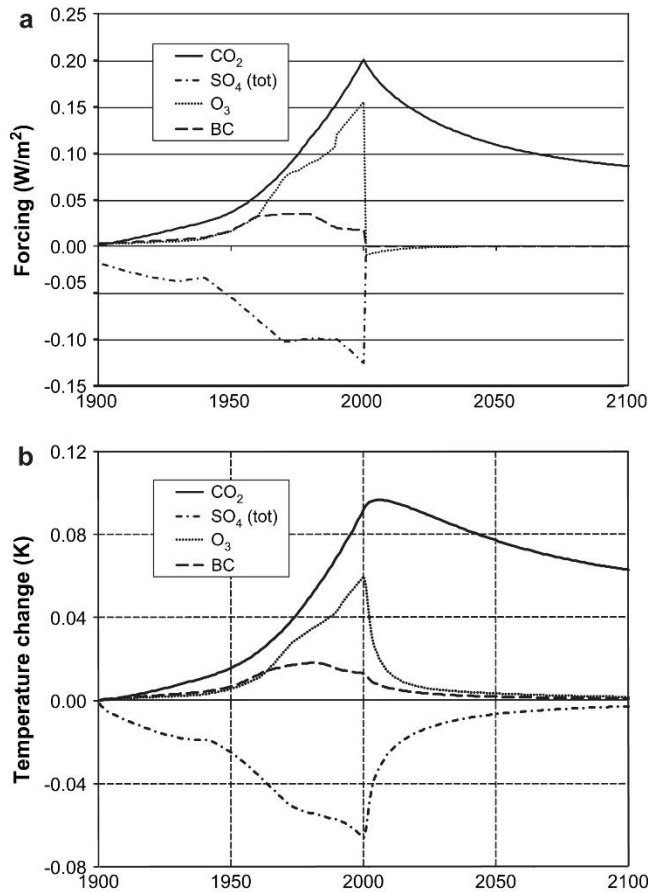
4201   Figure 11.1: Consequences for RF of different agents and associated temperature response over
4202   time from an assumed scenario when a selection of emissions from the transport sector is
4203   instantaneously reduced to zero in 2000.

4204
4205

12. Climate Response to Radiative Forcings

4209
4210
4211 Radiative forcing is an essential component in understanding historical changes in climate and

4212 their attribution to both natural and anthropogenic causes. Attribution of anthropogenic climate

4213 change requires both models and observations and consists of three steps: (i) detecting a change

4214 in climate; (ii) establishing that this change is consistent with the expected response to the

4215 estimated anthropogenic net forcing; and (c) establishing that this change cannot be explained

4216 by other mechanisms, such as internal variability or natural forcings. Without quantitative

4217 information on the magnitude, spatial structure and temporal evolution of both natural and

4218 anthropogenic radiative forcings, understanding the causes of historical changes in climate,

4219 from glacial-interglacial periods to the change in climate over the past century, would not be

4220 possible.

4221

4222 As an illustration of this process, Figure 12-1 (left column) compares the observed and model

4223 simulated global-mean temperature anomalies from 1860-2012 with that predicted from a multi-

4224 model ensemble of coupled ocean-atmosphere models from CMIP3 (gray lines) and

4225 CMIP5(yellow lines) that are integrated under three different forcing scenarios: historical

4226 natural and anthropogenic forcings (top), natural forcings only (middle), and anthropogenic

4227 greenhouse gas forcings only (bottom). The right columns show the corresponding ERF for

4228 each of these forcing scenarios derived from the CMIP5 simulations following Forster et al.

4229 (2013

4230
4231

4232
4233
4234
4235
4236
4237
4238
4239
4240
4241
4242
4243
4244
4245
4246
4247
4248
4249
4250
4251
4252
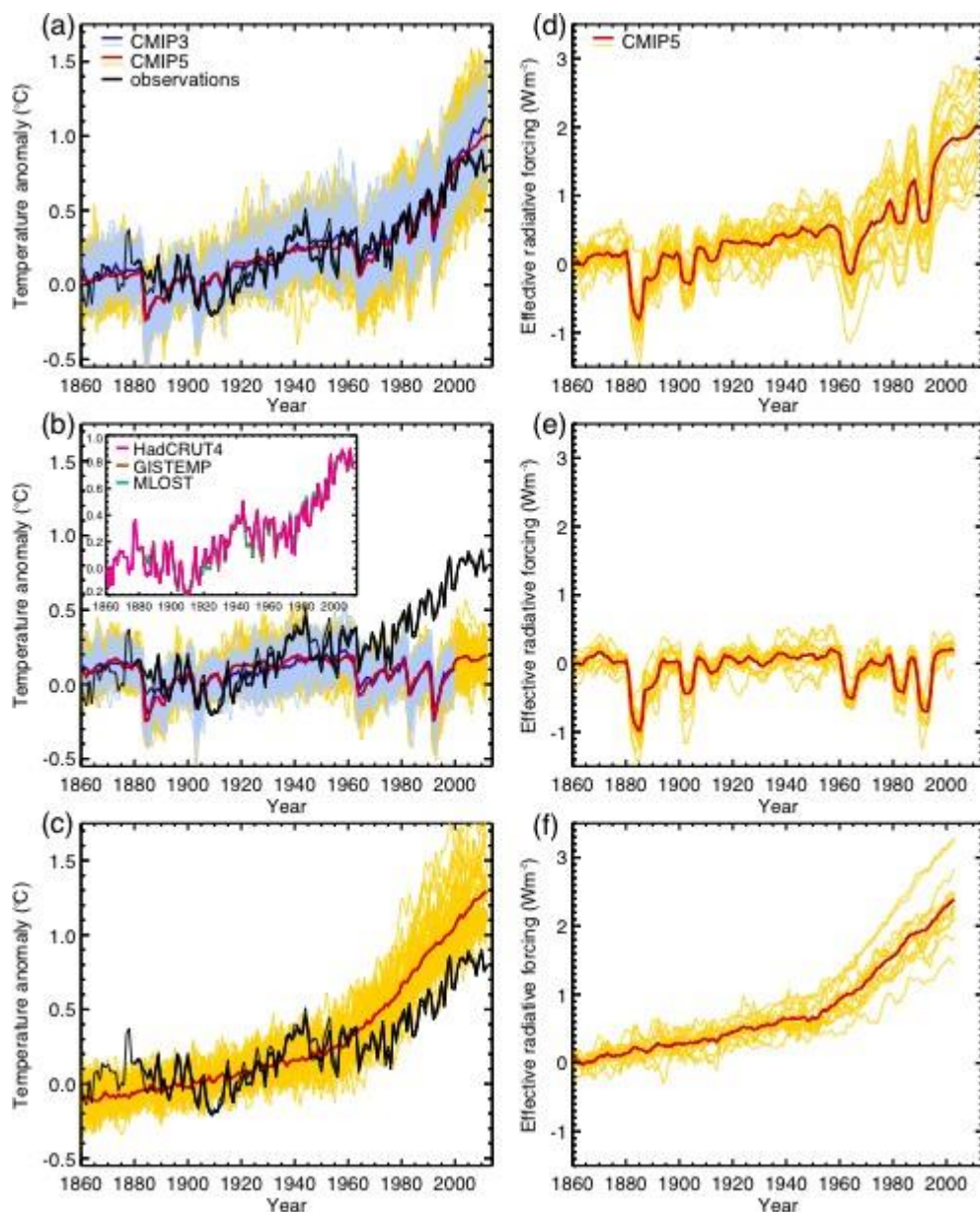
4253 **Figure 12-1: Left-hand column:** A comparison of observational estimates of global mean

4254 surface temperature (GMST, black lines) and climate model simulations [CMIP3 – blue lines;

4255 CMIP5 models – yellow lines] using both anthropogenic and natural forcings (a), natural

4256 forcings only (b) and greenhouse gas (GHG) forcing only (c). Thick red and blue lines depict the

213

4257   multi-model ensemble mean across all CMIP5 and CMIP3 simulations respectively. Note that

4258   CMIP3 simulations are not available for GHG forcing only (c). Inset to (b) shows the three

4259   observational data sets distinguished by different colours. **Right-hand column:** The effective

4260   radiative forcing (ERF) in CMIP5 models due to anthropogenic and natural forcings (d), natural

4261   forcings only (e) and GHGs only (f). Individual ensemble members are shown by thin yellow

4262   lines, and CMIP5 multi-model means are shown as thick red lines. From Bindoff et al. 2013.

4263
4264
4265
4266   This set of simulations highlight the basis for the attribution of recent warming to human-

4267   influenced activities. The simulations with natural forcing alone (center left panel) are unable to

4268   explain the rise in global mean temperature from the mid 20th Century to present. However,

4269   when natural and anthropogenic forcings are combined (top left panel), the model simulations

4270   are in excellent agreement with the observed temperature anomalies. Contrasting these

4271   simulations with the GHG only simulations (bottom panels), serves to illustrate how aerosols

4272   have partially offset a significant fraction of the GHG warming; without aerosols forcing, the

4273   present day global-mean temperatures would have increased another ~0.5 K. Since

4274   anthropogenic aerosols occur primarily in the Northern Hemisphere, these differences also have

4275   a distinct signature on the hemispheric contrast in temperature and precipitation as discussed

4276   below. Thus, accurate knowledge of both GHG and aerosol forcings is critical to understanding

4277   past and projecting future changes in climate, both globally and regionally.

4278

4279   Early attribution studies focused primarily on the changes in global-mean surface temperature

4280

4281   (e.g., Wigley and Raper 1990; Stouffer et al. 1994). These evolved into more complex studies

4282   that considered the spatial pattern or 'fingerprints' of climate change that were predicted by

4283   climate models and used more elaborate statistical methods to search for their presence in the

4284   observed record (Santer et al. 1996b). The fingerprints of anthropogenic climate change were

4285   expanded beyond simply the regional pattern of surface temperature, to consider the vertical

4286   structure of temperature change in the atmosphere and oceans, temperature extremes, and the

4287   diurnal and seasonal cycles of temperature, as well as other variables such as precipitation and

4288   sea level pressure (Santer et al., 1995, Hegerl et al., 1996, 1997, 2006; Stott et al., 2000, 2004;

4289   Vecchi et al. 2006; Meehl et al. 2009; Min et al. 2011; Zhang et al 2007). While each of these

4290   quantities have a defined response to anthropogenic forcing, the use of multivariate changes

4291   enhances the confidence in the attribution process. For example, both solar and GHG forcings

4292   can warm the surface, however they have very different impacts on the diurnal temperature

4293   cycle, precipitation change, and the temperature response in the stratosphere. Across all of these

4294   quantities, the observed changes are only explained through the inclusion of anthropogenic

4295   forcing. Thus, the concept of radiative forcing is fundamental to methods used to identify a

4296   human influence on climate.

4297
4298
4299

12.1 The Spatial Structure of Forcing and Response

As noted in Sections 2, 5, anthropogenic forcing from well-mixed GHGs and aerosols over the historical period have distinctly different spatial patterns – the former being positive and more spatially uniform, whereas the latter is a net negative and largely confined to the Northern Hemisphere. As noted above, this hemispheric asymmetry in the pattern of forcing, has significant impacts on both the detection and attribution of anthropogenic climate change (Bindoff et al., 2013) as well as the transient climate response to forcing in both historical simulations and future projections (Shindell, 2014).

For example, rainfall observations reveal a coherent southward shift of the tropical rain belt over the latter half of the 20th Century, which has been associated with severe droughts over the Sahel and portions of South America (Folland et al. 1986; Allen et al 2002). Observations in the last few decades of the 20th Century have revealed a weakening of the monsoon (Ramanathan et al., 2005, Chung and Ramanathan, 2006; Lau and Kim, 2006). This tropical precipitation shift has been linked to changes in the cross-equatorial energy transport driven by the interhemispheric contrast in the warming of the surface temperatures that arise from the combination of a spatially inhomogeneous shortwave forcing by aerosols and a relatively more homogeneous longwave forcing by WMGHGs (Kang et al. 2008). This type of a spatial structure in the radiative forcing leads to a decrease of the shortwave flux, primarily felt at the surface in the northern hemisphere (e.g., Chen and Ramaswamy, 1996; IPCC, 2001), and an increase in the heating of the atmosphere and surface

4324   globally due to the longwave effects of the WMGHGs (e.g., Ramanathan et al., 1981). The

4325   model- simulated response to this pattern of hemispheric asymmetry in the forcing enhances the

4326
4327   temperature gradient, induces a change in the meridional circulation and intensifies the heat and
4328
4329   moisture exchange between the two hemispheres across the equator, effectively moving the
4330
4331   tropical precipitation belt towards the warmer hemisphere (Ramaswamy and Chen, 1997).
4332
4333   Subsequent studies with improved models have affirmed this characteristic for realistic aerosol
4334
4335   and WMGHG forcings (Rotstayn and Lohman 2002; Ming and Ramaswamy, 2009; Hwang et

4336   al. 2013; Shindell et al. 2015; Wang 2015).

4337
4338
4339   Both aerosols and WMGHG influence the spatial pattern of warming. Anthropogenic aerosols

4340   introduce hemispheric asymmetry by preferentially cooling the northern hemisphere, while

4341   WMGHG warms the northern hemisphere more than the southern hemisphere due of the

4342   differing thermal inertia between the two hemispheres (Friedman et al. 2013). When forced by

4343   historical changes in both anthropogenic aerosols and greenhouse gases, the cooling effect of

4344   the aerosols dominates and climate models simulate less warming in the northern hemisphere

4345   compared to the southern hemisphere.

4346
4347   Aerosols induce an anomalous meridional circulation, which reduces the ascent in the northern

4348   tropics and opposes the local Hadley circulation. The hemispheric temperature gradient initiated

4349   reduces the southward cross-equatorial energy transport accompanying the weakening of the

4350   Hadley circulation (Hwang et al 2013; Allen et al. 2002; Bollasina et al. 2011; Soden and

4351   Chung 2017). This change in the large-scale atmospheric circulation, in turn, drives meridional

4352   shifts in the tropical precipitation bands; most notably a southward shift in tropical precipitation

4353   compared to simulations in which only GHG or natural forcings are included. The aerosol-

4354   induced effect on the cross-equatorial circulation and precipitation changes emerges as a strong

4355   spatial feature vis-à-vis WMGHG effects. In addition   the poleward transport of heat in both

4356   atmosphere and ocean are affected by aerosols differently

4357
4358   than in the case of the WMGHGs (Ocko et al., 2013). Polson et al. (2014) note a correlation

4359   between the trend of precipitation in the last few decades of the 20th Century and sulfur

4360   emissions. Recent work has also highlighted the role of aerosol-cloud interactions that induce

4361   adjustments in cloud interactions in amplifying this response. Aerosol forcing is found to induce

4362   secondary changes in the model simulated cloud radiative properties through both microphysical

4363   (Chung and Soden 2017) and large-scale dynamical changes. These changes act to further

4364   increase the hemispheric contrast in forcing, thereby amplifying both the circulation and

4365   precipitation changes. However, the broad spatial pattern of the climate response to aerosols and

4366   well mixed GHG forcings is more similar than would be expected given the differing

4367   geographic distributions of their emissions and forcings (e.g. Boer and Yu, 2003; Levy et al.,

4368   2013; Xie et al., 2013).

4369
4370   Boer and Yu (2003) showed that the CO_2 forcing spatial pattern (with maxima in the sub-tropics

4371   and a minima at high latitudes) explains very little of the surface temperature response pattern

4372   (generally increasing with latitude). While the aerosol forcing pattern explained more of the

4373   aerosol response pattern, the correlation remained small; indeed, the CO_2 and aerosol surface

4374   temperature responses were better correlated with each other than with their "parent" forcing

4375   pattern. Recent studies suggest that atmospheric feedbacks to the different patterns of forcing

4376   serve to homogenize the radiative perturbations, resulting in a more spatially similar pattern of

4377   response for both temperature and precipitation (Ganguly et al., 2012; Xie et al., 2013; Hill et

4378   al., 2015; Tian et al., 2016; Persad et al. 2018;). The rapid atmosphere-only adjustments to the

4379   forcing have been found to be particularly effective at homogenizing the response to aerosols

4380   and GHG forcings.

4381
4382

     Another spatial dimension to be considered is the vertical. An important parameter to consider in

the presence of WMGHG, tropospheric aerosol, and stratospheric ozone forcings is the manner of

changes in the vertical structure of the thermal profile, and comparison of model simulations with

observations (Santer et al., 1996). In the troposphere, there is a warming of the surface and

troposphere primarily due to the combined effect of the positive forcings primarily by WMGHGs

(with smaller contributions from short-lived gases and tropospheric ozone), and negative forcing

by tropospheric aerosols (Mitchell et al., 1990). In the stratosphere, there is a reduction of

temperature due to loss of stratospheric ozone, and increases in CO_2, tropospheric ozone and

stratospheric water vapor (Shine, 1991; Hansen et al., 1995; Ramaswamy et al., 1996; Forster and

Shine, 1997). The confirmation of the model simulations by observed temperature trends, from the

troposphere to the stratosphere and the temporal evolution of the vertical profile of temperature

changes, has helped affirm our knowledge of the radiative forcing agents, the radiative

perturbations they exert on the atmosphere and surface, and the manner of their influences on the

spatial dimensions of the climate system (Hansen et al., 1995; Santer et al., 2005; Fu et al., 2011;

Stott et al., 2004; Ramaswamy et al.,2006).

4383
4384
4385
4386

13. Solar and terrestrial radiation management

13.1 Introduction

The growth in the understanding and quantification of RF, its consequences for climate

change, and the attribution of observed phenomena to forcings, as described in the prior

sections, has initiated conceptual thinking on potential management of the forcing/s to

mitigate climate change. The principal pursuit is on how the long-term WMGHG forcings

can be partially offset or mitigated. The idea of solar and terrestrial radiation

management (STRM), sometimes also referred to as geoengineering, has over the last decade

become one of the research areas in which the concept of radiative forcing has been applied. t

But, the idea is by no means new. As early as the 1960s, Budyko wrote about "...the possibility

of implementing in future some projects of active influence on the climate..." (Budyko 1969).

Ironically, Budyko discussed this possibility as a way to prevent a new ice age, while the current

discussion is focused chiefly on the possibility of intentionally imposing a negative radiative

forcing on the Earth System, and thus introducing a cooling tendency. Specifically, current

research mainly explores the potential of using a few different STRM strategies to counter some

or all of the warming from increasing greenhouse gas concentrations in the atmosphere. While

the first research on this controversial topic began as early as the 1980s (Keith and Dowlatabadi

1992), it was not until Crutzen (2006) that extensive research on   various types of solar and

terrestrial radiation management began. The field represents one of the most recent examples of

how the radiative forcing concept can be useful for a range of research topics. Several

comprehensive reviews and assessments of this literature have been written (Royal society 2009;

4411   Caldeira et al. 2013; Ocean Studies Board 2015). They all share the conclusion that more

4412   research on the risks and benefits of STRM is urgently needed.

4413
4414   To date, research on the topic has been carried out almost exclusively with numerical models,

4415   and assessment has been based on the modeling activity organized by the Geoengineering

4416   Model Intercomparison Project (GeoMIP) (Kravitz et al. 2013). In the following, we review the

4417   major findings that have emerged from numerical modeling to date, with a focus on the

4418   *viability* and *climate response* of the three types of STRM that have gained the most attention

4419   : Stratospheric Aerosol Injection (SAI), Marine Sky Brightening (MSB) and Cirrus

4420   Cloud Thinning (CCT). While the former two strategies fall in the category of Solar

4421   Radiation Management (SRM), the latter belongs to what we can be labeled as Terrestrial

4422   Radiation Management (TRM). Viability in this context refers to the likelihood that the STRM

4423   mechanism in question can produce negative forcings of a magnitude sufficient to counter a

4424   considerable proportion of anthropogenic greenhouse gas forcing (currently at approximately 3

4425 Wm^{-2}, see Section 3).

4426

4427   Here we focus exclusively on the physical science related to STRM, and thus review the

4428   literature to-date and identify important knowledge gaps related to that aspect only. We do

4429   not discuss here any aspect of potential implementation concepts nor factors underlying them.

4430
4431

13.2 Solar radiation management (SRM)

4433

4434

4435   In the following, studies on the two types of SRM that have so far received the most attention

4436   are discussed (Sections 13.2.1 and 13.2.2). SRM strategies that have been proposed but received

4437   limited attention thus far, including surface albedo enhancements and the introduction of

4438   mirrors in space, will not be reviewed here. A review of literature on the climate response to

4439   SRM, with a focus on changes to the hydrological cycle, is presented in Section 13.2.3.

4440

4441

4442

4443

13.2.1 Stratospheric Aerosol Injection (SAI)

Extensive research focused on the major volcanic eruptions of the last century have clearly

demonstrated the conceptual viability of stratospheric aerosol injection as an SRM strategy (see

Section 9). However, reported forcings from GCM studies of SAI over the last decade span a

wide range, with differences

that can mainly be attributed to differing assumptions regarding

injection location and height, injection rates and aerosol sizes; estimates of RF range from -

8.5 to -1.2Wm^{-2}, and the associated global mean cooling ranges from 0.5 to 3.2K 0.5 to 3.2K

(e.g., Rasch et al., 2008, Robock et al., 2008, Jones et al. 2010, Berdahl et al., 2014, Crook et

al., 2015 and Timmreck and Niemeier, 2015). Thus, even the most conservative estimates

suggest that SAI likely has the potential to offset an appreciable proportion of anthropogenic

GHG forcing to date.

Most studies to date have considered stratospheric injection of SO_2, which in many respects

mimic the climate impact of major volcanic eruptions. The advantage of this is that the

global-mean response of the climate system to large injections of sulfur into the stratosphere

is well understood, largely due to studies of the 1991 Mt Pinatubo eruption and other well-

observed volcanic eruptions (see Section 9). However, the spatial responses due to the

volcanic aerosol perturbations are not well-understood and there are knowledge gaps with

respect to the climate feedback processes operating on the time scale of duration of the

stratospheric particles (e.g., cloud interactions, air-sea interactions). Further, the relationship

between the sulfur injection rates and the resulting forcing remains poorly understood and is

4467   expected to be nonlinear. The non-linearity with increasing emission rates arises in part

4468   because of the corresponding increase in aerosol size, which decreases aerosol lifetime and

4469   scattering efficiency. As a result, studies with prescribed aerosol sizes, regardless of emission

4470
4471   rate, may overestimate forcing, especially for high emission rates. A major uncertainty in

4472
4473   this respect is the aerosol coagulation rate in a freshly injected plume under stratospheric

4474
4475   conditions.

4476

4477

4478   Solid materials have also been considered for the purpose of SAI (Weisenstein et al. 2015;
4479   Jones et al. 2016) and could

4480
4481   considerably reduce the stratospheric ozone destruction that follows from injection of sulfur in
4482   the stratosphere. But apart from a few isolated

4483
4484   studies, the associated forcing is largely

4485
4486   unexplored. Irrespective of the injected material, there is broad agreement that large and

4487
4488   negative forcings are achievable through SAI, but considerably less agreement when it comes

4489
4490   to the climate response beyond the intended global mean cooling, which will be discussed

4491   further in Section 13.2.3.

4492
4493

4494

4495

4496

4497

4498

4499

4500

4501
4502
4503
4504
4505
4506
4507
4508
4509
4510
4511
4512

4513

4514
4515

13.2.2 Marine sky brightening (MSB)

While the very first STRM studies focused on SAI, research to explore the alternative strategy

of marine cloud brightening (MCB) also emerged almost three decades ago. Notably, Slingo

(1990) demonstrated how even modest perturbations of cloud properties could induce strong

radiative forcings. This understanding triggered the idea of intentionally perturbing marine

stratocumulus clouds for the purpose of cooling the climate (Latham 1990). Follow-up research

based on satellite observations has since identified the most susceptible regions for the purpose

of MCB as the subtropical regions off the west coasts of the major continents (Alterskjær et al.

2012). By injecting cloud condensation nuclei into the marine boundary layer of these regions,

cloud albedo could be increased through the creation of artificial ship tracks, through the

mechanisms discussed in Section 5. Hill and Ming (2012) employed a coupled-mixed-layer-

ocean-atmosphere GCM to conduct marine stratocumulus brightening experiments and found

that over half of the radiative cooling is due to scattering of solar radiation by the added sea-salt

aerosols while the rest arose from enhancement of the local cloud albedo. This finding was

recently supported by Ahlm et al. (2017), and suggests that the term *Marine Sky Brightening* is

more appropriate for this STRM strategy, as the forcing would manifest both under clear and

cloudy skies.

While no studies of SAI to date have produced positive forcings, Alterskjær & Kristjánsson

(2013) reported from a GCM study that depending on the size of the injected particles (usually

assumed to be sea salt), the competition for the available water vapor could actually lead to a

reduction in cloud droplet number concentrations, leading to a positive forcing. The opposite of

the desired brightening effect has also been reported from studies using large-eddy-simulations,

4541   depending on the background aerosol concentration and humidity (Wang et al. 2011).

4542   Therefore, despite the 17 GCM studies included in Figure 2 supporting the conceptual viability

4543   of MCB as a STRM strategy, important knowledge gaps remain. Notably, many of the early

4544   GCM studies on MCB, which produced very large negative radiative forcings, simply

4545   prescribed an increase in cloud droplet number in marine clouds, and thus could not capture

4546   buffering effects like the one described above.

4547

4548   .

4549

4550
4551

4552

4553

4554

4555
4556

4557

4558 **13.3 Climate response to SRM**

4559

4560 Beyond the global mean cooling which SRM strategies are designed to produce, the following

4561 common features of the simulated climate response to SRM have been identified:

4562
4563 i) SRM naturally yields negative forcings that maximize in the tropics, where insolation is

4564 strong. Consequently, SRM tends to cool the low latitudes more than it cools the polar regions,

4565 and for a global mean cancellation of a given GHG forcing it will generally produce over-

4566 cooling in the tropics while only partly cancelling the high-latitude GHG warming. This would

4567 in turn reduce the equator-to-pole temperature gradient and generate atmospheric circulation

4568 changes.

4569
4570 ii) Along with the cooling comes a reduction in global mean precipitation, as expected. There

4571 is consensus among GCMs that a complete cancellation of GHG warming by SRM in the

4572 global mean will lead to an over-compensation in global mean precipitation. This net

4573 precipitation reduction is a consequence of the relative changes to the surface- and atmospheric

4574 radiation budgets in a climate with both increased GHG forcing and SRM (Bala et al. 2008). It

4575 may therefore prove more beneficial to only partly compensate for the increase in GHG forcing

4576 (MacMartin et al. 2013).

4577
4578 iii) A novel finding is that the reduction of shortwave radiation to the surface that would result

4579 from SRM may have detrimental effects on agriculture, in contrast to what has been reported in

4580 previous studies (Proctor et al. 2018). This finding warrants further investigation.

4581

229

4582   **13.3 Terrestrial radiation management (TRM)**

4583

4584

4585   Only one TRM method has so far received sufficient research attention to merit review

4586   here, namely cirrus cloud thinning (CCT). In the following, the research on CCT and the

4587   associated climate response are reviewed.

4588

4589

13.3.1 Cirrus cloud thinning (CCT)

Taking advantage of the fact that most cirrus clouds exert a net positive cloud radiative effect, this TRM strategy proposes to reduce cirrus cloud coverage and lifetime, and thus generate a negative forcing. The mechanism by which this could be achieved is through seeding of the cold (< 40 C) upper troposphere with ice nucleating particles (INPs), which would allow ice crystals to nucleate and grow even for very slight supersaturations, and thus prevent the abundance of ice crystals that results if saturation ratios becomes high enough for ubiquitous tiny solution droplets to freeze spontaneously (~150%). The resulting large ice crystals would sediment out and reduce cirrus cloud cover and upper tropospheric water vapor, both producing a negative ERF (Mitchell and Finnegan 2009). In theory, this should produce the desired cooling effect, but GCM studies to date produce conflicting results on the matter. The mechanism relies on assumptions about the balance between the dominant ice nucleating mechanisms in the upper troposphere, which is poorly understood in the present. The fact that different studies yield different ERFs should therefore not be surprising.

An additional concern with CCT is the risk of "over seeding", that is, injecting too many artificial INPs which ultimately yield higher cirrus ice crystal concentrations than would have occurred in an unperturbed case, and thus a positive ERF (Storelvmo et al. 2013). For this TRM mechanism, the viability is thus still a topic of ongoing research, but recent cloud-resolving modeling results appear to support viability (Gruber et al. 2019) and reinforce the idea that CCT appears to be most promising in the instance of wintertime cirrus clouds at high latitudes.

231

4614

4615

4616

4617

4618

4619

4620

4621

4622

4623

4624

4625
4626

4627

4628

4629

4630

4631

4632
4633
4634
4635

4636

13.3. 2 Climate response to TRM

CCT does not reduce global mean precipitation to the same extent as SRM. The few GCM

studies on the climate response to CCT that have been carried out to date suggest that the

global mean hydrological sensitivity (i.e., the precipitation change for a unit temperature

change) is similar for CCT and GHG forcing, and that simultaneous compensation of

temperature and precipitation changes could thus be possible (Kristjánsson et al. 2015). This

appears to hold primarily for mid- and high latitudes (Kristjánsson et al. 2015). The

geographical distribution of cooling also more closely mirrors that of GHG warming. With

the caveat that the literature on this topic is still limited, it therefore appears that the climate

response to TRM is better suited to compensate for GHG warming than SRM. However, as

noted above, whether CCT is in fact a viable STRM strategy remains unclear.

13.4 Conclusion, key unknowns, outlook

STRM remains a scientifically pursued but controversial topic, and arguments have been

presented in the literature for why even theoretical and modeling studies on the topic should be

conducted with caution. The current understanding of the forcings associated with STRM

strategies can be summarized as follows:

1) Stratospheric Aerosol Injection (SAI) can produce strong negative forcings, but the non-

linear relationship between the injected mass and forcing is poorly understood.

2) Marine Sky brightening (MSB) through, for example, sea salt injection will very likely

achieve negative forcings of the desired magnitude, but there is a non-negligible chance that

forcing of the opposite sign could result under some conditions. Forcing per mass of injected

sea salt aerosol is poorly understood, and is highly dependent on the injected aerosol size.

3) Ocean albedo modification could generate strong negative forcings but does not seem

viable because of the likely interference with ocean ecosystems. A multi-disciplinary team of

experts is needed to fully address its viability.

4) Proposed land surface albedo modifications are deemed ineffective for the purpose of

STRM.

5) Mirrors in space can produce negative forcings of the desired magnitude, but viability

depends on the engineering question of whether it is feasible to arrange for sufficient reflective

material at the location in space where this would be optimal .

234

4680   6)   In part due to conflicting modeling results, it is still unclear whether cirrus cloud thinning

4681   (CCT) can produce sufficiently strong negative forcings to be a viable TRM strategy.

4682

4683   7)   Using SAI and MCB to completely cancel global-mean GHG warming would likely cause

4684   a net reduction of precipitation relative to pre-industrial conditions. A partial compensation of

4685   global mean GHG warming could lead to a lesser effect on precipitation.

4686

4687   8)   Should it prove viable as a STRM strategy, CCT appears more suited for an an offset of the

4688   climate response to increased GHG concentrations.

4689

4690   Common for many of the unknowns related to STRM strategies is that they are related to

4691   uncertainties about the unperturbed atmosphere, and to processes that are highly relevant for our

4692   understanding of the present atmosphere and anthropogenic perturbations to it. STRM research

4693   efforts are best directed towards activities which have the dual benefit of increasing

4694   understanding both of how past inadvertent and potential future advertent forcings affect the

4695   Earth's global climate system.

4696
4697

4698

14. Overall Summary and Challenges

4699

4700

4701

14.1 Summary

4702

4703

4704

4705 This paper has traced the evolution of the concept of radiative forcing over the past century. It

4706 has also described the historical milestones in the scientific community's understanding of the

4707 RF agents, their quantification including the total or net RF, and some important applications

4708 stemming from the concept. Beginning with the fundamentals of radiation physics, principally

4709 with the developments in the late 18th and through the 19th and 20th centuries to the present,

4710 that growth has established a powerful framework to quantify the factors that force the climate

4711 system by perturbing the shortwave and longwave energy disposition in the Earth System. We

4712 have focused on the forcing as defined from pre-industrial time (~1750) to present,

4713 approximately the mid-2010s. (We note that IPCC AR6 will be completing a major assessment

4714 in 2021 which will represent a major full update since the IPCC (2013) assessment). We have

4715 treated the fundamental developments by considering the major inflection points of scientific

4716 advances, more particularly as they relate to the quantification of the estimates together with the

4717 uncertainties. For some agents, such periods are well marked by times prior to approximately

4718 the 1950s (say, before the International Geophysical Year, 1957), between 1950s and the advent

4719 of the satellite era of global measurements (1979), and the onset of the major international

4720 assessments since mid-1980s. We have highlighted especially those points in time when the

4721 literature saw more robustness added to the knowledge especially with regards to quantification.

4722 The stages in growth evolved differently for the different forcing agents, with the complexity of

236

4723   some still hindering a rapidity of growth in confidence in the quantitative estimates (e.g.,

4724   aerosol indirect forcing).

4725
4726   The forcing concept has been conceptualized and applied with the intent to define a metric that

4727   would be helpful in providing a first-order estimate of the global-mean climate impact, and

4728   most specifically the effect on surface temperature. Perhaps the most important application has

4729   been the use of the RF estimates to comparatively estimate the climate responses due to

4730   different agents, both for policy decisions concerning mitigation and adaptation, and for the

4731   scientific understanding of the relative importance of the forcing agents. In recent years, the

4732   forcing concept has been extended to investigate the comparative impact of forcings on changes

4733   on circulation patterns, including consideration of both anthropogenic and natural forcings, and

4734   taking into account the internal variability of the climate system. The RF concept has also been

4735   used to formulate simple metrics for the warming potential of various agents and for ideas in

4736   radiation management.

4737
4738   There are several limitations encountered with both the RF and the more recent ERF concepts.

4739   These include: accounting for the growing recognition of the complexity of some of the forcers;

4740   inadequacies in characterizing and narrowing uncertainties in the determination of the forcings;

4741   uncertainties in precursor parameters to determining the forcing (e.g., preindustrial emissions);

4742   reliance on numerical models for estimates of forcing; and difficulties in achieving consistency

4743   across different numerical models and their estimates. The above issues in turn affect the

4744   synthesis of the estimate and uncertainty of the total RF of climate.

4745
4746   RF and ERF remain theoretical concepts well-suited to computational estimates and computer

4747   modeling of the climate system including the agents that drive climate change. However, there

237

4748 are shortcomings. These include: inability to observe/measure/quantify parameters of relevance

4749 in forcing estimates; and inability to monitor on a continuous basis key radiative flux and

4750 associated parameters to a high degree of accuracy; difficulties in verifying the theoretically-

4751 formulated radiative forcing against practically measurable observations since the latter are not

4752 rigorously able to measure the changes in the state of the system without feedbacks; theoretical

4753 (and laboratory measurement) gaps inhibiting the knowledge of the processes that lead to the

4754 agent's forcing of climate.

4755
4756 Weaknesses in the application of the concept include propagation of the uncertainties in

4757 different factors leading to the forcing estimate. This in turn affects the evaluation of the

4758 feedbacks and response due to the forcing. It also impacts linkages to detection-and-attribution

4759 of climate change, ability to link observed phenomena (e.g., extreme events) to forcing of the

4760 climate system, and narrowing uncertainties in climate projections.

4761
4762 It is important to note that the RF concept has been more than just an arbitrary or an academic

4763 formulation. It has gone beyond just a routine definition to express a metric concerning climate

4764 driving/forcing agent. Despite its limitations, there have been remarkable successes with this

4765 metric in understanding the way global climate responds to different forcings. Many findings

4766 have been demonstrated to be highly useful, e.g.: links to emissions/sources/precursors and

4767 relative effectiveness of the different forcers; ability to inter-compare models to quantify the

4768 changes in climate parameters; policy applications (e.g., GWPs). .

4769
4770
4771 Additional relevance with regards to climate impacts are the following points:

4772

4773 • The RF concept has found usefulness in the policy context as a precursor to Global Warming

4774 Potential – paralleling Ozone Depletion Potentials in the ozone loss context. It has become

4775 possible to link RFs of forcers to their influences on surface temperature, thus allowing cross-

4776 comparison of the climate change effectiveness of different forcers. It has also enabled

4777 thinking to develop along the lines of mitigation of anthropogenic greenhouse gas effects such

4778 as in Solar Radiation Management (Royal Society, 2009).

4779
4780
4781 • RF has become intertwined in the linkage from emissions to responses. A degree of robustness

4782 has been obtained using 3D global climate models to connect RF and responses in a simple

4783 manner. This started with global-means but has also included regional-based quantitative

4784 estimates in the case of some forcers. The variable in question has been principally surface

4785 temperature, but extensions have been made to other climate parameters through physical

4786 connections (hydrologic cycle and precipitation, sea-level rise).

4787
4788 • Forcing at the TOA/tropopause, that at the surface, and their physical relevance have been

4789 identified with changes in parameters describing the physical climate change. While surface

4790 flux change does not relate easily to surface temperature change, it can be linked to

4791 hydrological cycle and precipitation. (e.g., Asian monsoon and hemispheric/global spin-down

4792 of precipitation caused by aerosols).

4793
4794 • Significance of the question: what is the Earth's climate sensitivity to radiative forcings?

4795 Estimating climate sensitivity from observed temperature changes depends crucially on our

4796 knowledge of RF. If net anthropogenic RF over the past century has been the result of a

4797 significant offset of the positive forcings by negative forcings, that would suggest a strong

239

4798   climate sensitivity. But if positive forcing has been the dominant type, then the system is

4799   relative less sensitive. The dependence on an accurate RF to obtain a good estimate of climate

4800   sensitivity crucially determines in turn how severe climate impacts are likely to be under the

4801   influence of increased GHG emissions in the 21st Century estimates. Accompanying this task

4802   should be the sustained monitoring of changes in aerosol and related properties e.g., aerosol

4803   optical depths, vertical profile, clear- and all-sky spectral and total radiative fluxes.

4804

4805 • Characterizing and, to the extent possible, narrowing the uncertainties in the pre-industrial state

4806   especially for short-lived climate forcers (e.g., ozone, aerosols). Non-linearities and interactions

4807   between forcings and its invariable relation to feedbacks (e.g. dependencies on cloud, water

4808   vapor, surface albedo).

4809
4810 • Continue to explore the potential for direct observation of radiative forcing (e.g., stratospheric

4811   aerosols in the aftermath of a volcanic eruption, solar irradiance, spectrally- resolved TOA and

4812   surface observations).

4813
4814 • As the ERF concept advances, clarifying and documenting the nuances that differentiate his

4815   from RF e.g., the uncertainties arising due to different treatments of physical processes in

4816   different models, efficacy factors etc.

4817
4818
4819

14.2 Important research challenges in the coming decades

14.2.1 Improving the accuracy of the forcing estimate

The principal challenge in arriving at a definitive estimate of the net forcing since preindustrial times is made starkly evident by the IPCC Assessments. The last IPCC assessment report (2013) conclusion that the 1750-2011 net anthropogenic forcing (best estimate of 2.3 W m-2, with a range from 1.1 to 3.3 W m-2) indicates that the remaining uncertainties are very large compared to the best-estimate net forcing; this significantly hinders efforts to derive, for example, climate sensitivity given observed temperature changes, and inhibits understanding of the effectiveness of proposed mitigation pathways, with knock-on impacts on the confidence in the advice that can be given to policymakers.

- Ensuring GCM radiation codes faithfully represent radiative processes – with linkages to available observations. One particularly demanding task is to reduce the undesirable spread in the CO_2 forcing especially for the purposes of computing accurate climate responses in climate models. The World Climate Research Program Radiative Forcing Model Intercomparison Projects have enabled the community to calibrate models against robust reference calculations. The latest venture (Pincus et al., 2017) is expected to sustain the momentum and push the frontiers further forward.

- Deployment and utilization of observations from multiplicity of platforms for characterizing fully the four-dimensional distribution of forcing agents and their time evolution, especially for natural forcers such as solar irradiance and volcanic aerosols, and for short-lived climate forcers such as aerosols and related cloud microphysics, and ozone.

241

4847

4848 • A better process understanding of aerosol forcing and in particular aerosol-cloud interactions,

4849   which has been a main contributor to uncertainty in anthropogenic forcing.

4850

14.2.2 Computational and observational determinations that need to be carried out include:

● Taking advantage of the rapid advances in the past few years in computational

architectures, algorithmic formalisms, and computing capacities. Recent advances include the

facilitation of machine learning and neural networks (e.g., Krasnopolsky et al., 2005),

performing line-by-line benchmark computations over the entire global scale of a model (e.g.,

Jones et al., 2017).

● Processes and model parameterizations that enable translating the radiative forcing to

climate change, including the physical, chemical, and dynamical responses to the forcing, and

the modulation of extant circulation patterns throughout the integrated system.

● Continuous monitoring of the agents (concentrations, radiative properties) with the

highest possible accuracy and repeatability.

● Resolution of differences among observed (to the degree feasible) and modelled absolute

variations and changes in forcings.

● Improving the ability of climate models to capture the responses to the natural and

anthropogenic forcings, and evaluate the resulting responses to climate.

It is sobering to realize that RF largely evolved as a theoretical concept, a simple metric to

compare effects due to different forcers initially formulated for well-mixed greenhouse gases,

and shown to be somewhat easily relatable to simulated surface temperature change. In the

243

4878   past, when running climate model calculations was computationally taxing, RF proved tobe an

4879   invaluable quantifying capability. With increased computational resources now to run climate

4880   responses of single forcings or subsets of forcings or all forcings somewhat inexpensively, is

4881   RF or ERF a redundant concept? Recognizing the caveats and deficiencies noted above, and

4882   with the newer nuances in the forcing definition (e.g., adoption of ERF as the new forcing

4883   metric, Section 2), a legitimate question arises – what is the future of the radiative forcing

4884   concept?

4885
4886

14.3 Grand Challenge

The answer to the above question is that investigations into forcing and estimating it may no longer be independent of considerations of the rest of the climate system. For instance, adjustments (feedbacks) in climate parameters may need to be increasingly considered in order to relate to surface temperature change, which was the initial quest in determining RFs. RF and ERF remain useful physically-based constructs that, despite the fact that they cannot be in general observationally verified, still retain a simple link to climate responses, at least in the context of global-mean surface temperature.

Going forward, the *Grand Challenge* lies in viewing RF and forcing in general not as a separate entity in the trinity of forcing, feedback, and response, but to put it into a broader perspective. A picture of this might comprise looking at the Earth System in its broader scope than just temperature and only the physical climate system. Instead, in combining forcing, feedback, and response – we are entering the era of an Earth System challenge that needs to account for feedbacks e.g., ERF departs from RF in allowance for fast feedbacks to be factored into the forcing estimate (Section 2). This increase in complexity is manifest for the various forcing agents (Sections 3-9). These complexities then add to the body of uncertainties in the net forcing and its applications (Sections 10-13), with concomitant impacts on societal adaptation and mitigation planning and measures. There are thus significant facets to the Grand Challenge regarding the application of RF and ERF in the future and the societal utilization of this science for decision-making.

4911   Radiative forcing in the climate science and climate change context is emerging after a century

4912   of exploration and investigations with a firm qualitative sense but still with limitations in its

4913   quantitative certainty. There is considerable ground still to be covered in order to achieve a

4914   comprehensive resolution of the remaining uncertainties while retaining the simplicity of the

4915   concept, and meeting the demand for more accurate quantification of both the agent-wise and

4916   net anthropogenic forcing.

4917

4918

APPENDIX

4920

4921   AATSR: Advanced Along Track Scanning Radiometer

4922   ACCENT: Atmospheric Composition Change: the European NeTwork of excellence

4923   ACCMIP: Atmospheric Chemistry and Climate Model Intercomparison Project

4924   ACE: Aerosol Characterization Experiment

4925   ACI: Aerosol cloud interactions

4926   ACP: Atmospheric Chemistry and Physics

4927   ACRIM: Active Cavity Radiometer Irradiance Monitor

4928   ACRIM3: ACRIM 3

4929   ACRIMSAT: Active Cavity Radiometer Irradiance Monitor Satellite

4930   AERONET Aerosol Robotic Network

4931   AFCRL: Air Force Cambridge Research Laboratory

4932   AGCM: Atmospheric General Circulation Model

4933   AIRS: Atmospheric Infrared Sounder

4934   AMOC: Atlantic Meridional Overturning Circulation

4935   AMS: Aerosol Mass Spectrometer

4936

4937   AOD: Aerosol Optical Depth

4938   AQUA: an Earth observing satellite mission

4939   MODIS AQUA in the name of the platform

4940   AR: Assessment Report

4941   AR4 Fourth Assessment Report

4942   AR5: Fifth Assessment Report

4943   AR6: Sixth Assessment Report

4944   ARM Atmospheric Radiation Measurements

4945

4946   ARs: Assessment Reports

4947

4948   AVHRR: Advanced Very High Resolution Radiometer

4949   AerChemMIP: Aerosols and Chemistry Model Intercomparison Project

4950   BAMS: Bulletin of the American Meteorological Society

4951   BC: Black Carbon

4952   BGC: Biogeochemistry

4953

4954   C4MIP: Coupled Climate-Carbon Cycle Model Intercomparison Project

4955   CALIOP: Cloud-aerosol Lidar with Orthogonal Polarization

4956   CALIPSO: Cloud-Aerosol Lidar and Infrared Pathfinder Satellite Observation

4957   CAM: Community Atmospheric Model

4958   CATS: Cloud-Aerosol Transport System

4959   CCM: chemistry-climate model

4960   CCN: Cloud condensation nuclei

4961   CCSP: Climate Change Science Program

4962   CCT: Cirrus cloud thinning

4963   CDNC: Cloud droplet number concentration

4964   CDR: Carbon dioxide Removal

4965   CERES: Clouds and the Earth's Radiant Energy Sytem

4966   CF4: Carbon tetrafluoride

4967   CFC:chlorofluorocarbon

4968   CFCs: chlorofluorocarbons

4969   CH4: methane

4970

4971   CICERO: Centre for International Climate and Environmental Research

4972   CLARIFY Cloud aerosol interaction and forcing

4973   CLM4: Community Land Model Version 4

4974   CM2: GFDL's Coupled Model version 2

4975   CMIP: Coupled Model Intercomparison Project

4976   CMIP3: Coupled Model Intercomparison Project Phase 3

4977   CMIP5: Coupled Model Intercomparison Project Phase 5

4978   CMIP6: Coupled Model Intercomparison Project Phase 6

4979   CO: carbon monoxide

4980   CO2: Carbon dioxide

4981   CTM: Chemistry Transport Model

4982

4983

4984   DIRTMAP: The geological map of dust

4985   DMS: Dimethyl Sulfide

4986   DU: Dobson Unit

4987   ECHAM: climate model developed at the Max Planck Institut fur Meteorologie,

4988   Hamburg

4989   ECHAM4: ECHAM version 4

4990   ECHAM5: ECHAM version 5

4991   ECMWF: European Centre for Medium-Range Weather Forecasting

4992   EESC: effective equivalent stratospheric chlorine

4993   ENSO: El Nino Southern Oscillation

4994   ERF: effective radiative forcing

4995   ERFs: effective radiative forcings

4996   ESM: Earth System Model

4997

4998   FAR: First Assessment Report

4999   FDH: Fixed Dynamical Heating

5000   FFBC – fossil fuel black carbon

5001   FFOC – fossil fuel organic carbon

5002

5003   GCM: General Circulation Model

5004   GCTMs: Global Chemical Transport Models

5005   GEISA – Gestion et Etude des Informations Spectroscopiques Atmospheriques

5006   GFDL: Geophysical Fluid Dynamics Laboratory

5007   GHG: Greenhouse gas

5008   GISS: Goddard Institute for Space Studies

5009   GWP: Global Warming Potential

5010   GWPs: Global Warming Potentials

5011   GeoMIP: geoengineering model intercomparison project

5012

5013   H2S Hydrogen Sulfide

5014   H2SO4 Sulfuric Acid

5015   HALOE: Halogen Occultation Experiment

5016   HCFC -- Hydrochlorofluorocarbons

5017   HCFCs -- Hydrochlorofluorocarbons

5018   HFCs -- Hydroflourocarbons

5019

5020   HIRS: High resolution Infrared Sounder

5021   HITRAN -- High-resolution transmission molecular absorption

5022   HITRAN2016 – HITRAN version issues in 2016

5023   HNO3: Nitric Acid

5024   HO2: Peroxy hydroxyl

5025   HadGEM2: UK Hadley Centre Global Environment Model version 2

5026

5027   IEEE: Institute of Electrical and Electronic Engineers

5028   IGY: International Geophysical Year

5029

5030   IPCC: Intergovernmental Panel on Climate Change

5031   IR: Infrared Radiation

5032   IRF: Instantaneous radiative forcing

5033   IRIS: Interface Region Imaging Spectrograph

252

5034	IS92: An emissions scenario
5035	ISAMS: Improved Stratospheric and Mesopspheric Sounder
5036	ISCCP: International Satellite Cloud Climatology Project
5037	ISS; international Space Station
5038	ITCZ: InterTropical Convergence Zone
5039	
5040	JAS: Journal of the Atmospheric Sciences
5041	
5042	LASIC: Layered Atlantic Smoke Interactions with Clouds
5043	LBL: Line-by-line
5044	LH: Latent heat
5045	LMD – Laboratoire de Meteorologie Dynamique
5046	
5047	LOSU: level of scientific understanding
5048	LULCC: Land Use Land Cover Change
5049	LUMIP Land use model intercomparison Project
5050	LW: Longwave radiation
5051	
5052	MEGAN Model of Emissions of Gases and Aerosols from Nature

253

5053   MIPAS: Michelson Interferometer for Passive Atmospheric Sounding

5054   MIPs: Model Intercomparison Projects

5055   MISR: multi-angle imaging spectroradiometer

5056   MIT: Massachusetts Institute of Technology

5057   ML: Mixed Layer

5058

5059   MODIS: moderate resolution imaging spectrometer

5060   MSB: Marine sky brightening

5061   MSU: microwave sounding unit

5062

5063   NASA: National Aeronautics and Space Administration

5064   NATO: North Atlantic Treaty Organization

5065   NCAR: National Center for Atmospheric Research

5066   NERC: Natural environment research council

5067   NH3: ammonia

5068   NMHCs: Non-methane hydrocarbons

5069   NO: nitrogen oxide

5070   NO2: nitrogen dioxide

5071   NOAA: National Oceanic Atmospheric Administration

5072   NOx: nitrogen oxides

5073   N2: Nitrogen

5074   NRC: National Research Council

5075   NRLTSI2: Naval Research laboratory Total Solar Irradiance 2

5076   NRLSSI2: Naval Research Laboratory Solar Spectral Irradiance 2

5077

5078

5079   OCS: Carbonyl Sulfide

5080   ODSs: Ozone Depleting Substances

5081   OH: hydroxyl

5082   OK: Oklahoma

5083   OMI: ozone monitoring instrument

5084   OMPS: ozone mapping and profiling suite

5085   ORACLES: ObseRvations of Aerosols above CLouds and their intEractionS

5086   OSIRIS: Optical Spectrograph and InfraRed Imaging System

5087

5088   PARASOL: Polarization and Anisotropy of Reflectances for Atmospheric Sciences

5089   PD: present-day

5090   PDF: probability distribution function

5091

5092   PI: pre-industrial

5093   PMIP: Paleoclimate Model Intercomparison Project

5094   PMIP4: Paleoclimate Model Intercomparison Project (version 4)

5095   PMOD: Physikalish-Meteorologistics Observatorium Davos

5096   PNAS: Proceedings of the National Academy of Sciences

5097   POAM: Polar Ozone and Aerosol Measurement

5098   POLDER: POLarization and Directionality of the Earth's Reflectances

5099   PSD: Particle Size Distribution

5100

5101

5102   QBO: Quasi-Biennial Oscillation

5103

5104   RCP2.6: Representative Concentration Pathway 2.6

5105   RCP8.5: Representative Concentration Pathway 8.5

5106   RCPs: Representative Concentration Pathways

5107   RE: Radiative efficiency

5108   REs: Radiative efficiencies

5109   RF: Radiative forcing

5110   RFMIP: Radiative Forcing Model Intercomparison Project

5111   RFP: Radiative Flux Perturbation

5112   RFs: Radiative forcings

5113   RH: Relative Humidity

5114

5115   SA: South Africa

5116   SAFARI: Southern African Regional Science Initiative

5117   SAGE: Stratospheric Gas and Aerosol Experiment

5118   SAI: Stratospheric aerosol injection

5119   SAR: Second Assessment Report

5120   SATIRE: Spectral and Total Irradiance Reconstruction

5121

5122   SBUV Solar Backscatter Ultraviolet

5123   SCHIAMACHY (this is wrong abbreviation)

5124   SCIAMACHY SCanning Imaging Absorption SpectroMeter for Atmospheric

5125   CHartographY SCanning

5126

5127   SF6: sulfur hexafluoride

5128   SH: sensible heat

5129	SKYHI: generic name for a general circulation model at NOAA/Geophysical Fluid

5130	Dynamics Laboratory

5131	SLCF: short-lived climate forcer

5132

5133	SME Solar Mesosphere Explorer

5134	SMIC: Study of Man's Impact on Climate (a report)

5135	SMM Solar Maximum Mission

5136	SO2: Sulfur Dioxide

5137	SOHO Solar Heliospheric Observatory

5138	SORCE Solar Radiation and Climate Experiment

5139	SPARC: Stratospheric Tropospheric Processes and theor Role in Climate

5140	SRM: solar radiation management

5141	SST: sea surface temperature

5142	SSTs: sea surface temperatures

5143

5144	STRM: Solar and terrestrial radiation management

5145	SUCCESS

5146	SW: Shortwave radiation

5147

5148	TAR: Third Assessment Report

5149   TERRA: name of MODIS satellite

5150   TIM Total Irradiance Monitor

5151   TOA: top of atmosphere

5152   TOMS: total ozone mapping spectrometer

5153   TRM: Terrestrial radiation management

5154   TSI Total Spectral Irradiance

5155   TSIS Total and Spectral Irradiance Sensor

5156   TTL Tropical Tropopause Layer

5157

5158   UARS Upper Atmosphere Research Satellite

5159   UK: United Kingdom

5160   UKCA: UK chemistry and aerosol

5161   UM: Unified Model

5162   UN: United Nations

5163   UNFCCC: United Nations Framework Convention on Climate Change

5164   US : United States

5165   USA: United States of America

5166   UV: Ultraviolet

5167   VIRGO: a French-Italian project

259

5168   VIIRS: Visible Infrared Imaging Radiometer Suite

5169   VolMIP: Volcanic Forcings Model Intercomparison Project

5170   WACCM: Whole Atmosphere Community Climate Model

5171   WCRP – World Climate Research Programme

5172   WGI – Working Group I

5173   WMGHG: Well-mixed greenhouse gas

5174   WMGHGs: Well-mixed greenhouse gases

5175   WMO: World Meteorological Organization |

5176

5177

REFERENCES

5178

5179

5180 Aamaas, B., T. K. Berntsen, J. S. Fuglestvedt, K. P. Shine, and W. J. Collins, 2017: Regional
5181   temperature change potentials for short-lived climate forcers based on radiative forcing
5182   from multiple models, *Atmos. Chem. Phys.*, **17**, 10795-10809,https://doi.org/10.5194/acp-
5183   17-10795-2017

5184 Abbott, C.G. and Fowle, F.E. (1908). Recent determination of the solar constant of
5185   radiation. *Terr. Magnetism and Atmos. Electricity 13: doi: 10.1029/TE013i002p00079. issn:*
5186   *0096-8013.*

5187 Ackerman, Andy S., O. B. Toon, D. E. Stevens, A. J. Heymsfield, V. Ramanathan, and E. J.
5188   Welton. Reduction of tropical cloudiness by soot. *Science* 288, no. 5468 (2000): 1042-1047.

5189 Adams, J. B., M. E. Mann, and C. M. Ammann (2003), Proxy evidence for an El Nino-like
5190   response to volcanic forcing. *Nature*, 426, 274-278.

5191 Adams, P. J., Seinfeld, J. H., Koch, D., Mickley, L., & Jacob, D. (2001). General circulation
5192   model assessment of direct radiative forcing by the sulfate-nitrate-ammonium-water
5193   inorganic aerosol system. *Journal of Geophysical Research: Atmospheres*, *106*(D1), 1097-
5194   1111.

5195 Ahlm, L., A. Jones, W. C. Stjern, H. Muri, B. Kravitz, and J. E. Kristjánsson, 2017: Marine
5196   cloud brightening - As effective without clouds. *Atmos. Chem. Phys.*, doi:10.5194/acp-17-
5197   13071-2017.

5198 Albani, S., Balkanski, Y., Mahowald, N., Winckler, G., Maggi, V. and Delmonte, B.: Aerosol-
5199   Climate Interactions During the Last Glacial Maximum, Curr. Clim. Chang. Reports, 4(2),
5200   99–114, doi:10.1007/s40641-018-0100-7, 2018.

5201 Albrecht, B. A. Aerosols, cloud microphysics, and fractional cloudiness. *Science* **245,** 1227-1230
5202   (1989).

5203 Alexander, B., and L. J. Mickley, 2015: Paleo-Perspectives on Potential Future Changes in the

Oxidative Capacity of the Atmosphere Due to Climate Change and Anthropogenic Emissions. *Curr. Pollut. Reports*, **1**, 57–69, doi:10.1007/s40726-015-0006-0.

Allen, R. J., Evan, A. T. & Booth, B. B. B. Interhemispheric aerosol radiative forcing and tropical precipitation shifts during the late twentieth century. *J. Clim.* **28,** 8219-8246 (2015).

Alterskjær, K., and J. E. Kristjánsson, 2013: The sign of the radiative forcing from marine cloud brightening depends on both particle size and injection amount. *Geophys. Res. Lett.*, doi:10.1029/2012GL054286.

——, ——, and Ø. Seland, 2012: Sensitivity to deliberate sea salt seeding of marine clouds – observations and model simulations. *Atmos. Chem. Phys.*, **12**, 2795–2807, doi:10.5194/acp-12-2795-2012. https://www.atmos-chem-phys.net/12/2795/2012/ (Accessed December 20, 2018).

Altshuller, A. P., and J. J. Bufalini, 1965: Photochemical aspects of air pollution: a review. *Photochem. Photobiol.*, **4**, 97–146, doi:doi:10.1111/j.1751-1097.1965.tb05731.x. https://doi.org/10.1111/j.1751-1097.1965.tb05731.x.

Amman, C., G. Meehl, W. Washington, and C. Zender (2003), A monthly and latitudinally varying forcing dataset in simulations of 20th century climate. *Geophys Res Lett*, 30, 1657.

Anchukaitis, K. J., B. M. Buckley, E. R. Cook, B. I. Cook, R. D. D'Arrigo, and C. M. Ammann (2010), Influence of volcanic eruptions on the climate of the Asian monsoon region. *Geophysical Research Letters*, 37, L22703.

Andela, N., Morton, D. C., Giglio, L., Chen, Y., Van Der Werf, G. R., Kasibhatla, P. S., DeFries, R. S., Collatz, G. J., Hantson, S., Kloster, S., Bachelet, D., Forrest, M., Lasslop, G., Li, F., Mangeon, S., Melton, J. R., Yue, C. and Randerson, J. T.: A human-driven decline in global burned area, Science (80-.)., 356(6345), 1356–1362, doi:10.1126/science.aal4108, 2017.

Anderson, T. R., E. Hawkins, and P. D. Jones, 2016: CO2, the greenhouse effect and global warming: from the pioneering work of Arrhenius and Callendar to today's Earth System Models. Endeavor, 40, 3, pp178-187. https://doi.org/10.1016/endeavour.2016.07.002

Andersson, S., B. Martinsson, J.-P. Vernier, J. Friberg, C. A. M. Brenninkmeijer, M. Hermann, P. van Velhoven, and A. Zahn (2014), Significant radiative impact of volcanic aerosol in the lowermost stratosphere, Nature Communications, doi:10.1038/NCOMMS8692.

Andreae, M. O. and Merlet, P.: Emission of trace gases and aerosols from biomass burning, Global Biogeochem. Cycles, 15(4), 955–966, 2001.

Andrews, T. and Forster, P.: CO2 forcing induces semi-direct effects with consequences for climate feedback interpretations, Geophysical Research Letters, 35, L04802, 2008.

Andrews, T., Forster, P., Boucher, O., Bellouin, N. and Jones, A.: Precipitation, radiative forcing and global temperature change, Geophysical Research Letters, 37, L14701, 2010.

Andrews, T., Gregory, J. M., Forster, P. M. and Webb, M. J.: Cloud Adjustment and its Role in CO2 Radiative Forcing and Climate Sensitivity: A Review, Surveys in Geophysics, 33(3-4), 619-635, 2012.

Andrews, T. (2014). Using an AGCM to diagnose historical effective radiative forcing and mechanisms of recent decadal climate change. *Journal of Climate*, *27*(3), 1193-1209.

Angel, R., 2006: Feasibility of cooling the Earth with a cloud of small spacecraft near the inner Lagrange point (L1). *Proc. Natl. Acad. Sci.*, doi:10.1073/pnas.0608163103.

Antico, A., and M. E. Torres, 2015: Evidence of a decadal solar signal in the Amazon River: 1903 to 2013, Geophys. Res. Lett., 42, doi:10.1002/2015GL066089.

Antuña, J. C., A. Robock, G. L. Stenchikov, J. Zhou, C. David, J. Barnes, and L. Thomason (2003), Spatial and temporal variability of the stratospheric aerosol cloud produced by the 1991 Mount Pinatubo eruption. *J Geophys Res*, 108, 4624.

Aquila, V., L. D. Oman, R. S. Stolarski, P. R. Colarco, and P. A. Newman (2012), Dispersion of the volcanic sulfate cloud from a Mount Pinatubo–like eruption. *Journal of Geophysical Research-Atmospheres*, 117, D06216.

5255   Aquila, V., C. I. Garfinkel, P. A. Newman, L. D. Oman, and D. W. Waugh (2014), Modifications
5256   of the quasi-biennial oscillation by a geoengineering perturbation of the stratospheric aerosol
5257   layer. *Geophysical Research Letters*, 41, 1738-1744.

5258   Archer, D., and S. Ramstorf, 2010: The Climate Crisis, ISBN 978-0-521-73255-0
5259   (paperback version). Cambridge University Press, 250 pages.

5260   Arfeuille, F., and Coauthors (2013), Modeling the stratospheric warming following the Mt.
5261   Pinatubo eruption: uncertainties in aerosol extinctions. *Atmos Chem Phys*, 13, 11221-11234.

5262   Armour, K. C., C. M. Bitz, and G. H. Roe (2013), Time-varying climate sensitivity from regional
5263   feedbacks, J. Clim., 26, 4518–4534, doi:10.1175/jcli-d-12-00544.1.

5264   Arneth, A., Harrison, S., Zaehle, S., Tsigaridis, K., Menon, S., Bartlein, P., Feichter, J., Korhola,
5265   A., Kulmala, M., O'Donnell, D., Schurgers, G., Sorvari, S. and Vesala, T.: Terrestrial
5266   biogeochemical feedbacks in the climate system, Nature-geoscience, 3, 525–532; DOI:
5267   10.1038/NGEO905, 2010.

5268   Arrhenius, S., 1896: On the influence of carbonic acid in the air upon the temperature of the
5269   ground. *Phil. Mag. and J. Science*, Ser. 5, vol. 41, pp 237-276.

5270

5271   Bala, G., Caldeira, K. and Nemani, R.: Fast versus slow response in climate change: implications
5272   for the global hydrological cycle, Climate Dynamics, 35(2-3), 423-434, 2010.

5273   Bala, G., P. B. Duffy, and K. E. Taylor, 2008: Impact of geoengineering schemes on the global
5274   hydrological cycle. *Proc. Natl. Acad. Sci.*, doi:10.1073/pnas.0711648105.

5275   Balmaseda, M. A., K. Mogensen, and A. T. Weaver (2013), Evaluation of the ECMWF ocean
5276   reanalysis system ORAS4. *Quarterly Journal of the Royal Meteorological Society*, 139,
5277   1132-1161.

5278   Baran, A. J., and J. S. Foot (1994), New application of the operational sounder HIRS in
5279   determining a climatology of sulphuric acid aerosol from the Pinatubo eruption, J. Geophys.
5280   Res., 99(D), 25,673–25,679, doi:10.1029/94JD02044.

5281 Ban-Weiss, G., Cao, L., Bala, G. and Caldeira, K.: Dependence of climate forcing and response
5282   on the altitude of black carbon aerosols, Climate Dynamics, 897-911, 2011.

5283 Banerjee, A., A. C. Maycock, A. T. Archibald, N. L. Abraham, P. Telford, P. Braesicke, and J.
5284   A. Pyle, 2016: Drivers of changes in stratospheric and tropospheric ozone between year
5285   2000 and 2100. *Atmos. Chem. Phys.*, **16**, 2727–2746, doi:10.5194/acp-16-2727-2016.
5286   https://www.atmos-chem-phys.net/16/2727/2016/ (Accessed October 1, 2018).

5287 Bardeen, C. G., O. B. Toon, E. J. Jensen, D. R. Marsh, and V. L. Harvey (2008), Numerical
5288   simulations of the three-dimensional distribution of meteoric dust in the mesosphere and
5289   upper stratosphere, J. Geophys. Res., 113, D17202, doi:10.1029/2007JD009515.

5290 Barnes, J. E., and D. J. Hofmann (1997), Lidar measurements of stratospheric aerosol over Mauna
5291   Loa, Geophys. Res. Lett., 24, 1923-1926.

5292 Barriopedro, D., R. Garcıa-Herrera, and R. Huth, 2008: Solar modulation of Northern
5293   Hemisphere winter blocking, J. Geophys. Res., 113, D14118, doi:10.1029/2008JD009789.

5294 Bates, D. R., and M. Nicolet, 1950: The photochemistry of atmospheric water vapor. *J. Geophys.*
5295   *Res.*, **55**, 301–327, doi:doi:10.1029/JZ055i003p00301.
5296   https://doi.org/10.1029/JZ055i003p00301.

5297 Bates, D. R., and A. E. Witherspoon, 1952: The photochemistry of some minor constituents of
5298   the Earth's atmosphere (CO2, CO, CH4, N2O)*. *Geophys. J. Int.*, **6**, 324,
5299   doi:doi:10.1111/j.1365-246X.1952.tb03020.x. https://doi.org/10.1111/j.1365-
5300   246X.1952.tb03020.x.

5301 Baumgardner, D., J. E. Dye, R. G. Knollenberg and B. W. Gandrud (1992), Interpretation of
5302   measurements made by the FSSP-300X during the Airborne Arctic Stratospheric Expedition,
5303   J. Geophys. Res., 97, 8035-8046.

5304 Bellouin, N. Boucher, O., Haywood, J.M., and Reddy, M.S., Global estimate of aerosol direct
5305   radiative forcing from satellite measurements, Nature, 428, doi: 10.1038/nature04348, 2005.

5306 Bellouin, N., J. Rae, A. Jones, C. Johnson, J.M. Haywood , O. Boucher Aerosol forcing in the
5307   CMIP5 simulations by HadGEM2-ES and the role of ammonium nitrate, J Geophys. Res.,
5308   doi:10.1029/2011JD016074, 2011.

5309

5310

5311 Berdahl, M., Alan Robock, Duoying Ji, John C. Moore, Andy Jones, Ben Kravitz, and Shingo
5312   Watanabe, 2014: Arctic cryosphere response in the Geoengineering Model Intercomparison
5313   Project G3 and G4 scenarios, *J. Geophys. Res. Atmospheres*.
5314   https://doi.org/10.1002/2013JD020627

5315

5316 Berntsen, T. K., I. S. A. Isaksen, G. Myhre, J. S. Fuglestvedt, F. Stordal, T. A. Larsen, R. S.
5317   Freckleton, and K. P. Shine, 1997: Effects of anthropogenic emissions on tropospheric
5318   ozone and its radiative forcing. *J. Geophys. Res. Atmos.*, **102**, 28101–28126,
5319   doi:doi:10.1029/97JD02226. https://doi.org/10.1029/97JD02226.

5320 Bindoff, N.L., P.A. Stott, K.M. AchutaRao, M.R. Allen, N. Gillett, D. Gutzler, K. Hansingo, G.
5321   Hegerl, Y. Hu, S. Jain, I.I. Mokhov, J. Overland, J. Perlwitz, R. S. and X. Z., 2013:
5322   Detection and attribution of climate change: From global to regional. *Climate Change 2013*
5323   *the Physical Science Basis: Working Group I Contribution to the Fifth Assessment Report*
5324   *of the Intergovernmental Panel on Climate Change*.

5325 Bingen, C., D. Fussen, and F. Vanhellemont (2004a), A global climatology of stratospheric aerosol
5326   size distribution parameters derived from SAGE II data over the period 1984 – 2000: 1.
5327   Methodology and climatological observations, J. Geophys. Res., 109, D06201.

5328 Bingen, C., D. Fussen, and F. Vanhellemont (2004b), A global climatology of stratospheric aerosol
5329   size distribution parameters derived from SAGE II data over the period 1984–2000: 2.
5330   Reference data, J. Geophys. Res., 109, D06202.

5331 Bischoff T, Schneider T (2014), Energetic constraints on the position of the intertropical
5332   convergence zone, J Clim., 27(13), 4937–4951

5333 Bischoff T, Schneider T (2016), The equatorial energy balance, ITCZ position, and double-ITCZ
5334   bifurcations, J Clim., 29(8), 2997–3013.

5335 Bock, L., and U. Burkhardt (2016), Reassessing properties and radiative forcing of contrail cirrus
5336   using a climate model, J. Geophys. Res. Atmos., 121, 9717–9736,
5337   doi:10.1002/2016JD025112.

5338 Bock, L. and Burkhardt, U.: Contrail cirrus radiative forcing for future air traffic, Atmos. Chem.
5339   Phys., 19, 8163-8174, https://doi.org/10.5194/acp-19-8163-2019, 2019.

5340 Bolin, B. and Charlson, R. J. (1976), On the role of the tropospheric sulfur cycle in the
5341   shortwave radiative climate of the earth, Ambio 5,47-54.

5342 Bollasina, M. A., Ming, Y. & Ramaswamy, V. Anthropogenic aerosols and the weakening of the
5343   South Asian summer monsoon. *Science* **334,** 502-505 (2011).

5344 Bonan, G.: Forests and climate change: Forcings, Feedbacks and the Climate Benefits of Forests,
5345   Science (80-.)., 320, 1444–1448; DOI: 10.1126/science.1155121, 2008.

5346 Bond, T. C., and Coauthors, 2013: Bounding the role of black carbon in the climate system: A
5347   scientific assessment. *J. Geophys. Res. Atmos.*, **118**, 5380–5552, doi:10.1002/jgrd.50171.

5348 Bony, S., and Coauthors, 2006: How Well Do We Understand and Evaluate Climate Change
5349   Feedback Processes? J. Clim., 19, 3445–3482, doi:10.1175/JCLI3819.1.
5350   https://doi.org/10.1175/JCLI3819.1.

5351 Borrmann S., A. Thomas, V. Rudakov, V. Yushkov, B. Lepuchov, T. Deshler, N. Vinnichenko,
5352   V. Khattatov, L. Stefanutti (2000), Stratospheric aerosol measurements in the Arctic winter
5353   of 1996/1997 with the M-55 Geophysika high-altitude research aircraft, Tellus B, 52 (4),
5354   1088-1103.

5355 Boucher, O., and J. Haywood, 2001: On summing the components of radiative forcing of climate
5356   change. *Clim. Dyn.*, **18**, 297–302.

5357   Boucher, O. *et al.* Clouds and Aerosols. In: *Climate Change 2013: The Physical Science Basis.*
5358   *Contribution of Working Group I to the Fifth Assessment Report of the Intergovernmental*
5359   *Panel on Climate Change* (eds Stocker TF, et al.) (Cambridge Univ. Press, 2013).

5360   Boucher, O., and U. Lohmann, 1995: The sulfate-CCN-cloud albedo effect - a sensitivity study
5361   with 2 general-circulation models. Tellus Ser. B-Chemical Phys. Meteorol., 47, 281–300.

5362   Boucher, O., Randall, D., Artaxo, P., Bretherton, C., Feingold, G., Forster, P., Kerminen, V.-M.,
5363   Kondo, Y., Liao, H., Lohmann, U., Rasch, P., Satheesh, S. K., Sherwood, S., Stevens, B.
5364   and Zhang, X.-Y., Clouds and Aerosols. In: Climate Change 2013: The Physical Science
5365   Basis. Contribution of Working Group I to the Fifth Assessment Report of the
5366   Intergovernmental Panel on Climate Change. T. F. Stocker, D. Qin, G.-K. Plattner, M.
5367   Tignor, S. K. Allen et al. (Editors), Cambridge University Press, Cambridge, United
5368   Kingdom and New York, NY, USA, pp. 571-657, 2013.

5369   Boucher, O. (1995). GCM estimate of the indirect aerosol forcing using satellite-retrieved cloud
5370   droplet effective radii. *Journal of climate*, *8*(5), 1403-1409.

5371   Boucher, O., & Anderson, T. L. (1995). General circulation model assessment of the sensitivity of
5372   direct climate forcing by anthropogenic sulfate aerosols to aerosol size and chemistry. *Journal*
5373   *of Geophysical Research: Atmospheres*, *100*(D12), 26117-26134.

5374   Boucher, O., & Lohmann, U. (1995). The sulfate-CCN-cloud albedo effect. *Tellus B: Chemical*
5375   *and Physical Meteorology*, *47*(3), 281-300.

5376   Boucher, O., et al., 1998. Intercomparison of models representing direct shortwave radiative
5377   forcing by sulfate aerosols. J. Geophys. Res., 103, 16979-16998.

5378   Boucher, O., & Tanré, D. (2000). Estimation of the aerosol perturbation to the Earth's radiative
5379   budget over oceans using POLDER satellite aerosol retrievals. *Geophysical research letters*,
5380   *27*(8), 1103-1106.

5381   Boucher, O., and Haywood, J.M., 2001. On summing the components of radiative forcing of
5382   climate change. Climate Dynamics, 18, 297-302.

5383   Boucher, O., Randall, D., Artaxo, P., Bretherton, C., Feingold, G., Forster, P., Kerminen, V.-M.,

5384   Kondo, Y., Liao, H., Lohman, U., Rasch, P., Satheesh, S., Sherwood, S., Stevens, B.,

5385   Zhang, X.-Y., Lohmann, U., Rasch, P., Satheesh, S., Sherwood, S., Stevens, B. and Zhang,

5386   X.-Y.: Clouds and Aerosols, in Climate Change 2013: The Physical Science Basis.

5387   Contribution of Working Group I to the Fifth Assessment Report of the Intergovernmental

5388   Panel on Climate Change, edited by V. B. and P. M. M. Stocker, T.F., D. Qin, G.-K.

5389   Plattner, M. Tignor, S.K. Allen, J. Boschung, A. Nauels, Y. Xia, pp. 573–657, Cambridge

5390   University Press, United Kingdom., 2013.

5391   Bourassa, A. E., Degenstein, D. A., Gattinger, R. L., and Llewellyn, E. J. (2007), Stratospheric

5392   aerosol retrieval with OSIRIS limb scatter measurements, J. Geophys. Res., 112, D10 217,

5393   doi:10.1029/2006JD008079.

5394   Bourassa, A. E., Degenstein, D. A., and Llewellyn, E. J. (2008), Retrieval of stratospheric aerosol

5395   size information from OSIRIS limb scattered sunlight spectra, Atmos. Chem. Phys., 8, 6375-

5396   6380.

5397   Bousquet, P., D. A. Hauglustaine, P. Peylin, C. Carouge, and P. Ciais, 2005: Two decades of OH

5398   variability as inferred by an inversion of atmospheric transport and chemistry of methyl

5399   chloroform. *Atmos. Chem. Phys.*, **5**, 2635–2656, doi:10.5194/acp-5-2635-2005.

5400   https://www.atmos-chem-phys.net/5/2635/2005/.

5401   Bovensmann, H. Burrows, J. P., Buchwitz, M., Frerick, J., Noël, S., Rozanov et al. (1999),

5402   SCIAMACHY: Mission Objectives and Measurement Modes, J. Atmos. Sci., 56, 127 – 150,

5403   doi: 10.1175/1520-0469.

5404   Brasseur, G. P., 2009: Implications of Climate Change for Air Quality. *WMO Bulletin*, 10–15.

5405   Brasseur, G., and C. Granier (1992), Mount Pinatubo aerosols, chlorofluorocarbons and ozone

5406   depletion. Science, 257, 1239–1242.

5407   Brasseur, G. P., J. T. Kiehl, J.-F. Müller, T. Schneider, C. Granier, X. Tie, and D. Hauglustaine,

5408   1998: Past and future changes in global tropospheric ozone: Impact on radiative forcing.

5409   *Geophys. Res. Lett.*, **25**, 3807–3810, doi:doi:10.1029/1998GL900013.

5410   https://doi.org/10.1029/1998GL900013.

Brenguier, J.-L., P. Y. Chuang, Y. Fouquart, D. W. Johnson, F. Parol, H. Pawlowska, J. Pelon, L. Schu¨ller, F. Schro¨der, and J. Snider, An overview of the ACE-2 CloudyColumn Closure Experiment, Tellus, Ser. B, 52, 815–827, 2000a.

Brimblecombe, P., Bowler, C. (1990) Air pollution history, York 1850–1900, in: Brimblecombe, P., Pfister, C. (editors), The Silent Countdown, pp. 182–195, Springer Verlag.

Brock, C. A., P. Hamill, J. C. Wilson, H. H. Jonsson, and K. R. Chan (1995), Particle formation in the upper tropical troposphere: A source of nuclei for the stratospheric aerosol, Science, 270(5242), 1650–1653, doi:10.2307/2887916.

Broccoli, A., K. Dixon, T. Delworth, T. Knutson, and R. Stouffer (2003), Twentieth-century temperature and precipitation trends in ensemble climate simulations including natural and anthropogenic forcing. *J Geophys Res*, 108, 4798.

Bryan, K., S. Manabe, and M. Spelman, 1988: Interhemispheric asymmetry in the transient response of a coupled ocean-atmosphere model to a CO_2 forcing. *J. Phys. Oceanography*, **18(6)**, 851-867.

Bluth, G. J. S., S. D. Doiron, C. C. Schnetzler, A. J. Krueger and L. S. Walter (1992), Global tracking of the SO2 clouds from the June 1991 Mount Pinatubo eruptions, Geophys. Res. Lett., 19, 151-154.

Bluth, G. J. S., C. C. Schnetzler, A. J. Krueger and L. S. Walter (1993), The contribution of explosive volcanism to global atmospheric sulphur dioxide concentrations, Nature, 366, 327-329.

Bruhl, C., J. Lelieveld, P. J. Crutzen, and H. Tost, (2012), The role of carbonyl sulphide as a source of stratospheric sulphate aerosol and its impact on climate, Atmos. Chem. Phys., 12, 1239-1253, doi:10.5194/acp-12-1239-2012.

Brühl, C., J. Lelieveld, H. Tost, M. Höpfner, and N. Glatthor (2015), Stratospheric sulphur and its implications for radiative forcing simulated by the chemistry climate model EMAC, J. Geophys. Res. Atmos., 120, 2103–2118, doi:10.1002/2014JD022430.

5438   Budyko, M. I., 1969: The effect of solar radiation variations on the climate of the Earth. *Tellus*,
5439   doi:10.3402/tellusa.v21i5.10109.

5440   Burrows J. P., E. Hölzle, A. P. H. Goede, H. Visser, and W. Fricke (1995), SCIAMACHY –
5441   Scanning Imaging Absorption Spectrometer for Atmospheric Chartography, Acta
5442   Astronautica, 35(7), 445 – 451.

5443

5444   Cadle, R. D., and E. R. Allen, 1970: Atmospheric Photochemistry. *Science (80-.).*, **167**, 243 LP-
5445   263. http://science.sciencemag.org/content/167/3916/243.abstract.

5446   Carn, S. A., A. J. Krueger, G. J. S. Bluth, S. J. Schaefer, N. A. Krotkov, I. M. Watson and S. Datta
5447   (2003), Volcanic eruption detection by the Total Ozone Mapping Spectrometer (TOMS)
5448   instruments: a 22-year record of sulfur dioxide and ash emissions. In: Volcanic Degassing
5449   (eds. C. Oppenheimer, D. M. Pyle, and J. Barclay), Geological Society, London, Special
5450   Publications, 213, 177-202.

5451   Carn, S. A., Clarisse, L., and Prata, A. J. (2016), Multi-decadal satellite measurements of global
5452   volcanic degassing, J. Volcanol. Geotherm. Res., 311, 99 – 134.

5453   Caldeira, K., G. Bala, and L. Cao, 2013: The Science of Geoengineering. *Annu. Rev. Earth*
5454   *Planet. Sci.*, doi:10.1146/annurev-earth-042711-105548.

5455

5456

5457   Callendar, G. S. (1941). Infra-red absorption by carbon dioxide, with special reference to
5458   atmospheric radiation. *Quarterly Journal of the Royal Meteorological Society*, *67*(291),
5459   263–275. http://doi.org/10.1002/qj.49706729105

5460   Callendar, G. S., 1938: The artificial production of carbon dioxide and its influence on
5461   temperature. Quart. J. Roy. Meteor. Soc., doi: 10.1002/qj.49706427503
5462   (https://dx.doi.org/10.1002/qj.49706427503).

5463   Callis, L. B., M. Natarajan, and R. E. Boughner, 1983: On the relationship between the

greenhouse effect, atmospheric photochemistry, and species distribution. *J. Geophys. Res. Ocean.*, **88**, 1401–1426, doi:doi:10.1029/JC088iC02p01401. https://doi.org/10.1029/JC088iC02p01401.

Carbon Dioxide and Climate: A Scientific Assessment. (1979). Washington D.C., U.S.A.: National Academy of Sciences. http://doi.org/10.17226/12181

Carslaw, K. S., Boucher, O., Spracklen, D., Mann, G., Rae, J. G., Woodward, S. and Kumala, M.: A review of natural aerosol interactions and feedbacks within the Earth System, Atmos. Chem. Phys., 10, 1701–1737, 2010.

Carslaw, K. S., Lee, L., Reddington, C., Pringle, K., Rap, A., Forster, P., Mann, G., Spracklen, D., Woodhouse, M., Regayre, L. and Pierce, J.: Large contribution of natural aerosols to uncertainty in indirect forcing, Nature, 503(doi:10.1038/nature12674), 67–71, 2013.

Carslaw, K.S., Gordon, H., Hamilton, D.S. et al. 2017: Aerosols in the Pre-industrial Atmosphere, Curr Clim Change Rep, *3*, https://doi.org/10.1007/s40641-017-0061-2

Carslaw, K. S., Lee, L. A., Reddington, C. L., Pringle, K. J., Rap, A., Forster, P. M., … and Pierce, J. R. Large contribution of natural aerosols to uncertainty in indirect forcing. *Nature*, *503*(7474), 67, 2013.

Charlson, R. J., Langner, J., Rodhe, H., Leovy, C. B., & Warren, S. G. (1991). Perturbation of the northern hemisphere radiative balance by backscattering from anthropogenic sulfate aerosols. *Tellus A: Dynamic Meteorology and Oceanography*, *43*(4), 152-163.

Charlson, R. J., Schwartz, S. E., Hales, J. M., Cess, R. D., Coakley, J. J., Hansen, J. E., & Hofmann, D. J. (1992). Climate forcing by anthropogenic aerosols. *Science*, *255*(5043), 423-430.

Cess, R.D., 1976: Climate Change: An Appraisal of Atmospheric Feedback Mechanisms Employing Zonal Climatology. *J. Atmos. Sci.,* **33**, 1831–1843, https://doi.org/10.1175/1520-0469(1976)033<1831:CCAAOA>2.0.CO;2

Cess, R. D., Zhang, M.-H., Potter, G. L., Barker, H. W., Colman, R. A., Dazlich, D. A., … Wetherald, R. T. (1993). Uncertainties in Carbon Dioxide Radiative Forcing in Atmospheric

272

General Circulation Models. *Science*, *262*(5137), 1252–1255.

http://doi.org/10.1126/science.262.5137.1252

Cess, R. D., and Coauthors, 1990: Intercomparison and interpretation of climate feedback processes in 19 atmospheric general circulation models. J. Geophys. Res. Atmos., 95, 16601–16615, doi:10.1029/JD095iD10p16601. https://doi.org/10.1029/JD095iD10p16601.

——, and Coauthors, 1993: Uncertainties in Carbon Dioxide Radiative Forcing in Atmospheric General Circulation Models. Science (80-.)., 262, 1252 LP-1255, doi:10.1126/science.262.5137.1252. http://science.sciencemag.org/content/262/5137/1252.abstract.

Cess, R. D., et al. (1996), Cloud feedback in atmospheric general circulation models: An update, J. Geophys. Res., 101, 12,791–12,794

Cess, R.D., *et al.*, Uncertainties in carbon dioxide radiative forcing, *Science*262,1252(1993).

Chamberlain, J. W., H. M. Foley, G. J. MacDonald, and M. A. Ruderman, 1982: In Carbon dioxide review 1982, W. Clark, Ed., Oxford University Press, Clarendon, England, 255–277.

Chameides, W., and J. C. G. Walker, 1973: A photochemical theory of tropospheric ozone. *J. Geophys. Res.*, **78**, 8751–8760, doi:10.1029/JC078i036p08751. http://dx.doi.org/10.1029/JC078i036p08751.

Chameides, W. L., and R. J. Cicerone, 1978: Effects of nonmethane hydrocarbons in the atmosphere. *J. Geophys. Res. Ocean.*, **83**, 947–952, doi:doi:10.1029/JC083iC02p00947. https://doi.org/10.1029/JC083iC02p00947.

Chapman, S., 1930: On ozone and atomic oxygen in the upper atmosphere. *Philos. Mag.*, **10**, 369–383.

Chanin, M.-L., and V. Ramaswamy, 1998: Chapter 5. Trends in Stratospheric Temperatures. *Scientific Assessment of Ozone Depletion: 1998*, D.L. Albritton, R.. Watson, P.J. Aucamp, and G. Megie, Eds.

5517　Charlson, R. J., J. Langner, H. Rodhe, C. B. Leovy, and S. G. Warren, 1991: Perturbation of the
5518　　　Northern-Hemisphere Radiative Balance by Backscattering from Anthropogenic Sulfate
5519　　　Aerosols. Tellus Ser. a-Dynamic Meteorol. Oceanogr., 43, 152–163.

5520　Charlson, R. J., Langner, J., Rodhe, H., Leovy, C. B., & Warren, S. G. (1991). Perturbation of
5521　　　the northern hemisphere radiative balance by backscattering from anthropogenic sulfate
5522　　　aerosols. *Tellus A: Dynamic Meteorology and Oceanography*, *43*(4), 152-163.

5523　Charlson, R. J., Schwartz, S. E., Hales, J. M., Cess, R. D., Coakley, J. J., Hansen, J. E., &
5524　　　Hofmann, D. J. (1992). Climate forcing by anthropogenic aerosols. *Science*, *255*(5043),
5525　　　423-430.

5526　Chédin A, Husson N, Scott NA. Une banque de données pour l'étude des phénomènes de
5527　　　transfert radiatif dans les atmosphères planétaires: la banque GEISA. Bull Inform Centre
5528　　　Données Stellaires (France) 1982;22:121–121.

5529　Chen, C.-T., and V. Ramaswamy, 1996: Sensitivity of Simulated Global Climate to Perturbations
5530　　　in Low Cloud Microphysical Properties. Part II: Spatially Localized Perturbations. *J.*
5531　　　*Clim.*, **9**, 2788–2801, doi:10.1175/1520-
5532　　　0442(1996)009<2788:SOSGCT>2.0.CO;2. https://doi.org/10.1175/1520-
5533　　　0442(1996)009%3C2788:SOSGCT%3E2.0.CO.

5534　Chen, Y. C., Christensen, M. W., Diner, D. J., & Garay, M. J. (2015). Aerosol-cloud interactions
5535　　　in ship tracks using Terra MODIS/MISR. *Journal of Geophysical Research: Atmospheres*,
5536　　　*120*(7), 2819-2833.

5537　Chen, C.-C. and Gettelman, A.: Simulated 2050 aviation radiative forcing from contrails and
5538　　　aerosols, Atmos. Chem. Phys., 16, 7317-7333, https://doi.org/10.5194/acp-16-7317-2016,
5539　　　2016.

5540　Chiang, J. C. H. & Bitz, C. M. Influence of high latitude ice cover on the marine Intertropical
5541　　　Convergence Zone. *Clim. Dyn.* **25,** 477-496 (2005).

5542　Chiodo, G., L. M. Polvani, D. R. Marsh, A. Stenke, W. Ball, E. Rozanov, S. Muthers, and K.
5543　　　Tsigaridis, 2018: The Response of the Ozone Layer to Quadrupled CO2 Concentrations. *J.*

Clim., **31**, 3893–3907, doi:10.1175/JCLI-D-17-0492.1. https://doi.org/10.1175/JCLI-D-17-0492.1.

Chiou, E. W., L. W. Thomason, and W. P. Chu (2006), Variability of Stratospheric Water Vapor Inferred from SAGE II, HALOE, and Boulder (Colorado) Balloon Measurements, J. Climate, 19, 4121-4133.

Christoforou, P, and S. Hameed, 1997: Solar cycle and the Pacific 'centers of action', Geophys. Res. Lett., 24, 293-296.

Chuang, C. C., J. E. Penner, K. E. Taylor, and J. J. Walton, 1993: Climate effects of anthropogenic sulfate: Simulations from a coupled chemistry/climate model. 7. http://inis.iaea.org/search/search.aspx?orig_q=RN:25046956.

Chung, E.-S., and B. J. Soden, 2015: An Assessment of Direct Radiative Forcing, Radiative Adjustments, and Radiative Feedbacks in Coupled Ocean–Atmosphere Models. J. Clim., 28, 4152–4170, doi:10.1175/JCLI-D-14-00436.1. https://doi.org/10.1175/JCLI-D-14-00436.1.

Chylek, P., & Wong, J. (1995). Effect of absorbing aerosols on global radiation budget. *Geophysical research letters*, *22*(8), 929-931.

Chylek, P., and J. Wong, 1995: Effect of absorbing aerosols on global radiation budget. Geophys. Res. Lett., 22, 929–931, doi:10.1029/95GL00800. https://doi.org/10.1029/95GL00800.

Ciais, P., Gasser, T., Paris, J., Caldeira, K., Raupach, M., Canadell, J., Patwardhan, A., Friedlingstein, P., Piao, S., Gitz, V., Raupauch, M., Canadell, J., Patwardhan, A., Friedlingstein, P., Piao, S. and Gitze, V.: Attributing the increase in atmospheric CO2 to emitters and absorbers, Nat. Clim. Chang., 3(doi:10.1038/nclimate1942), 926–930, 2013a.

Ciais, P., Sabine, C., Bala, G., Bopp, L., Brovkin, V., Canadell, J., Chhabra, A., DeFries, R., Galloway, J., Heimann, M., Jones, C., Quéré, C. Le, Myneni, R. B., Piao, S. and Thornton, P.: Carbon and Other Biogeochemical Cycles, Clim. Chang. 2013 - Phys. Sci. Basis, 465–570, doi:10.1017/CBO9781107415324.015, 2013b.

5571   Clark, W. C. (ed.)., 1982: Carbon dioxide review 1982. Oxford University Press, Clarendon,
5572   England, United States, https://www.osti.gov/servlets/purl/5963903.

5573   Clette, F. and L. Lefèvre, 2016: The new sunspot number: Assembling all corrections, Sol. Phys.
5574   291, 2629–2651, https://doi.org/10.1007/s11207-016-1014-y

5575   Coakley, J. A., Bernstein, R. L., & Durkee, P. A. (1987). Effect of ship-stack effluents on cloud
5576   reflectivity. *Science*, *237*(4818), 1020-1022.

5577   Coakley, J. Jr. (1981), Stratospheric Aerosols and the Tropospheric Energy Budget: Theory Versus
5578   Observations, J. Geophys. Res., 86, 9761-9766.

5579   Coddington, O., J. L. Lean, P. Pilewskie, M. Snow, and D. Lindholm, 2106: A solar irradiance
5580   climate data record, Bulletin American Meteor. Soc., BAMS.

5581   Cole-Dai, J. (2010), Volcanoes and climate, WIREs Climate Change, doi:10.1002/wcc.76.

5582   Collins, J. W., and Coauthors, 2017: AerChemMIP: Quantifying the effects of chemistry and
5583   aerosols in CMIP6. *Geosci. Model Dev.*, **10**, 585–607, doi:10.5194/gmd-10-585-2017.

5584   Collins, W. D., Feldman, D. R., Kuo, C., & Nguyen, N. H. (2018). Large regional shortwave
5585   forcing by anthropogenic methane informed by Jovian observations. *Science Advances*,
5586   *4*(9). http://doi.org/10.1126/sciadv.aas9593

5587   Collins, W. J., S. Sitch, and O. Boucher, 2010: How vegetation impacts affect climate metrics for
5588   ozone precursors. *J. Geophys. Res.*, **115**, D23308, doi:10.1029/2010jd014187.
5589   http://dx.doi.org/10.1029/2010JD014187.

5590   Collins, W. J., M. M. Fry, H. Yu, J. S. Fuglestvedt, D. T. Shindell, and J. J. West: Global and
5591   regional temperature-change potentials for near-term climate forcers, *Atmos. Chem.*
5592   *Phys.*, **13**, 2471-2485, https://doi.org/10.5194/acp-13-2471-2013.

5593   Collins, W. D., and Coauthors, 2006: Radiative forcing by well-mixed greenhouse gases:
5594   Estimates from climate models in the Intergovernmental Panel on Climate Change (IPCC)
5595   Fourth Assessment Report (AR4). J. Geophys. Res., 111, D14317.

5596   Collins, W. D., Ramaswamy, V., Schwarzkopf, M. D., Sun, Y., Portmann, R. W., Fu, Q., …

5597   Zhong, W. Y. (2006). Radiative forcing by well-mixed greenhouse gases: Estimates from

5598   climate models in the Intergovernmental Panel on Climate Change (IPCC) Fourth

5599   Assessment Report (AR4). *Journal of Geophysical Research Atmospheres*, *111*(14), 1–15.

5600   http://doi.org/10.1029/2005JD006713

5601   Collins, W. J., Lamarque, J., Schulz, M., Boucher, O., Eyring, V., Hegglin, I., Maycock, A.,

5602   Myhre, G., Prather, M., Shindell, D. and Smith, S. J.: AerChemMIP : quantifying the effects

5603   of chemistry and aerosols in, , 585–607, doi:10.5194/gmd-10-585-2017, 2017.

5604   Colman, R. A., and S. B. Power (2010), Atmospheric radiative feedbacks associated with transient

5605   climate change and climate variability, Clim. Dyn., 34, 919–933, doi:10.1007/s00382-009-

5606   0541-8.

5607   Conover, John H. "Anomalous cloud lines." *Journal of the Atmospheric Sciences* 23, no. 6

5608   (1966): 778-785.

5609   Cooke, W. F., & Wilson, J. J. (1996). A global black carbon aerosol model. *Journal of*

5610   *Geophysical Research: Atmospheres*, *101*(D14), 19395-19409.

5611   Cooke, W. F., Liousse, C., Cachier, H., & Feichter, J. (1999). Construction of a 1× 1 fossil fuel

5612   emission data set for carbonaceous aerosol and implementation and radiative impact in the

5613   ECHAM4 model. *Journal of Geophysical Research: Atmospheres*, *104*(D18), 22137-22162.

5614   Costantino, L., & Bréon, F. M. (2013). Aerosol indirect effect on warm clouds over South-East

5615   Atlantic, from co-located MODIS and CALIPSO observations. *Atmos. Chem. Phys*, *13*(1),

5616   69-88.

5617   Crook, J. A., L. S. Jackson ,S. M. Osprey, P. M. Forster , 2015: A comparison of temperature

5618   and precipitation responses to different Earth radiation management geoengineering

5619   schemes, *J. Geophys. Res. Atmospheres*, https://doi.org/10.1002/2015JD023269

5620

5621   Crutzen, P. J., 1970: The influence of nitrogen oxides on the atmospheric ozone content. *Q. J. R.*

5622   *Meteorol. Soc.*, **96**, 320–325, doi:10.1002/qj.49709640815.

5623   https://doi.org/10.1002/qj.49709640815.

5624

Crutzen, P. J., 1972a: SST's: A Threat to the Earth's Ozone Shield. *Ambio*, **1**, 41–51. http://www.jstor.org/stable/4311946.

Crutzen, P. J., 1972b: *Gas-phase nitrogen and methane chemistry in the atmosphere*. Stockholm, 20 pp.

Crutzen, P. J., 1973: *A discussion of the chemistry of some minor constituents in the stratosphere and troposphere*. Stockholm,.

Crutzen, P. J., 1979: The role of NO and NO2 in the chemistry of the troposphere and stratosphere. *Annu. Rev. Earth Planet. Sci.*, **7**, 443–472.

——, and J. Lelieveld, 2001: Human Impacts on Atmospheric Chemistry. *Annu. Rev. Earth Planet. Sci.*, **29**, 17–45.

Crutzen, P. J. (1976), The possible importance of CSO for the sulfate layer of the stratosphere, Geophys. Res. Lett., 3, 73–76, doi:10.1029/GL003i002p00073.

Crutzen, P. (2006), Albedo Enhancement by Stratospheric Sulfur Injections: A Contribution to Resolve a Policy Dilemma? *Climatic Change*, 77, 211-220.

Crutzen, P. J., 2006: Albedo enhancement by stratospheric sulfur injections: A contribution to resolve a policy dilemma? *Clim. Change*, doi:10.1007/s10584-006-9101-y.

Cubasch, U., R. Voss, G. C. Hegerl, J. Waszkewitz, and T. J. Crowley, 1997: Simulation of the influence of solar radiation variations on the global climate with an ocean-atmosphere general circulation model, Climate Dynamics, 13, 757-767.

5644

Damon, P., and J. Jirikowic, 1992: The Sun as a Low-Frequency Harmonic Oscillator. Radiocarbon, 34(2), 199-205. doi:10.1017/S003382220001362X.

Daniel, J. S., and S. Solomon, 1998: On the climate forcing of carbon monoxide. *J. Geophys. Res. Atmos.*, **103**, 13249–13260, doi:doi:10.1029/98JD00822.

5649 https://doi.org/10.1029/98JD00822.

de Graaf, M., Tilstra, L. G., Wang, P., & Stammes, P. (2012). Retrieval of the aerosol direct
radiative effect over clouds from spaceborne spectrometry. *Journal of Geophysical
Research: Atmospheres*, 117(D7).

de Graaf, M., N. Bellouin, L.G. Tilstra, J.M. Haywood, and P. Stammes, Aerosol direct radiative
effect from episodic smoke emissions over the southeast Atlantic Ocean from 2006 to 2009,
Geophy. Res. Letts, 41, 21, 7723–7730, DOI: 10.1002/2014GL061103, 2014.

Delworth, T. L., V. Ramaswamy, and G. L. Stenchikov (2005), The impact of aerosols on
simulated ocean temperature, heat content, and sea level in the 20th century. *Geophys Res
Lett*, 32, L24709.

Delworth, T. L., et al. (2006), GFDL's CM2 global coupled climate models. Part I: Formulation
and simulation characteristics, J. Clim., 19, 643–674, doi:10.1175/JCLI3629.1.

DeLand, M. T., and R. P. Cebula, 1998: NOAA 11 Solar Backscatter Ultraviolet, model 2
(SBUV/2) instrument solar spectral irradiance measurements in 1989–1994: 2. Results,
validation, and comparisons, J. Geophys. Res., 103(D13), 16251–16273,
doi:10.1029/98JD01204.

DeLand, M. T., and R. P. Cebula, 2008: Creation of a composite solar ultraviolet irradiance data
set, J. Geophys. Res., 113, A11103, doi:10.1029/2008JA013401.

Delaygue, G. and E. Bard, 2011: An Antarctic view of Beryllium-10 and solar activity for the
past millennium. Clim. Dyn. 36: 2201. https://doi.org/10.1007/s00382-010-0795-1

Denman, K. L., and Coauthors, 2007: Couplings Between Changes in the Climate System and
Biogeochemistry. *Climate Change 2007: The Physical Science Basis. Contribution of
Working Group I to the Fourth Assessment Report of the Intergovernmental Panel on
Climate Change*, D. Qin, M. Manning, Z. Chen, M. Marquis, K.B. Averyt, M. Tignor, and
H.L. Miller, Eds., Cambridge University Press, Cambridge, United Kingdom and New
York, NY, USA.

Denman, K. L., Brasseur, G., Chidthaisong, A., Ciais, P., Cox, P. M., Dickinson, R. E.,

5676   Hauglustaine, D., Heinze, C., Holland, E., Jacob, D., Lohmann, U., Ramachandran, S., Dias,

5677   P. L. da S., Wofsy, S. C. and Zhang, X.: Couplings between changes in the climate system

5678   and biogeochemistry, in Climate Change 2007: The Physical Science Bases. Contribution of

5679   Working Group I to the Fourth Assessment Report of the Intergovernmental Panel on

5680   Climate Change, edited by S. Solomon D. Qin, M. Manning, Z. Chen, M. Marquis, K.B.

5681   Averyt, M.Tignor and H.L. Miller, Cambridge University Press, Cambridge, UK., 2007.

5682   Derwent, R. G. (1990), Trace gases and their relative contribution to the greenhouse effect, Rep,

5683   Atomic Energy Research Establishment Harwell Oxon UK. Report AERE- R13716.

5684   Deshler, T., M. E. Hervig, D. J. Hofmann, J. M. Rosen, and J. B. Liley (2003), Thirty years of in

5685   situ stratospheric aerosol size distribution measurements from Laramie, Wyoming (41°N),

5686   using   balloon-borne   instruments,   J.   Geophys.   Res.,   108(D5),   4167,

5687   doi:10.1029/2002JD002514

5688   Deshler, T., R. Anderson-Sprecher, H. Jager, J. Barnes, D. J. Hoffmann, B Clemesha, D. Simonich,

5689   M. Osborn, R. J. Grainger, S. Godin-Beekmann (2006), Trends in the nonvolcanic component

5690   of stratospheric aerosol over the period 1971-2004, J. Geophys Res., 111, D01201,

5691   doi:10.1029/2005JD006089.

5692   Deshler, T. (2008), A review of global stratospheric aerosol: Measuremnts, importance, life cycle,

5693   and local stratospheric aerosol, Atmospheric research, 90, 223-232.

5694   Dessler, A. E., M. R. Schoeberl, T. Wang, S.M. Davis, K. H. Rosenlof, and J.-P. Vernier (2014),

5695   Variations of stratospheric water vapor over the past three decades, J. Geophys. Res. Atmos.,

5696   119, 12,588–12,598, doi:10.1002/2014JD021712.

5697   Despres, V., Huffman, J., Burrows, S. M., Hoose, C., Safatov, A., Buryak, G., Frohlich-

5698   Nowoisky, J., Elbert, W., M. Andreae, Polsch, U. and Jaenicke, R.: Primary biological

5699   aerosol particles in the atmosphere: a review, Tellus B, 64(15598),

5700   doi:10.3402/tellusb.v64i0.15598, 2012.

5701   Deuzé, J.L., Bréon, F.M., Devaux, C., Goloub, P.H., Herman, M., Lafrance, B., Maignan, F.,

5702   Marchand, A., Nadal, F., Perry, G. and Tanré, D., 2001. Remote sensing of aerosols over

5703   land surfaces from POLDER-ADEOS-1 polarized measurements. *Journal of Geophysical*

5704   *Research: Atmospheres*, *106*(D5), pp.4913-4926.

5705 Dhomse, S., K. Emmerson, G. Mann, N. Bellouin, K. Carslaw, M. Chipperfield, R. Hommel, N.

5706   Abraham, P. Telford, P. Braesicke, M. Dalvi, C. Johnson, F. O'Connor, O. Morgenstern, J.

5707   Pyle, T. Deshler, J. Zawodny, and L. Thomason (2014), Aerosol microphysical simulations

5708   of the Mt. Pinatubo eruption with the UM-UKCA composition-climate model, Atmos. Chem.

5709   Phys., 14,11221-11246, doi:10.5194/ACP-14-11221-2014.

5710 Dickinson, R. E., and R. J. Cicerone, 1986: Future global warming from atmospheric trace gases.

5711   *Nature*, 319, 109–115, doi:10.1038/319109a0. https://doi.org/10.1038/319109a0.

5712 Dickinson, R.E., S.C. Liu, and T.M. Donahue, 1978: Effect of Chlorofluoromethane Infrared

5713   Radiation on Zonal Atmospheric Temperatures. J. Atmos. Sci., 35, 2142–

5714   2152,https://doi.org/10.1175/1520-0469(1978)035<2142:EOCIRO>2.0.CO;2

5715 Dickinson, R.E., S.C. Liu, and T.M. Donahue, 1978: Effect of Chlorofluoromethane Infrared

5716   Radiation on Zonal Atmospheric Temperatures. J. Atmos. Sci., 35, 2142–

5717   2152,https://doi.org/10.1175/1520-0469(1978)035<2142:EOCIRO>2.0.CO;2

5718 Dines, W. H., 1917: The heat balance of the atmosphere. Quart. J. Roy. Meteor. Soc., vol. 43,

5719   issue 182, pp 151-158. https://doi.org/10.1002/qj.49704318203.

5720 Donner, L. J., and V. Ramanathan, 1980: Methane and nitrous oxide: their effects on the

5721   terrestrial climate. *Journal of the Atmospheric Sciences*. 37:119-124

5722 Donner, L. and V. Ramanathan, 1980: Methane and Nitrous Oxide: Their Effects on the

5723   Terrestrial Climate. J. Atmos. Sci., 37, 119–124, https://doi.org/10.1175/1520-

5724   0469(1980)037<0119:MANOTE>2.0.CO;2

5725 Doutriaux-Boucher, M., Webb, M., Gregory, J. and Boucher, O.: Carbon dioxide induced

5726   stomatal closure increases radiative forcing via a rapid reduction in low cloud, Geophysical

5727   Research Letters, -, 2009.

5728 Dorland, R., F. J. Dentener, and J. Lelieveld, 1997: Radiative forcing due to tropospheric ozone

5729   and sulfate aerosols. *J. Geophys. Res. Atmos.*, **102**, 28079–28100,

5730   doi:doi:10.1029/97JD02499. https://doi.org/10.1029/97JD02499.

5731 Dogar, M., G. Stenchikov, S. Osipov, B Wyman, M. Zhao (2017), Sensitivity of the Regional
5732   Climate in the Middle East and North Africa to Volcanic Perturbations, J. Geophys. Res.
5733   Atmos., 122, doi:10.1002/2017JD026783.

5734 Doughty, C. E., C. B. Field, and A. M. S. McMillan, 2011: Can crop albedo be increased through
5735   the modification of leaf trichomes, and could this cool regional climate? *Clim. Change*,
5736   doi:10.1007/s10584-010-9936-0.

5737 Douglass, D. H. and B. D. Clader, 2002: Climate sensitivity of the Earth to solar irradiance,
5738   Geophys. Res. Lett., 29, 10.1029/2002GL015345.

5739 Drayson, S.R., (1976). Rapid computation of the Voigt profile, Journal of Quantitative
5740   Spectroscopy and Radiative Transfer, 16(7), 611—614. https://doi.org/10.1016/0022-
5741   4073(76)90029-7

5742 Dubovik, O., and M. King, A flexible inversion algorithm for retrieval of aerosol optical
5743   properties from Sun and sky radiance measurements, J. Geophys. Res., 105, 20,673–20,696,
5744   2000.

5745 Duce, R. A., LaRoche, J., Altieri, K., Arrigo, K. R., Baker, A. R., Capone, D. G., Cornell, S.,
5746   Dentener, F., Galloway, J., Ganeshram, R. S., Geider, R. J., Jickells, T., Kuypers, M. M.,
5747   Langlois, R., Liss, P. S., Liu, S. M., Middelburg, J. J., Moore, C. M., Nickovic, S., Oschlies,
5748   A., Pedersen, T., Prospero, J., Schlitzer, R., Seitzinger, S., Sorensen, L. L., Uematsu, M.,
5749   Ulloa, O., Voss, M., Ward, B. and Zamora, L.: Impacts of Atmospheric Anthropogenic}
5750   Nitrogen on the Open Ocean, Science (80-.)., 320(5878), 893–897,
5751   doi:10.1126/science.1150369, 2008.

5752 Duda, D. P., Bedka, S. T., Minnis, P., Spangenberg, D., Khlopenkov, K., Chee, T., and Smith Jr.,
5753   W. L.: Northern Hemisphere contrail properties derived from Terra and Aqua MODIS data
5754   for 2006 and 2012, Atmos. Chem. Phys., 19, 5313-5330, https://doi.org/10.5194/acp-19-
5755   5313-2019, 2019.

5756   Dudok de Wit, T., Kopp, G., Fröhlich, C., and M. Schöll, 2017: Methodology to create a new

5757   total solar irradiance record: Making a composite out of multiple data records. Geophys.

5758   Res. Lett., 44, 1196–1203, doi:10.1002/2016GL071866.

5759   Dutton, E. G., and J. R. Christy (1992), Solar radiative forcing at selected locations and evidence

5760   for global lower tropospheric cooling following the eruptions of El Chichón and Pinatubo,

5761   Geophys. Res. Lett., 19, 2313-2316.

5762   Dykema, J. A., D. W. Keith, J. G. Anderson, and D. Weisenstein, 2014: Stratospheric controlled

5763   perturbation experiment: A small-scale experiment to improve understanding of the risks of

5764   solar geoengineering. *Philos. Trans. R. Soc. A Math. Phys. Eng. Sci.*,

5765   doi:10.1098/rsta.2014.0059.

5766

5767   Eddy, J. A., 1976: The Maunder Minimum, Science, New Series, 192, 4245, 1189-1202.

5768   Ekholm, N., 1901: On the variations of the climate of the geological and historical past and their

5769   causes. *Quart. J. Roy. Meteor. Soc.*, 27, 117, 1-62.

5770   Ellingson, R. G., & Fouquart, Y. (1991). The intercomparison of radiation codes in climate

5771   models: An overview. *Journal of Geophysical Research: Atmospheres*, *96*(D5), 8925–8927.

5772   http://doi.org/10.1029/90JD01618

5773   English, J., O. Toon, and M. Mills (2013), Microphysical simulations of large volcanic eruptions:

5774   Pinatubo and Toba, J. Geophys. Res. Atmos., 118, 1880-1895, doi:10.1002/JGRD.50196.

5775   Etminan, M., Myhre, G., Highwood, E. J., & Shine, K. P. (2016). Radiative forcing of carbon

5776   dioxide, methane, and nitrous oxide: A significant revision of the methane radiative forcing.

5777   *GEOPHYSICAL RESEARCH LETTERS*, *43*(24), 12614–12623.

5778   http://doi.org/10.1002/2016GL071930

5779   Etminan, M., Myhre, G., Highwood, E. J. and Shine, K. P.: Radiative forcing of carbon dioxide,

5780   methane, and nitrous oxide: A significant revision of the methane radiative forcing,

5781   Geophysical Research Letters, 43(24), 12614-12623, 2016.

Evan, A., Flamant, C., Gaetani, M. and Guichard, F.: The past, present and future of African dust, Nature, 531, 493–495, 2016.

Evan, A. T. (2012), Atlantic hurricane activity following two major volcanic eruptions, J. Geophys. Res. 117, D06101.

Eyring, V., and Coauthors, 2013: Long-term ozone changes and associated climate impacts in CMIP5 simulations. *J. Geophys. Res. Atmos.*, **118**, 5029–5060, doi:10.1002/jgrd.50316. http://dx.doi.org/10.1002/jgrd.50316.

Eyring, V., S. Bony, G. A. Meehl, C. A. Senior, B. Stevens, R. J. Stouffer, and K. E. Taylor, 2016: Overview of the Coupled Model Intercomparison Project Phase 6 (CMIP6) experimental design and organization. *Geosci. Model Dev.*, **9**, 1937–1958, doi:10.5194/gmd-9-1937-2016. https://www.geosci-model-dev.net/9/1937/2016/

Fabian, P., and P. G. Pruchniewicz, 1977: Meridional distribution of ozone in the troposphere and its seasonal variations. *J. Geophys. Res.*, **82**, 2063–2073, doi:doi:10.1029/JC082i015p02063. https://doi.org/10.1029/JC082i015p02063.

Fahey, D.W. U. Schumann, S. Ackerman, P. Artaxo, O. Boucher, M. Danilin, B. Kärcher, P. Minnis, T. Nakajima, and O. B. Toon (1999). Aviation-Produced Aerosols and Cloudiness. In Aviation and the Global Atmosphere. A Special Report of IPCC Working Groups I and III J.E. Penner, D.H. Lister, D.J. Griggs, D.J. Dokken, M. McFarland (Eds). Cambridge University Press, Cambridge, UK, 65−120.

Feddema, J., Oleson, K., Bonan, G., Mearns, L., Buja, L., Meehl, G. and Washington, W.: The importance of land-cover change in simulating future climates, Science (80-.)., 310, 1674–1678, 2005.

Feichter, J., U. Lohmann and I. Schult, 1997: The atmospheric sulfur cycle in ECHAM-4 and its impact on the shortwave radiation. Climate Dynamics, 13, 235−246.

Fels, S. B., J. D. Mahlman, M. D. Schwarzkopf, and R. W. Sinclair, 1980: Stratospheric Sensitivity to Perturbations in Ozone and Carbon Dioxide: Radiative and Dynamical

5809   Response. J. Atmos. Sci., 37, 2265–2297, doi:10.1175/1520-
5810   0469(1980)037<2265:SSTPIO>2.0.CO;2. https://doi.org/10.1175/1520-
5811   0469(1980)037%3C2265:SSTPIO%3E2.0.CO.

5812   Fels, S. B., Kiehl, J. T., Lacis, A. A., & Schwarzkopf, M. D. (1991). Infrared cooling rate
5813   calculations in operational general circulation models: Comparisons with benchmark
5814   computations. *J. Geophys. Res.*, *96*, 9105–9120. http://doi.org/10.1029%2F91JD00516.

5815   Field, C. B., Barros, V. R., Mach, K. J., Mastrandrea, M. D., Aalst, M. van, Adger, W. N., Arent,
5816   D. J., Barnett, J., Betts, R., Bilir, T. E., Birkmann, J., Carmin, J., Chadee, D. D., Challinor,
5817   A. J., Chatterjee, M., Cramer, W., Davidson, D. J., Estrada, Y. O., Gattuso, J.-P., Hijioka,
5818   Y., Hoegh-Guldberg, O., Huang, H.-Q., Insarov, G. E., Jones, R. N., Kovats, R. S., Lankao,
5819   P. R., Larsen, J. N., Losada, I. J., Marengo, J. A., McLean, R. F., Mearns, L. O., Mechler,
5820   R., Morton, J. F., Niang, I., Oki, T., Olwoch, J. M., Opondo, M., Poloczanska, E. S.,
5821   Pörtner, H.-O., Redsteer, M. H., Reisinger, A., Revi, A., Schmidt, D. N., Shaw, M. R.,
5822   Solecki, W., Stone, D. A., Stone, J. M. R., Strzepek, K. M., Suarez, A. G., Tschakert, P.,
5823   Valentini, R., Vicuña, S., Villamizar, A., Vincent, K. E., Warren, R., White, L. L.,
5824   Wilbanks, T. J., Wong, P. P. and Yohe, G. W.: Technical Summary, in Climate Change
5825   2014: Impacts, Adaptation, and Vulnerability. Part A: Global and Sectoral Aspects.
5826   Contribution of Working Group II to the Fifth Assessment Report of the Intergovernmental
5827   Panel on Climate Change, edited by C. B. Field, V. R. Barros, D. J. Dokken, K. J. Mach, M.
5828   D. Mastrandrea, T. E. Bilir, M. Chatterjee, K. L. Ebi, Y. O. Estrada, R. C. Genova, B.
5829   Girma, E. S. Kissel, A. N. Levy, S. MacCracken, P. R. Mastrandrea, and L. L. White, pp.
5830   35–94, Cambridge University Press, Cambridge, UK and New York, NY, USA., 2014.

5831   Fiocco, G., and G. Grams (1964), Observations of the aerosol layer at 20 km by optical radar, J.
5832   Atmos. Sci., 21, 323–324.

5833   Fiore, A. M., and Coauthors, 2012: Global air quality and climate. *Chem. Soc. Rev.*, **41**, 6663–
5834   6683. http://dx.doi.org/10.1039/C2CS35095E.

5835   Fiore, A. M., V. Naik, and E. M. Leibensperger, 2015: Air Quality and Climate Connections. *J.
5836   Air Waste Manage. Assoc.*, **65**, 645–685, doi:10.1080/10962247.2015.1040526.
5837   http://www.tandfonline.com/doi/full/10.1080/10962247.2015.1040526.

5838   Fisher, D., C. Hales, W-C. Wang, M. Ko, N. D. Sze, 1990: Model calculations of the relative

5839   effects of CFCs and their replacements on global warming. *Nature* 344(6266):513-516.

5840   DOI: 10.1038/344513a0.

5841   Fisher, D. A., C. H. Hales, W. C. Wang, M. K. W. Ko, and N. D. Sze (1990), Model-calculations

5842   of the relative effects of CFCs and their replacements on global warming, Nature, 344(6266),

5843   513–516, doi:10.1038/344513a0.

5844   Fisher et al., 1990D.A. Fisher, C.H. Hales, W.C. Wang, M.K.W. Ko, N.D. SzeModel

5845   calculations of the relative effects of CFCs and their replacements on global warming

5846   Nature, 344 (1990), pp. 513-516

5847   Fisher, D., C.H. Hales, W.C. Wang, M.K.W. Ko, N.D. Sze, 1990: Model calculations of the

5848   relative effects of CFCs and their replacements on global warming Nature, 344 (1990),

5849   pp. 513-516.

5850   Fishman, J., and P. J. Crutzen, 1978: The origin of ozone in the troposphere. *Nature*, **274**, 855–

5851   858. http://dx.doi.org/10.1038/274855a0.

5852   Fishman, J., V. Ramanathan, P. J. Crutzen, and S. C. Liu, 1979a: Tropospheric ozone and

5853   climate. *Nature*, **282**, 818–820. http://dx.doi.org/10.1038/282818a0.

5854   Fishman, J., S. Solomon, and P. J. Crutzen, 1979b: Observational and theoretical evidence in

5855   support of a significant in-situ photochemical source of tropospheric ozone. *Tellus*, **31**, 432–

5856   446, doi:10.1111/j.2153-3490.1979.tb00922.x. https://doi.org/10.1111/j.2153-

5857   3490.1979.tb00922.x.

5858   Fläschner, D., Mauritsen, T. and Stevens, B.: Understanding the inter-model spread in global-

5859   mean hydrological sensitivity, Journal of Climate, 29, 801-817, 2016.

5860   Fleming, J. R., 2007: The Callendar Effect, American Meteorological Society, Boston, MA.

5861   Fleming, J. R., 1998: Historical perspectives on climate change. Oxford University Press. ISBN

5862   978-0195078701.

5863   Folland, C. K., Palmer, T. N. & Parker, D. E. Sahel rainfall and worldwide sea temperatures, 1901-
5864   85. *Nature* **320,** 602-607 (1986).

5865   Forster, P., V. Ramaswamy, P. Artaxo, T. Berntsen, R. Betts, D.W. Fahey, J. Haywood, J. Lean,
5866   D.C. Lowe, G. Myhre, J. Nganga, R. Prinn, G. Raga, M. Schulz and R. Van Dorland, 2007:
5867   Changes in Atmospheric Constituents and in Radiative Forcing. In: Climate Change 2007:
5868   The Physical Science Basis. Contribution of Working Group I to the Fourth Assessment
5869   Report of the Intergovernmental Panel on Climate Change [Solomon, S., D. Qin, M.
5870   Manning, Z. Chen, M. Marquis, K.B. Averyt, M.Tignor and H.L. Miller (eds.)]. Cambridge
5871   University Press, Cambridge, United Kingdom and New York, NY, USA.

5872   Forster, P. M., Richardson, T., Maycock, A. C., Smith, C. J., Samset, B. H., Myhre, G.,
5873   Andrews, T., Pincus, R. and Schulz, M.: Recommendations for diagnosing effective
5874   radiative forcing from climate models for CMIP6, Journal of Geophysical Research:
5875   Atmospheres, 121(20), 12460-12475, 2016.

5876   Forster, P., and Coauthors, 2007: Changes in Atmospheric Constituents and in Radiative
5877   Forcing. Climate Change 2007: The Physical Science Basis. Contribution of Working
5878   Group I to the Fourth Assessment Report of the Intergovernmental Panel on Climate
5879   Change, D. Qin, M. Manning, Z. Chen, M. Marquis, K.B. Averyt, M. Tignor, and H.L.
5880   Miller, Eds., Cambridge University Press, Cambridge, United Kingdom and New York,
5881   NY, USA.

5882   Forster, P. M., 2016: Inference of Climate Sensitivity from Analysis of Earth's Energy Budget.
5883   Annu. Rev. Earth Planet. Sci., 44, 85–106, doi:doi:10.1146/annurev-earth-060614-105156.
5884   http://www.annualreviews.org/doi/abs/10.1146/annurev-earth-060614-105156.

5885   Forster, P., and Coauthors, 2007: Changes in Atmospheric Constituents and in Radiative
5886   Forcing. *Climate Change 2007: The Physical Science Basis. Contribution of Working
5887   Group I to the Fourth Assessment Report of the Intergovernmental Panel on Climate
5888   Change*, D. Qin, M. Manning, Z. Chen, M. Marquis, K.B. Averyt, M. Tignor, and H.L.
5889   Miller, Eds., Cambridge University Press, Cambridge, United Kingdom and New York,
5890   NY, USA.

Forster, P. M., 1999: Radiative forcing due to stratospheric ozone changes 1979–1997, using updated trend estimates. *J. Geophys. Res. Atmos.*, **104**, 24395–24399, doi:doi:10.1029/1999JD900770. https://doi.org/10.1029/1999JD900770.

Forster, P. M., and K. P. Shine, 1997: Radiative forcing and temperature trends from stratospheric ozone changes. *J. Geophys. Res. Atmos.*, **102**, 10841–10855, doi:doi:10.1029/96JD03510. https://doi.org/10.1029/96JD03510.

Forster, P. M., and K. P. Shine, 1999: Stratospheric water vapour changes as a possible contributor to observed stratospheric cooling. *Geophys. Res. Lett.*, **26**, 3309–3312, doi:doi:10.1029/1999GL010487. https://doi.org/10.1029/1999GL010487.

Foster, G., and S. Rahmstorf, 2011: Global temperature evolution 1979–2010, Environ. Res. Lett., 6, doi:10.1088/1748-9326/6/4/044022.

Forster, P., Ramaswamy, V., Artaxo, P., Berntsen, T., Betts, R., Fahey, D. W., Haywood, J., Lean, J., Lowe, D. C., Myhre, G., Nganga, J., Prinn, R., Raga, G. and Dorland, R. Van: Changes in Atmospheric Constituents and in Radiative Forcing, in Climate Change 2007: The Physical Science Basis. Contribution of Working Group I to the Fourth Assessment Report of the Intergovernmental Panel on Climate Change, edited by S. Solomon D. Qin, M. Manning, Z. Chen, M. Marquis, K.B. Averyt, M.Tignor and H.L. Miller, pp. 130–234, Cambridge University Press, Cambridge, United Kingdom and New York, NY, USA., 2007.

Forster, P., V. Ramaswamy, P. Artaxo, T. Berntsen, R. Betts, D.W. Fahey, J. Haywood, J. Lean, D.C. Lowe, G. Myhre, J. Nganga, R. Prinn, G. Raga, M. Schulz and R. Van Dorland (2007), Changes in Atmospheric Constituents and in Radiative Forcing. In: Climate Change 2007: The Physical Science Basis. Contribution of Working Group I to the Fourth Assessment Report of the Intergovernmental Panel on Climate Change [Solomon, S., D. Qin, M. Manning, Z. Chen, M. Marquis, K.B. Averyt, M.Tignor and H.L. Miller (eds.)]. Cambridge University Press, Cambridge, United Kingdom and New York, NY, USA.

Forster, P., and Coauthors, 2007: Changes in Atmospheric Constituents and in Radiative Forcing. *Climate Change 2007: The Physical Science Basis. Contribution of Working*

Group I to the Fourth Assessment Report of the Intergovernmental Panel on Climate Change, D. Qin, M. Manning, Z. Chen, M. Marquis, K.B. Averyt, M. Tignor, and H.L. Miller, Eds., Cambridge University Press, Cambridge, United Kingdom and New York, NY, USA.

Forster, P. M., Richardson, T., Maycock, A. C., Smith, C. J., Samset, B. H., Myhre, G., Andrews, T., Pincus, R., and Schulz, M. (2016), Recommendations for diagnosing effective radiative forcing from climate models for CMIP6, *J. Geophys. Res. Atmos.*, 121, 12,460– 12,475, doi:10.1002/2016JD025320.

Forster, P. M. *et al.* Evaluating adjusted forcing and model spread for historical and future scenarios in the CMIP5 generation of climate models. *J. Geophys. Res. Atmos.* **118,** 1139-1150 (2013).

Forster, P.M. (2016) Inference of Climate Sensitivity from Analysis of Earth's Energy Budget Annual Review of Earth and Planetary Sciences 2016 44:1, 85-106

Forsyth, P. Y., In the wake of Etna, 44 B.C., Classical Antiq., 7, 49-57, 1988.

Foukal, P., 1981: Sunspots and changes in the global output of the sun. Proc. The Physics of Sunspots, 1981, Sunspot, NM, A83-18101 06-92), 391-423.

Foukal, P. and J. Lean, 1988: Magnetic modulation of solar luminosity by photospheric activity, Astrophys. J., 328, 347-357.

Foukal, P. and J. Lean, 1990: An empirical model of total solar irradiance variations between 1874-1988, Science, 247, 556-558.

Foukal, P. V., Mack, P. E., and J. E. Vernazza, 1977: The effect of sunspots and faculae on the solar constant, Astrophysical Journal, Part 1, vol. 215, Aug. 1, 1977, p. 952-959.

Foukal, P. North, G. and T. Wigley, 2004: A Stellar View on Solar Variations and Climate, Science, 306, 5693, pp. 68-69, DOI: 10.1126/science.1101694

Fourier, J.B. 1824: M6moire sur les temp6ratures du globe terrestre et des espaces planetaires. Mem. Acad. Sci. Inst. Fr. 7, 569-604.

5945 Franklin, B., Meteorological imaginations and conjectures, 1784: Manchr. Lit. Philos. Soc. Mem.
5946   Proc., 2, 122. (Reprinted in Weatherwise, 35, 262, 1982.).

5947 Franklin, B., Meteorological imaginations and conjectures, Manchr. Lit. Philos. Soc. Mem. Proc.,
5948   2, 122, 1784. (Reprinted in Weatherwise, 35, 262, 1982.)

5949 Friedman, A., Y-Hwang, J. Chiang. and D. Frierson, 2013: Interhemispheric temperature
5950   asymmtery over the 20th Century and in future projections. J. Climate 26(15), 5419-5433

5951 Friedlingstein, P., Cox, P., Betts, R., Bopp, L., Bloh, W. von, Brovkin, V., P. Cadule, Doney, S.,
5952   Eby, M., I. Fung, G. Bala, J. John, C. Jones, F. Joos, T. Kato, M. Kawamiya, Knorr, W., K.
5953   Lindsay, H. D. Mathews, T. Raddatz, P. Rayner, Reick, C., E. Roeckner, Schnitzler, K.-G.,
5954   Schnurr, R., K. Strassmen, A. J. Weaver, C. Yoshikawa and Zeng, N.: Climate-carbon cycle
5955   feedback analysis, results from the C4MIP Model intercomparison, J. Clim., 19, 3337–
5956   3353, 2006.

5957 Free, M. and J. Angell (2002), Effect of volcanoes on the vertical temperature profile in radiosonde
5958   data, J. Geophys. Res., 107, No. D10, 10.1029/2001JD001128.

5959 Free, Melissa, and A. Robock (1998), Global warming in the context of the Little Ice Age. *J.*
5960   *Geophys. Res.*, **104**, 19,057-19,070.

5961 Friis-Christensen, E., and K Lassen, 1991: Length of the Solar Cycle: An Indicator of Solar
5962   Activity Closely Associated with Climate, Science, 254, pp. 698-700, DOI:
5963   10.1126/science.254.5032.698

5964 Fröhlich, C., 2013: Total Solar Irradiance: What Have We Learned from the Last Three Cycles
5965   and the Recent Minimum? Space Sci Rev, 176: 237. https://doi.org/10.1007/s11214-011-
5966   9780-1

5967 Fröhlich, C. and J. Lean, 2004: Solar radiative output and its variability: Evidence and
5968   Mechanisms, Astron. Astrophys. Rev., 12 (4), 273-320, doi: 10.1007/s00159-004-0024-1.

5969 Fröhlich, C., Romero, J., Roth, H. et al., 1995: VIRGO: Experiment for helioseismology and
5970   solar irradiance monitoring, Sol Phys 162: 101. https://doi.org/10.1007/BF00733428

5971   Fry, M. M., et al., 2012: The influence of ozone precursor emissions from four world regions on

5972   tropospheric composition and radiative climate forcing, *J. Geophys. Res.,* **117**, D07306,

5973   doi:10.1029/2011JD017134.

5974   Fuglestvedt, J. S., I. S. A. Isaksen, and W. Wang, 1996: Estimates of indirect global warming

5975   potentials for CH4, CO and NOX. *Clim. Change*, **34**, 405–437.

5976   Fuglestvedt, J. S., T. K. Berntsen, I. S. A. Isaksen, H. Mao, X.-Z. Liang, and W.-C. Wang, 1999:

5977   Climatic forcing of nitrogen oxides through changes in tropospheric ozone and methane;

5978   global 3D model studies. *Atmos. Environ.*, **33**, 961–977, doi:10.1016/s1352-

5979   2310(98)00217-9. http://www.sciencedirect.com/science/article/pii/S1352231098002179.

5980   Fuglestvedt, J. S., K. P. Shine, T. Berntsen, J. Cook, D. S. Lee, A. Stenke, R. B. Skeie, G. J. M.

5981   Velders, and I. A.Waitz (2010), Transport impacts on atmosphere and climate: Metrics,

5982   Atmos. Environ., 44(37), 4648–4677, doi:10.1016/j.atmosenv.2009.04.044.

5983   Fueglistaler, S., A. E. Dessler, T. J. Dunkerton, I. Folkins, Q. Fu, and P. W. Mote (2009), Tropical

5984   tropopause layer, Rev. Geophys., 47, RG1004, doi:10.1029/2008RG000267.

5985   Fueglistaler, S., Liu, Y. S., Flannaghan, T. J., Haynes, P. H., Dee, D. P., Read et al. (2013), The

5986   relation between atmospheric humidity and temperature trends for stratospheric water, J.

5987   Geophys. Res. Atmos., 118, 105 –1074.

5988   Fyfe, J. C., K. von Salzen, J. N. S. Cole, N. P. Gillett, and J. P. Vernier (2013), Surface response

5989   to stratospheric aerosol changes in a coupled atmosphere-ocean model. *Geophysical Research*

5990   *Letters*, 40, 584-588.

5991   Ganguly, D., Rasch, P. J., Wang, H. & Yoon, 2012: J. Fast and slow responses of the South

5992   Asian monsoon system to anthropogenic aerosols. *Geophys. Res. Lett.* **39**, L18804

5993   Gao, C., Robock, A., & Ammann, C. (2008). Volcanic forcing of climate over the past 1500

5994   years: An improved ice core-based index for climate models. *Journal of Geophysical*

5995   *Research: Atmospheres*, *113*(D23).

5996   Gao, C., A. Robock, and C. Ammann (2008), Volcanic forcing of climate over the past 1500 years:

5997   An improved ice core-based index for climate models, J. Geophys. Res., 113, D23111,

5998   doi:10.1029/2008JD010239.

5999   Gasser, T., Peters, G. P., Fuglestvedt, J. S., Collins, W. J., Shindell, D. T., and Ciais, P.: Accounting

6000   for the climate–carbon feedback in emission metrics, Earth Syst. Dynam., 8, 235-253,

6001   https://doi.org/10.5194/esd-8-235-2017, 2017.

6002   Gasser, T. and Ciais, P.: A theoretical framework for the net land-to-atmosphere CO_2 flux and

6003   its implications in the definition of "emissions from land-use change," Earth Syst. Dyn., 4,

6004   171–186, doi:10.5194/esd-4-171–2013, 2013.

6005   Gassó, S. (2008). Satellite observations of the impact of weak volcanic activity on marine clouds.

6006   *Journal of Geophysical Research: Atmospheres*, *113*(D14).

6007   Gauss, M., and Coauthors, 2006: Radiative forcing since preindustrial times due to ozone change

6008   in the troposphere and the lower stratosphere. *Atmos. Chem. Phys.*, **6**, 575–599.

6009   Ghan, S. J.: Technical Note: Estimating aerosol effects on cloud radiative forcing, Atmospheric

6010   Chemistry and Physics, 13(19), 9971-9974, 2013.

6011   Ghan, S.J., Easter, R.C., Chapman, E.G., Abdul-Razzak, H., Zhang, Y., Leung, L.R., Laulainen,

6012   N.S., Saylor, R.D. and Zaveri, R.A., 2001. A physically based estimate of radiative forcing

6013   by anthropogenic sulfate aerosol. *Journal of Geophysical Research: Atmospheres*, *106*(D6),

6014   pp.5279-5293.

6015   Ghan, S et al. Challenges in constraining anthropogenic aerosol effects on cloud radiative forcing

6016   using present-day spatiotemporal variability. PNAS, 113, 5804–5811, 2016.

6017   Gidden, M. J., Riahi, K., Smith, S. J., Fujimori, S., Luderer, G., Kriegler, E., van Vuuren, D. P.,

6018   van den Berg, M., Feng, L., Klein, D., Calvin, K., Doelman, J. C., Frank, S., Fricko, O.,

6019   Harmsen, M., Hasegawa, T., Havlik, P., Hilaire, J., Hoesly, R., Horing, J., Popp, A.,

6020   Stehfest, E. and Takahashi, K.: Global emissions pathways under different socioeconomic

6021   scenarios for use in CMIP6: a dataset of harmonized emissions trajectories through the end

6022   of the century, Geosci. Model Dev. Discuss., (November), 1–42, doi:10.5194/gmd-2018-

6023   266, 2018.

6024   Ginoux, P., Prospero, J., Gill, T. E., Hsu, N. C. and Zhao, M.: Global scale attribution of
6025   anthropogenic and natural dust sources and their emission rates based on MODIS deep blue
6026   aerosol products, Rev. Geophys., 50,(RG3005,), DOI:10.1029/2012RG000388, 2012.

6027   Gitz, V. and Ciais, P.: Amplifying effects of land-use change on future atmospheric CO2 levels,
6028   Global Biogeochem. Cycles, 17(1), 1024; doi:10.1029/2002GB001963, 2003.

6029   Gomez Martin, J. C., J. S. Brooke, W. Feng, M. Hopfner, M. J. Mills, and J. M. C. Plane (2017),
6030   Impacts of meteoric sulfur in the Eart's atmosphere, J. Geophys. Res. Atmos., 122,
6031   doi:10.1002/2017JD027218.

6032   Goody, R. M., and Y. L. Yung, 1985: Atmospheric Radiation: Theoretical Basis. Second edition.
6033   Oxford University Press, New York, 1989. 519 pp.

6034   Goody, R. M., & Yung, Y. L. (1995). *Atmospheric Radiation : Theoretical Basis.* Oxford
6035   University Press. Retrieved from https://global.oup.com/academic/product/atmospheric-
6036   radiation-9780195102918#.W9NLN4c8GC4.mendeley

6037   Govindasamy, B., and K. Caldeira (2000), Geoengineering Earth's radiation balance to mitigate
6038   CO2-induced climate change. *Geophysical Research Letters*, 27, 2141-2144.

6039   Granier, C., K. P. Shine, J. S. Daniel, I. E. Hansen, S. Lal, and F. Stordal, 1999: Climate Effects
6040   of Ozone and Halocarbon Changes. *Scientific Assessment of Ozone Depletion: 1998*, D.L.
6041   Albritton, P.J. Aucamp, G. Mégie, and R.T. Watson, Eds.

6042   Granier, C., and Coauthors, 2011: Evolution of anthropogenic and biomass burning emissions of
6043   air pollutants at global and regional scales during the 1980–2010 period. *Clim. Change*,
6044   **109**, 163–190, doi:10.1007/s10584-011-0154-1. http://dx.doi.org/10.1007/s10584-011-
6045   0154-1.

6046   Graf, H.-F., J. Feichter and B. Langmann, 1997: Volcanic sulfur emissions: Estimates of source
6047   strength and its contribution to the global sulfate distribution. J. Geophys. Res., 102,
6048   10727−10738.

6049 Graham, B., Guyon, P., Maenhaut, W., Taylor, P. E., Ebert, M., Matthias-Maser, S., Mayol-
6050   Bracero, O. L., Godoi, R. H. M., Artaxo, P., Meixner, F. X., Moura, M. A. L., Rocha, C. H.
6051   E., VanGrieken, R., Globsky, M. M., Flagan, R. C. and Andreae, M. O.: Composition and
6052   diurnal variability of the natural Amazonian aerosol, J. Geophys. Res., 108(D24), 4765,
6053   doi:10.1029/2003JD004049, 2003.

6054 Grattan, J., Brayshay, M., Sadler, J. (1998), Modelling the distal impacts of past volcanic gas
6055   emissions: evidence of Europewide environmental impacts from gases emitted during the
6056   eruption of Italian and Icelandic volcanoes in 1783. Quaternaire 9, 25– 35.

6057 Gray, L. J., et al., 2010: Solar influences on climate, Rev. Geophys., 48, RG4001,
6058   doi:10.1029/2009RG000282.

6059 Gregory, J. M., and Coauthors, 2004: A new method for diagnosing radiative forcing and climate
6060   sensitivity. Geophys. Res. Lett., 31, L03205, doi:10.1029/2003gl018747.

6061 ——, C. D. Jones, P. Cadule, and P. Friedlingstein, 2009: Quantifying Carbon Cycle Feedbacks.
6062   J. Clim., 22, 5232–5250, doi:10.1175/2009JCLI2949.1.
6063   https://doi.org/10.1175/2009JCLI2949.1.

6064 Greene, M. T. (2000), High achiever, Nature, 407, pp 947.

6065 Gregory, J. M., Bi, D., Collier, M. A., Dix, M. R., Hirst, A. C., Hu, A., Huber, M., Knutti, R.,
6066   Marsland, S. J., Meinshausen, M., Rashid, H. A., Rotstayn, L. D., Schurer, A. and Church, J.
6067   A. (2013), Climate models without pre-industrial volcanic forcing underestimate historical
6068   ocean thermal expansion. Geophysical Research Letters, 40 (8). pp. 1600-1604. ISSN 0094-
6069   8276 doi: https://doi.org/10.1002/grl.50339

6070 Gruner, P., Kleinert, H., (1927), Die dammerung erscheinen, Probl. Kosm. Phys., 10, 1-113.

6071 Gruber, S., Blahak, U., Haenel, F., Kottmeier, C., Leisner, T., Muskatel, H., Storelvmo, T. ,
6072   Vogel, B., 2019: A process study on thinning of Arctic winter cirrus clouds with high-
6073   resolved ICON-ART simulations. *J. Geophys. Res.*, **Under revi**.

6074 Guenther, A., Karl, T., Harley, P., Wiedinmyer, C., Palmer, P. I. and Geron, C.: Estimates of
6075   global terrestrial emissions using MEGAN (Model of Emissions of Gases and Aerosols

6076   from Nature), Atmos. Chem. Phys., 6, 3181–3210, doi:10.5194/acp-6-3181-2006, 2006.

6077 Guo, S., G. J. S. Bluth, W. I. Rose, I. M. Watson, and A. J. Prata (2004a), Re-evaluation of SO2
6078   release of the 15 June 1991 Pinatubo eruption using ultraviolet and infrared satellite sensors,
6079   Geochem. Geophys. Geosyst., 5, Q04001, doi:10.1029/2003GC000654.

6080 Guo, S., W. I. Rose, G. J. S. Bluth, and I. M. Watson (2004b), Particles in the great Pinatubo
6081   volcanic cloud of June 1991: The role of ice, Geochem. Geophys. Geosyst., 5, Q05003,
6082   doi:10.1029/2003GC000655.

6083

6084 Haagen-Smit, A. J., 1952: Chemistry and Physiology of Los Angeles Smog. *Ind. Eng. Chem.*, **44**,
6085   1342–1346.

6086 Haberreiter, M., M. Scholl, T. D. de Wit, M. Kretzschmar, S. Misios, K. Tourpali, and W.
6087   Schmutz, 2017: A new observational solar irradiance composite, J Geophys Res-Space,
6088   122(6), 5910-5930, doi: 10.1002/2016ja023492.

6089 Hameed, S., and R. D. Cess, 1983: Impact of a global warming on biospheric sources of methane
6090   and its climatic consequences. *Tellus B*, **35B**, 1–7, doi:doi:10.1111/j.1600-
6091   0889.1983.tb00001.x. https://doi.org/10.1111/j.1600-0889.1983.tb00001.x.

6092 Hameed, S., R. D. Cess, and J. S. Hogan, 1980: Response of the global climate to changes in
6093   atmospheric chemical composition due to fossil fuel burning. *J. Geophys. Res. Ocean.*, **85**,
6094   7537–7545, doi:doi:10.1029/JC085iC12p07537. https://doi.org/10.1029/JC085iC12p07537.

6095 Hamill, P., E. J. Jensen, P. B. Russell, J. J. Bauman (1997), The life cycle of stratospheric aerosol
6096   particles, Bull. Amer. Meteorol. Soc., 7, 1395-1410.

6097 Hamilton, D. S., Hantson, S., Scott, C. E., Kaplan, J. O., Pringle, K. J., Nieradzik, L. P., Rap, A.,
6098   Folberth, G. A., Spracklen, D. V. and Carslaw, K. S.: Reassessment of pre-industrial fire
6099   emissions strongly affects anthropogenic aerosol forcing, Nat. Commun., 9(1),
6100   doi:10.1038/s41467-018-05592-9, 2018.

6101 Hampson, J., 1965: Chemiluminescent emission observed in the stratosphere and mesosphere.

Les Problems Meteorologiques de la Stratosphere et de la Mesosphere, Presses Universitaires de France, Paris, p. 393.

Hartmann, D. L., Klein Tank, A., Alexander, L., Bronnimann, S., Charabi, Y., Dentener, F. J., Easterling, D. R., Kaplan, A., Soden, B., Thorne, P., Wild, M. and Zhai, P. M.: Observations: Atmosphere and Surface, in Climate Change 2013: The Physical Science Basis. Contribution of Working Group I to the Fifth Assessment Report of the Intergovernmental Panel on Climate Change, pp. 159–218., 2013.

Haug, G. H., D. Günther, L. C. Peterson, D. M. Sigman, K. A. Hughen, and B. Aeschlimann, 2003: Climate and the collapse of Maya Civilization, Science, 299, 1731-1735

Han, Q., Rossow, W. B., & Lacis, A. A. (1994). Near-global survey of effective droplet radii in liquid water clouds using ISCCP data. *Journal of Climate*, *7*(4), 465-497.

Hansen, J. E., Sato, M., Lacis, A., Ruedy, R., Tegen, I., & Matthews, E. (1998). Climate forcings in the industrial era. *Proceedings of the National Academy of Sciences*, *95*(22), 12753-12758.

Hansen, J., and Coauthors, 1997a: Forcings and chaos in interannual to decadal climate change. *J. Geophys. Res. Atmos.*, **102**, 25679–25720, doi:doi:10.1029/97JD01495. https://doi.org/10.1029/97JD01495.

——, M. Sato, and R. Ruedy, 1997b: Radiative forcing and climate response. *J. Geophys. Res. Atmos.*, **102**, 6831–6864, doi:doi:10.1029/96JD03436. https://doi.org/10.1029/96JD03436.

Hansen, J., 2002: Climate forcing in Goddard Institute for Space Studies SI2000 simulations. *J Geophys Res*, 107, 4347.

Hansen, J. E., A. Lacis, and S. A. Lebedeff, 1982: In Carbon dioxide review 1982, W. Clark, Ed., Oxford University Press, Clarendon, England, 284–289.

Hansen, J. E., and Andrew A. Lacis, 1990: Sun and dust versus greenhouse gases: an assessment of their relative roles in global climate change. Nature volume 346, pages 713–719.

6127 Hansen, J., A. Lacis, D. Rind, G. Russell, P. Stone, I. Fung, R. Ruedy, and J. Lerner, 1984:

6128   Climate sensitivity: Analysis of feedback mechanisms. In *Climate Processes and Climate*

6129   *Sensitivity*. J.E. Hansen and T. Takahashi, Eds., AGU Geophysical Monograph 29, Maurice

6130   Ewing Vol. 5. American Geophysical Union, pp. 130-163. 10.1029/GM029.

6131 Hansen, J., A. Lacis, R. Ruedy, M. Sato, and H. Wilson, 1993: How Sensitive Is the Worlds

6132   Climate. *Natl. Geogr. Res. Explor.*, **9**, 142–158.

6133 ——, M. Sato, R. Ruedy, A. Lacis, and V. Oinas, 2000: Global warming in the twenty-first

6134   century: An alternative scenario. *Proc. Natl. Acad. Sci. U. S. A.*, **97**, 9875–9880.

6135 Hansen, J., D. Johnson, A. Lacis, S. Lebedeff, P. Lee, D. Rind, and G. Russell, 1981: Climate

6136   Impact of Increasing Atmospheric Carbon Dioxide. Science, 213, 957 LP-966,

6137   doi:10.1126/science.213.4511.957.

6138   http://science.sciencemag.org/content/213/4511/957.abstract.

6139 Hansen, J., D. Johnson, A. Lacis, S. Lebedeff, P. Lee, D. Rind, and G. Russell, 1981: Climate

6140   Impact of Increasing Atmospheric Carbon Dioxide. *Science*, 213, 957 LP-966,

6141   doi:10.1126/science.213.4511.957. http://science.sciencemag.org/content/213/4511/957.

6142 ——, I. Fung, A. Lacis, D. Rind, S. Lebedeff, R. Ruedy, G. Russell, and P. Stone, 1988: Global

6143   climate changes as forecast by Goddard Institute for Space Studies three-dimensional

6144   model. J. Geophys. Res. Atmos., 93, 9341–9364, doi:10.1029/JD093iD08p09341.

6145   https://doi.org/10.1029/JD093iD08p09341.

6146 ——, A. Lacis, R. Ruedy, M. Sato, and H. Wilson, 1993: How Sensitive Is the Worlds Climate.

6147   Natl. Geogr. Res. Explor., 9, 142–158.

6148 ——, M. Sato, and R. Ruedy, 1997: Radiative forcing and climate response. J. Geophys. Res.,

6149   102, 6831–6864.

6150 ——, and Coauthors, 2005: Efficacy of climate forcings. J. Geophys. Res., 110, D18104,

6151   doi:10.1029/2005JD005776.

6152 Harshvardhan (1979), Perturbation of the Zonal Radiation Balance by a Stratospheric Aerosol

6153   Layer, J. Atmos. Sci., 36, 1274-1285.

6154   Hauglustaine, D. A., C. Granier, G. P. Brasseur, and G. Mégie, 1994: The importance of
6155   atmospheric chemistry in the calculation of radiative forcing on the climate system. J.
6156   Geophys. Res. Atmos., 99, 1173–1186, doi:10.1029/93JD02987.
6157   https://doi.org/10.1029/93JD02987.

6158   Haywood, J.M., and Shine, K.P., 1995. The effect of anthropogenic sulfate and soot aerosol on
6159   the clear sky planetary radiation budget. Geophys. Res. Letts., 22, 5, 603-606.

6160   Haywood, J.M. and Shine, K.P., 1997. Multi-spectral Calculations of the Direct Radiative
6161   Forcing of Tropospheric Sulfate and Soot Aerosols using a Column Model. Quart. J. of the
6162   Roy. Meteorol. Soc., 123, 1907-1930.

6163   Haywood, J.M., Roberts, D.L., Slingo, A., Edwards, J.M. and Shine, K.P., 1997. General
6164   Circulation Model Calculations of the Direct Radiative Forcing by Anthropogenic Sulfate
6165   and Fossil-Fuel Soot Aerosol. J. Clim., 10, 1562-1577.

6166   Haywood, J.M. and Ramaswamy, V., 1998. Global sensitivity studies of the direct radiative
6167   forcing of sulfate and black carbon aerosol. J. Geophys. Res., 103, 6043-6058.

6168   Haywood, J.M., Ramaswamy, V., and Soden, B.J., 1999. Tropospheric aerosol climate forcing in
6169   clear-sky satellite observations over the oceans. Science, 283, 1299-1305.

6170   Haywood, J.M., Francis, P.N., Glew, M.D., Dubovik, O., and Holben, B.N, Comparison of
6171   aerosol size distributions, radiative properties, and optical depths determined by aircraft
6172   observations and Sun photometers during SAFARI-2000. *J. Geophys. Res.,* 108(D13),
6173   8471, doi:10.1029/2002JD002250, 2003.

6174   Haywood, J. M., M. D. Schwarzkopf, and V. Ramaswamy, 1998: Estimates of radiative forcing
6175   due to modeled increases in tropospheric ozone. *J. Geophys. Res. Atmos.*, **103**, 16999–
6176   17007, doi:doi:10.1029/98JD01348. https://doi.org/10.1029/98JD01348.

6177   Haywood, J. M., Jones, A., Bellouin, N. & Stephenson, D. Asymmetric forcing from stratospheric
6178   aerosols impacts Sahelian rainfall. *Nat. Clim. Change* **3,** 660-665 (2013).

6179   Haywood, J. M., A. Jones, N. Bellouin, and D. Stephenson (2013), Asymmetric forcing from
6180   stratospheric aerosols impacts Sahelian rainfall. *Nat Clim Change*, 3, 660-665.

6181 Haywood, J. M., A. Jones, and G. S. Jones, 2014: The impact of volcanic eruptions in the period
6182   2000–2013 on global mean temperature trends evaluated in the HadGEM2-ES climate model.
6183   *Atmospheric Science Letters*, 15, 92-96.

6184 Haywood, J. M., and K. P. Shine, 1995: The effect of anthropogenic sulfate and soot aerosol on
6185   the clear-sky planetary radiation budget. Geophys. Res. Lett., 22, 603–606.

6186 Hauglustaine, D. A., and G. P. Brasseur, 2001: Evolution of tropospheric ozone under
6187   anthropogenic activities and associated radiative forcing of climate. *J. Geophys. Res.*, **106**,
6188   32337–32360.

6189 Hauglustaine, D. A., C. Granier, and G. P. Brasseur, 1995: Impact of increased methane
6190   emissions on the atmospheric composition and related radiative forcing on the climate
6191   system. *Atmospheric Ozone as a Climate Gas, NATO-ASI Series*, W.-C. Wang and I.
6192   Isaksen, Eds., Springer-Verlag, Berlin, Germany, 189–203.

6193 Heald, C. and Spracken, D.: Land use change impacts on air quality and climate, Chem. Rev.,
6194   225(10), 4476–4496; DOI: 10.1021/cr500446g, 2015.

6195 Hegerl, G.C., et al., 1996: Detecting greenhouse-gas-induced climate change with an optimal
6196   fingerprint method. *J. Clim.*, **9**, 2281–2306.

6197 Hegerl, G.C., et al., 1997: Multi-fingerprint detection and attribution of greenhouse-gas and
6198   aerosol-forced climate change. *Clim. Dyn.*, **13**, 613–634.

6199 Hegerl, G. C. *et al.* Challenges in quantifying changes in the global water cycle. *Bull. Am.*
6200   *Meteorol. Soc.* **96,** 1097-1115 (2015).

6201 Heckendorn, P., and Coauthors (2009), The impact of geoengineering aerosols on stratospheric
6202   temperature and ozone. *Environ Res Lett*, 4, 045108.

6203 Hegglin, M. I., and T. G. Shepherd, 2009: Large climate-induced changes in ultraviolet index
6204   and stratosphere-to-troposphere ozone flux. *Nat. Geosci*, **2**, 687–691,
6205   doi:http://www.nature.com/ngeo/journal/v2/n10/suppinfo/ngeo604_S1.html.
6206   http://dx.doi.org/10.1038/ngeo604.

6207   Hergesell, M., 1919: Die Strahlung der Atmosphäre unter Zungrundlegung bon Lindeberger

6208   Temperatur: und Feuchtigkeits Messungen. *Die Arbeiten des Preusslichen Aero-*

6209   *nautischen Observatoriums bei Lindenberg,* Vol. 13, Braunschweig, Germany, Firedr.

6210   Vieweg and Sohn, 1-24.

6211   Herring, W. S., and T. R. Borden, Jr., 1965: Mean distributions of ozone density over

6212   North America, 1963-1964. Environ- mental Research Papers, No. 162. AFCRL 65-

6213   913, Air Force Cambridge Research Laboratories, Bedford, Mass., 19 pp.

6214   Hickey, J. R., Stowe, L. L., Jacobowitz, H., Pellegrino, P., Maschhoff, R. H., House, F., and T.

6215   H. Vonder Haar, 1980: Initial Solar Irradiance Determinations from Nimbus 7 Cavity

6216   Radiometer Measurements, Science, 208, 281-283, DOI: 10.1126/science.208.4441.281

6217   Hill, S. A., Ming, Y. & Held, 2015: I. M. Mechanisms of forced tropical meridional energy flux

6218   change. *J. Clim.* **28**, 1725–1742

6219   Hill, S., and Y. Ming, 2012: Nonlinear climate response to regional brightening of tropical

6220   marine stratocumulus. *Geophys. Res. Lett.*, doi:10.1029/2012GL052064.

6221   Hodnebrog Ø, Etminan M, Fuglestvedt JS, Marston G, Myhre G, Nielsen CJ, Shine KP,

6222   Wallington TJ 2013: Global Warming Potentials and Radiative Efficiencies of Halocarbons

6223   and Related Compounds: A Comprehensive Review Reviews of Geophysics 51:300-378

6224   10.1002/rog.20013.

6225   Hoesly, R. M., and Coauthors, 2017: Historical (1750–2014) anthropogenic emissions of reactive

6226   gases and aerosols from the Community Emission Data System (CEDS). *Geosci. Model*

6227   *Dev. Discuss.*, **2017**, 1–41, doi:10.5194/gmd-2017-43. [http://www.geosci-model-dev-](http://www.geosci-model-dev-discuss.net/gmd-2017-43/)

6228   [discuss.net/gmd-2017-43/](http://www.geosci-model-dev-discuss.net/gmd-2017-43/).

6229   Hofmann, D. J., J. M. Rosen, T. J. Pepin, and R. G. Pinnick (1975), Stratospheric aerosol

6230   measurements I: Time variations at northern midlatitudes, J. Atmos. Sci., 32, 1446–1456.

6231   Holben, Brent N., T. F Eck, I Slutsker, D. Tanre, J. P. Buis, A. Setzer, E. Vermote et al.

6232   "AERONET—A federated instrument network and data archive for aerosol

6233   characterization." *Remote sensing of environment* 66, no. 1 (1998): 1-16.

6234 Holton, J.R., P. H. Haynes, M. E.. McIntyre, A. R. Douglass, R. B. Rood, L. Pfister (1995),
6235   Stratosphere-troposphere exchange, Rev. Geophys., 33, 403-439.

6236 Hood, L. L., S. Misios, D. M. Mitchell, E. Rozanov, L. J. Gray, K. Tourpali, K. Matthes, H.
6237   Schmidt, G. Chiodo, R. Thiéblemont, D. Shindell, and A. Krivolutsky, 2015: Solar signals
6238   in CMIP-5 simulations: the ozone response, Quarterly Journal Roy. Meteor. Soc., 141, I692,
6239   2670-2689, Part A DOI10.1002/qj.2553.

6240 Höpfner, M., Glatthor, N., Grabowski, U., Kellmann, S., Kiefer, M., Linden et al. (2013), Sulfur
6241   dioxide (SO2) as observed by MIPAS/Envisat: temporal development and spatial distribution
6242   at 15–45 km altitude, Atmos. Chem. Phys., 13, 10405 − 10423, doi:10.5194/acp-13-10405-
6243   2013.

6244 Höpfner, M., Boone, C. D., Funke, B., Glatthor, N., Grabowski, U., Günther et al. (2015), Sulfur
6245   dioxide (SO2) from MIPAS in the upper troposphere and lower stratosphere 2002 − 2012,
6246   Atmos. Chem. Phys., 15, 7017 − 7037, doi:10.5194/acp-15-7017-2015.

6247 Hough, A. M., and R. G. Derwent, 1990: Changes in the global concentration of tropospheric
6248   ozone due to human activities. *Nature*, **344**, 645–648.

6249 Houghton, J. T., 1963: Absorption in the stratosphere by some water vapor lines in the v_2
6250   band. *Quart. J. Roy. Meteor. Soc.,* **89,** 332-338.

6251 Houghton, R.: Interactions between land-use change and climate-carbon cycle feedbacks, Curr.
6252   Clim. Chang. Reports, 4(2), 115–127, 2018.

6253 Howard, J. N., D. L. Burch and D. Williams, 1955: Near-infrared transmission through
6254   synthetic atmosphere. Geophysics Research Papers, No. 40, Air Force Cambridge
6255   Research Center, AFCRC-TR-55-213, 214 pp.

6256 Hoyt, D. V., and K. H. Schatten, 1997: The Role of the Sun in Climate Change, Oxford
6257   University Press.

6258 Hoyt, D. V., 1979. The Smithsonian Astrophysical Observatory solar constant program. Revs.
6259   Geophys. and Space Physics, 17, 427-458.

6260   Hoyt, D. V., and K. H. Schatten, 1997: The Role of the Sun in Climate Change, Oxford
6261   University Press.

6262   Hudson, H.S., Silva, S., Woodard, M. et al., 1982: The effects of sunspots on solar irradiance,
6263   Solar Physics 76: 211. https://doi.org/10.1007/BF00170984

6264   Hulburt, E. O. (1931). The temperature of the lower atmosphere of the earth. *Physical Review*,
6265   *38*(10), 1876–1890. http://doi.org/10.1103/PhysRev.38.1876

6266   Humphreys, W. J. (1913), Volcanic dust and other factors in the production of climatic changes,
6267   and their possible relation to ice gases, J. Franklin Inst., Aug. 131-172.

6268   Humphreys, W. J. (1940), Physics of the Air, McGraw-Hill, New York, 676 pp.

6269   Huneeus, N., Schulz, M., Balkanski, Y., Griesfeller, J., Prospero, M. J., Kinne, S., ... & Diehl, T.
6270   (2011). Global dust model intercomparison in AeroCom phase I. *Atmospheric Chemistry*
6271   *and Physics*, *11*, 7781-7816.

6272   Husar, R. B., Prospero, J. M., & Stowe, L. L. (1997). Characterization of tropospheric aerosols
6273   over the oceans with the NOAA advanced very high resolution radiometer optical thickness
6274   operational product. *Journal of Geophysical Research: Atmospheres*, *102*(D14), 16889-
6275   16909.

6276   Husson, N. B. Bonnet, N.A. Scott, & A. Chédin. (1992). Management and study of
6277   spectroscopic information: the GEISA program. *J. Quant. Spectrosc. Rad. Trans., 48*, 509-
6278   518. https://doi.org/10.1016/0022-4073(92)90116-L

6279   Hsu, N. C., Tsay, S. C., King, M. D., & Herman, J. R. (2006). Deep blue retrievals of Asian
6280   aerosol properties during ACE-Asia. *IEEE Transactions on Geoscience and Remote*
6281   *Sensing*, *44*(11), 3180-3195.

6282   Hwang, Y.-T., Frierson, D. M. W. & Kang, S. M. Anthropogenic sulfate aerosol and the southward
6283   shift of tropical precipitation in the late 20th century. *Geophys. Res. Lett.* **40,** 2845-2850
6284   (2013).

6285

Iacobellis, S. F., Frouin, R., & Somerville, R. C. (1999). Direct climate forcing by biomass-burning aerosols: Impact of correlations between controlling variables. *Journal of Geophysical Research: Atmospheres*, *104*(D10), 12031-12045.

I.E. Gordon, L.S. Rothman, C. Hill, R.V. Kochanov, Y. Tan, P.F. Bernath, M. Birk, V. Boudon, A. Campargue, K.V. Chance, B.J. Drouin, J.-M. Flaud, R.R. Gamache, J.T. Hodges, D. Jacquemart, V.I. Perevalov, A. Perrin, K.P. Shine, M.-A.H. Smith, J. Tennyson, G.C. Toon, H. Tran, V.G. Tyuterev, A. Barbe, A.G. Császár, V.M. Devi, T. Furtenbacher, J.J. Harrison, J.-M. Hartmann, A. Jolly, T.J. Johnson, T. Karman, I. Kleiner, A.A. Kyuberis, J. Loos, O.M. Lyulin, S.T. Massie, S.N. Mikhailenko, N. Moazzen-Ahmadi, H.S.P. Müller, O.V. Naumenko, A.V. Nikitin, O.L. Polyansky, M. Rey, M. Rotger, S.W. Sharpe, K. Sung, E. Starikova, S.A. Tashkun, J. Vander Auwera, G. Wagner, J. Wilzewski, P. Wcisło, S. Yu, E.J. Zak, The HITRAN2016 molecular spectroscopic database, Journal of Quantitative Spectroscopy and Radiative Transfer, Volume 203, 2017, Pages 3-69, ISSN 0022-4073, https://doi.org/10.1016/j.jqsrt.2017.06.038.

Iles, C. E., G. C. Hegerl, A. P. Schurer, and X. Zhang (2013), The effect of volcanic eruptions on global precipitation, J. Geophys. Res., 118, 8770-8786, doi:10.1002/JGRD.50678.

IPCC, Annex II: Climate System Scenario Tables . *Climate Change 2013: The Physical Science Basis. Contribution of Working Group I to the Fifth Assessment Report of the Intergovernmental Panel on Climate Change*, T.F. Stocker D. Qin, G.-K. Plattner, M. Tignor, S.K. Allen, J. Boschung, A. Nauels, Y. Xia, V. Bex and P.M. Midgley, Ed., Cambridge University Press, Cambridge, United Kingdom and New York, NY, USA, 1395–1446.

Isaksen, I. S. A., and Ø. Hov, 1987: Calculation of trends in the tropospheric concentration of O3, OH, CO, CH4 and NOx. *Tellus B*, **39B**, 271–285, doi:doi:10.1111/j.1600-0889.1987.tb00099.x. https://doi.org/10.1111/j.1600-0889.1987.tb00099.x.

Isaksen, I. S. A., J. S. Fuglestvedt, Y.-P. Lee, C. Johnson, R. Atkinson, J. Lelieveld, H. Sidebottom, and A. M. Thompson, 1991: Tropospheric Processes: Observations and interpretation. *Scientific Assessment of Ozone Depletion: 1991*, D.L. Albritton, R.T. Watson, S. Solomon, R.F. Hampson, and F. Ormond, Eds.

6315 ——, V. Ramaswamy, H. Rodhe, and T. M. L. Wigley, 1992: Radiative Forcing of Climate.

6316 *Climate Change 1992: The Supplementary Report to the IPCC Scientific Assessment*, J.T.

6317 Houghton, B.A. Callander, and S.K. Varney, Eds., Cambridge University Press, Cambridge,

6318 U.K., New York, NY, USA, Victoria, Australia.

6319 Isaksen, I. S. A., and Coauthors, 2009: Atmospheric composition change: Climate-Chemistry

6320 interactions. *Atmos. Environ.*, **43**, 5138–5192, doi:10.1016/j.atmosenv.2009.08.003.

6321 http://www.sciencedirect.com/science/article/pii/S1352231009006943.

6322 Isaksen, I., V. Ramaswamy, H. Rodhe, and T. M. L. Wigley, 1992: Radiative forcing of climate.

6323 Climate Change 1992: The Supplementary Report to the IPCC Scientific Assessment, 47–

6324 67.

6325 Iversen,T.,A. Kirkevåg,J. E. Kristjansson,and Ø. Seland,2000:Climate effects of sulfate and

6326 black carbon estimated in a global climate model. In Air Pollution Modeling and its

6327 Application XIV, S.-E. Gryning and F.A. Schiermeier,Eds. Kluwer/Plenum Publishers,New

6328 York, 335-342.

6329

6330 Jacquinet-Husson, N., R. Armante, N.A. Scott, A. Chédin, L. Crépeau, C. Boutammine, A.

6331 Bouhdaoui, C. Crevoisier, V. Capelle, C. Boonne, N. Poulet-Crovisier, A. Barbe, D. Chris

6332 Benner, V. Boudon, L.R. Brown, J. Buldyreva, A. Campargue, L.H. Coudert, V.M. Devi,

6333 M.J. Down, B.J. Drouin, A. Fayt, C. Fittschen, J.-M. Flaud, R.R. Gamache, J.J. Harrison, C.

6334 Hill, Ø. Hodnebrog, S.-M. Hu, D. Jacquemart, A. Jolly, E. Jiménez, N.N. Lavrentieva, A.-

6335 W. Liu, L. Lodi, O.M. Lyulin, S.T. Massie, S. Mikhailenko, H.S.P. Müller, O.V.

6336 Naumenko, A. Nikitin, C.J. Nielsen, J. Orphal, V.I. Perevalov, A. Perrin, E. Polovtseva, A.

6337 Predoi-Cross, M. Rotger, A.A. Ruth, S.S. Yu, K. Sung, S.A. Tashkun, J. Tennyson, Vl.G.

6338 Tyuterev, J. Vander Auwera, B.A. Voronin, & A. Makie. (2016). The 2015 edition of the

6339 GEISA spectroscopic database, *Journal of Molecular Spectroscopy*, *327*, 31-72.

6340 https://doi.org/10.1016/j.jms.2016.06.007.

6341 Jacob, D. J., and D. A. Winner, 2009: Effect of climate change on air quality. *Atmos. Environ.*,

6342 **43**, 51–63, doi:10.1016/j.atmosenv.2008.09.051.

http://www.sciencedirect.com/science/article/B6VH3-4TNWH49-
4/2/30b98e804a7d8cab841c22038bc0c264.

Jacobson, M. Z. (2001). Global direct radiative forcing due to multicomponent anthropogenic
and natural aerosols. *Journal of Geophysical Research: Atmospheres*, *106*(D2), 1551-1568.

Jacobson, M. Z., and J. E. Ten Hoeve, 2012: Effects of urban surfaces and white roofs on global
and regional climate. *J. Clim.*, doi:10.1175/JCLI-D-11-00032.1.

Jethva, H., Torres, O., Remer, L. A., & Bhartia, P. K. (2013). A color ratio method for
simultaneous retrieval of aerosol and cloud optical thickness of above-cloud absorbing
aerosols from passive sensors: Application to MODIS measurements. *IEEE Transactions on
Geoscience and Remote Sensing*, *51*(7), 3862-3870.

Jickells, T. D., An, Z. S., Andersen, K. K., Baker, A. R., Bergametti, C., Brooks, N., Cao, J. J.,
Boyd, P. W., Duce, R. A., Hunter, K. A., Kawahata, H., Kubilay, N., LaRoche, J., Liss, P.
S., Mahowald, N., Prospero, J. M., Ridgwell, A. J., Tegen, I. and Torres, R.: Global iron
connections between desert dust, ocean biogeochemistry, and climate, Science (80-.).,
308(5718), doi:10.1126/science.1105959, 2005.

Jimenez, JL, et al. Evolution of organic aerosols in the atmosphere. Science 326, 1525-1529,
2009,

Johnson, B. T., Shine, K. P., & Forster, P. M. (2004). The semi-direct aerosol effect: Impact of
absorbing aerosols on marine stratocumulus. *Quarterly Journal of the Royal Meteorological
Society*, *130*(599), 1407-1422.

Jones, A., Roberts, D. L. and Slingo, A. 1994. A climate model study of the indirect radiative
forcing by anthropogenic sulfate aerosols. Nature 370, 450–453.

Jones, A., Roberts, D. L., Woodage, M. J., and Johnson, C. E., 2001. Indirect sulfate aerosol
forcing in a climate model with an interactive sulfur cycle, *J. Geophys. Res*., **106**, 20293-
20310, doi:10.1029/2000JD000089

Jones, A., D. L. Roberts, and A. Slingo, 1994: A climate model study of indirect radiative
forcing by anthropogenic sulfate aerosols. Nature, 370, 450–453.

6370 A. Jones, J. Haywood, O. Boucher, B. Kravitz, and A. Robock, 2010: Geoengineering by
6371   stratospheric SO2 injection: results from the Met Office HadGEM2 climate model and
6372   comparison with the Goddard Institute for Space Studies ModelE; *Atmos. Chem. Phys.*, 10,
6373   5999–6006, doi:10.5194/acp-10-5999-2010

6374

6375 Jones, A. C., J. M. Haywood, and A. Jones, 2016: Climatic impacts of stratospheric
6376   geoengineering with sulfate, black carbon and titania injection. *Atmos. Chem. Phys.*, **16**,
6377   2843–2862, doi:10.5194/acp-16-2843-2016. https://www.atmos-chem-
6378   phys.net/16/2843/2016/ (Accessed December 20, 2018).

6379 Jones, Alexandra L., D Feldman, Stuart Freidenreich, David J Paynter, V Ramaswamy, W D
6380   Collins, and R Pincus, 2017: **A New Paradigm for Diagnosing Contributions to Model**
6381   **Aerosol Forcing Error**. *Geophysical Research Letters*, **44(23)**,
6382   DOI:10.1002/2017GL075933

6383 Johnson, C., J. Henshaw, and G. Mclnnes, 1992: Impact of aircraft and surface emissions of
6384   nitrogen oxides on tropospheric ozone and global warming. *Nature*, **355**, 69.
6385   https://doi.org/10.1038/355069a0.

6386 Johnson, C. E., and R. G. Derwent, 1996: Relative radiative forcing consequences of global
6387   emissions of hydrocarbons, carbon monoxide and NOx from human activities estimated
6388   with a zonally-averaged two-dimensional model. *Clim. Change*, **34**, 439–462.

6389 Johnston, H., 1971: Reduction of Stratospheric Ozone by Nitrogen Oxide Catalysts from
6390   Supersonic Transport Exhaust. *Science (80-.).*, **173**, 517–522.
6391   http://www.jstor.org/stable/1732244.

6392 Junge, C. E., 1962: Global ozone budget and exchange between stratosphere and troposphere.
6393   *Tellus*, **14**, 363–377, doi:doi:10.1111/j.2153-3490.1962.tb01349.x.
6394   https://doi.org/10.1111/j.2153-3490.1962.tb01349.x.

6395 Jungclaus, J. H., Bard, E., Baroni, M., Braconnot, P., Cao, J., Chini, L. P., et al., 2017: The
6396   PMIP4 contribution to CMIP6 - Part 3: the Last Millennium, scientific objective and

6397   experimental design for the PMIP4 past1000 simulations. Geoscientific Model

6398   Development, 10, 4005-4033. doi:10.5194/gmd-2016-278.

6399

6400   Kaplan, L. D. (1952). On the Pressure Dependence of Radiative Heat Transfer in the

6401   Atmosphere. *Journal of Meteorology*. http://doi.org/10.1175/1520-

6402   0469(1952)009<0001:OTPDOR>2.0.CO;2

6403   Kang, S., I. Held, D. Frierson, and M. Zhao, 2008: The response of the ITCZ to extratropical

6404   thermal forcing: Idealized slab ocean experiments with a GCM. J. Climate, 21(14), 3521-

6405   3532.

6406   Kaplan, L. D., 1960: The influence of carbon dioxide variations on the atmospheric heat

6407   balance. *Tellus*, **12,** 204-208.

6408   Kärcher, Bernd (2018) *Formation and Radiative Forcing of Contrail Cirrus.* Nature

6409   Communications, pp. 1-17. Nature Publishing Group. DOI: 10.1038/s41467-018-04068-0

6410   ISSN 2041-1723.

6411   Kaufman, Y. J., Tanre, D. and Boucher, O.: A satellite view of aerosols in the climate system,

6412   Nature, 419(6903), 215-223, 2002.

6413   Keeling, C. D., 1960: The concentration and isotopic abundances of carbon dioxide in the

6414   atmosphere. *Tellus*, 12, 2, 200-203.

6415   Keith, D. W., and H. Dowlatabadi, 1992: a serious look at geoengineering. *Eos, Trans. Am.*

6416   *Geophys. Union*, doi:10.1029/91EO00231.

6417

6418   Kiehl, J. T., T. L. Schneider, R. W. Portmann, and S. Solomon, 1999: Climate forcing due to

6419   tropospheric and stratospheric ozone. *J. Geophys. Res.*, **104**, 31239–31254.

6420   Kiehl, J.T. and B.A. Boville, 1988: The Radiative-Dynamical Response of a Stratospheric-

6421   Tropospheric General Circulation Model to Changes in Ozone. J. Atmos. Sci., 45, 1798–

6422   1817, https://doi.org/10.1175/1520-0469(1988)045<1798:TRDROA>2.0.CO;2

6423 Kiehl, J. T., and B. P. Briegleb, 1993: The relative roles of sulfate aerosols and greenhouse gases

6424 in climate forcing. Science (80-.)., 260, 311–314, doi:10.1126/science.260.5106.311.

6425 http://science.sciencemag.org/content/260/5106/311.abstract

6426 Kiehl, J. T., and B. P. Briegleb, 1993: The relative roles of sulfate aerosols and greenhouse gases

6427 in climate forcing. *Science (80-.).*, **260**, 311–314, doi:10.1126/science.260.5106.311.

6428 http://science.sciencemag.org/content/260/5106/311.abstract.

6429 Kiehl, J. T., & Briegleb, B. P. (1993). The relative roles of sulfate aerosols and greenhouse gases

6430 in climate forcing. *Science*, *260*(5106), 311-314.

6431 Kiehl, J. T., and H. Rodhe, Modeling geographical and seasonal forcing due to aerosols, in

6432 Proceedings of the Dahlem Workshop on Aerosol Forcing of Climate, edited by R. J.

6433 Chaffson and J. Heintzenberg, pp. 281-296, John Wiley, New York, 1995.

6434 Kirchner, I., G. Stenchikov, H. Graf, A. Robock, J. Antuña, 1999: Climate Model Simulation of

6435 Winter Warming and Summer Cooling Following the 1991 Mount Pinatubo Volcanic

6436 Eruption, *J. Geophys. Res.,* **104***,* 19,039-19,055.

6437 Kirtman, B., and Coauthors, 2013: Near-term Climate Change: Projections and Predictability.

6438 *Climate Change 2013: The Physical Science Basis. Contribution of Working Group I to the*

6439 *Fifth Assessment Report of the Intergovernmental Panel on Climate Change*, T.F. Stocker et

6440 al., Eds., Cambridge University Press, Cambridge, United Kingdom and New York, NY,

6441 USA.

6442 Kirschke, S., Bousquet, P., Ciais, P., Saunois, M., Canadell, J., Dlugokencky, E., Bergamashi, P.,

6443 Berman, D., Blake, D., Bruhwiler, L., Cameron-Smith, P., Castaldi, S., Chevalier, F., Feng,

6444 L., Fraser, A., Heimann, M., Hodson, E., Houweling, S., Josse, B., Fraser, P., Krummel, P.,

6445 Lamarque, J. F., Langenfelds, R., LeQuere, C., Naik, V., O'Doherty, S., Palmer, P., Pison,

6446 I., Plummer, D., Poulter, B., Prinn, R., Rigby, M., Ringeval, B., Santini, M., Schmidt, M.,

6447 Shindel, D., Simpson, I., Spahni, R., Steele, L., Strode, S., Sudo, K., Szopa, S., G.R., van

6448 der W., Voulgarakis, A., van Weele, M., Weiss, R., Williams, J. and Zeng, G.: Three

6449 decades of global methane sources and sinks, Nature-geoscience, 6, 813–823, 2013.

6450 Krasnopolsky, M. V., M.S. Fox-Rabinovitz, and D.V. Chalikov, 2005, New Approach to
6451   Calculation of Atmospheric Model Physics: Accurate and Fast Neural Network Emulation
6452   of Longwave Radiation in a Climate Model Monthly Weather Review, **133**., 1370-1383

6453 Kravitz, B., A. Robock, P. M. Forster, J. M. Haywood, M. G. Lawrence, and H. Schmidt, 2013:
6454   An overview of the Geoengineering Model Intercomparison Project (GeoMIP). *J. Geophys.*
6455   *Res. Atmos.*, doi:10.1002/2013JD020569.

6456 Kravitz, B., and Coauthors (2013), Climate model response from the Geoengineering Model
6457   Intercomparison Project (GeoMIP). *Journal of Geophysical Research-Atmospheres*, 118,
6458   8320-8332.

6459 Kremser, S., Thomason, L. W., von Hobe, M., Hermann, M., Deshler, T., Timmreck et al.:
6460   Stratospheric aerosol – Observations, processes, and impact on climate, Rev. Geophys., 54,
6461   278 – 335, doi:10.1002/2015RG000511, 2016.

6462 Krivova, N.A. and S. K. Solanki, 2008: Models of solar irradiance variations: Current status, J
6463   Astrophys Astron, 29: 151. https://doi.org/10.1007/s12036-008-0018-x

6464 Krivova, N. A., Vieira, L. E. A., and S. K. Solanki, 2010: Reconstruction of solar spectral
6465   irradiance since the Maunder minimum. J. Geophys. Res., 115, A12112,
6466   doi:10.1029/2010JA015431.

6467 Krueger, A. J., S. J. Schaefer, N. A. Krotkov, G. Bluth, and S. Barker (2000), Ultraviolet remote
6468   sensing of volcanic emissions. Remote sensing of active volcanism. *Geophys Monograph*,
6469   116, 25-43.

6470 Ko, M. K. W., and Coauthors, 1995: Model simulations of stratospheric ozone. *Scientific*
6471   *Assessment of Ozone Depletion: 1994*, D.L. Albritton, R.T. Watson, and P.J. Aucamp, Eds.

6472 Kopp, G. and G. Lawrence, 2005: The Total Irradiance Monitor (TIM): Instrument Design, Sol
6473   Phys, 230: 91. https://doi.org/10.1007/s11207-005-7446-4

6474 Kopp, G., and J. L. Lean, 2011: A new low value of Total Solar Irradiance: evidence and climate
6475   significance, Geophys. Res. Lett., 38, L01706, doi:10.1029/2010GL045777.

Kopp, G., N. Krivova, Chi-Ju Wu, and J. Lean, 2016: The impact of the revised sunspot record on solar irradiance reconstructions, Solar Phys., DOI 10.1007/s11207-016-0853-x

Kvalevåg, M. M., and G. Myhre, 2013: The effect of carbon-nitrogen coupling on the reduced land carbon sink caused by tropospheric ozone. *Geophys. Res. Lett.*, **40**, 3227–3231, doi:doi:10.1002/grl.50572. https://doi.org/10.1002/grl.50572.

Kristjánsson, J. E., H. Muri, and H. Schmidt, 2015: The hydrological cycle response to cirrus cloud thinning. *Geophys. Res. Lett.*, doi:10.1002/2015GL066795.

Kinne, S., Schulz, M., Textor, C., Guibert, S., Balkanski, Y., Bauer, S., Berntsen, E., Berglen, T.F., Boucher, O., Chin, M. and Collins, W., 2006. An AeroCom initial assessment–optical properties in aerosol component modules of global models. *Atmospheric Chemistry and Physics*, *6*, pp.1815-1834.

Koffi, B., Schulz, M., Bréon, F.M., Griesfeller, J., Winker, D., Balkanski, Y., Bauer, S., Berntsen, T., Chin, M., Collins, W.D. and Dentener, F., 2012. Application of the CALIOP layer product to evaluate the vertical distribution of aerosols estimated by global models: AeroCom phase I results. *Journal of Geophysical Research: Atmospheres*, *117*(D10).

Kloster, S., Mahowald, N. M., Randerson, J. T., Thornton, P. E., Hoffman, F. M., Levis, S., Lawrence, P. J., Feddema, J. J., Oleson, K. W. and Lawrence, D. M.: Fire dynamics during the 20th century simulated by the Community Land Model, Biogeosciences, 7(6), doi:10.5194/bg-7-1877-2010, 2010.

Kondratiev, K. Y., and H. I. Niilisk, 1960: On the question of carbon dioxide heat radiation in the atmosphere. *Geofts. Pura Appl., 46, 216-230.*

Koschmeider H. 1924. Therie der horizontalen sichtweite. Beitr. Phys. Freien Atmos. 12: 33–35. Langner, J. and H. Rodhe, J. Atmos. Chem. 13, 225 (1991)

Kotchenruther, R.A. and Hobbs, P.V., 1998. Humidification factors of aerosols from biomass burning in Brazil. *Journal of Geophysical Research: Atmospheres*, *103*(D24), pp.32081-32089.

6502   Kotchenruther, R.A., Hobbs, P.V. and Hegg, D.A., 1999. Humidification factors for atmospheric

6503   aerosols off the mid-Atlantic coast of the United States. *Journal of Geophysical Research:*

6504   *Atmospheres*, *104*(D2), pp.2239-2251.

6505   Kohfeld, K. E. and Harrison, S. P.: DIRTMAP: The geological record of dust, Earth Sci. Rev.,

6506   54, 81–114, 2001.

6507

6508   Lacis, A., 1985: Chlorofluorocarbons and stratospheric ozone. *Global Environmental Problems*,

6509   S.F. Singer, Ed., Paragon House, New York.

6510   Lacis, A. A., D. J. Wuebbles, and J. A. Logan, 1990: Radiative forcing of climate by changes in

6511   the vertical distribution of ozone. *J. Geophys. Res. Atmos.*, **95**, 9971–9981,

6512   doi:doi:10.1029/JD095iD07p09971. https://doi.org/10.1029/JD095iD07p09971.

6513   Lacis., A., J. Hansen, M. Sato (1992), Geophys. Res. lett., 19, No. 15, 1607-1610.

6514   Lacis, A. A., D. J. Wuebbles, and J. A. Logan, 1990: Radiative forcing of climate by changes in

6515   the vertical distribution of ozone. J. Geophys. Res. Atmos., 95, 9971–9981,

6516   doi:10.1029/JD095iD07p09971. http://dx.doi.org/10.1029/JD095iD07p09971

6517   Lambert, A., R. G. Grainger, J. J. Remedios, C. D. Rodgers, M. Corney, and F. W. Taylor (1993),

6518   Measurements of the evolution of the Mt. Pinatubo aerosol cloud by ISAMS, Geophys. Res.

6519   Lett., 20(12), 1287–1290, doi:10.1029/93GL00827.

6520   Lamarque, J. F., and Coauthors, 2010: Historical (1850–2000) gridded anthropogenic and

6521   biomass burning emissions of reactive gases and aerosols: methodology and application.

6522   *Atmos. Chem. Phys.*, **10**, 7017–7039, doi:10.5194/acp-10-7017-2010. http://www.atmos-

6523   chem-phys.net/10/7017/2010/.

6524   ——, and Coauthors, 2013: The Atmospheric Chemistry and Climate Model Intercomparison

6525   Project (ACCMIP): overview and description of models, simulations and climate

6526   diagnostics. *Geosci. Model Dev.*, **6**, 179–206, doi:10.5194/gmd-6-179-2013.

6527   http://www.geosci-model-dev.net/6/179/2013/.

6528 Lamarque, J.-F., Bond, T. C., Eyring, V., Granier, C., Heil, A., Klimont, Z., Lee, D., Liousse, C.,
6529   Mieville, A., Owen, B., Schultz, M. G., Shindell, D., Smith, S. J., Stehfest, E., Van
6530   Aardenne, J., Cooper, O. R., Kainuma, M., Mahowald, N., McConnell, J. R., Naik, V.,
6531   Riahi, K. and Van Vuuren, D. P.: Historical (1850-2000) gridded anthropogenic and
6532   biomass burning emissions of reactive gases and aerosols: Methodology and application,
6533   Atmos. Chem. Phys., 10(15), doi:10.5194/acp-10-7017-2010, 2010.

6534 Lamarque, J. F., Kyle, P. P., Meinshausen, M., Riahi, K., Smith, S. J., van Vuuren, D. P.,
6535   Conley, A. J. and Vitt, F.: Global and regional evolution of short-lived radiatively-active
6536   gases and aerosols in the Representative Concentration Pathways, Clim. Change, 109(1),
6537   191–212, doi:10.1007/s10584-011-0155-0, 2011.

6538 Langley, S.P. 1884. Researches on solar heat and its absorption by the Earth's atmosphere. A
6539   report of the Mount Whitney Expedition. Professional Papers of the Signal Service, No. 15,
6540   Government Printing office, Washington, DC.

6541 Lawrence, D. M., Hurtt, G. C., Arneth, A., Brovkin, V., Calvin, K. V., Jones, A. D., Jones, C. D.,
6542   Lawrence, P. J., Noblet-Ducoudré, N. De, Pongratz, J., Seneviratne, S. I. and Shevliakova,
6543   E.: The Land Use Model Intercomparison Project (LUMIP) contribution to CMIP6:
6544   Rationale and experimental design, Geosci. Model Dev., 9(9), 2973–2998,
6545   doi:10.5194/gmd-9-2973-2016, 2016.

6546 Lashof, D. A., and D. R. Ahuja (1990), Relative contributions of greenhouse gas emissions to
6547   global warming, Nature, 344(6266), 529–531, doi:10.1038/344529a0.

6548 Lashof, D. A., 1989: The dynamic greenhouse: Feedback processes that may influence future
6549   concentrations of atmospheric trace gases and climatic change. *Clim. Change*, **14**, 213–242.
6550   https://doi.org/10.1007/BF00134964.

6551 Latham, J., 1990: Control of global warming? [10]. *Nature*, doi:10.1038/347339b0.

6552 Lean, J., 2017: Sun Climate Connections, Oxford Research Encyclopedias, Climate Science,
6553   DOI: 10.1093/acrefore/9780190228620.013.9.

6554   Lean, J., 2018a: Estimating solar irradiance since 850, Earth and Space Science, doi:
6555   10.1002/2017EA000357

6556   Lean, J., 2018b: Observation-Based Detection and Attribution of Twenty-first Century Climate
6557   Change, WIREs Climate Change, 9, doi: 10.1002/wcc.511

6558   Lean, J. and D. Rind, 2008: How natural and anthropogenic Influences alter Global and regional
6559   surface temperatures: 1889 to 2006, Geophys. Res. Lett., 35, L18701,
6560   doi:10.1029/2008GL034864.

6561   Lean, J. L., and M. T. DeLand, 2012: How Does the Sun's Spectrum Vary? J. Clim., 25, 2556-
6562   2560.

6563   Lean, J., Skumanich, A., and O. R. White, 1992: Estimating the Sun's Radiative Output During
6564   the Maunder Minimum, Geophysical Research Letters, 19,1591-1495.

6565   Lean, J., J. Beer and R. Bradley, 1995: Reconstruction of solar irradiance since 1610:
6566   Implications for climate change, Geophys. Res. Lett., 22, 3195-3198.

6567   Lean, J. L., G.J. Rottman, H.L. Kyle, T.N. Woods, J.R. Hickey, and L.C. Puga, 1997: Detection
6568   and parameterization of variations in solar mid and near ultraviolet radiation (200 to 400
6569   nm), J. Geophys. Res., 102, 29939-29956.

6570   Lean, J., Wang, Y.-M., and N. R. Sheeley, Jr., 2002: The effect of increasing solar activity on the
6571   Sun's total and open magnetic flux during multiple cycles; Implications for solar forcing of
6572   climate, Geophys. Res. Lett., 29, doi:10.1029/2002GL015880.

6573   Lean, J. L., G. Rottman, J. Harder and G Kopp, 2005: SORCE contributions to new
6574   understanding of global change and solar variability, Solar Phys., 230:27-53.

6575   LeGrande, A., K. Tsigaridis, S. Bauer (2016), Role of atmospheric chemistry in the climate
6576   impacts of stratospheric volcanic injections, Nature Geosci., doi:10.1038/NGEO2771.

6577   Lejeune, Q., Davin, E. L., Gudmundsson, L., Winckler, J. and Seneviratne, S. I.: Historical
6578   deforestation locally increased the intensity of hot days in northern mid-latitudes, Nat. Clim.
6579   Chang., 8(5), 386–390, doi:10.1038/s41558-018-0131-z, 2018.

6580   Lelieveld, J., and P. J. Crutzen, 1992: Indirect chemical effects of methane on climate warming.
6581   *Nature*, **355**, 339. https://doi.org/10.1038/355339a0.

6582   Lelieveld, J. O. S., P. J. Crutzen, and F. J. Dentener, 1998: Changing concentration, lifetime and
6583   climate forcing of atmospheric methane. *Tellus B*, **50**, 128–150, doi:doi:10.1034/j.1600-
6584   0889.1998.t01-1-00002.x. https://doi.org/10.1034/j.1600-0889.1998.t01-1-00002.x.

6585   Levy, H., 1971: Normal Atmosphere: Large Radical and Formaldehyde Concentrations
6586   Predicted. *Science (80-.).*, **173**, 141–143.

6587   Lesins, G., Chylek, P., & Lohmann, U. (2002). A study of internal and external mixing scenarios
6588   and its effect on aerosol optical properties and direct radiative forcing. *Journal of
6589   Geophysical Research: Atmospheres*, *107*(D10), AAC-5.

6590   Lilensten, J., T. Dudok de Wit, and K. Matthes (eds), 2015: Earth's climate response to a
6591   changing Sun, EDP Science, doi: 10.1051/9782759817337.

6592   Liou, K-N., 2002: An Introduction to Atmospheric Radiation. Academic Press, San Diego, CA,
6593   583pp.

6594   Lippmann, M., & Albert, R. E. (1969). The effect of particle size on the regional deposition of
6595   inhaled aerosols in the human respiratory tract. *American Industrial Hygiene Association
6596   Journal*, *30*(3), 257-275.

6597   Liu, S. C., 1977: Possible effects on froposheric O 3 and OH due to No emissions. *Geophys.
6598   Res. Lett.*, **4**, 325–328, doi:doi:10.1029/GL004i008p00325.
6599   https://doi.org/10.1029/GL004i008p00325.

6600   Liu, S. C., D. Kley, M. McFarland, J. D. Mahlman, and H. Levy, 1980: On the origin of
6601   tropospheric ozone. *J. Geophys. Res. Ocean.*, **85**, 7546–7552,
6602   doi:doi:10.1029/JC085iC12p07546. https://doi.org/10.1029/JC085iC12p07546.

6603   ——, M. Trainer, F. C. Fehsenfeld, D. D. Parrish, E. J. Williams, D. W. Fahey, G. Hübler, and P.
6604   C. Murphy, 1987: Ozone production in the rural troposphere and the implications for
6605   regional and global ozone distributions. *J. Geophys. Res. Atmos.*, **92**, 4191–4207,
6606   doi:doi:10.1029/JD092iD04p04191. https://doi.org/10.1029/JD092iD04p04191.

6607 Lockwood, M., R G Harrison, T Woollings and S K Solanki, 2010: Are cold winters in Europe
6608   associated with low solar activity? Environ. Res. Lett. 5 (2010) 024001.

6609 Loffler, M., S. Brinkop, P. Jockel (2016), Impact of major volcanic eruptions on stratospheric
6610   water vapour, Atmos. Chem. Phys., 16, 6547–6562, 2016, www.atmos-chem-
6611   phys.net/16/6547/2016/, doi:10.5194/acp-16-6547-2016.

6612 Lohmann, U., Rotstayn, L., Storelvmo, T., Jones, A., Menon, S., Quaas, J., Ekman, A. M. L.,
6613   Koch, D. and Ruedy, R.: Total aerosol effect: radiative forcing or radiative flux
6614   perturbation?, Atmospheric Chemistry and Physics, 10(7), 3235-3246, 2010.

6615 London, J., 1962: Mesospheric dynamics, Part III. Final Report, Contract No. AF19
6616   (604)-5492, Department of Meteorology and Oceanography, New York University,
6617   99 pp.

6618 Lovelock, J. E., Maggs, R. J., & Wade, R. J. (1973). Halogenated Hydrocarbons in and over the
6619   Atlantic. *Nature*, *241*, 194. Retrieved from https://doi.org/10.1038/241194a0

6620 Loeb, N. G., & Kato, S. (2002). Top-of-atmosphere direct radiative effect of aerosols over the
6621   tropical oceans from the Clouds and the Earth's Radiant Energy System (CERES) satellite
6622   instrument. *Journal of Climate*, *15*(12), 1474-1484.

6623 Loeb, N. G., & Manalo-Smith, N. (2005). Top-of-atmosphere direct radiative effect of aerosols
6624   over global oceans from merged CERES and MODIS observations. *Journal of Climate*,
6625   *18*(17), 3506-3526.

6626 Lohmann, U., J. Feichter, J. Penner, and R. Leaitch, Indirect effect of sulfate and carbonaceous
6627   aerosols: A mechanistic treatment, J. Geophys. Res., 105, 12,193–12,206, 2000.

6628 Lohmann, U., Rotstayn, L., Storelvmo, T., Jones, A., Menon, S., Quaas, J., ... & Ruedy, R.
6629   (2010). Total aerosol effect: radiative forcing or radiative flux perturbation?. *Atmospheric
6630   Chemistry and Physics*, *10*(7), 3235-3246.

6631 Le Quéré, C., Andrew, R. M., Canadell, J. G., Sitch, S., Ivar Korsbakken, J., Peters, G. P.,
6632   Manning, A. C., Boden, T. A., Tans, P. P., Houghton, R. A., Keeling, R. F., Alin, S.,
6633   Andrews, O. D., Anthoni, P., Barbero, L., Bopp, L., Chevallier, F., Chini, L. P., Ciais, P.,

6634   Currie, K., Delire, C., Doney, S. C., Friedlingstein, P., Gkritzalis, T., Harris, I., Hauck, J.,

6635   Haverd, V., Hoppema, M., Klein Goldewijk, K., Jain, A. K., Kato, E., Körtzinger, A.,

6636   Landschützer, P., Lefèvre, N., Lenton, A., Lienert, S., Lombardozzi, D., Melton, J. R.,

6637   Metzl, N., Millero, F., Monteiro, P. M. S., Munro, D. R., Nabel, J. E. M. S., Nakaoka, S. I.,

6638   O'Brien, K., Olsen, A., Omar, A. M., Ono, T., Pierrot, D., Poulter, B., Rödenbeck, C.,

6639   Salisbury, J., Schuster, U., Schwinger, J., Séférian, R., Skjelvan, I., Stocker, B. D., Sutton,

6640   A. J., Takahashi, T., Tian, H., Tilbrook, B., Van Der Laan-Luijkx, I. T., Van Der Werf, G.

6641   R., Viovy, N., Walker, A. P., Wiltshire, A. J. and Zaehle, S.: Global Carbon Budget 2016,

6642   Earth Syst. Sci. Data, 8(2), 605–649, doi:10.5194/essd-8-605-2016, 2016.

6643 Le Quere, C., Andres, R. J., Boden, T., Conway, T., Houghton, R. A., House, J. I., Marland, G.,

6644   Peters, G. P., van der Werf, G. R., Ahlstrom, A., Andrew, R. M., Bopp, L., Canadell, J. G.,

6645   Ciais, P., Doney, S. C., Enright, C., Friedlingstein, P., Huntingford, C., Jain, A. K.,

6646   Jourdain, C., Kato, E., Keeling, R. F., Klein Goldewijk, K., Levis, S., Levy, P., Lomas, M.,

6647   Poulter, B., Raupach, M. R., Schwinger, J., Sitch, S., Stocker, B. D., Viovy, N., Zaehle, S.

6648   and Zeng, N.: The global carbon budget 1959–2011, Earth Syst. Sci. Data, 5, 165–185,

6649   doi:10.5194/essd-5-165–2013, 2013.

6650 Logan, J. A., 1985: Tropospheric ozone: Seasonal behavior, trends, and anthropogenic influence.

6651   *J. Geophys. Res. Atmos.*, **90**, 10463–10482, doi:10.1029/JD090iD06p10463.

6652   http://dx.doi.org/10.1029/JD090iD06p10463.

6653 Logan, J. A., M. J. Prather, S. C. Wofsy, and M. B. McElroy, 1978: Atmospheric chemistry:

6654   response to human influence. *Philos. Trans. R. Soc. London A Math. Phys. Eng. Sci.*, **290**,

6655   187–234, doi:10.1098/rsta.1978.0082.

6656   http://rsta.royalsocietypublishing.org/content/290/1367/187.

6657 Logan, J. A., M. J. Prather, S. C. Wofsy, and M. B. McElroy, 1981: Tropospheric chemistry: A

6658   global perspective. *J. Geophys. Res.*, **86**, 7210–7254, doi:10.1029/JC086iC08p07210.

6659   http://dx.doi.org/10.1029/JC086iC08p07210.

6660 Luther, F. M., 1982: In Carbon dioxide review 1982, W. Clark, Ed., Oxford University Press,

6661   Clarendon, England, 290–295.

6662

Machta, L., and T. Carpenter, 1971: Trends in high cloudiness at Denver and Salt Lake City. *Man's Impact on the Climate* (W. H. Matthews, W. W. Kellogg and G. D. Robinson, Eds.), MIT Press, pp. 410–415.

Machta, L., and T. Carpenter, 1971: Trends in high cloudiness at Denver and Salt Lake City. *Man's Impact on the Climate* (W. H. Matthews, W. W. Kellogg and G. D. Robinson, Eds.), MIT Press, pp. 410–415.

MacKay, R. M., M. K. W. Ko, R.-L. Shia, Y. Yang, S. Zhou, and G. Molnar, 1997: An Estimation of the Climatic Effects of Stratospheric Ozone Losses during the 1980s. *J. Clim.*, **10**, 774–788, doi:10.1175/1520-0442(1997)010<0774:AEOTCE>2.0.CO;2. https://doi.org/10.1175/1520-0442(1997)010%3C0774:AEOTCE%3E2.0.CO.

MacMartin, D. G., D. W. Keith, B. Kravitz, and K. Caldeira, 2013: Management of trade-offs in geoengineering through optimal choice of non-uniform radiative forcing. *Nat. Clim. Chang.*, doi:10.1038/nclimate1722.

Mahowald, N.: Aerosol indirect effect on biogeochemical cycles and climate, Science (80-.)., 334(6057), doi:10.1126/science.1207374, 2011.

Mahowald, N., Ward, D. S., Kloster, S., Flanner, M. G., Heald, C. L., Heavens, N. G., Hess, P. G., Lamarque, J.-F. and Chuang, P. Y.: Aerosol impacts on climate and biogeochemistry., 2011.

Mahowald, N. M., Scanza, R., Brahney, J., Goodale, C. L., Hess, P. G., Moore, J. K. and Neff, J.: Aerosol Deposition Impacts on Land and Ocean Carbon Cycles, Curr. Clim. Chang. Reports, 3(1), 16–31, doi:10.1007/s40641-017-0056-z, 2017a.

Mahowald, N. M., Ward, D. S., Doney, S. C., Hess, P. G. and Randerson, J. T.: Are the impacts of land use on warming underestimated in climate policy?, Environ. Res. Lett., 12(9), doi:10.1088/1748-9326/aa836d, 2017b.

Mahowald, N. M., Randerson, J. T., Lindsay, K., Munoz, E., Doney, S. C., Lawrence, P., Schlunegger, S., Ward, D. S., Lawrence, D. and Hoffman, F. M.: Interactions between land

6689   use change and carbon cycle feedbacks, Global Biogeochem. Cycles, 31(1), 96–113,

6690   doi:10.1002/2016GB005374, 2017c.

6691   Mahowald, N. M. M., Kloster, S., Engelstaedter, S., Moore, J. K. K., Mukhopadhyay, S.,

6692   McConnell, J. R. R., Albani, S., Doney, S. C. C., Bhattacharya, A., Curran, M. A. J. A. J.,

6693   Flanner, M. G. G., Hoffman, F. M. M., Lawrence, D. M. M., Lindsay, K., Mayewski, P. A.

6694   A., Neff, J., Rothenberg, D., Thomas, E., Thornton, P. E. E. and Zender, C. S. S.: Observed

6695   20th century desert dust variability: impact on climate and biogeochemistry, Atmos. Chem.

6696   Phys., 10(22), 10875–10893, doi:10.5194/acp-10-10875-2010, 2010.

6697   Mahowald, N. N. M.: Anthropocence changes in desert area: sensitivity to climate model

6698   predictions, Geophys. Res. Lett., 34(L18817), doi:10.1029/2007GL030472,

6699   doi:10.1029/2007GL030472, 2007.

6700   Malinina, E., Rozanov, A., Rozanov, V., Liebing, P., Bovensmann, H., and Burrows, J. P. (2018),

6701   Aerosol particle size distribution in the stratosphere retrieved from SCIAMACHY limb

6702   measurements, Atmos. Meas. Tech., 11, 2085-2100, https://doi.org/10.5194/amt-11-2085-

6703   2018.

6704   Mann, M. E., M. A. Cane, S. E. Zebiak, and A. Clement, 2005: Volcanic and solar forcing of the

6705   tropical Pacific over the past 1000 Years, J. Clim.,18, 447-456.

6706   Mann, M. E., Z. Zhang, S. Rutherford, R. S. Bradley, M. K. Hughes, D. Shindell, C. Ammann,

6707   G. Faluvegi, and F. Ni, 2009: Global Signatures and Dynamical Origins of the Little Ice

6708   Age and Medieval Climate Anomaly, Science, 326, 5957, 1256-1260, DOI:

6709   10.1126/science.1177303.

6710   Manabe, S., & Wetherald, R. T. (1967). Thermal Equilibrium of the Atmosphere with a Given

6711   Distribution of Relative Humidity. *Journal of the Atmospheric Sciences*, *24*(3), 241–259.

6712   http://doi.org/10.1175/1520-0469(1967)024<0241:TEOTAW>2.0.CO;2

6713   Manabe, S., & Wetherald, R. T. (1975). The Effects of Doubling the CO_2 Concentration on the

6714   climate of a General Circulation Model. *Journal of the Atmospheric Sciences*, *32*(1), 3–15.

6715   http://doi.org/10.1175/1520-0469(1975)032<0003:TEODTC>2.0.CO;2

6716 Manabe, S., and R. T. Wetherald, 1967: Thermal Equilibrium of the Atmosphere with a Given
6717   Distribution of Relative Humidity. *J. Atmos. Sci.*, **24**, 241–259, doi:10.1175/1520-
6718   0469(1967)024<0241:TEOTAW>2.0.CO;2. https://doi.org/10.1175/1520-
6719   0469(1967)024%3C0241:TEOTAW%3E2.0.CO.

6720 Manabe, S., and R. T. Wetherald, 1967: Thermal Equilibrium of the Atmosphere with a Given
6721   Distribution of Relative Humidity. J. Atmos. Sci., 24, 241–259, doi:10.1175/1520-
6722   0469(1967)024<0241:teotaw>2.0.co;2. http://journals.ametsoc.org/doi/abs/10.1175/1520-
6723   0469%281967%29024%3C0241%3ATEOTAW%3E2.0.CO%3B2.

6724 Manabe, S., and F. Moller, 1961: On the radiative equilibrium and heat balance of the
6725   atmosphere. *Mon. Wea. Rev., 89, 503-532.*

6726 —---, and R. F. Strickler, 1964: Thermal equilibrium of the atmosphere with a convective
6727   adjustment. *J. Atmos. Sci., 21, 361-385.*

6728 —---, and R. Wetherald, 1967: Thermal equilibrium of the atmosphere with a given distribution of
6729   relative humidity. *J. Atmos. Sci.*, **24(3)**, 241-259.

6730 —---, and R. Wetherald, 1975: The effects of doubling CO_2 concentration on the climate of
6731   general circulation model. *J. Atmos. Sci.*, **32(1)**, 3-15.

6732 —---, and R. J. Stouffer, 1980: Sensitivity of a global climate model to an increase of
6733 CO_2concentration in the atmosphere. *J. Geophys. Res.*, **85(C10)**, 5529-5554.

6734 Marlon, J., Bartlein, P., Carcaillet, C., Gavin, D., Harrison, S., Higuera, P., Joos, F., Power, M.
6735   and Prentice, I. C.: Climate and human influences on global biomass burning over the past
6736   two millennia, Nature-Geosciences, 1, 697–701, 2008.

6737 Marlon, J. R., Bartlein, P. J., Gavin, D. G., Long, C. J., Anderson, R. S., Briles, C. E., Brown, K.
6738   J., Colombaroli, D., Hallett, D. J., Power, M. J., Scharf, E. A. and Walsh, M. K.: Long-term
6739   perspective on wildfires in the western USA, Proc. Natl. Acad. Sci., 109(9), E535–E543,
6740   doi:10.1073/pnas.1112839109, 2012.

6741 Martin, J. H., Gordon, M. and Fitzwater, S. E.: The case for iron, Limnol. Oceanogr., 36(8),
6742   1793–1802, doi:10.4319/lo.1991.36.8.1793, 1991.

6743 Martin, P. E., & Barker, E. F. (1932). The Infrared Absorption Spectrum of Carbon Dioxide.
6744   *Phys. Rev.*, *41*(3), 291–303. http://doi.org/10.1103/PhysRev.41.291

6745 Martin, G. M., D. W. Johnson, and An Spice. "The measurement and parameterization of
6746   effective radius of droplets in warm stratocumulus clouds." *Journal of the Atmospheric*
6747   *Sciences* 51, no. 13 (1994): 1823-1842.

6748

6749 Marsh, D. R., J.-F. Lamarque, A. J. Conley, and L. M. Polvani, 2016: Stratospheric ozone
6750   chemistry feedbacks are not critical for the determination of climate sensitivity in
6751   CESM1(WACCM). *Geophys. Res. Lett.*, **43**, 3928–3934, doi:doi:10.1002/2016GL068344.
6752   https://doi.org/10.1002/2016GL068344.

6753 Marvel, K., Schmidt, G. A., Miller, R. L. and Nazarenko, L. S.: Implications for climate
6754   sensitivity from the response to individual forcings, Nature Climate Change, 6, 386, 2015.

6755   Mastenbrook, H. **J.,** 1963: Frost-point hygrometer measurement in the stratosphere and the
6756   problem of moisture contamination. *Humidity and Moisture,* Vol. 2, New York,
6757   Reinhold Publishing Co., 480-485.

6758 Matthes, K., Funke, B., Andersson, M., Barnard, L., Beer, J., et al., 2017: Solar forcing for
6759   CMIP6 (v3.2). Geoscientific Model Development, Katlenburg-Lindau Vol. 10, Iss. 6: 2247-
6760   2302.

6761 Mathews, E. and Fung, I.: Methane emission from natural wetlands: Global distribution, area and
6762   environmental characterics of sources, Global Biogeochem. Cycles, 1(1), 61–86, 1987.

6763 Matthews, H. D., Graham, T. L., Keverian, S., Lamontagne, C., Seto, D. and Smith, T. J.:
6764   National contributions to observed global warming, Environ. Res. Lett., 9(1),
6765   doi:10.1088/1748-9326/9/1/014010, 2014.

6766 Mauceri, S., Pilewskie, P., Richard, E. et al., 2018: Revision of the Sun's Spectral Irradiance as
6767   Measured by SORCE SIM, Sol Phys 293: 161. https://doi.org/10.1007/s11207-018-1379-1.

6768 Maycock AC, Joshi MM, Shine KP, Scaife AA 2013: The circulation response to idealized

6769   changes in water vapor. J Climate 26:545-561 DOI: 10.1175/JCLI-D-12-00155.1

6770 Moore, C. M. M., Mills, M. M. M., Arrigo, K. R. R., Berman-Frank, I., Bopp, L., Boyd, P. W.

6771   W., Galbraith, E. D. D., Geider, R. J. J., Guieu, C., Jaccard, S. L. L., Jickells, T. D. D., La

6772   Roche, J., Lenton, T. M. M., Mahowald, N. M. M., Marañón, E., Marinov, I., Moore, J. K.

6773   K., Nakatsuka, T., Oschlies, A., Saito, M. A. A., Thingstad, T. F. F., Tsuda, A. and Ulloa,

6774   O.: Processes and patterns of oceanic nutrient limitation, Nat. Geosci., 6(9), 701–710,

6775   doi:10.1038/ngeo1765, 2013.

6776 McCracken, K. G., J. Beer, F. Steinhilber, and J. Abreu, 2013: The Heliosphere in Time, Space

6777   Sci. Rev., 176, 59-71 DOI 10.1007/s11214-011-9851-3.

6778 McClatchey, R. A., Benedict, W. S., Clough, S. A., Burch, D. E., Calfee, R. F., Fox, K., …

6779   Garing, J. S. (1973). *AFCRL Atmospheric Absorption Line Parameters Compilation*.

6780   Bedford, MA.

6781 McConnell, J. C., M. B. McElroy, and S. C. Wofsy, 1971: Natural Sources of Atmospheric CO.

6782   *Nature*, **233**, 187. http://dx.doi.org/10.1038/233187a0.

6783 McCormick, M.P. (1987), SAGE II: An overview. Adv. Space Res., 7, 219–226.

6784 McCormick, R. A., & Ludwig, J. H. (1967). Climate modification by atmospheric aerosols.

6785   *Science*, *156*(3780), 1358-1359.

6786 McCoy, D. T., & Hartmann, D. L. (2015). Observations of a substantial cloud-aerosol indirect

6787   effect during the 2014–2015 Bárðarbunga-Veiðivötn fissure eruption in Iceland.

6788   *Geophysical Research Letters*, *42*(23), 10-409.

6789 McElroy, M. B., S. C. Wofsy, J. E. Penner, and J. C. McConnell, 1974: Atmospheric Ozone:

6790   Possible Impact of Stratospheric Aviation. *J. Atmos. Sci.*, **31**, 287–304, doi:10.1175/1520-

6791   0469(1974)031<0287:AOPIOS>2.0.CO;2. https://doi.org/10.1175/1520-

6792   0469(1974)031%3C0287:AOPIOS%3E2.0.CO.

6793 ——, ——, and Y. L. Yung, 1977: The nitrogen cycle: perturbations due to man and their

6794   impact on atmospheric N2O and O3. *Philos. Trans. R. Soc. London B Biol. Sci.*, **277**, 159–

6795 181, doi:10.1098/rstb.1977.0009.

6796 http://rstb.royalsocietypublishing.org/content/277/954/159.

6797 McGregor, S., and A. Timmermann (2011), The effect of explosive tropical volcanism on ENSO,

6798 J. Clim., 24(8), 2178–2191.

6799 Meehl, G. A., and Coauthors, 2007: Global Climate Projections. *Climate Change 2007: The*

6800 *Physical Science Basis. Contribution of Working Group I to the Fourth Assessment Report*

6801 *of the Intergovernmental Panel on Climate Change*, D. Qin, M. Manning, Z. Chen, M.

6802 Marquis, K.B. Averyt, M. Tignor, and H.L. Miller, Eds., Cambridge University Press,

6803 Cambridge, United Kingdom and New York, NY, USA.

6804 Meehl, G. A., J. M. Arblaster, K. Matthes, F. Sassi, and H. van Loon, 2009: Amplifying the

6805 Pacific Climate System Response to a Small 11-Year Solar Cycle Forcing, Science, 325,

6806 1114-1118, DOI: 10.1126/science.1172872.

6807 Meehl, G. A. *et al.* Relative increase of record high maximum temperatures compared to record

6808 low minimum temperatures in the US. *Geophys. Res. Lett.* **36**, L23701 (2009).

6809 Meehl, G. A., J. M. Arblaster, J. T. Fasullo, A. Hu, and K. E. Trenberth (2011), Model-based

6810 evidence of deep-ocean heat uptake during surface-temperature hiatus periods. *Nature Clim*

6811 *Change*, 1, 360-364.

6812 Meftah, M., L. Damé, D. Bolsée, A. Hauchecorne, N. Pereira, D. Sluse, G. Cessateur, A. Irbah1,

6813 J. Bureau, M. Weber3, K. Bramstedt, T. Hilbig3, R. Thiéblemont, M. Marchand, F.

6814 Lefèvre1, A. Sarkissian and S. Bekki, (2018): SOLAR-ISS: A new reference spectrum

6815 based on SOLAR/SOLSPEC observations, A&A 611, A1 https://doi.org/10.1051/0004-

6816 6361/201731316

6817 Meyer, K., Platnick, S., & Zhang, Z. (2015). Simultaneously inferring above-cloud absorbing

6818 aerosol optical thickness and underlying liquid phase cloud optical and microphysical

6819 properties using MODIS. *Journal of Geophysical Research: Atmospheres*, *120*(11), 5524-

6820 5547.

322

6821 Michaels, P. J., and P. C. Knappenberger, 2000: Natural Signals in the MSU lower tropospheric
6822   temperature Record, Geophys. Res. Lett., 27, 2,905-2,908.

6823 Mickley, L. J., P. P. Murti, D. J. Jacob, J. A. Logan, D. M. Koch, and D. Rind, 1999: Radiative
6824   forcing from tropospheric ozone calculated with a unified chemistry-climate model. *J.*
6825   *Geophys. Res. Atmos.*, **104**, 30153–30172, doi:doi:10.1029/1999JD900439.
6826   https://doi.org/10.1029/1999JD900439.

6827 Mie, G., 1908: Beiträge zur Optik trüber Medien, speziell kolloidaler Metallösungen. *Annalen*
6828   *der Physik*. **330**(3): 377–445.

6829 Migeotte, M. V. (1948). Spectroscopic Evidence of Methane in the Earth's Atmosphere. *Phys.*
6830   *Rev.*, *73*(5), 519–520. http://doi.org/10.1103/PhysRev.73.519.2

6831 Ming, Y., Ramaswamy, V. and Persad, G.: Two opposing effects of absorbing aerosols on
6832   global-mean precipitation, Geophysical Research Letters, 37, L13701, 2010.

6833 Minnis, P., E. F. Harrison, L. L. Stowe, G. G. Gibson, F. M. Denn, D. R. Doelling, and W. L.
6834   Smith, 1993: Radiative Climate Forcing by the Mount Pinatubo Eruption. Science (80-.).,
6835   259, 1411 LP-1415, doi:10.1126/science.259.5100.1411.
6836   http://science.sciencemag.org/content/259/5100/1411.abstract.

6837 Minnis, P., Young, D.F., Garber, D.P., Nguyen, L., Smith, W.L. and Palikonda, R., 1998.
6838   Transformation of contrails into cirrus during SUCCESS. *Geophysical Research Letters*,
6839   *25*(8), pp.1157-1160.

6840 Minnis, P., Schumann, U., Doelling, D.R., Gierens, K.M. and Fahey, D.W., 1999. Global
6841   distribution of contrail radiative forcing. *Geophysical Research Letters*, *26*(13), pp.1853-
6842   1856.

6843 Mills, M., A. Schmidt, R.Easter, S. Solomon, D. Kinnison, S. Ghan,R. Neely III, D. Marsh, A.
6844   Conley, C. Bardeen, and A. Gettelman (2016), Global volcanic aerosol properties derived
6845   from emissions, 1990-2014, using CESM1(WACCM), J. Geophys. Res., Atmos., 121,
6846   doi:10.1002/2015JD024290.

6847 Min, S. K. *et al.* Human contribution to more-intense precipitation extremes. *Nature* **470**, 378–381
6848   (2011).

6849 Ming, Y. & Ramaswamy, V. A model investigation of aerosol-induced changes in tropical
6850   circulation. *J. Clim.* **24,** 5125-5133 (2011).

6851 Minnis, P., E. F. Harrison, L. L. Stowe, G. G. Gibson, F. M. Denn, D. R. Doelling, and W. L.
6852   Smith Jr. (1993), Radiative climate forcing by the Mt. Pinatubo eruption. *Science*, 259, 1411-
6853   1415.

6854 Misios, S., D. M. Mitchell, L. J. Gray, K. Tourpali, K. Matthes, L. Hood, H. Schmidt, G. Chiodo,
6855   R. Thiéblemont, E. Rozanov, and A. Krivolutsky, 2015: Solar signals in CMIP-5
6856   simulations: effects of atmosphere-ocean coupling, Q.J.R. Meteorol. Soc.. doi:
6857   10.1002/qj.2695.

6858 Mishchenko, M. I., Geogdzhayev, I. V., Cairns, B., Rossow, W. B., & Lacis, A. A. (1999).
6859   Aerosol retrievals over the ocean by use of channels 1 and 2 AVHRR data: sensitivity
6860   analysis and preliminary results. *Applied Optics*, *38*(36), 7325-7341.

6861 Mitchell, J. F., Johns, T. C., Gregory, J. M., & Tett, S. F. B. (1995). Climate response to
6862   increasing levels of greenhouse gases and sulfate aerosols. *Nature*, *376*(6540), 501.

6863 Mitchell, D. L., and W. Finnegan, 2009: Modification of cirrus clouds to reduce global warming.
6864   *Environ. Res. Lett.*, doi:10.1088/1748-9326/4/4/045102.

6865 Mitchell, D. M., S. Misios, L. J. Gray, K. Tourpali, K. Matthes, L. Hood, H. Schmidt, G. Chiodo,
6866   R. Thiéblemont, E. Rozanov, D.Shindell, and A. Krivolutsky, 2015: Solar signals in CMIP-
6867   5 simulations: the stratospheric pathway. Q.J.R. Meteorol. Soc., 141: 2390–2403. doi:
6868   10.1002/qj.2530.

6869 Mitchell, J F., S. Manabe, T Tokioka, and V Meleshko, 1990: Equilibrium climate
6870   change In *Climate Change: The IPCC Scientific Assessment*, Cambridge, UK, Cambridge
6871   University Press, 131-172.

6872 Mlynczak, M. G., Daniels, T. S., Kratz, D. P., Feldman, D. R., Collins, W. D., Mlawer, E. J., …
6873   Mast, J. C. (2016). The spectroscopic foundation of radiative forcing of climate by carbon

6874   dioxide. *Geophysical Research Letters*, *43*(10), 5318–5325.

6875   http://doi.org/10.1002/2016GL068837

6876   Molina, M. J., and F. S. Rowland, 1974: Stratospheric Sink for Chlorofluoromethanes: Chlorine

6877   Atom Catalyzed Destruction of Ozone. *Nature*, 810–812.

6878   Möller, F., 1963: On the influence of changes in the CO2 concentration in air on the

6879   radiation balance of the earth's surface and on the climate. *J. Geophys. Res.,* **68,** 3877-

6880   3886.

6881   Monks, P. S., and Coauthors, 2015: Tropospheric ozone and its precursors from the urban to the

6882   global scale from air quality to short-lived climate forcer. *Atmos. Chem. Phys.*, **15**, 8889–

6883   8973, doi:10.5194/acp-15-8889-2015. https://www.atmos-chem-phys.net/15/8889/2015/.

6884   Montzka, S. A., M. Krol, E. Dlugokencky, B. Hall, P. Jöckel, and J. Lelieveld, 2011: Small

6885   Interannual Variability of Global Atmospheric Hydroxyl. *Science (80-.).*, **331**, 67–69.

6886   http://www.sciencemag.org/content/331/6013/67.abstract.

6887   Murray, L. T., L. J. Mickley, J. O. Kaplan, E. D. Sofen, M. Pfeiffer, and B. Alexander, 2014:

6888   Factors controlling variability in the oxidative capacity of the troposphere since the Last

6889   Glacial Maximum. *Atmos. Chem. Phys.*, **14**, 3589–3622, doi:Doi 10.5194/Acp-14-3589-

6890   2014.

6891   Murgatroyd, R. J., 1960: Some recent measurements by aircraft of humidity up to

6892   50,000 ft. in the tropics and their relation- ship to meridional circulation: *Proc.*

6893   *Symp. Atmos. Ozone,* Oxford, 20-25 July 1959, IUGG Monogr. No. 3, Paris, p. 30.

6894   Myhre, G., Highwood, E. J., Shine, K. P., & Stordal, F. (1998). New estimates of radiative

6895   forcing due to well mixed greenhouse gases. *Geophysical Research Letters*, *25*(14), 2715–

6896   2718. http://doi.org/10.1029/98GL01908

6897   Myhre, G., Shindel, D., Breon, G.-M., Collins, W., Fuglestvedt, J., Huang, J., Koch, D.,

6898   Lamarque, J. F., Lee, D., Mendoza, B., Nakajima, T., Robock, A., Stephens, G., Takemura,

6899   T. and Zhang, H.: Anthropogenic and Nature Radiative Forcing, in Climate Change 2013:

6900   The Physical Science Basis. Contribution of Working Group I to the Fifth Assessment

6901   Report of the Intergovernmental Panel on Climate Change, edited by T. Stocker, D. Qin, G.

6902   K. Plattner, M. Tignor, S. Allen, J. Boschung, A. Nauels, Y. Xia, V. Bex, and P. Midgley,

6903   pp. 659–740, Cambridge University Press, Cambridge, UK., 2013.

6904   Myhre, G., and Coauthors, 2013: Anthropogenic and Natural Radiative Forcing. *Climate Change*

6905   *2013: The Physical Science Basis. Contribution of Working Group I to the Fifth Assessment*

6906   *Report of the Intergovernmental Panel on Climate Change*, T.F. Stocker et al., Eds.,

6907   Cambridge University Press, Cambridge, U.K. and New York, NY, USA, 659–740.

6908   Myhre, G., and Coauthors, 2013: Anthropogenic and Natural Radiative Forcing. *Climate Change*

6909   *2013: The Physical Science Basis. Contribution of Working Group I to the Fifth Assessment*

6910   *Report of the Intergovernmental Panel on Climate Change*, T.F. Stocker et al., Eds.,

6911   Cambridge University Press, Cambridge, U.K. and New York, NY, USA, 659–740.

6912   Myhre, G., Shindell, D., Bréon, F.-M., Collins, W., Fuglestvedt, J., Huang, J., Koch, D.,

6913   Lamarque, J.-F., Lee, D., Mendoza, B., Nakajima, T., Robock, A., Stephens, G., Takemura,

6914   T. and Zhang, H., Anthropogenic and Natural Radiative Forcing. In: Climate Change 2013:

6915   The Physical Science Basis. Contribution of Working Group I to the Fifth Assessment

6916   Report of the Intergovernmental Panel on Climate Change. T. F. Stocker, D. Qin, G.-K.

6917   Plattner, M. Tignor, S. K. Allen et al. (Editors), Cambridge University Press, Cambridge,

6918   United Kingdom and New York, NY, USA, pp. 659-740, 2013.

6919   Myhre, G., E. J. Highwood, K. P. Shine, and F. Stordal, 1998: New estimates of radiative forcing

6920   due to well mixed greenhouse gases. Geophys. Res. Lett., 25.

6921   ——, and Coauthors, 2018: Quantifying the Importance of Rapid Adjustments for Global

6922   Precipitation Changes. Geophys. Res. Lett., 45, 11,399-11,405, doi:10.1029/2018gl079474.

6923   Myhre, G. *et al.* Anthropogenic and Natural Radiative Forcing. In: *Climate Change 2013: The*

6924   *Physical Science Basis. Contribution of Working Group I to the Fifth Assessment Report of*

6925   *the Intergovernmental Panel on Climate Change* (eds Stocker TF, et al.) (Cambridge Univ.

6926   Press, 2013).

6927   Myhre, G., D. Shindell, F.-M. Bréon, W. Collins, J. Fuglestvedt, J. Huang, D. Koch, J.-F.

6928   Lamarque, D. Lee, B. Mendoza, T. Nakajima, A. Robock, G. Stephens, T. Takemura and H.

6929   Zhang (2013), Anthropogenic and Natural Radiative Forcing. In: Climate Change (2013), The

6930   Physical Science Basis. Contribution of Working Group I to the Fifth Assessment Report of

6931   the Intergovernmental Panel on Climate Change [Stocker, T.F., D. Qin, G.-K. Plattner, M.

6932   Tignor, S.K. Allen, J. Boschung, A. Nauels, Y. Xia, V. Bex and P.M. Midgley (eds.)].

6933   Cambridge University Press, Cambridge, United Kingdom and New York, NY, USA

6934   Myhre, G., O. Boucher, F.-M. Bréon, P. Forster, and D. Shindell, 2015: Declining uncertainty in

6935   transient climate response as CO_2 forcing dominates future climate change. *Nat.*

6936   *Geosci.*, **8**, doi:10.1038/ngeo2371.

6937   Myhre, D. Shindell, F.-M. Bréon, W. Collins, J. Fuglestvedt, J. Huang, D. Koch, J.-F. Lamarque,

6938   D. Lee, B. Mendoza, T. Nakajima, A. Robock, G. Stephens, T. Takemura and H. Zhang, G.,

6939   Anthropogenic and Natural Radiative Forcing. *Climate Change 2013: The Physical Science*

6940   *Basis. Contribution of Working Group I to the Fifth Assessment Report of the*

6941   *Intergovernmental Panel on Climate Change*, T.F. Stocker D. Qin, G.-K. Plattner, M.

6942   Tignor, S.K. Allen, J. Boschung, A. Nauels, Y. Xia, V. Bex and P.M. Midgley, Ed.,

6943   Cambridge University Press, Cambridge, United Kingdom and New York, NY, USA, 659–

6944   740.

6945   Myhre, G., and F. Stordal (1997), Role of spatial and temporal variations in the computation of

6946   radiative forcing and GWP, J.Geophys. Res., 102(D10), 11181–11200,

6947   doi:10.1029/97JD00148.

6948   Myhre, G., Shindell, D., Bréon, F.-M., Collins, W., Fuglestvedt, J., Huang, J., Koch, D.,

6949   Lamarque, J.-F., Lee, D., Mendoza, B., Nakajima, T., Robock, A., Stephens, G., Takemura,

6950   T. and Zhang, H., Anthropogenic and Natural Radiative Forcing. In: Climate Change 2013:

6951   The Physical Science Basis. Contribution of Working Group I to the Fifth Assessment

6952   Report of the Intergovernmental Panel on Climate Change. T. F. Stocker, D. Qin, G.-K.

6953   Plattner, M. Tignor, S. K. Allen et al. (Editors), Cambridge University Press, Cambridge,

6954   United Kingdom and New York, NY, USA, pp. 659-740, 2013.

6955   Myhre, G., F. Stordal, K. Restad and I.S.A. Isaksen, 1998: Estimation of the direct radiative

6956   forcing due to sulfate and soot aerosols. Tellus, 50B, 463−477.

van Marle, M. J. E., and Coauthors, 2017: Historic global biomass burning emissions for CMIP6 (BB4CMIP) based on merging satellite observations with proxies and fire models (1750-2015). *Geosci. Model Dev.*, **10**, 3329–3357, doi:10.5194/gmd-10-3329-2017. https://doi.org/10.5194/gmd-10-3329-2017.

Van Marle, M. J. E., Kloster, S., Magi, B. I., Marlon, J. R., Daniau, A. L., Field, R. D., Arneth, A., Forrest, M., Hantson, S., Kehrwald, N. M., Knorr, W., Lasslop, G., Li, F., Mangeon, S., Yue, C., Kaiser, J. W. and Van Der Werf, G. R.: Historic global biomass burning emissions for CMIP6 (BB4CMIP) based on merging satellite observations with proxies and fire models (1750-2015), Geosci. Model Dev., 10(9), 3329–3357, doi:10.5194/gmd-10-3329-2017, 2017.

Nadelhoffer, K. J., Emmett, B. A., Gundersen, P., Kjønaas, O. J., Koopmans, C. J., Schleppi, P., Tietema, A. and Wright, R. F.: Nitrogen deposition makes a minor contribution to carbon sequestration in temperate forests, Nature, 398(March 11, 1999), 145–148 [online] Available from: http://www.nature.com, 1999.

Naik, V., and Coauthors, 2013: Preindustrial to present-day changes in tropospheric hydroxyl radical and methane lifetime from the Atmospheric Chemistry and Climate Model Intercomparison Project (ACCMIP). *Atmos. Chem. Phys.*, **13**, 5277–5298, doi:10.5194/acp-13-5277-2013.

National Research Council 1979. *Carbon Dioxide and Climate: A Scientific Assessment*. Washington, DC: The National Academies Press, . https://doi.org/10.17226/12181.

National Research Council, 1982. *Carbon dioxide and Climate: A Second Assessment.* Washington, DC: The National Academies Press, 96 pages. https://doi.org/10.17226/18524

National Research Council, 1996: A plan for a research program on Aerosol Radiative Forcing and Climate Change. Washington, DC: The National Academies Press, 161pp.

6983 National Research Council, 2005: Radiative Forcing of Climate Change: Expanding the Concept
6984   and Addressing Uncertainties. The National Academies Press, Washington, DC, 208pp.
6985   https://www.nap.edu/catalog/11175/radiative-forcing-of-climate-change-expanding-the-
6986   concept-and-addressing.

6987 National Research Council, 2005: *Radiative Forcing of Climate Change: Expanding the Concept*
6988   *and Addressing Uncertainties.* The National Academies Press, 224 pp.

6989 National Research Council, 2005: Radiative Forcing of Climate Change: Expanding the Concept
6990   and Addressing Uncertainties. The National Academies Press, Washington, DC,
6991   https://www.nap.edu/catalog/11175/radiative-forcing-of-climate-change-expanding-the-
6992   concept-and-addressing

6993 Neff, U., S. J. Burns, A. Mangini, M. Mudelsee, D. Fleitmann, and A. Matter, 2001: Strong
6994   coherence between solar variability and the monsoon in Oman between 9 and 6 kyr ago,
6995   Nature, 411, 290-293.

6996 Niemeier, U., C. Timmreck, H. F. Graf, S. Kinne, S. Rast, and S. Self (2009), Initial fate of fine
6997   ash and sulfur from large volcanic eruptions. *Atmos Chem Phys*, 9, 9043-9057.

6998 Niemeier, U. and S. Tilmes (2017), Sulfur injections for a cooler planet, *Science* 357, no. 6348,
6999   246-248.

7000 U. Niemeier and C. Timmreck (2015), What is the limit of climate engineering by stratospheric
7001   injection of SO2?, *Atmos. Chem. Phys.,* 15, 9129–9141, 2015
7002   https://doi.org/10.5194/acp-15-9129-2015

7003

7004 Nowack, P. J., N. Luke Abraham, A. C. Maycock, P. Braesicke, J. M. Gregory, M. M. Joshi, A.
7005   Osprey, and J. A. Pyle, 2015: A large ozone-circulation feedback and its implications for
7006   global warming assessments. *Nat. Clim. Chang.*, **5**, 41–45, doi:10.1038/nclimate2451.
7007   http://dx.doi.org/10.1038/nclimate2451.

7008 Novello, V. F., Vuille, M, Cruz, F. W., Stríkis, N. M., de Paula, M. S., Edwards, R. L., Cheng,
7009   H., Karmann, I., Jaqueto, P. F., Trindade, R. I. F., Hartmann, G. A., Moquet, Jean S., 2016:

7010   Centennial-scale solar forcing of the South American Monsoon System recorded in

7011   stalagmites, Scientific Reports, 6, Article number: 24762

7012

7013 Ocean Studies Board, 2015: Climate Intervention: Reflecting Sunlight to Cool the Earth. *Natl.*

7014   *Acad. Press*, doi:10.17226/18988.

7015 Ohba, M., H. Shiogama, T. Yokohata, and M. Watanabe (2013), Impact of strong tropical volcanic

7016   eruptions on ENSO simulated in a coupled GCM, J. Clim., 26(14), 5169–5182.

7017 Oman, L., A. Robock, G. Stenchikov, G. A. Schmidt, and R. Ruedy (2005), Climatic response to

7018   high latitude volcanic eruptions. *J Geophys Res*, 110, D13103.

7019 Oman, L., A. Robock, G. Stenchikov, T. Thordarson, D. Koch, D. Shindell, and C. Gao (2006a),

7020   Modeling the distribution of the volcanic aerosol cloud from the 1783-1784 Laki eruption. *J*

7021   *Geophys Res*, 111, D12209.

7022 Oman, L., A. Robock, G. L. Stenchikov, and T. Thordarson (2006b), High-latitude eruptions cast

7023   shadow over the African monsoon and the flow of the Nile. *Geophys Res Lett*, 33, L18711.

7024 Olson, J., and Coauthors, 1997: Results from the Intergovernmental Panel on Climatic Change

7025   Photochemical Model Intercomparison (PhotoComp). *J. Geophys. Res. Atmos.*, **102**, 5979–

7026   5991, doi:doi:10.1029/96JD03380. https://doi.org/10.1029/96JD03380.

7027 Owens, A. J., C. H. Hales, D. L. Filkin, C. Miller, and M. McFarland, 1985: Multiple scenario

7028   ozone change calculations: The subtractive perturbation approach. *Atmospheric Ozone*, C.S.

7029   Zerefos and A. Ghazi, Eds., D. Reidel, Dordrecht, 82–86.

7030

7031 Paudel, R., Mahowald, N. M., Hess, P. G. M., Meng, L. and Riley, W. J.: Attribution of changes

7032   in global wetland methane emissions from pre-industrial to present using CLM4.5-BGC,

7033   Environ. Res. Lett., 11(3), doi:10.1088/1748-9326/11/3/034020, 2016.

7034 Paulot, F., D. Paynter, P. Ginoux, V. Naik, and L. W. Horowitz, 2018: Changes in the aerosol

7035   direct radiative forcing from 2001 to 2015: observational constraints and regional

7036   mechanisms. *Atmos. Chem. Phys.*, **18**, 13265–13281, doi:10.5194/acp-18-13265-2018.

7037 Pausata, F. S., L. Chafik, R. Caballero, and D. S. Battisti (2015), Impacts of high-latitude volcanic

7038   eruptions on ENSO and AMOC, Proc. Natl. Acad. Sci. U.S.A., 112(45), 13,784–13,788.

7039 Pechony, O. and Shindell, D. T.: Driving forces of global wildfires over the past millennium and

7040   the forthcoming century, Proc. Natl. Acad. Sci., 107(45), 19167–19170,

7041   doi:10.1073/pnas.1003669107, 2010

7042 Peers, F., Waquet, F., Cornet, C., Dubuisson, P., Ducos, F., Goloub, P., ... & Thieuleux, F.

7043   (2015). Absorption of aerosols above clouds from POLDER/PARASOL measurements and

7044   estimation of their direct radiative effect. *Atmospheric Chemistry and Physics*, *15*(8), 4179-

7045   4196.

7046 Penner, J. E., Dickinson, R. E., & O'Neill, C. A. (1992). Effects of aerosol from biomass burning

7047   on the global radiation budget. Science, 256(5062), 1432-1434.Stanhill, G., & Moreshet, S.

7048   (1992). Global radiation climate changes: The world network. *Climatic Change*, *21*(1), 57-

7049   75.

7050 Penner, J. E., Chuang, C. C., & Grant, K. (1998). Climate forcing by carbonaceous and sulfate

7051   aerosols. *Climate Dynamics*, *14*(12), 839-851.

7052 Penner et al., IPCC, 2001.

7053 Penner, J. E., R. E. Dickinson, and C. A. O'Neill, 1992: Effects of aerosol from biomass burning

7054   on the global radiation budget. *Science (80-.).*, **256**, 1432–1434,

7055   doi:10.1126/science.256.5062.1432.

7056   http://science.sciencemag.org/content/256/5062/1432.abstract.

7057 Penner, J. E. and J. S. Chang, 1978: Possible variations in atmospheric ozone related to the

7058   eleven-year solar cycle, Geophys. Res. Lett., 5, 817.

7059 Penner, J. E., Dickinson, R. E., & O'Neill, C. A. (1992). Effects of aerosol from biomass burning

7060   on the global radiation budget. *Science*, 256(5062), 1432-1434.

331

Penner, J. E., R. E. Dickinson, and C. A. O'Neill, 1992: Effects of aerosol from biomass burning on the global radiation budget. Science (80-.)., 256, 1432–1434, doi:10.1126/science.256.5062.1432. http://science.sciencemag.org/content/256/5062/1432.abstract.

Perlwitz, J., and H.-F. Graf (2001), Troposphere-stratosphere dynamic coupling under strong and weak polar vortex conditions. Geophys. Res. Lett., 28, 271–274.

Perner, D., D. H. Ehhalt, H. W. Pätz, U. Platt, E. P. Röth, and A. Volz, 1976: OH - Radicals in the lower troposphere. *Geophys. Res. Lett.*, **3**, 466–468, doi:doi:10.1029/GL003i008p00466. https://doi.org/10.1029/GL003i008p00466.

Persad, G., D J Paynter, Y Ming, and V Ramaswamy, 2017: Competing Atmospheric and Surface-Driven Impacts of Absorbing Aerosols on the East Asian Summertime Climate. *Journal of Climate*, **30(22)**, DOI:10.1175/JCLI-D-16-0860.1.

Peters, L. K., and Coauthors, 1995: The current state and future direction of Eulerian models in simulating the tropospheric chemistry and transport of trace species: a review. *Atmos. Environ.*, **29**, 189–222, doi:http://dx.doi.org/10.1016/1352-2310(94)00235-D. http://www.sciencedirect.com/science/article/pii/135223109400235D.

Pierrehumbert, R. T. (2011). Infrared radiation and planetary temperature. *Physics Today*, *64*(1), 33–38. http://doi.org/10.1063/1.3653855

Pilewski, P., G. Kopp, E. Richard, O. Coddington, S. Mauceri, T. Sparn, and T. Woods, 2018: TSIS-1 and continuity of the total and spectral solar irradiance climate data record, European Geosciences Union General Assembly 2018, Vienna, Austria, April 9-13.

Pinto, J. P., R. P. Turco, and O. B. Toon (1989), Self-limiting physical and chemical effects in volcanic eruption clouds, J. Geophys. Res., 94(D8), 11,165–11,174, doi:10.1029/JD094iD08p11165.

7086 Pinnock, S., M. D. Hurley, K. P. Shine, T. J. Wallington, and T. J. Smyth (1995), Radiative

7087   forcing of climate by hydrochlorofluorocarbons and hydrofluorocarbons, *J. Geophys. Res.*,

7088   100(D11), 23227–23238, doi:10.1029/95JD02323.

7089 Pincus, R., Forster, P. M., & Stevens, B. (2016). The Radiative Forcing Model Intercomparison

7090   Project (RFMIP): experimental protocol for CMIP6. *GEOSCIENTIFIC MODEL*

7091   *DEVELOPMENT*, *9*(9), 3447–3460. http://doi.org/10.5194/gmd-9-3447-2016

7092 Pincus, R., Forster, P. M., & Stevens, B. (2016): The Radiative Forcing Model Intercomparison

7093   Project (RFMIP): experimental protocol for CMIP6. *GEOSCIENTIFIC MODEL*

7094   *DEVELOPMENT*, *9*(9), 3447–3460. http://doi.org/10.5194/gmd-9-3447-2016

7095 Pinnock, S., M. D. Hurley, K. P. Shine, T. J. Wallington, and T. J. Smyth (1995), Radiative

7096   forcing of climate by hydrochlorofluorocarbons and hydrofluorocarbons, *J. Geophys. Res.*,

7097   100(D11), 23227–23238, doi:10.1029/95JD02323

7098 Pitari, G., and Coauthors (2014), Stratospheric ozone response to sulfate geoengineering: Results

7099   from the Geoengineering Model Intercomparison Project (GeoMIP). *Journal of Geophysical*

7100   *Research-Atmospheres*, 119, 2629-2653.

7101 Pitari, G., Schumann, U., Stordal, F., Zerefos, C., 2005. Aviation radiative forcing in 2000: an

7102   update of IPCC (1999). Meteorol. Zeit 114, 555–561.

7103 Plass, G. N. (1956a). Effect of Carbon Dioxide Variations on Climate. *American Journal of*

7104   *Physics*, *24*(5), 376–387. http://doi.org/10.1119/1.1934233

7105 Plass, G. N. (1956b). Infrared Radiation in the Atmosphere. *American Journal of Physics*, *24*(5),

7106   303–321. http://doi.org/10.1119/1.1934220

7107 Plass, G. N. (1956). The influence of the 15µ carbon-dioxide band on the atmospheric infra-red

7108   cooling rate. *Quarterly Journal of the Royal Meteorological Society*, *82*(353), 310–324.

7109   http://doi.org/10.1002/qj.49708235307

7110 Plass, G. N. (1956). The Carbon Dioxide Theory of Climatic Change. *Tellus*, *8*(2), 140–154.

7111   http://doi.org/10.1111/j.2153-3490.1956.tb01206.x

7112   Plass, G. N., 1956: The influence of the 15-micron carbon dioxide band on the atmospheric

7113   infrared cooling rate. *Quart. J. Roy. Meteor. Soc.,* **82,** 310-324.

7114   Platnick, S., 2018: The Earth Observer, vol. 30, Issue 2, pp1-3.

7115

7116

7117   Polson, D., M. Bollasina, G, C, Hegerl, and L. J. Wilcox, 2014: Decreased monsoon precipitation

7118   in the Northern Hemisphere due to anthropogenic aerosols, Geophys. Res. Lett., 41, 6023-

7119   6029. https://doi.org/10.1002/2014GL060811

7120

7121   Polvani, L, A. Banerjee, A. Schmidt, Northern Hemisphere continental winter warming following

7122   the 1991 Mt. Pinatubo eruption: reconciling models and observations (2019), Atmos. Chem.

7123   Phys., 19, 6351-6366, 2019,https://doi.org/10.5194/acp-19-6351-2019

7124   Ponater, M., Pechtl, S., Sausen, R., Schumann, U., and Hüttig, G. (2006) Potential of the

7125   cryoplane technology to reduce aircraft climate impact: a state-of-the-art assessment.

7126   Atmos. Environ., 40, 6928–6944.

7127   Portmann, R. W., S. Solomon, J. Fishman, J. R. Olson, J. T. Kiehl, and B. Briegleb, 1997:

7128   Radiative forcing of the Earth's climate system due to tropical tropospheric ozone

7129   production. *J. Geophys. Res.*, **102**, 9409–9418.

7130   Prather, M. J., 1994: Lifetimes and eigenstates in atmospheric chemistry. *Geophys. Res. Lett.*, **21**,

7131   801–804, doi:doi:10.1029/94GL00840. https://doi.org/10.1029/94GL00840.

7132   Prather, M., R. Sausen, A. S. Grossman, J. M. Haywood, D. Rind, and B. H. Subbaraya, 1999:

7133   Potential Climate Change from Aviation. IPCC Special Report on Aviation and the Global

7134   Atmosphere, 185–215.

7135   Prather, M. J., R. G. Derwent, D. Ehhalt, P. J. Fraser, E. Sanhueza, and X. Zhou, 1995: Other

7136   Trace Gases and Atmospheric Chemistry. *Climate Change 1994: Radiative Forcing of*

7137   *Climate Change and An Evalaution of the IPCC IS92 Emision Scenarios*, J.T. Houghton,

L.G. Meira Filho, J. Bruce, H. Lee, B.A. Callandar, E. Haites, N. Harris, and K. Maskell, Eds., Cambridge, U.K., New York, NY, USA, Melbourne, Australia.

Prather, M. J., and Coauthors, 2001: Atmospheric Chemistry and Greenhouse Gases. *Climate Change 2001: The Physical Science Basis. Contribution of Working Group I to the Third Assessment Report of the Intergovernmental Panel on Climate Change*, Y. Ding, D.J. Griggs, M. Noguer, P.J. van der Linden, X. Dai, K. Maskell, and C.A. Johnson, Eds., Cambridge University Press, Cambridge, United Kingdom and New York, NY, USA.

——, and Coauthors, 2018: How well can global chemistry models calculate the reactivity of short-lived greenhouse gases in the remote troposphere, knowing the chemical composition. *Atmos. Meas. Tech.*, **11**, 2653–2668, doi:10.5194/amt-11-2653-2018. https://www.atmos-meas-tech.net/11/2653/2018/.

Predybaylo, E., G. L. Stenchikov, A. T. Wittenberg, and F. Zeng (2017), Impacts of a Pinatubo-Size Volcanic Eruption on ENSO, J. Geophys. Res. Atmos., 122, 925–947, doi:10.1002/2016JD025796.

Previdi, M.: Radiative feedbacks on global precipitation, Environmental Research Letters, 5(2), 025211, 2010.

Prinn, R. G., and Coauthors, 2001: Evidence for Substantial Variations of Atmospheric Hydroxyl Radicals in the Past Two Decades. *Science (80-.).*, **292**, 1882 LP-1888, doi:10.1126/science.1058673. http://science.sciencemag.org/content/292/5523/1882.abstract.

Proctor, J., S. Hsiang, J. Burney, M. Burke, and W. Schlenker, 2018: Estimating global agricultural effects of geoengineering using volcanic eruptions. *Nature*, doi:10.1038/s41586-018-0417-3.

Pueschel, R. F. (1996), Stratospheric Aerosols: Formation, Properties, Effects, J. Aerosol Sci., 27, No. 3, 383-402.

7164   Quaas, J., Ming, Y., Menon, S., Takemura, T., Wang, M., Penner, J. E., ... & Sayer, A. M.

7165   (2009). Aerosol indirect effects–general circulation model intercomparison and evaluation

7166   with satellite data. *Atmospheric Chemistry and Physics*, *9*(22), 8697-8717.

7167

7168   Ramanathan, V. (1975). Greenhouse Effect Due to Chlorofluorocarbons: Climatic

7169   Implications. *Science*, *190*(4209), 50 LP-52 http://doi.org/10.1126/science.190.4209.50.

7170   Ramanathan, V., Lian, M. S., & Cess, R. D. (1979). Increased atmospheric CO2: Zonal and

7171   seasonal estimates of the effect on the radiation energy balance and surface

7172   temperature. *Journal of Geophysical Research: Oceans*, *84*(C8), 4949–4958.

7173   http://doi.org/10.1029/JC084iC08p04949

7174   _____, and A. Vogelmann, 1997: Greenhouse effect, atmospheric solar absorption, and the

7175   Earth's Radiation Budget: From the Arrhenius-Langley era to the 1990s. Ambio, 26, 1,

7176   pp38-46.

7177   Ramanathan, V., Crutzen, P. J., Kiehl, J. T. and Rosenfeld, D.: Atmosphere - Aerosols, climate,

7178   and the hydrological cycle, Science, 294(5549), 2119-2124, 2001.

7179   Ramanathan, V. (1975). Greenhouse Effect Due to Chlorofluorocarbons: Climatic Implications.

7180   *Science*, *190*(4209), 50 LP-52. http://doi.org/10.1126/science.190.4209.50

7181   Ramanathan, V. (1980). Climatic Effects of Anthropogenic Trace Gases. In W. Bach, J.

7182   Pankrath, & J. Williams (Eds.), *Interactions of Energy and Climate: Proceedings of an*

7183   *International Workshop held in Münster, Germany, March 3–6, 1980* (pp. 269–280).

7184   Dordrecht, Holland: D. Reidel Publishing Company. http://doi.org/10.1007/978-94-009-

7185   9111-8

7186   Ramanathan, V., Callis, L. B., & Boughner, R. E. (1976). Sensitivity of Surface Temperature and

7187   Atmospheric Temperature to Perturbations in the Stratospheric Concentration of Ozone and

7188   Nitrogen Dioxide. *Journal of the Atmospheric Sciences*, *33*(6), 1092–1112.

7189   http://doi.org/10.1175/1520-0469 (1976)033<1092:SOSTAA>2.0.CO;2

7190   Ramanathan, V., Cicerone, R. J., Singh, H. B., & Kiehl, J. T. (1985). Trace gas trends and their

7191   potential role in climate change. *Journal of Geophysical Research: Atmospheres*, *90*(D3),

7192   5547–5566. http://doi.org/10.1029/JD090iD03p05547

7193   Ramanathan, V., Lian, M. S., & Cess, R. D. (1979). Increased atmospheric CO2: Zonal and

7194   seasonal estimates of the effect on the radiation energy balance and surface temperature.

7195   *Journal of Geophysical Research: Oceans*, *84*(C8), 4949–4958.

7196   http://doi.org/10.1029/JC084iC08p04949

7197   Ramanathan, V., L. Callis, R. Cess, J. Hansen, I. Isaksen, W. Kuhn, A. Lacis, F. Luther, J.

7198   Mahlman, R. Reck, & M. Schlesinger(1987), Climate-chemical interactions and effects of

7199   changing atmospheric trace gases, *Rev. Geophys.*, 25(7), 1441–1482,

7200   doi:10.1029/RG025i007p01441.

7201   Ramanathan, V., and R. E. Dickinson, 1979: The Role of Stratospheric Ozone in the Zonal and

7202   Seasonal Radiative Energy Balance of the Earth-Troposphere System. J. Atmos. Sci., 36,

7203   1084–1104, doi:10.1175/1520-0469(1979)036<1084:TROSOI>2.0.CO;2.

7204   https://journals.ametsoc.org/doi/abs/10.1175/1520-

7205   0469%281979%29036%3C1084%3ATROSOI%3E2.0.CO%3B2.

7206   ——, M. S. Lian, and R. D. Cess, 1979: Increased atmospheric CO2: Zonal and seasonal

7207   estimates of the effect on the radiation energy balance and surface temperature. J. Geophys.

7208   Res. Ocean., 84, 4949–4958, doi:10.1029/JC084iC08p04949.

7209   https://doi.org/10.1029/JC084iC08p04949.

7210   ——, R. J. Cicerone, H. B. Singh, and J. T. Kiehl, 1985: Trace gas trends and their potential role

7211   in climate change. J. Geophys. Res. Atmos., 90, 5547–5566,

7212   doi:10.1029/JD090iD03p05547. https://doi.org/10.1029/JD090iD03p05547.

7213   ——, and Coauthors, 1987: Climate-chemical interactions and effects of changing atmospheric

7214   trace gases. Rev. Geophys., 25, 1441–1482, doi:10.1029/RG025i007p01441.

7215   https://doi.org/10.1029/RG025i007p01441.

7216   Ramanathan, V., 1975: Greenhouse Effect Due to Chlorofluorocarbons: Climatic Implications.

7217   Science (80-.)., 190, 50 LP-52, doi:10.1126/science.190.4209.50.

7218   http://science.sciencemag.org/content/190/4209/50.abstract.

——, 1981: The Role of Ocean-Atmosphere Interactions in the CO2 Climate Problem. J. Atmos. Sci., 38, 918–930, doi:10.1175/1520-0469(1981)038<0918:TROOAI>2.0.CO;2. https://doi.org/10.1175/1520-0469(1981)038%3C0918:TROOAI%3E2.0.CO.

Ramanathan, V., 1982: In Carbon dioxide review 1982, W. Clark, Ed., Oxford University Press, Clarendon, England, 278–283.

Ramanathan, V., 1981: The Role of Ocean-Atmosphere Interactions in the CO2-Climate Problems. J. Atmos. Sci., 38: 918-930.

Ramanathan, V., C. Chung, D. Kim, T. Bettge, L. Buja, J. T. Kiehl, W. M. Washington, Q. Fu, D. R. Sikka, and M. Wild, 2005: Atmospheric Brown Clouds: Impacts on South Asian Climate and Hydrological Cycle. *PNAS*, Vol. 102, No. 15, 5326-5333.

Ramanathan, V., and R. E. Dickinson, 1979: The Role of Stratospheric Ozone in the Zonal and Seasonal Radiative Energy Balance of the Earth-Troposphere System. *J. Atmos. Sci.*, **36**, 1084–1104, doi:10.1175/1520-0469(1979)036<1084:TROSOI>2.0.CO;2. https://journals.ametsoc.org/doi/abs/10.1175/1520-0469%281979%29036%3C1084%3ATROSOI%3E2.0.CO%3B2.

——, L. B. Callis, and R. E. Boughner, 1976: Sensitivity of Surface Temperature and Atmospheric Temperature to Perturbations in the Stratospheric Concentration of Ozone and Nitrogen Dioxide. *J. Atmos. Sci.*, **33**, 1092–1112, doi:10.1175/1520-0469(1976)033<1092:SOSTAA>2.0.CO;2. https://doi.org/10.1175/1520-0469(1976)033%3C1092:SOSTAA%3E2.0.CO.

Ramanathan, V., and Coauthors, 1985: Trace gas effects on climate. *World Meteorological Organization Global Ozone Research and Monitoring Project Report NO. 16 Atmospheric Ozone 1985 - Assessment of our Understanding of the Processes Controlling its Present Distribution and Change*.

Ramanathan, V., and Coauthors, 1987: Climate-chemical interactions and effects of changing atmospheric trace gases. *Rev. Geophys.*, **25**, 1441–1482, doi:doi:10.1029/RG025i007p01441. https://doi.org/10.1029/RG025i007p01441.

Ramaswamy, V, M D Schwarzkopf, W J Randel, B D Santer, B J Soden, and G Stenchikov, 2006: Anthropogenic and natural influences in the evolution of lower stratospheric cooling. *Science*, **311(5764)**, DOI:10.1126/science.1122587

7249 Ramaswamy, V, J W Hurrell, G A Meehl, A Phillips, B D Santer, M Daniel Schwarzkopf, D J
7250   Seidel, S C Sherwood, and P W Thorne, 2006: Why do temperatures vary vertically (from
7251   the surface to the stratosphere) and what do we understand about why they might vary and
7252   change over time? In *Temperature Trends in the Lower Atmosphere: Steps for*
7253   *Understanding and Reconciling Differences*, Karl, T R, S J Hassol, C D Miller, W L
7254   Murray, eds., Washington, DC, A Report by the Climate Change Science
7255   Program/Subcommittee on Global Change Research, 15-28.

7256 Ramaswamy, V., and Coauthors, 2001: Radiative Forcing of Climate Change. *Climate Change*
7257   *2001: Working Group I: The Scientific Basis*, F. Joos and J. Srinivasan, Eds.

7258 Ramaswamy, V., Boucher, O., Haigh, J., Hauglustaine, D., Haywood, J.M., Myhre, G.,
7259   Nakajima, T., Shi, G.Y., and Solomon, S., Radiative Forcing of Climate Change. Climate
7260   Change: The Scientific Basis. Contribution of Working Group I to the Third Assessment
7261   Report of the Intergovernmental Panel on Climate Change [Houghton, J.T., Y. Ding, D.J.
7262   Griggs, M. Noguer, P.J. van der Linden, X. Dai, K. Maskell, and C.A. Johnson (eds.)].
7263   Cambridge University Press, Cambridge, United Kingdom and New York, NY, USA, 349-
7264   416, 881pp, 2001.

7265 Ramaswamy, V, and C-T Chen, 1997: Linear additivity of climate response for combined albedo
7266   and greenhouse perturbations. *Geophysical Research Letters*, **24(5)**, 567-570.

7267 Ramaswamy, V, M D Schwarzkopf, and W J Randel, 1996: Fingerprint of ozone depletion in the
7268   spatial and temporal pattern of recent lower-stratospheric cooling. *Nature*, **382**, 616-618.

7269 Ramaswamy, V., M. D. Schwarzkopf, and K. P. Shine, 1992: Radiative forcing of climate from
7270   halocarbon-induced global stratospheric ozone loss. *Nature*, **355**, 810–812,
7271   doi:10.1038/355810a0. https://doi.org/10.1038/355810a0.

7272 Ramaswamy, V., K. Shine, C. Leovy, W.-C. Wang, H. Rodhe, and D. Wuebbles, 1991:
7273   Radiative forcing of climate. *Scientific Assessment of Ozone Depletion: 1991*, D.L.
7274   Albritton, R.T. Watson, S. Solomon, R.F. Hampson, and F. Ormond, Eds.

7275 Ramaswamy, V., Boucher, O., Haigh, J., Hauglustaine, D., Haywood, J.M., Myhre, G.,
7276   Nakajima, T., Shi, G.Y., and Solomon, S., Radiative Forcing of Climate Change. Climate
7277   Change: The Scientific Basis. Contribution of Working Group I to the Third Assessment

Report of the Intergovernmental Panel on Climate Change [Houghton, J.T., Y. Ding, D.J. Griggs, M. Noguer, P.J. van der Linden, X. Dai, K. Maskell, and C.A. Johnson (eds.)]. Cambridge University Press, Cambridge, United Kingdom and New York, NY, USA, 349-416, 881pp, 2001.

Ramaswamy, V., et al., (2006), Anthropogenic and natural infl uences in the evolution of lower stratospheric cooling. Science, 311, 1138–1141

Ramaswamy, V., M. D. Schwarzkopf, and K. P. Shine, 1992: Radiative forcing of climate from halocarbon-induced global stratospheric ozone loss. Nature, 355, 810–812, doi:10.1038/355810a0. https://doi.org/10.1038/355810a0.

——, and Coauthors, 2001: Radiative Forcing of Climate Change. Climate Change 2001: The Scientific Basis. Contribution of Working Group I to the Third Assessment Report of the Intergovernmental Panel on Climate Change, Y. Ding, D.J. Griggs, M. Noguer, P.J. Van der Linden, X. Dai, K. Maskell, and C.A. Johnson, Eds., Cambridge University Press, Cambridge, United Kingdom and New York, NY, USA.

Ramaswamy, V & Boucher, Olivier & Haigh, Joanna & Hauglustaine, D & Haywood, J & Myhre, Gunnar & Nakajima, T & Y Shi, G & Solomon, S. (2001). Radiative Forcing of Climate Change. In: *Climate Change 2001: The Scientific Basis. Contribution of Working Group I to the Third Assessment Report of the Intergovernmental Panel on Climate Change* [Houghton, J.T., Y. Ding, D.J. Griggs, M. Noguer, P.J. van der Linden, X. Dai, K. Maskell, and C.A. Johnson (eds.)]. Cambridge University Press, Cambridge, United Kingdom and New York, NY, USA, 881pp.

Ramachandran, S., V. Ramaswamy, G.L. Stenchikov, and A. Robock (2000), Radiative impact of the Mt. Pinatubo volcanic eruption: Lower stratospheric response. J. Geophys. Res., 105(D19), 24409–24429.

Randall, C. E., R. M. Bevilacqua, J. D. Lumpe, and K. W. Hoppel, (2001), Validation of POAM III aerosols: Comparison to SAGE II and HALOE. *J Geophys Res*, 106, 27,525-527,536.

Randall, C. E., R. M. Bevilacqua, J. D. Lumpe, K. W. Hoppel, D. W. Rusch, and E. P. Shettle (2000), Comparison of polar ozone and aerosol measurement (POAM) II and Stratospheric

7306   Aerosol and Gas Experiment (SAGE) II aerosol measurements from 1994 to 1996. *J Geophys*

7307   *Res*, 105, 3929-3942.

7308   Randel, W., F. Wu, S. Oltmans, K. Rosenlof, G. Nedoluha (2004), Interannual Changes of

7309   Stratospheric Water vapor and Correlations with Tropical Tropopause Temperatures, J.

7310   Atmos. Res., 61, 2133-2148.

7311   Rap, A., Forster, P.M., Haywood, J.M., Jones, A., and Boucher, O. (2010) Estimating the climate

7312   impact of linear contrails using the UK Met Office climate model. Geophys. Res. Lett., 37,

7313   L20703.

7314   Rasch, P.J., Simone Tilmes , Richard P Turco, Alan Robock, Luke Oman, Chih-Chieh (Jack)

7315   Chen, Georgiy L Stenchikov and Rolando R Garcia, 2008: An overview of geoengineering

7316   of climate using stratospheric sulphate aerosols, *Philosophical Transactions of the Royal*

7317   *Society –A- Mathematical, Physical and Engineering Sciences*

7318   https://doi.org/10.1098/rsta.2008.0131

7319

7320   Rayleigh, Lord (Strutt, Hon. J, W.), 1871: On the light from the sky, its polarization and

7321   colour. *The London, Edinburgh, and Dublin Philosophical Magazine and Journal of*

7322   *Science*. **41** (271): 107–120. doi:10.1080/14786447108640452.

7323   Rayleigh, Lord, 1881: On the electromagnetic theory of light. *The London, Edinburgh, and*

7324   *Dublin Philosophical Magazine and Journal of Science*. **12** (73): 81-

7325   101. doi:10.1080/14786448108627074.

7326   Richardson, T. B., and Coauthors, 2019: Efficacy of climate forcings in PDRMIP models.

7327   Submitted.

7328   Robock, A. (2000), Volcanic eruptions and climate, Rev. Geophys., 38(2), 191–219,

7329   doi:10.1029/1998RG000054.

7330   Robock, A., Jerch, K. and Bunzl, M., 2008. 20 reasons why geoengineering may be a bad idea.

7331   *Bulletin of the Atomic Scientists*, *64*(2), pp.14-59.

7332 Robock, A., Luke Oman, Georgiy L. Stenchikov, 2008: Regional climate responses to
7333   geoengineering with tropical and Arctic SO2 injections; *Journal of Geophysical Research*
7334   *Atmospheres*. https://doi.org/10.1029/2008JD010050

7335

7336 Roe, G. H., N. Feldl, K. C. Armour, Y.-T. Hwang, and D. M. W. Frierson (2015), The remote
7337   impacts of climate feedbacks on regional climate predictability, Nat. Geosci., 8, 135–139,
7338   doi:10.1038/ngeo2346.

7339 Rose, B. E. J., K. C. Armour, D. S. Battisti, N. Feldl, and D. D. B. Koll (2014), The dependence
7340   of transient climate sensitivity and radiative feedbacks on the spatial pattern of ocean heat
7341   uptake, Geophys. Res. Lett., 41, 1071–1078, doi:10.1002/2013GL058955.

7342 Rotstayn, L. D. & Lohmann, U. Tropical rainfall trends and the indirect aerosol effect. *J. Clim.* **15,**
7343   2103-2116 (2002).

7344 Rotstayn, L. D., and J. E. Penner, 2001: Indirect Aerosol Forcing, Quasi Forcing, and Climate
7345   Response. J. Clim., 14, 2960–2975, doi:10.1175/1520-
7346   0442(2001)014<2960:IAFQFA>2.0.CO;2. https://doi.org/10.1175/1520-
7347   0442(2001)014%3C2960:IAFQFA%3E2.0.CO.

7348 Rotstayn, L., Indirect forcing by anthropogenic aerosols: A general circulation model calculation
7349   of the effective-radius and cloud lifetime effects, J. Geophys. Res., 104, 9369–9380, 1999.

7350 Regener, V. H., 1938: Messung des Ozongehalts der Luft in Bodennahe. *Met. Zeitschr*, **55**, 459–
7351   462.

7352 Renner, E. D., and G. E. Becker, 1970: Production of nitric oxide and nitrous oxide during
7353   denitrification by Corynebacterium nephridii. *J. Bacteriol.*, **101**, 821–826.
7354   https://www.ncbi.nlm.nih.gov/pubmed/5438050.

7355 Rigby, M., and Coauthors, 2017: Role of atmospheric oxidation in recent methane growth. *Proc.*
7356   *Natl. Acad. Sci. U. S. A.*, **114**, 5373–5377, doi:10.1073/pnas.1616426114.

7357 Robinson, E., and R. C. Robbins, 1970: Gaseous Atmospheric Pollutants from Urban and

7358   Natural Sources BT - Global Effects of Environmental Pollution: A Symposium Organized

7359   by the American Association for the Advancement of Science Held in Dallas, Texas,

7360   December 1968. S.F. Singer, Ed., Springer Netherlands, Dordrecht, 50–64

7361   https://doi.org/10.1007/978-94-010-3290-2_7.

7362   Roelofs, G.-J., J. Lelieveld, and R. Dorland, 1997: A three-dimensional chemistry/general

7363   circulation model simulation of anthropogenically derived ozone in the troposphere and its

7364   radiative climate forcing. *J. Geophys. Res. Atmos.*, **102**, 23389–23401,

7365   doi:doi:10.1029/97JD02210. https://doi.org/10.1029/97JD02210.

7366   Rohrer, F., and Coauthors, 2014: Maximum efficiency in the hydroxyl-radical-based self-

7367   cleansing of the troposphere. *Nat. Geosci.*, **7**, 559–563, doi:10.1038/ngeo2199.

7368   Royal Society, 2009: Geoengineering the climate. Science, governance, and uncertainty. Report

7369   10/09, Royal Society, London, UK, 82 pp.

7370   Ringeval, B., de Noblet-ducoudre, N., Ciais, P., Bousquet, P., Prigeent, C., Papa, F. and Rossow,

7371   W.: An attempt to quantify the impact of changes in wetland extent on methane emissions

7372   on the seasonal and interannual time scales, Global Biogeochem. Cycles, 24(GB2003),

7373   doi:10.1029/2008gb003354, 2010.

7374   Roger A. Pielke, S.: Land Use and Climate Change, Science (80-.)., 310, 1624–1625,

7375   doi:10.1126/science.1120529, 2005.

7376   Read, W. G., L. Froidevaux, and J. W. Waters (1993), Microwave limb sounder measurement of

7377   stratospheric SO2 from the Mount Pinatubo volcano, Geophys. Res. Lett., 20, 1299–1302,

7378   doi:10.1029/93GL00831.

7379   Robock, A. (2000), Volcanic eruptions and climate, Rev. Geophys., 38(2), 191–219,

7380   doi:10.1029/1998RG000054.

7381   Robock, A., C. M. Ammann, L. Oman, D. Shindell, S. Levis, and G. Stenchikov (2009), Did the

7382   Toba volcanic eruption of 74 ka B.P. produce widespread glaciation? *Journal of Geophysical*

7383   *Research-Atmospheres*, 114, D10107.

7384 Robock, A., M. Bunzl, B. Kravitz, and G. L. Stenchikov (2010), A Test for Geoengineering?
7385   *Science*, 327, 530-531.

7386 Russell, P. B., J. M. Livingston, E. G. Dutton, R. F. Pueschel, J. A. Reagan, T. E. DeFoor, M. A.
7387   Box, D. Allen, P. Pilewskie, B. M. Herman, S. A. Kinne and D. J. Hofmann (1993), Pinatubo
7388   and pre-Pinatubo optical-depth spectra: Mauna Loa measurements, comparisons, inferred
7389   particle size distributions, radiative effects, and relationship to lidar data, J. Geophys. Res.,
7390   98, 22969-22985.

7391 Richard, E., D. Harber, J. Rutkowski, K. O'Malia, M. Triplett, G. Drake, J. Harder, P. Pilewskie,
7392   S. Brown, A. Smith, and K. Lykke, 2011: Future Long-term Measurements of Solar
7393   Spectral Irradiance by the TSIS Spectral Irradiance Monitor: Improvements in Measurement
7394   Accuracy and Stability. Proceedings 11th International Conference on New Developments
7395   and Applications in Optical Radiometry, Maui, HI, S. Park and E. Ikonen, Eds., paper
7396   INV004.

7397 Rind, D., J. Lean, and R. Healy, 1999: Simulated time-dependent climate response to solar
7398   radiative forcing since 1600, J. Geophys. Res., 104(D2), 1973–1990,
7399   doi:10.1029/1998JD200020.

7400 Rind, D., J. Lean, J. Lerner, P. Lonergan, C. McLinden and A. Leboissitier, 2008: Exploring the
7401   Stratospheric/Tropospheric Response to Solar Forcing, J. Geophys. Res. ,113, D24103,
7402   doi:10.1029/2008JD010114.

7403 Roth, R., and F. Joos, 2013: A reconstruction of radiocarbon production and total solar irradiance
7404   from the Holocene 14C and CO2 records: implications of data and model uncertainties.
7405   Clim. Past, 9, 1879–1909, doi:10.5194/cp-9-1879-2013

7406 Rottman, G., 2006: Measurements of total and spectral solar irradiance, Space Sci. Rev., 125, 39-
7407   51, DOI: 10.1007/s11214-006-9045-6.

7408 Rottman, G., Harder, J., and J. Fontenla, 2005: The Spectral Irradiance Monitor (SIM): Early
7409   Observations, Solar Physics, 230: 205. https://doi.org/10.1007/s11207-005-1530-7

7410

7411   Samset, B. H., and Coauthors, 2016: Fast and slow precipitation responses to individual climate

7412   forcers: A PDRMIP multimodel study. Geophys. Res. Lett., 43,

7413   doi:10.1002/2016GL068064.

7414   Santer, B.D., et al., 1995: Towards the detection and attribution of an anthropogenic effect on

7415   climate. *Clim. Dyn.*, **12**, 77–100.

7416   Santer, B.D., et al., 1996: A search for human influences on the thermal structure of the

7417   atmosphere. *Nature*, **382**, 39–46.

7418   Santer, B.D., T.M.L. Wigley, T.P. Barnett, and E. Anyamba, 1996b: Detection of climate change,

7419   and attribution of causes. In: *Climate Change 1995: The Science of Climate*

7420   *Change* [Houghton, J.T., et al. (eds.)]. Cambridge University Press, Cambridge, United

7421   Kingdom and New York, NY, USA, pp. 407–443.

7422   Sausen, R., Isaksen, I., Grewe, V., Hauglustaine, D., Lee, D.S., Myhre, G., Kö hler, M.O., Pitari,

7423   G., Schumann, U., Stordal, F., Zerefos, C., 2005. Aviation radiative forcing in 2000: an

7424   update of IPCC (1999). Meteorol. Zeit 114, 555–561.

7425   Schimel, D., and Coauthors, 1996: Radiative Forcing of Climate Change. *Climate Change 1995:*

7426   *The science of climate change*, J.T. Houghton, L.G. Meira Filho, B.A. Callandar, N. Harris,

7427   A. Kattenberg, and K. Maskell, Eds., Cambridge University Press, Cambridge, U.K., New

7428   York, NY, USA, Melbourne, Australia.

7429   Schimel, D. D., and Coauthors, 1996: Radiative forcing of climate change. (eds.). Contribution

7430   of Working Group I to the Second Assessment Report of the Intergovernmental Panel on

7431   Climate Change. Cambridge University Press, Cambridge, U.K. 572 pp. Climate Change

7432   1995—The Science of Climate Change, J.T. Houghton, L.G. Meira Filho, B.A. Callander,

7433   N. Harris, A. Kattenberg, and K. Maskell, Eds., Cambridge University Press, Cambridge,

7434   U.K., 65–131.

7435   Schimel, D., and Coauthors, 1996: Radiative Forcing of Climate Change. *Climate Change 1995:*

7436   *The science of climate change*, J.T. Houghton, L.G. Meira Filho, B.A. Callandar, N. Harris,

7437   A. Kattenberg, and K. Maskell, Eds., Cambridge University Press, Cambridge, U.K., New

7438   York, NY, USA, Melbourne, Australia.

7439 Schmidt, A et al., Satellite detection, long-range transport, & air quality impacts of volcanic

7440   sulfur dioxide from the 2014–2015 flood lava eruption at Bárðarbunga (Iceland). JGR,

7441   9739-9757, 2015.

7442 Schulz, M., Textor, C., Kinne, S., Balkanski, Y., Bauer, S., Berntsen, T., ... & Isaksen, I. S. A.

7443   (2006). Radiative forcing by aerosols as derived from the AeroCom present-day and pre-

7444   industrial simulations. *Atmospheric Chemistry and Physics*, *6*(12), 5225-5246.

7445 Schwarz, J. P., J. R. Spackman, R. S. Gao, L. A. Watts, P. Stier, M. Schulz, S. M. Davis, S. C.

7446   Wofsy, and D. W. Fahey (2010), Global-scale black carbon profiles observed in the remote

7447   atmosphere and compared to models, Geophys. Res. Lett., 37, L18812,

7448   doi:10.1029/2010GL044372.

7449 Stier, P., Feichter, J., Kinne, S., Kloster, S., Vignati, E., Wilson, J., Ganzeveld, L., Tegen, I.,

7450   Werner, M., Balkanski, Y., Schulz, M., Boucher, O., Minikin, A., and Petzold, A.: The

7451   aerosol climate model ECHAM5-HAM, Atmos. Chem. Phys., 5, 1125–1156, 2005,

7452   http://www.atmos-chem-phys.net/5/1125/2005/.

7453 Shindell, D. T., Faluvegi, G., Rotstayn, L. & Milly, G. Spatial patterns of radiative forcing and

7454   surface temperature response. *J. Geophys. Res. Atmos.* **120,** 5385-5403 (2015).

7455 Shindell, D. T., Faluvegi, G., Rotstayn, L. & Milly, G. Spatial patterns of radiative forcing and

7456   surface temperature response. *J. Geophys. Res. Atmos.* **120,** 5385-5403 (2015).

7457 Schumann, U., Baumann, R., Baumgardner, D., Bedka, S. T., Duda, D. P., Freudenthaler, V.,

7458   Gayet, J.-F., Heymsfield, A. J., Minnis, P., Quante, M., Raschke, E., Schlager, H., Vázquez-

7459   Navarro, M., Voigt, C., and Wang, Z.: Properties of individual contrails: a compilation of

7460   observations and some comparisons, Atmos. Chem. Phys., 17, 403-438,

7461   https://doi.org/10.5194/acp-17-403-2017, 2017.

7462 Schumann, U. and Mayer, B.: Sensitivity of surface temperature to radiative forcing by contrail

7463   cirrus in a radiative-mixing model, Atmos. Chem. Phys., 17, 13833-13848,

7464   https://doi.org/10.5194/acp-17-13833-2017, 2017.

Schneider, S. H., and R. E. Dickinson, 1974: Climate modeling. Rev. Geophys., 12, 447–493, doi:10.1029/RG012i003p00447. https://doi.org/10.1029/RG012i003p00447.

Scott, N.A., & Chedin, A. (1981) A Fast Line-by-Line Method for Atmospheric Absorption Computations: The Automatized Atmospheric Absorption Atlas. *Journal of Applied Meteorology*, *20(7),* 802—812, *https://doi.org/10.1175/1520-0450(1981)020<0802:AFLBLM>2.0.CO;2.*

Von Schneidemesser, E., and Coauthors, 2015: Chemistry and the Linkages between Air Quality and Climate Change. *Chem. Rev.*, **115**, 3856–3897, doi:10.1021/acs.chemrev.5b00089.

Schwarzkopf, M. D., and V. Ramaswamy, 1993: Radiative forcing due to ozone in the 1980s: Dependence on altitude of ozone change. *Geophys. Res. Lett.*, **20**, 205–208, doi:doi:10.1029/93GL00209. https://doi.org/10.1029/93GL00209.

Singh, H. B., 1977: Atmospheric halocarbons: Evidence in favor of reduced average hydroxyl radical concentration in the troposphere. *Geophys. Res. Lett.*, **4**, 101–104, doi:doi:10.1029/GL004i003p00101. https://doi.org/10.1029/GL004i003p00101.

Sitch, S., P. M. Cox, W. J. Collins, and C. Huntingford, 2007: Indirect radiative forcing of climate change through ozone effects on the land-carbon sink. *Nature*, **448**, 791-U4, doi:Doi 10.1038/Nature06059.

Seinfeld JH[1], Bretherton C[2], Carslaw KS[3], Coe H[4], DeMott PJ[5], Dunlea EJ[6], Feingold G[7], Ghan S[8], Guenther AB[9], Kahn R[10], Kraucunas I[8], Kreidenweis SM[5], Molina MJ[11], Nenes A[12], Penner JE[13], Prather KA[11], Ramanathan V[14], Ramaswamy V[15], Rasch PJ[8], Ravishankara AR[5], Rosenfeld D[16], Stephens G[17], Wood R[2]. 2016: Improving our fundamental understanding of the role of aerosol-cloud interactions in the climate system. Proc Natl Acad Sci, 113(21):5781-90. doi: 10.1073/pnas.1514043113.

Senior, C. A., and J. F. B. Mitchell (2000), The time dependence of climate sensitivity, Geophys. Res. Lett., 27, 2685–2688.

7490 Sherwood, S. C., Bony, S., Boucher, O., Bretherton, C., Forster, P. M., Gregory, J. M. and
7491   Stevens, B.: Adjustments in the Forcing-Feedback Framework for Understanding Climate
7492   Change, Bulletin of the American Meteorological Society, 96(2), 217-228, 2015.

7493 Shindell, D. T.: Inhomogeneous forcing and transient climate sensitivity, Nature Climate
7494   Change, 4(4), 274-277, 2014.

7495 Shindell, D., and Coauthors, 2013: Attribution of historical ozone forcing to anthropogenic
7496   emissions. *Nat. Clim. Chang.*, **3**, 567. https://doi.org/10.1038/nclimate1835.

7497 Shindell, D. T., G. Faluvegi, N. Bell, and G. A. Schmidt, 2005: An emissions-based view of
7498   climate forcing by methane and tropospheric ozone. *Geophys. Res. Lett.*, **32**, L04803,
7499   doi:10.1029/2004gl021900. http://dx.doi.org/10.1029/2004GL021900.

7500 Shindell, D. T., G. Faluvegi, N. Unger, E. Aguilar, G. A. Schmidt, D. M. Koch, S. E. Bauer, and
7501   R. L. Miller, 2006: Simulations of preindustrial, present-day, and 2100 conditions in the
7502   NASA GISS composition and climate model G-PUCCINI. *Atmos. Chem. Phys.*, **6**, 4427–
7503   4459, doi:10.5194/acp-6-4427-2006. http://www.atmos-chem-phys.net/6/4427/2006/.

7504 Shindell, D. T., G. Faluvegi, D. M. Koch, G. A. Schmidt, N. Unger, and S. E. Bauer, 2009:
7505   Improved Attribution of Climate Forcing to Emissions. *Science (80-.).*, **326**, 716–718,
7506   doi:10.1126/science.1174760. http://www.sciencemag.org/content/326/5953/716.abstract.

7507 Shindell, D., Kuylenstierna, J., Vignati, E., van Dingenen, R., Amann, M., Klimont, Z.,
7508   Anenberg, S., Muller, N., Janssens-Maenhout, G., Raes, F., Schwartz, J., Faluvegi, G.,
7509   Pozzoli, L., Kupiainen, K., Hoglund-Isaksson, L., Emberson, L., Streets, D., Ramanathan,
7510   V., Hicks, K., Oanh, N., Milly, G., Williams, M., Demkine, V. and Fowler, D.:
7511   Simultaneously mitigating near-term climate change and improving human health and food
7512   security, Science (80-.)., 335, 185–189, 2012.

7513 Shindell, D. T., Lamarque, J.-F., Schulz, M., Flanner, M., Jiao, C., Chin, M., Young, P. J., Lee,
7514   Y. H., Rotstayn, L., Mahowald, N., Milly, G., Faluvegi, G., Balkanski, Y., Collins, W. J.,
7515   Conley, A. J., Dalsoren, S., Easter, R., Ghan, S., Horowitz, L., Liu, X., Myhre, G.,
7516   Nagashima, T., Naik, V., Rumbold, S. T., Skeie, R., Sudo, K., Szopa, S., Takemura, T.,
7517   Voulgarakis, A., Yoon, J.-H. and Lo, F.: Radiative forcing in the ACCMIP historical and

7518   future climate simulations, Atmos. Chem. Phys., 13(6), doi:10.5194/acp-13-2939-2013,
7519   2013.

7520 Shindell, D. T., Borgford-Parnell, N., Brauer, M., Haines, A., Kuylenstierna, J., Leonard, S. A.,
7521   Ramanthan, V., Ravishankara, A. R., Amman, M. and Srivastava, L.: A climate policy
7522   pathway for near- and long-term benefits, Science (80-.)., 356(6337), 493–494, 2017.

7523 Shine, K. P., Y. Fouquart, V. Ramaswamy, S. Solomon, and J. Srinivasan., 1995: Radiative
7524   forcing. Climate Change 1994. Radiative Forcing of Climate Change and an Evaluation of
7525   the IPCC IS92 Emission Scenarios, J.T. Houghton, L.G.M. Filho, J. Bruce, H. Lee, B.A.
7526   Callander, E. Haites, N. Harris, and K. Maskell, Eds., Cambridge University Press,
7527   Cambridge, U.K., 163–203.

7528 Shine, K. P., Derwent, R. G., Wuebbles, D. J., & J-J. Morcrette. (1990). Radiative Forcing of
7529   Climate. In J. T. Houghton, G. J. Jenkins, & J. J. Ephraums (Eds.), *Climate Change: The*
7530   *IPCC Scientific Assessment (1990)* (p. 410). Cambridge, Great Britain, New York, NY,
7531   USA and Melbourne, Australia: Cambridge University Press.

7532 Shine, K. P., Cook, J., Highwood, E. J. and Joshi, M. M.: An alternative to radiative forcing for
7533   estimating the relative importance of climate change mechanisms, Geophysical Research
7534   Letters, 30(20), 2047, 2003.

7535 Shine, K. P., R. G. Derwent, D. J. Wuebbles, and J.-J. Morcrette, 1990: Radiative forcing of
7536   Climate. Radiative forcing of Climate, J.T. Houghton, G.J. Jenkins, and J.J. Ephraums,
7537   Eds., 41–68.

7538 ——, Y. Fouquart, V. Ramaswamy, S. Solomon, and J. Srinivasan., 1995: Radiative forcing.
7539   Climate Change 1994—Radiative Forcing of Climate Change and an Evaluation of the
7540   IPCC IS92 Emission Scenarios, J.T. Houghton, L.G.M. Filho, J. Bruce, H. Lee, B.A.
7541   Callander, E. Haites, N. Harris, and K. Maskell, Eds., Cambridge University Press,
7542   Cambridge, U.K., 163–203.

7543 Shine, K. P., Derwent, R. G., Wuebbles, D. J., & J-J. Morcrette. (1990). Radiative Forcing of
7544   Climate. In J. T. Houghton, G. J. Jenkins, & J. J. Ephraums (Eds.), *Climate Change: The*
7545   *IPCC Scientific Assessment (1990)* (p. 410). Cambridge, Great Britain, New York, NY,

7546   USA and Melbourne, Australia: Cambridge University Press.

7547   Shine, K. P., R. G. Derwent, D. J. Wuebbles, and J.-J. Morcrette, 1990: Radiative Forcing of
7548   Climate. *Climate Change: The IPCC Scientific Assessment (1990)*, J.T. Houghton, G.J.
7549   Jenkins, and J.J. Ephraums, Eds., Cambridge University Press, Cambridge, U.K. and New
7550   York, NY, USA.

7551   Shine, K. P., and Coauthors, 1995a: Radiative forcing due to changes in ozone: a comparison of
7552   different codes BT - Atmospheric Ozone as a Climate Gas. W.-C. Wang and I.S.A. Isaksen,
7553   Eds., Berlin, Heidelberg, Springer Berlin Heidelberg, 373–396.

7554   Shine, K. P., Y. Fouquart, V. Ramaswamy, S. Solomon, and J. Srinivasan, 1995b: Radiative
7555   Forcing. *Climate Change 1994: Radiative Forcing of Climate Change and An Evalaution of*
7556   *the IPCC IS92 Emision Scenarios*, J.T. Houghton, L.G. Meira Filho, J. Bruce, L. Hoesung,
7557   B.A. Callandar, E. Haites, N. Harris, and K. Maskell, Eds., Cambridge, U.K., New York,
7558   NY, USA, Melbourne, Australia.

7559   Shine, K. P., K. Labitzke, V. Ramaswamy, P. C. Simon, S. Solomon, and W.-C. Wang, 1995c:
7560   Radiative forcing and temperature trends. *Scientific Assessment of Ozone Depletion: 1994*,
7561   D.L. Albritton, R.T. Watson, and P.J. Aucamp, Eds., World Meteorological Organization
7562   (WMO), Geneva, Switzerland.

7563   Shine, K. P., Derwent, R. G., Wuebbles, D. J., & J-J. Morcrette. (1990). Radiative Forcing of
7564   Climate. In J. T. Houghton, G. J. Jenkins, & J. J. Ephraums (Eds.), Climate Change: The
7565   IPCC Scientific Assessment (1990) (p. 410). Cambridge, Great Britain, New York, NY,
7566   USA and Melbourne, Australia: Cambridge University Press.

7567   Shine, K. P.: 1991, 'On the cause of the relative greenhouse strength of gases such as the
7568   halocarbons', Journal of the Atmospheric Science 48, 1513–1518.

7569   Shine, K. P., and P. M. d. F. Forster, 1999: The effect of human activity on radiative forcing of
7570   climate change: a review of recent developments. *Glob. Planet. Change*, **20**, 205–225,
7571   doi:https://doi.org/10.1016/S0921-8181(99)00017-X.
7572   http://www.sciencedirect.com/science/article/pii/S092181819900017X.

7573   Smith, C. J., and Coauthors, 2018: Understanding Rapid Adjustments to Diverse Forcing Agents.

7574   Geophys. Res. Lett., 45, 12,12-23,31, doi:10.1029/2018GL079826.

7575   https://doi.org/10.1029/2018GL079826.

7576   Smith, H. J. P., Dube, D. J., Gardner, M. E., Clough, S. A., Kneizys, F. X., & L.S. Rothman.

7577   (1978). *FASCODE -- Fast Atmosphere Signature Code (Spectral Transmittance and*

7578   *Radiance)*. Hanscom AFB, MA.

7579   Smith, C. J., Kramer, R. J., Myhre, G., Forster, P., Soden, B., Andrews, T., Boucher, O.,

7580   Faluvegi, G., Fläschner, D., Hodnebrog, Ø., Kasoar, M., Kharin, V., Kirkevåg, A.,

7581   Lamarque, J. F., Mülmenstädt, J., Olivié, D., Richardson, T., Samset, B. H., Shindell, D.,

7582   Stier, P., Takemura, T., Voulgarakis, A. and Watson-Parris, D.: Understanding rapid

7583   adjustments to diverse forcing agents, Geophysical Research Letters, 45, 12023-

7584   12031, https://doi.org/10.1029/2018GL079826, 2018.

7585   Snow, M., Eparvier, F., Harder, J., Jones, A., McClintock, W., Richard, E., and T. Woods, 2018:

7586   Ultraviolet Solar Spectral Irradiance Variation on Solar Cycle Timescales. Proceedings of

7587   the International Astronomical Union, 13(S340), 203-208.

7588   doi:10.1017/S1743921318001278

7589   Steinhilber, F, Abreu, J. A., Beer, J., Brunner, I., Christl, M., Fischer, H., Heikkila, U., Kubik, P.

7590   W., Mann, M., McCracken, K. G., Miller, H., Miyahara, H., Oerter, H., and Wilhelms, F.,

7591   2012: 9,400 years of cosmic radiation and solar activity from ice cores and tree rings.

7592   Proceedings of the National Academy of Sciences, 109, i16, 5967-5971 DOI

7593   10.1073/pnas.1118965109

7594   Stevens, M. J., and G. R. North, 1996: Detection of the climate response to the solar cycle, J.

7595   Atmos. Sci., 53, 2594-2608.

7596   Slingo, A., 1990: Sensitivity of the Earth's radiation budget to changes in low clouds.

7597   *Nature*, **343**, 49. https://doi.org/10.1038/343049a0.

7598   Stenchikov, G., T. L. Delworth, V. Ramaswamy, R. J. Stouffer, A. Wittenberg, and F. Zeng,

7599   2009: Volcanic signals in oceans. *J. Geophys. Res. Atmos.*, doi:10.1029/2008JD011673.

7600   Storelvmo, T., J. E. Kristjansson, H. Muri, M. Pfeffer, D. Barahona, and A. Nenes, 2013: Cirrus

7601   cloud seeding has potential to cool climate. *Geophys. Res. Lett.*,

7602   doi:10.1029/2012GL054201.

7603   Soden, B. J., Held, I. M., Colman, R., Shell, K. M., Kiehl, J. T. and Shields, C. A.: Quantifying

7604   Climate Feedbacks Using Radiative Kernels, Journal of Climate, 21(14), 3504-3520, 2008.

7605   Soden, B. J., Collins, W. D., & Feldman, D. R. (2018). Reducing uncertainties in climate models.

7606   *Science*, *361*(6400), 326–327. http://doi.org/10.1126/science.aau1864

7607   Soden, B. J., W. D. Collins, and D. R. Feldman, 2018: Reducing uncertainties in climate models.

7608   Science, 361, 326–327, doi:10.1126/science.aau1864.

7609   Soden, B. J., Collins, W. D. and Feldman, D. R.: Reducing uncertainties in climate models,

7610   Science, 361(6400), 326-327, 2018.

7611   Solomon, S., 1999: Stratospheric ozone depletion: A review of concepts and history. *Rev.*

7612   *Geophys*, **37**, 275–316.

7613   Stephens, G. L., 2005: Cloud Feedbacks in the Climate System: A Critical Review. J. Clim., 18,

7614   237–273, doi:10.1175/JCLI-3243.1. https://doi.org/10.1175/JCLI-3243.1.

7615   Stevenson, D. S., C. E. Johnson, W. J. Collins, R. G. Derwent, K. P. Shine, and J. M. Edwards,

7616   1998: Evolution of tropospheric ozone radiative forcing. *Geophys. Res. Lett.*, **25**, 3819–

7617   3822, doi:doi:10.1029/1998GL900037. https://doi.org/10.1029/1998GL900037.

7618   ——, and Coauthors, 2013: Tropospheric ozone changes, radiative forcing and attribution to

7619   emissions in the Atmospheric Chemistry and Climate Model Intercomparison Project

7620   (ACCMIP). *Atmos. Chem. Phys.*, **13**, 3063–3085, doi:10.5194/acp-13-3063-2013.

7621   http://www.atmos-chem-phys.net/13/3063/2013/.

7622   Stolarski, R., V. Fioletov, L. Bishop, S. Godin, R. D. Bojkov, V. Kirchhoff, M.-L. Chanin, and J.

7623   Zawodny, 1991: Ozone and temperature trends. *Scientific Assessment of Ozone Depletion:*

7624   *1991*, D.L. Albritton, R.T. Watson, S. Solomon, R.F. Hampson, and F. Ormond, Eds.

7625   Stone, D., L. K. Whalley, and D. E. Heard, 2012: Tropospheric OH and HO2 radicals: field

measurements and model comparisons. *Chem. Soc. Rev.*, **41**, 6348–6404, doi:10.1039/c2cs35140d.

Stordal, F., R. G. Derwent, I. S. A. Isaksen, D. J. Jacob, M. Kanakidou, J. A. Logan, and M. J. Prather, 1995: Model Simulations of global tropospheric ozone. *Scientific Assessment of Ozone Depletion: 1994*, D.L. Albritton, R.T. Watson, and P.J. Aucamp, Eds., World Meteorological Organization (WMO), Geneva, Switzerland.

Stouffer, R. J., S. Manabe, and K. Bryan, 1989): Interhemispheric asymmetry in climate response to a gradual increase of atmospheric CO_2. *Nature*, **342**, 660-662.

Stephens, G. L., 2005: Cloud feedbacks in the climate system: A critical review. J. Climate, 18, 237–273, doi:10.1175/JCLI-3243.1

Sterner EO and DJA Johansson (2017). The effect of climate–carbon cycle feedbacks on emission metrics Environ. Res. Lett. 12 034019 10.1088/1748-9326/aa61dc

Stott, P.A., et al., 2000: External control of 20th century temperature by natural and anthropogenic forcings. *Science*, **290**, 2133–2137.

Stott, P. A., Stone, D. A. & Allen, M. R. Human contribution to the European heatwave of 2003. *Nature* **432**, 610–614 (2004).

Stouffer, R.J., S. Manabe, and K.Y. Vinnikov, 1994: Model assessment of the role of natural variability in recent global warming. *Nature*, **367**, 634–636.

http://science.sciencemag.org/content/195/4279/673.abstract.

Sitch, S., Friedlingstein, P., Gruber, N., Jones, S., Murray-Tortarolo, G., Ahlstrom, A., Doney, S., Graven, H., Heinze, C., Huntingford, C., Levis, S., Levy, P., Lomas, M., Poulter, B., Viovy, N., Zaehle, S., Zeng, N., Piao, S., LeQuere, C., Smith, B., Zhu, Z. and Myneni, R.: Recent trends and drivers of regional sources and sinks of carbon dioxide, Biogeosciences, 12, 653–2015, 2015.

Santer, B. D., and Coauthors (2014), Volcanic contribution to decadal changes in tropospheric temperature. *Nature Geoscience*, 7, 185-189.

Sato, M., J. E. Hansen, M. P. McCormick, and J. B. Pollack (1993), Stratospheric aerosol optical depths, 1850–1990, J. Geophys. Res., 98(D12), 22,987–22,994, doi:10.1029/93JD02553.

Schmidt, G., et al. (2011), Climate forcing reconstructions for use in PMIP simulations of the last millennium (v1.0). *Geosci. Model Dev.*, **4**, 33–45.

Schneider, D. P., C. M. Ammann, B. L. Otto-Bliesner, and D. S. Kaufman (2009), Climate response to large, high-latitude and low-latitude volcanic eruptions in the Community Climate System Model. *J. Geophys. Res. Atmos.*, **114**, D15101.

Scope, J. P. (1862), Volcanoes: The character of their phenomena, their share in the structure and composition of the surface of the globe and their relation to its internal forces, 2nd ed., London: Longman, Green, Longmans, and Roberts.

Sekiya, T., K. Sudo, and T. Nagai (2016), Evolution of stratospheric sulfate aerosol from the 1991 Pinatubo eruption: Roles of aerosol microphysical processes, J. Geophys. Res. Atmos., 121, doi:10.1002/2015JD024313.

Sheng, J.-X., D. K. Weisentstein, B.-P. Luo, E. Rozanov, A. Stenke, J. Anet, H. Bingemer, and T. Peter (2015), Global atmospheric sulfur budget under volcanically quiescent conditions: Aerosol-chemistry-climate model predictions and validation, J Geophys. Res. Atmos., 120, 256-276, doi:10.1002/2014JD021985.

Shindell, D.T., G.A. Schmidt, R.L. Miller, and M. Mann (2003), Volcanic and solar forcing of climate change during the preindustrial era. J. Clim., 16, 4094–4107.

Shindell, D.T., G.A. Schmidt, M. Mann, and G. Faluvegi (2004), Dynamic winter climate response to large tropical volcanic eruptions since 1600. J. Geophys. Res., 109, D05104, doi:10.1029/2003JD004151.

Simkin, T., L. Siebert, L. McClelland, D. Bridge, C. G. Newhall, J. H. Latter (1981), Volcanoes of the World, New York, Hutchinson Ross.

Simkin, T. (1993), Terrestrial volcanism in space and time, Annu. Rev. Earth. Planet. Sci., 21, 427-452.

7678 Soden, B. J., R. T. Wetherald, G. L. Stenchikov, and A. Robock (2002), Global cooling following

7679   the eruption of Mt. Pinatubo: A test of climate feedback of water vapor. *Science*, 296, 727-

7680   730.

7681 Solomon, S., J. S. Daniel, R. R. Neely, J. P. Vernier, E. G. Dutton, and L. W. Thomason (2011),

7682   The Persistently Variable "Background" Stratospheric Aerosol Layer and Global Climate

7683   Change. *Science*, 333, 866-870.

7684 Stenchikov, G., R. Dickerson, K. Pickering, W. Ellis, B. Doddridge, S. Kondragunta, O. Poulida,

7685   J. Scala, W.-K. Tao (1996), Stratosphere-Troposphere Exchange in a Mid-Latitude Mesoscale

7686   Convective Complex: Part 2, Numerical Simulations, *J. Geophys. Res.,* **101**, 6837-6851.

7687 Stenchikov, G.L., et al. (1998), Radiative forcing from the 1991 Mount Pinatubo volcanic eruption.

7688   J. Geophys. Res., 103(D12), 13837–13857.

7689 Stenchikov, G.L., et al. (2002), Arctic Oscillation response to the 1991 Mount Pinatubo eruption:

7690   effects of volcanic aerosols and ozone depletion. J. Geophys. Res., 107(D24), 4803,

7691   doi:10.1029/2002JD002090.

7692 Stenchikov, G., et al. (2004), Arctic Oscillation response to the 1991 Pinatubo eruption in the

7693   SKYHI GCM with a realistic quasi-biennial oscillation. J. Geophys. Res., 109, D03112,

7694   doi:10.1029/2003JD003699.

7695 Stenchikov, G., et al. (2006), Arctic Oscillation response to volcanic eruptions in the IPCC AR4

7696   climate models. J. Geophys. Res., 111, D07107, doi:10.1029/2005JD006286.

7697 Stenchikov, G., T. L. Delworth, V. Ramaswamy, R. J. Stouffer, A. Wittenberg, and F. Zeng (2009),

7698   Volcanic signals in oceans, J. Geophys. Res., D16104, 114, doi:10.1029/2008JD011673.

7699 Stenchikov, G. (2016), The role of volcanic activity in climate and global change, In the book

7700   Climate Change, Observed Impact on Planet Earth, 2nd Edition, Trevor Letcher, Ed., ISBN:

7701   978-0-444-63524-2, pp. 419-448.

7702 Stothers, R. (1996), Major optical depth perturbations to the stratosphere from volcanic eruptions:

7703   Pyrheliometric period, 1881-1960, J. Geophys. Res., 101, No. D2, 3901-3920.

7704 Stothers, R. (1997), Stratospheric aerosol clouds due to very large volcanic eruptions of the early

7705   twentieth century: Effective particle size and conversion from pyrheliometric to visual optical

7706   depth, J. Geophys. Res., 102, No. D5, 6143-6151.

7707 Stothers, R., 2001a: Major optical depth perturbations to the stratosphere from volcanic eruptions:

7708   Stellar extinction period, 1961-1978. J. Geophys. Res., 106(D3), 2993–3003.

7709 Stothers, R., 2001b: A chronology of annual mean radii of stratospheric aerosol from volcanic

7710   eruptions during the twentieth century as derived from ground-based spectral extinction

7711   measurements. J. Geophys. Res., 106(D23), 32043–32049.

7712

7713 Tarasick, D, Galbally, I, Cooper, OR, Ancellet, G, Leblanc, T, Wallington, TJ, Ziemke, J,

7714   Liu, X, Steinbacher, M, Stähelin, J, Vigouroux, C, Hannigan, J, García, O, Foret, G,

7715   Zanis, P, Weatherhead, E, Petropavlovskikh, I, Worden, H, Osman, M, Liu, J, Lin, M,

7716   Schultz, M, Granados-Muñoz, M, Thompson, AM, Oltmans, SJ, Cuesta, J, Dufour, G,

7717   Thouret, V, Hassler, B and Trickl, T., 2018. Tropospheric Ozone Assessment Report

7718   (TOAR): Tropospheric ozone observations–How well do we know tropospheric ozone

7719   changes? *Elem. Sci. Anth* . in-review, 2019.

7720 Taylor, K. E., and J. E. Penner, 1994: Response of the climate system to atmospheric aerosols

7721   and greenhouse gases. Nature, 369, 734–737, doi:10.1038/369734a0.

7722   https://doi.org/10.1038/369734a0.

7723 Tebaldi, C., and R. Knutti, 2007: The use of the multi-model ensemble in probabilistic climate

7724   projections. *Philos. Trans. R. Soc. A Math. Phys. Eng. Sci.*, **365**, 2053–2075,

7725   doi:10.1098/rsta.2007.2076. https://doi.org/10.1098/rsta.2007.2076.

7726 Tegen, I., Lacis, A. A., & Fung, I. (1996). The influence on climate forcing of mineral aerosols

7727   from disturbed soils. *Nature*, *380*(6573), 419.

7728 Telegadas, K., and J. London, 1954: A physical model of Northern Hemisphere troposphere

7729   for winter and summer. Scientific Report No. 1, Contract AF19 (122)-165; Research

7730   Div. College of Engineering, New York University, 55. pp.

7731 Tett, S.F.B., et al. (2002), Estimation of natural and anthropogenic contributions to twentieth
7732   century temperature change. J. Geophys. Res., 107(D16), 4306, doi:10.1029/2000JD000028.

7733 Textor, C., Schulz, M., Guibert, S., Kinne, S., Balkanski, Y., Bauer, S., ... & Dentener, F. (2007).
7734   The effect of harmonized emissions on aerosol properties in global models–an AeroCom
7735   experiment. *Atmospheric Chemistry and Physics*, *7*(17), 4489-4501.

7736 The royal society, 2009: *Royal Society Geoengineering the climate: science, governance and*
7737   *uncertainty*.

7738 Thompson, A. M., and R. J. Cicerone, 1986: Possible perturbations to atmospheric CO, CH4,
7739   and OH. *J. Geophys. Res. Atmos.*, **91**, 10853–10864, doi:doi:10.1029/JD091iD10p10853.
7740   https://doi.org/10.1029/JD091iD10p10853.

7741 ——, R. W. Stewart, M. A. Owens, and J. A. Herwehe, 1989: Sensitivity of tropospheric
7742   oxidants to global chemical and climate change. *Atmos. Environ.*, **23**, 519–532,
7743   doi:https://doi.org/10.1016/0004-6981(89)90001-2.
7744   http://www.sciencedirect.com/science/article/pii/0004698189900012.

7745 Thornton, P. E., Doney, S. C., Lindsay, K., Moore, J. K. K., Mahowald, N., Randerson, J. T.,
7746   Fung, I., Lamarque, J.-F. F., Feddema, J. J., Lee, Y.-H. Y.-H., Peter E. Thornton K.
7747   Lindsay, J. K. Moore, N. Mahowald, J. T. Randerson, I. Fung, J.-F. Lamarque, J. Feddema,
7748   Y.-H. Lee, S. D., Thornton, P. E., Doney, S. C., Lindsay, K., Moore, J. K. K., Mahowald,
7749   N., Randerson, J. T., Fung, I., Lamarque, J.-F. F., Feddema, J. J. and Lee, Y.-H. Y.-H.:
7750   Carbon-nitrogen interactions regular climate-carbon cycle feedbacks: results from an
7751   atmosphere-ocean general circulation model, Biogeosciences, 6(10), 2009–2099, 2009.

7752 Tian, D., Dong, W., Gong, D., Guo, Y. & Yang, 2016: S. Fast responses of climate system to
7753   carbon dioxide, aerosols and sulfate aerosols without the mediation of SST in the CMIP5. *Int.*
7754   *J. Climatol*. **37**, 1156–1166.

7755 Toll, V., Christensen, M., Gassó, S., & Bellouin, N. (2017). Volcano and Ship Tracks Indicate
7756   Excessive Aerosol-Induced Cloud Water Increases in a Climate Model. *Geophysical*
7757   *research letters*, *44*(24).

7758 Turner, A. J., C. Frankenberg, P. O. Wennberg, and D. J. Jacob, 2017: Ambiguity in the causes

7759   for decadal trends in atmospheric methane and hydroxyl. *Proc. Natl. Acad. Sci.*,.

7760   http://www.pnas.org/content/early/2017/04/18/1616020114.abstract.

7761 ——, ——, and E. A. Kort, 2019: Interpreting contemporary trends in atmospheric methane.

7762   *Proc. Natl. Acad. Sci.*, **116**, 2805 LP-2813, doi:10.1073/pnas.1814297116.

7763   http://www.pnas.org/content/116/8/2805.abstract.

7764 Twomey, S. A.: The Nuclei of Natural Cloud Formation. Part II: The Supersaturation in Natural

7765   Clouds and the Variation of Cloud Droplet Concentrations, Geofis. Pure Appl., 43, 227–

7766   242, 1959.

7767 Twomey, S. A.: The influence of pollution on the shortwave albedo of clouds, J. Atmos. Sci., 34,

7768   1149–1152, 1977.

7769 Twomey, S. The influence of pollution on the shortwave albedo of clouds. *J. Atmos. Sci.* **34,** 1149-

7770   1152 (1977).

7771 Tyndall, J., 1861: On the Absorption and Radiation of Heat by Gases and Vapours, and on

7772   the Physical Connexion of Radiation, Absorption, and Conduction", *Philosophical*

7773   *Transactions of the Royal Society of London*, Volume 151, pages 1–36.

7774 Thomason, L. W., and G. Taha (2003), SAGE III aerosol extinction measurements: Initial results.

7775   *Geophys Res Lett*, 30, 1631.

7776 Thomason, L., and Th. Peter (Eds.) (2006), Assessment of Stratospheric Aerosol Properties

7777   (ASAP), WCRP-124, WMO/TD- No. 1295, SPARC Report No. 4, February 2006.

7778 Thomason, L. W., Ernest, N., Millán, L., Rieger, L., Bourassa, A., Vernier, J.-P. et al. (2018), A

7779   global space-based stratospheric aerosol climatology: 1979–2016, Earth Syst. Sci. Data, 10,

7780   469-492, https://doi.org/10.5194/essd-10-469-2018.

7781 Tilmes, S., R. R. Garcia, D. E. Kinnison, A. Gettelman, and P. J. Rasch (2009), Impact of

7782   geoengineered aerosols on the troposphere and stratosphere. *Journal of Geophysical*

7783   *Research-Atmospheres*, 114, D12305.

7784   Tilmes, S., and Coauthors, 2013: The hydrological impact of geoengineering in the
7785   Geoengineering Model Intercomparison Project (GeoMIP). *Journal of Geophysical*
7786   *Research-Atmospheres*, 118, 11036-11058.

7787   Timmreck, C., H.-F. Graf, and I. Kirchner (1999), A one and half year interactive MA/ECHAM4
7788   simulation of Mount Pinatubo Aerosol. *Journal of Geophysical Research-Atmospheres*, 104,
7789   9337-9359.

7790   Timmreck, C., H.-F. Graf, S. J. Lorenz, U. Niemeier, D. Zanchettin, D. Matei, J. H. Jungclaus, and
7791   T. J. Crowley (2010), Aerosol size confines climate response to volcanic super eruptions,
7792   Geophys. Res. Lett., 37, L24705, doi:10.1029/2010GL045464.

7793   Timmreck, C. (2012), Modeling the climatic effects of large explosive volcanic eruptions. *Wiley*
7794   *Interdisciplinary Reviews-Climate Change*, 3, 545-564.

7795   Toohey, M., K. Krüger, M. Bittner, C. Timmreck, and Schmidt, H. (2014), The Impact of Volcanic
7796   Aerosol on the Northern Hemisphere Stratospheric Polar Vortex: Mechanisms and Sensitivity
7797   to Forcing Structure, Atmos. Chem. Phys., 14(23), 13063 – 13079, doi:10.5194/acp-14-
7798   13063-2014.

7799   Toon, O. B., and J. B. Pollack (1976), A global average model of atmospheric aerosols for radiative
7800   transfer calculations, J. Appl. Meteorol., 15, 225-246.

7801   Trenberth, K., and A. Dai, 2007: Effect of Mount Pinatubo volcanic eruption on the hydrological
7802   cycle as analaog of geoengineering. *Geophys Res Lett*, **34,** L15702.

7803   Trepte, C. R., M. H. Hitchman (1992), Tropical stratospheric circulation deduced from satellite
7804   aerosol data, Nature, 355, 626-628.

7805   Turco, R. P., R. C. Witten and O. B. Toon (1982), Stratospheric Aerosols: Observation and Theory,
7806   Reviwes of Geophysics and Space Physics, 20, No. 2, 233-279.

7807

7808 Unger, N., T. C. Bond, J. S. Wang, D. M. Koch, S. Menon, D. T. Shindell, and S. Bauer, 2010:

7809   Attribution of climate forcing to economic sectors. *Proc. Natl. Acad. Sci.,* 107 (8) 3382-

7810   3387. https://doi.org/10.1073/pnas.0906548107

7811 Unger, N.: Human land-use driven reduction of forest volatiles cools global climate, Nat. Clim.

7812   Chang., doi:10.1038/nclimate2347, 2014.

7813 Unger, N., Bond, T., Wang, J. S., Koch, D. M., Menon, S., Shindell, D. and Bauer, S.:

7814   Attribution of climate forcing to economic sectors, Proc. Natl. Acad. Sci. USA, 107(8),

7815   3382–3387, 2010.

7816 Unruh, Y.C., S. K. Solanki, and M. Fligge, 2000: Modelling solar irradiance variations:

7817   Comparison with observations, including line-ratio variations. Space Sci. Rev., 94, 1-2,

7818   145-152, doi:10.1023/A:1026758904332.

7819

7820 van Dorland, R., Dentener, F. J., & Lelieveld, J. (1997). Radiative forcing due to tropospheric

7821   ozone and sulfate aerosols. *Journal of Geophysical Research: Atmospheres*, *102*(D23),

7822   28079-28100.

7823 Van de Hulst, H. C., 1957: Light scattering by small particles. By H. C. **van de Hulst**. New York

7824   (John Wiley and Sons), London (Chapman and Hall). 470pp

7825 von Savigny, C., Ernst, F., Rozanov, A., Hommel, R., Eichmann, K.-U., Rozanov, V., Burrows, J.

7826   P., and Thomason, L. W. (2015), Improved stratospheric aerosol extinction profiles from

7827   SCIAMACHY: validation and sample results, Atmos. Meas. Tech., 8, 5223 – 5235.

7828 Vecchi G. A., et al., Weakening of tropical Pacific atmospheric circulation due to anthropogenic

7829   forcing, *Nature*, **441**. 73 - 76 (2006).

7830 Vernier, J. P., et al. (2009), Tropical stratospheric aerosol layer from CALIPSO lidar observations,

7831   J. Geophys. Res., 114, D00H10, doi:10.1029/2009JD011946.

7832 Vernier, J.-P., L. W. Thomason, J.-P. Pommereau, A. Bourassa, J. Pelon, A. Garnier,

7833   A.Hauchecorne, L. Blanot, C. trepte, Doug Degenstein, and F. Vagras (2011), Major

7834   influence of tropical volcanic eruptions on the stratospheric aerosol layer during the last

7835   decade, Geophys. Res. Lett., 38, L12807, doi:10.1029/2011GL047563.

7836 Verschuren, D., K. R. Laird, and B. F. Cumming, 2000: Rainfall and drought in equatorial east

7837   Africa during the past 1,100 years, Nature, 403, 410-414 doi:10.1038/35000179

7838 Voigt, C., U. Schumann, A. Minikin, A. Abdelmonem, A. Afchine, S. Borrmann, M. Boettcher,

7839   B. Buchholz, L. Bugliaro, A. Costa, J. Curtius, M. Dollner, A. Dörnbrack, V. Dreiling, V.

7840   Ebert, A. Ehrlich, A. Fix, L. Forster, F. Frank, D. Fütterer, A. Giez, K. Graf, J. Grooß, S.

7841   Groß, K. Heimerl, B. Heinold, T. Hüneke, E. Järvinen, T. Jurkat, S. Kaufmann, M.

7842   Kenntner, M. Klingebiel, T. Klimach, R. Kohl, M. Krämer, T.C. Krisna, A. Luebke, B.

7843   Mayer, S. Mertes, S. Molleker, A. Petzold, K. Pfeilsticker, M. Port, M. Rapp, P. Reutter, C.

7844   Rolf, D. Rose, D. Sauer, A. Schäfler, R. Schlage, M. Schnaiter, J. Schneider, N. Spelten, P.

7845   Spichtinger, P. Stock, A. Walser, R. Weigel, B. Weinzierl, M. Wendisch, F. Werner, H.

7846   Wernli, M. Wirth, A. Zahn, H. Ziereis, and M. Zöger, 2017: ML-CIRRUS: The Airborne

7847   Experiment on Natural Cirrus and Contrail Cirrus with the High-Altitude Long-Range

7848   Research Aircraft HALO. *Bull. Amer. Meteor. Soc.,* **98**, 271–288,

7849   https://doi.org/10.1175/BAMS-D-15-00213.1

7850 Voulgarakis, A., and Coauthors, 2013: Analysis of present day and future OH and methane

7851   lifetime in the ACCMIP simulations. *Atmos. Chem. Phys.*, **13**, 2563–2587, doi:10.5194/acp-

7852   13-2563-2013.

7853

7854 Ward, D. S. S. and Mahowald, N. M.: Contributions of developed and developing countries to

7855   global climate forcing, Environ. Res. Lett., 9(074008), doi:10.1088/1748-9326/9/7/074008,

7856   doi:10.1088/1748-9326/9/7/074008, 2014.

7857 Ward, D. S. S. and Mahowald, N. M.: Local sources of global climate forcing from different

7858   cateogries of land use activities, Earth Syst. Dyn., 6(1), 175–2015, doi:10.5194/esd-6-175-

7859   2015, 2015.

7860 Ward, D. S. S., Mahowald, N. M. M. and Kloster, S.: Potential climate forcing of land use and

7861   land cover change, Atmos. Chem. Phys., 14(23), 12701–12724, doi:10.5194/acp-14-12701-

7862   2014, 2014.

7863   Wang, C. Anthropogenic aerosols and the distribution of past large-scale precipitation change.
7864   *Geophys. Res. Lett.* **42,** 10,876-10,884 (2015).

7865   Wang, W. C., Yung, Y. L., Lacis, A. A., Mo, T., & Hansen, J. E. (1976). Greenhouse Effects due
7866   to Man-Made Perturbations of Trace Gases. *Science*, *194*(4266), 685 LP-690.
7867   http://doi.org/10.1126/science.194.4266.685.

7868   Wang, W.-C., Y.-C. Zhuang, and R. D. Bojkov, 1993: Climate implications of observed changes
7869   in ozone vertical distributions at middle and high latitudes of the northern hemisphere.
7870   Geophys. Res. Lett., 20, 1567–1570, doi:10.1029/93GL01318.
7871   https://doi.org/10.1029/93GL01318.

7872   Wang, W. C., Yung, Y. L., Lacis, A. A., Mo, T., & Hansen, J. E. (1976). Greenhouse Effects due
7873   to Man-Made Perturbations of Trace Gases. *Science*, *194*(4266), 685 LP-690.
7874   http://doi.org/10.1126/science.194.4266.685

7875   Wang, C. C., and L. I. Davis, 1974: Measurement of Hydroxyl Concentrations in Air Using a
7876   Tunable uv Laser Beam. *Phys. Rev. Lett.*, **32**, 349–352, doi:10.1103/PhysRevLett.32.349.
7877   https://link.aps.org/doi/10.1103/PhysRevLett.32.349.

7878   ——, ——, C. H. Wu, S. Japar, H. Niki, and B. Weinstock, 1975: Hydroxyl Radical
7879   Concentrations Measured in Ambient Air. *Science (80-.).*, **189**, 797–800.
7880   http://www.jstor.org/stable/1740212.

7881   Wang, W.-C., and N. D. Sze, 1980: Coupled effects of atmospheric N2O and O3 on the Earth's
7882   climate. *Nature*, **286**, 589. http://dx.doi.org/10.1038/286589a0.

7883   Wang, H., P. J. Rasch, and G. Feingold, 2011: Manipulating marine stratocumulus cloud amount
7884   and albedo: A process-modelling study of aerosol-cloud-precipitation interactions in
7885   response to injection of cloud condensation nuclei. *Atmos. Chem. Phys.*, doi:10.5194/acp-
7886   11-4237-2011.

7887   Wang, Y.-M., J. L. Lean, and N. R. Sheeley, Jr., 2005: Modeling the Sun's magnetic field and
7888   irradiance since 1713, Astrophys. J., 625, 522–538.

7889 ——, D. J. Wuebbles, W. M. Washington, R. G. Isaacs, and G. Molnar, 1986: Trace gases and

7890   other potential perturbations to global climate. *Rev. Geophys.*, **24**, 110–140,

7891   doi:doi:10.1029/RG024i001p00110. https://doi.org/10.1029/RG024i001p00110.

7892 Wagner, J. Wilzewski, P. Wcisło, S. Yu, E.J. Zak, The HITRAN2016 molecular spectroscopic

7893   database, Journal of Quantitative Spectroscopy and Radiative Transfer, Volume 203, 2017,

7894   Pages 3-69, ISSN 0022-4073, https://doi.org/10.1016/j.jqsrt.2017.06.038

7895 Wallington, T. J., J. H. Seinfeld, and J. R. Barker, 2018: 100 Years of progress in gas-phase

7896   atmospheric chemistry research. *Meteorol. Monogr.*, doi:10.1175/AMSMONOGRAPHS-D-

7897   18-0008.1. https://doi.org/10.1175/AMSMONOGRAPHS-D-18-0008.1.

7898 Washington, W., and G. Meehl, 1989: Climate sensitivity due to increased CO_2: experiments

7899   with a coupled atmosphere and ocean general circulation model. Clim. Dyn., 4, 1, 1–38.

7900 Watson, R. J., H. Rodhe, H. Oeschger, and U. Siegenthaler, 1990: Greenhouse gases and

7901   aerosols. *Climate Change: The IPCC Scientific Assessment (1990)*, J.T. Houghton, G.J.

7902   Jenkins, and J.J. Ephraums, Eds., Cambridge, U.K. and New York, NY, USA.

7903 Weart, S. R. (1997). Global Warming, Cold War, and the Evolution of Research Plans.

7904   *Historical Studies in the Physical and Biological Sciences*, *27*(2), 319–356.

7905   http://doi.org/10.2307/27757782.

7906 Weisenstein, D. K., D. W. Keith, and J. A. Dykema, 2015: Solar geoengineering using solid

7907   aerosol in the stratosphere. *Atmos. Chem. Phys.*, **15**, 11835–11859, doi:10.5194/acp-15-

7908   11835-2015. https://www.atmos-chem-phys.net/15/11835/2015/ (Accessed December 20,

7909   2018).

7910 Wei, T., Yang, S., Moore, J. C., Shi, P., Cui, X., Duan, Q., Xu, B., Dai, Y., Yuan, W., Wei, X.,

7911   Yang, Z., Wen, T., Teng, F., Gao, Y., Chou, J., Yan, X., Wei, Z., Guo, Y., Jiang, Y., Gao,

7912   X., Wang, K., Zheng, X., Ren, F., Lv, S., Yu, Y., Liu, B., Luo, Y., Li, W., Ji, D., Feng, J.,

7913   Wu, Q., Cheng, H., He, J., Fu, C., Ye, D., Xu, G. and Dong, W.: Developed and developing

7914   world responsibilities for historical climate change and CO2 mitigation, Proc. Natl. Acad.

7915   Sci., 109(32), 12911–12915, doi:10.1073/pnas.1203282109, 2012.

W. H. Matthews, W. W. Kellogg and G. D. Robinson, 1971, *Man's Impact on the Climate* MIT Press.

Wigley, T. M. L., 1987: Relative contributions of different trace gases to the greenhouse effect. Clim. Monit., 16, 14–29.

Wigley, T. M. L., 1989: Possible climate change due to SO2-derived cloud condensation nuclei. Nature, 339, 365–367, doi:10.1038/339365a0. https://doi.org/10.1038/339365a0.

Winton, M., K. Takahashi, and I. M. Held (2010), Importance of ocean heat uptake efficacy to transient climate change, J. Clim., 23, 2333–2344, doi:10.1175/2009jcli3139.1.

WMO, 1982: Report of the meeting of experts on potential climatic effects of ozone and other minor trace gases. WMO Global Ozone Research and Monitoring Project Report No 14.

WMO, 1986: *Atmospheric Ozone 1985.* Global Ozone Research and Monitoring Project Report No. 16. World Meteorological Organization, Geneva. Volume III.

WMO, 1986: Global ozone research and monitoring project. Atmospheric Ozone. WMO, Geneva, Switzerland.

World Meteorological Organization Global Ozone Research and Monitoring Project Report NO. 16 Atmospheric Ozone 1985 - Assessment of our Understanding of the Processes Controlling its Present Distribution and Change.

——, J. C. McConnell, and M. B. McElroy, 1972: Atmospheric CH4, CO, and CO2. *J. Geophys. Res.*, **77**, 4477–4493, doi:doi:10.1029/JC077i024p04477. https://doi.org/10.1029/JC077i024p04477.

Wuebbles, D. J., F. M. Luther, and J. E. Penner, 1983: Effect of coupled anthropogenic perturbations on stratospheric ozone. *J. Geophys. Res. Ocean.*, **88**, 1444–1456, doi:doi:10.1029/JC088iC02p01444. https://doi.org/10.1029/JC088iC02p01444.

Wetherald, R. T., and S. Manabe, 1975: The Effects of Changing the Solar Constant on the Climate of a General Circulation Model, J.Atmos. Sciences, 32, 2044-2059, https://doi.org/10.1175/1520-0469(1975)032<2044:TEOCTS>2.0.CO;2

White, O. R., Skumanich, A., Lean, J,. Livingston, W. C., and Keil, S. L., 1992: The Sun in a Non-cycling State, Publications of the Astronomical Society of the Pacific, 104, 1139-1143.

White, W. B., J. Lean, D.R. Cayan, and M.D. Dettinger, 1997: Response of global upper ocean temperature to changing solar irradiance, J. Geophys. Res., 102, 3255-3266.

Wigley, T. M. L. and S. C. B. Raper, 1990: Climatic change due to solar irradiance changes, Geophys. Res. Lett. 17, 12, 2169-2172, 10.1029/GL017i012p02169.

Wigley, T. M. L. (2006), A combined mitigation/geoengineering approach to climate stabilization. *Science*, 314, 452-454.

Willson, R. C., 1979: Active cavity radiometer type IV, Applied Optics, 18, 179-188, https://doi.org/10.1364/AO.18.000179

Willson, R.C., 2014: ACRIM3 and the total solar irradiance database, Astrophys Space Sci 352: 341. https://doi.org/10.1007/s10509-014-1961-4

Willson, R. C., Gulkis, S., Janssen, M., Hudson, H. S., and Chapman. G. A., 1981: Observations of Solar Irradiance Variability, Science 211, 4483, 700-702, DOI: 10.1126/science.211.4483.700

Woods, T. N., W. K. Tobiska, G. J. Rottman, and J. R. Worden, 2000: Improved solar Lyman α irradiance modeling from 1947 through 1999 based on UARS observations, J. Geophys. Res., 105(A12), 27195–27215, doi:10.1029/2000JA000051.

Xie, S.-P., Lu, B. & Xiang, 2013: B. Similar spatial patterns of climate responses to aerosol and greenhouse gas changes. *Nat. Geosci.* **6**, 828–832.

Yamamoto, G., and T. Sasamori, 1958: Calculation of the absorption of the 15 μ carbon dioxide band. *Sci. Rept. Tohoku Univ. Fifth Ser.,* **10,** No. 2, 37-57.

Young, P. J., and Coauthors, 2013: Pre-industrial to end 21st century projections of tropospheric

7967   ozone from the Atmospheric Chemistry and Climate Model Intercomparison Project

7968   (ACCMIP). *Atmos. Chem. Phys.*, **13**, 2063–2090, doi:10.5194/acp-13-2063-2013.

7969   http://www.atmos-chem-phys.net/13/2063/2013/ (Accessed July 16, 2018).

7970 Young, P. Y., and Coauthors, 2018: Tropospheric Ozone Assessment Report: Assessment of

7971   global-scale model performance for global and regional ozone distributions, variability, and

7972   trends. *Elem Sci Anth.*, **6**, doi:http://doi.org/10.1525/elementa.265.

7973 Yorks, J. E., Palm, S. P. McGill, M. J. Hlavka, D. L. Hart, W. D., Selmer, P. A., and Nowottnick

7974   (2015), E. P.: CATS Algorithm Theoretical Basis Document, 1st ed., NASA, 2015.

7975

7976 Zennaro, P., Kehrwald, N., McConnell, J. R., Schüpbach, S., Maselli, O. J., Marlon, J.,

7977   Vallelonga, P., Leuenberger, D., Zangrando, R., Spolaor, A., Borrotti, M., Barbaro, E.,

7978   Gambaro, A. and Barbante, C.: Fire in ice: Two millennia of boreal forest fire history from

7979   the Greenland NEEM ice core, Clim. Past, 10(5), 1905–1924, doi:10.5194/cp-10-1905-

7980   2014, 2014.

7981 Zhang, J., Christopher, S. A., Remer, L. A., & Kaufman, Y. J. (2005). Shortwave aerosol

7982   radiative forcing over cloud-free oceans from Terra: 2. Seasonal and global distributions.

7983   *Journal of Geophysical Research: Atmospheres*, *110*(D10).

7984 Zhang, Y., 2008: Online-coupled meteorology and chemistry models: history, current status, and

7985   outlook. *Atmos. Chem. Phys.*, **8**, 2895–2932, doi:10.5194/acp-8-2895-2008.

7986   https://www.atmos-chem-phys.net/8/2895/2008/.

7987 Zhang X, et al. (2007) Detection of human influence on twentieth-century precipitation trends.

7988   Nature **448**:461–465.

7989 Zimmermann, P H., Feichter, J., Rath, H. K., Crutzen, P. J., and Weiss, W. (1989), A global

7990   three- dimensional source receptor model investigation using KrX5, Atmos. Environ. 23,25-

7991   35.

7992 1984: *Global Tropospheric Chemistry: A Plan for Action*. 194 pp.

1985: *World Meteorological Organization Global Ozone Research and Monitoring Project Report NO. 16 Atmospheric Ozone 1985 - Assement of our Understanding of the Processes Controlling its Present Distribution and Change*.

Zanchettin, Davide, Myriam Khodri, Claudia Timmreck, Matthew Toohey, Anja Schmidt, Edwin P. Gerber, Gabriele Hegerl, Alan Robock, Francesco S. R. Pausata, William T. Ball, Susanne E. Bauer, Slimane Bekki, Sandip S. Dhomse, Allegra N. LeGrande, Graham W. Mann, Lauren Marshall, Michael Mills, Marion Marchand, Ulrike Niemeier, Virginie Poulain, Eugene Rozanov, Angelo Rubino, Andrea Stenke, Kostas Tsigaridis, and Fiona Tummon (2016), The Model Intercomparison Project on the climatic response to Volcanic forcing (VolMIP): experimental design and forcing input data for CMIP6, Geosci. Model Dev., 9, 2701-2719, https://doi.org/10.5194/gmd-9-2701-2016.

Zeilinga de Boer, J., D. T. Sanders (2002), Volcanoes and Human History, Princeton University Press, Princeton, NJ.

Zielinski, G. (2000), Use of paleo-records in determining variability within the volcanism-climate system, Quarterly Science reviews, 19, 417-438.